

Phenomenology of the Non-sterile Electroweak-scale Right-handed Neutrino Model

Ajinkya Shrish Kamat

Mumbai, India

M.Sc. Physics, Indian Institute of Technology Bombay,

Mumbai, India, 2009

B.Sc. Physics, University of Mumbai, India, 2007

A Dissertation presented to
the Graduate Faculty of the University of Virginia
in Candidacy for the Degree of
Doctor of Philosophy

Department of Physics

University of Virginia

May, 2015

Dedicated to my mother Medha S. Kamat,

father Shrish D. Kamat,

sister Preeti N. Telang,

Sharmistha Sahoo,

and

to the memory of my teachers Late Dr. G. A. Desai and

Late Mr. L. S. Jogalekar

Acknowledgements

I take this opportunity to express my gratitude to my advisor Prof. Pham Q. Hung. My doctoral research and this dissertation would not have been possible without his mentoring, support and encouragement. While working under his tutelage I have not only learned about particle physics, but also how the thought-process behind a scientific endeavor develops.

I am grateful to Prof. Hank Thacker for his guidance and collaboration during early years of my Ph.D. as well as for supporting me through graduate research assistantship for a number of semesters.

I also thank members of my research review committee, Prof. Hung, Prof. Thacker and Prof. Xiaochao Zheng, for taking time to review my research and giving their valuable feedback on the progress of my research, annually. In addition, I am thankful to them as well as Prof. Roger Chevalier for agreeing to be on my dissertation committee and giving time out of their busy schedules to review my dissertation and for my doctoral defense.

I am also thankful to Prof. Simonetta Liuti for her support and guidance during early time of my doctoral years. I also thank my colleague and friend Vinh V. Hoang for his collaboration and cooperation, during my doctoral research.

My gratitude to my parents and my sister cannot be expressed in words. Without them by my side throughout my life, it would not have been possible for me to reach

this juncture.

In addition, I am also thankful and grateful to:

The University of Virginia (UVA) and the Department of Physics for my life as a graduate student here has shaped me as a researcher as well as a person and a professional; the administrative staff at the Department, for their support right from the first day I joined UVA; the Graduate Directors Prof. Sackett, Prof. Louca and Prof. Nilanga for their guidance and support, especially Prof. Nilanga for supporting me with a departmental fellowship in the final year; the faculty and staff in the Department under whom I have served as a teaching assistant and a grader, for it gave me an opportunity to gain experience in teaching physics, in addition to just learning it; Melissa Hurst, the Director of Professional Development in UVA's Office of Graduate and Postdoctoral Affairs, for her guidance and support; all my colleagues, with whom I shared office over the years, for even casual discussions with them have been not only informative, but at times relaxing; all my teachers during my school years, undergraduate, master's and doctoral education, for it is because of the knowledge that I gained from them, I became capable of completing my doctoral studies; all my friends at UVA, especially Sharmistha Sahoo, Jay Nottingham, Sachith Dissanayake, Kirti Chawla, and likewise my friends elsewhere for their support and encouragement; all of my roommates in Charlottesville over the years, for their company has been relaxing amidst stressful times of my graduate life.

I also thank all those people whom I could not explicitly mention in this note, but interactions with whom have shaped me into the person I am today.

Abstract

In this dissertation we have discussed the phenomenology of the non-sterile Electroweak-scale Right-handed Neutrino ($\text{EW}\nu_R$) model. In the $\text{EW}\nu_R$ model, a right-handed neutrino can naturally acquire a mass around the electroweak scale $\Lambda_{EW} \approx 246$ GeV. This model adds the mirror fermions and an interesting Higgs sector to the particle spectrum in the Standard Model. We demonstrate that a significant part of the parameter space in the original $\text{EW}\nu_R$ model agrees with the precision constraints from the “Oblique Parameter” measurements. We then discuss the development of a minimal extension to the original $\text{EW}\nu_R$ model. This extended $\text{EW}\nu_R$ model includes the 125-GeV scalar that possesses “a dual nature”: it can either be a SM-like Higgs OR an impostor very different from the SM Higgs, both of which have the signal strengths compatible with experiments.

Foreword

Particle physics is a branch of science that explores the constituents of matter and energy in the Universe. It probes the most fundamental building blocks in the Nature. Research endeavors in particle physics - experimental and theoretical alike - inspire and invigorate far beyond their specific fields [1]. They not only add to our understanding of the Universe we live in, but also lay the foundations for technological advancements in the next-century and thereafter, we can only begin to imagine!

There are four fundamental forces in the Nature - gravitational, electromagnetic, weak nuclear and strong nuclear forces, all of which are studied in particle physics. The nature of these forces and the behavior of the fundamental constituents of matter and energy are explained with the help of various theoretical frameworks. The development of these theories is generally directed by experimental discoveries. Theoretical research enables us to make sense out of the experimental data and make predictions of new phenomena, to be tested experimentally in the future. Testing new theories often leads to new experimental observations, which can potentially direct the development of new theories. It is such dynamics in the research enterprise that drives the advancement of any scientific field, not only particle physics.

We believe that to further this advancement through theoretical research, the following steps should be followed while developing and analyzing any theoretical framework:

1. Verifying the agreement of the framework with the results from experiments in the past.
2. Verifying the agreement of the framework with results from the contemporary experiments; interpreting the experimental data from the perspective of the framework.
3. Analyzing implications of the framework for future experimentation; predicting phenomena peculiar to the framework, *which can be experimentally tested and which could conclusively confirm or disprove the framework.*

In this dissertation, we present the doctoral research that follows this approach of theoretical research, and attempts to address mainly two of the most profound questions in particle physics.

Many decades and centuries of in-depth study of the fundamental forces has revealed to us many exciting secrets of the Nature. Particle physicists often try to explain many of these features by theoretically formulating different *symmetries* in the Nature. The symmetry that the electromagnetic and weak nuclear forces obey is referred to as the “electroweak” symmetry. This symmetry existed only for a very short time at the beginning of the Universe, after which the symmetry was *broken*. It has been a long-standing question in particle physics to experimentally confirm the mechanism, through which the electroweak symmetry was broken.

Different elementary particles behave differently under the effects of the broken and unbroken symmetries in the Nature. Among these particles are a type of particles called “Neutrinos”. They are the second most abundant type of particles in the Universe (the first one being photons - the constituents of light). More than 20 trillion neutrinos coming from the Sun pass through our body every second. More than 100 billion billion neutrinos can come out of a nuclear reactor every second. Neutrinos are

so abundant, but the origin of their masses has not been experimentally validated.

The nature of the electroweak symmetry breaking and the origin of neutrino masses have been two of the most pressing problems in particle physics. In 2012, a new particle called a “Higgs boson” was discovered at the Large Hadron Collider - a particle physics experimental facility on French-Swiss border and also the largest machine ever built! This could be a crucial ingredient in the process of breaking the electroweak symmetry, which leads to masses of many elementary particles. The discovery of a Higgs boson in 2012 will certainly go a long way in resolving the first of the aforementioned mysteries. However, the mystery of the origin of neutrino masses still remains an open question.

There have been several attempts to theoretically realize the origin of neutrino masses, but none of these theoretical models have been experimentally confirmed. It may not be possible to conclusively confirm or disprove many of them at the Large Hadron collider or other experiments in the near future.

Is it possible to develop a theoretical framework, which explains the origin of neutrino masses and can also be conclusively tested at the Large Hadron Collider and other experiments in the near future?

And, is such theoretical framework possible without adding any more fundamental forces to the four known forces in the Nature?

These questions are the primary motivations behind the doctoral research presented here. They were answered affirmatively by a theoretical model - the Electroweak-scale Right-handed Neutrino Model - put forward a few years ago. Readers would find a detailed analysis of different aspects of this model as well as development and implications of an extension of this model, in the light of the Higgs discovery, covered in this dissertation.

We hope the readers enjoy reading this dissertation.

Contents

Acknowledgements	i
Abstract	iii
Foreword	iv
1 The Standard Model	3
1.1 How does the $SU(2)$ symmetry emerge?	4
1.1.1 Fermi's model of β -decay	4
1.1.2 Unitarity requires W^\pm, W^0	6
1.1.3 Conclusion of the section	15
1.2 'Gauging' the $SU(2)$ symmetry	16
1.2.1 Global vs. local $SU(2)$ symmetry	17
1.2.2 The covariant derivative and non-invariant mass terms	18
1.3 The Higgs mechanism and generating the masses of gauge bosons and fermions	22
1.3.1 Steps in the Higgs mechanism	24
1.3.2 The Higgs mechanism for the $SU(2)$ gauge theory	25
1.3.3 Generating masses of the fermions	28
1.3.4 Summary of this section	29

1.4	The Standard Model of particle physics	29
1.4.1	Existence of a $U(1)_Y$ gauge theory	30
1.4.2	Gauging the $SU(2)_L \times U(1)_Y$ symmetry	32
1.4.3	Breaking the $SU(2)_L \times U(1)_Y$ gauge symmetry spontaneously	33
1.5	Features and Limitations of the Standard Model	40
2	Neutrino Oscillations and Models of Neutrino Masses	44
2.1	The PMNS matrix and various mixing angles	45
2.1.1	PMNS matrix	47
2.1.2	Global fit values	49
2.2	Seesaw mechanism of neutrino masses	50
2.2.1	Different types of ν -mass terms	51
2.2.2	Type-I Seesaw mechanism	53
2.2.3	Type-II Seesaw mechanism	54
2.2.4	Type-III Seesaw mechanism	55
2.3	Left-Right symmetric models	57
2.4	Summary of the chapter	58
3	Hung's Minimal $EW\nu_R$ Model	60
3.1	Building the model	61
3.1.1	The fermion sector	62
3.1.2	The scalar sector	65
3.2	Breaking of the electroweak symmetry	69
3.2.1	The physical scalars	73
3.3	Summary of the minimal $EW\nu_R$ model	76
3.3.1	What's the advantage of the mirror fermions?	77
3.3.2	Why don't we see mirror fermions today?	78

3.3.3	Doesn't ν_R contribute to the total energy density?	78
3.3.4	Does this model have a 'dark matter' candidate?	79
3.3.5	Main features of the model	79
4	Contributions to Oblique Parameters in the $\text{EW}\nu_R$ Model	81
4.1	Defining Oblique Parameters	81
4.1.1	What are Oblique Parameters?	81
4.1.2	Why are Oblique Parameters relevant?	86
4.2	Calculating new physics contributions to Oblique Parameters	87
4.3	Calculation of One Loop Contributions to the Oblique Parameters in the $\text{EW}\nu_R$ model	88
4.3.1	Contributions to Oblique Parameters from the scalar sector in the $\text{EW}\nu_R$ model	89
4.3.2	Contributions to the Oblique Parameters from the fermion sector in the $\text{EW}\nu_R$ model	92
4.4	Comparison with the experimental constraints	95
4.4.1	Ranges of relevant parameters	95
4.4.2	Unconstrained \tilde{S} and \tilde{T} parameters for the scalar and the mirror fermion sectors	98
4.4.3	Constrained \tilde{S} and \tilde{T} parameters for the scalar and the mirror fermion sectors	101
4.5	Conclusions of the chapter	103
5	An Extended $\text{EW}\nu_R$ Model and the Dual Nature of the 125-GeV Scalar	105
5.1	Can the minimal $\text{EW}\nu_R$ model accommodate a 125-GeV Higgs? . . .	107
5.2	An extended $\text{EW}\nu_R$ model	111

5.2.1	Field content of the model	111
5.2.2	Symmetry breaking	113
5.2.3	Physical particle spectrum in the extended $\text{EW}\nu_R$ model . . .	118
5.2.4	A comment on oblique contributions in the extended $\text{EW}\nu_R$ model	119
5.2.5	A comment on the pseudo Nambu-Goldstone bosons in the $\text{EW}\nu_R$ model	119
5.3	Partial decay widths of neutral Higgs	121
5.3.1	$\mathbf{H} \rightarrow \mathbf{g}\mathbf{g}$	121
5.3.2	$\mathbf{H}^0 \rightarrow \gamma\gamma$	123
5.3.3	Tree level decays of \tilde{H}	126
5.4	The Dual Nature of the 125-GeV Scalar	128
5.4.1	Methodology for comparing the $\text{EW}\nu_R$ model predictions with data	130
5.4.2	\tilde{H} as 125-GeV Higgs candidate with a dominant SM-like com- ponent	137
5.4.3	\tilde{H} as the 125-GeV Higgs candidate with a sub-dominant SM- like component	144
5.4.4	The next heavier neutral scalar \tilde{H}'	150
5.4.5	Conclusions about the 125-GeV Higgs candidate in the $\text{EW}\nu_R$ model	153
6	Conclusions	156
A	Loop Integrals and Functions	160
B	Feynman rules in the minimal $\text{EW}\nu_R$ Model	165

C	Loop Contributions to Oblique Parameters in the $\text{EW}\nu_R$ model	169
C.1	One Loop Contributions to \tilde{S}_{scalar} and \tilde{T}_{scalar}	169
C.2	One Loop Contributions to $\tilde{S}_{fermion}$ and $\tilde{T}_{fermion}$	180
D	Feynman rules in the extended $\text{EW}\nu_R$ model	187

List of Figures

1.1	Fermi's 4 fermion interaction.	5
1.2	One loop process Fermi's 4 fermion interactions.	7
1.3	$e^- \nu_\mu \rightarrow \mu^- \nu_e$ process with W^\pm reduces to Fermi's 4 fermion interaction at $q^2 \ll M_W^2$	9
1.4	$\nu_e \bar{\nu}_e \rightarrow W_L W_L$ by exchanging an electron.	10
1.5	$\nu_e \bar{\nu}_e \rightarrow W_L W_L$ by exchanging the W^0 boson.	11
1.6	EW ν_R model mirror fermion loop examples	12
1.7	$\nu_e \bar{\nu}_e \rightarrow W_L W_L$ by exchanging an electron.	13
1.8	$\nu_e \bar{\nu}_e \rightarrow W_L W_L$ by exchanging an electron.	13
1.9	$\nu_e \bar{\nu}_e \rightarrow W_L W_L$ by exchanging the W^0 boson.	13
1.10	The Standard Model particle content. Image source: Wikipedia	41
3.1	Physical particle spectrum in the minimal EW ν_R model	77
4.1	Mass of ν_R versus mass of charged mirror fermion f^M with constraints due to perturbativity of the Yukawa couplings. Thus, the final constraints are $M_Z/2 \leq M_R \leq 300 \text{ GeV}$ and $m_{f^M} \leq 610 \text{ GeV}$ (small purple area).	97
4.2	\tilde{T} versus \tilde{S} for the scalar sector with the 1 and 2 σ experimental contours (about 500 points). Plotted by Vinh V. Hoang.	99

4.3	\tilde{T} versus \tilde{S} for the mirror fermion sector with the 1 and 2 σ experimental contours (about 500 points). Plotted by Vinh V. Hoang.	100
4.4	Total \tilde{T} versus \tilde{S} with the 1 and 2 σ experimental contours. Plotted by Vinh V. Hoang.	102
5.1	Courtesy: CMS collaboration, CMS-PAS-HIG-13-002, March 2013	110
5.2	Physical particle spectrum in the extended EW ν_R model.	118
5.3	Figure shows the predictions of $\mu(\tilde{H} \rightarrow b\bar{b}, \tau\bar{\tau}, \gamma\gamma, W^+W^-, ZZ)$ in the EW ν_R model for examples 1 and 2 in <i>Dr. Jekyll</i> and example 1, 2 and 3 in <i>Mr. Hyde</i> scenarios, in comparison with corresponding best fit values by CMS [51, 52, 53, 54].	143
5.4	Predicted signal strength of $\tilde{H}' \rightarrow W^+W^-$ in 4 example scenarios (blue and purple squares). The results of the search for SM-like Higgs boson up to 600 GeV with the 1 σ (green band) and 2 σ (yellow band) limits on the SM background (dotted curve) and CMS data (solid black curve) are also displayed.	151
C.1	EW ν_R model mirror fermion loop examples	181
C.2	Standard Model fermion loop examples	182

List of Tables

1.1	Vertices in the theory of weak interactions.	14
2.1	Global fit values of neutrino oscillation measurements, given in [21] for “free fluxes”. “NH” → Normal Hierarchy; “IH” → Inverted Hierarchy.	50
5.1	Allowed ranges of VEVs and parameters defined in Eq. (5.14). All values are given in GeV	134
5.2	Partial width of $H \rightarrow gg$ as the measure of the production cross section, partial widths and branching ratios for various channels in SM (for $m_{H_{SM}} = 125.7$ GeV with total width = 4.17E-3 GeV , and the EW ν_R model for <i>Dr. Jekyll</i> example 2 scenario: $a_{1,1M} = -0.0025$, where $m_{\tilde{H}} = 125.7$ GeV, total width = 4.45E-3 GeV and $\tilde{H} \sim H_1^0$. All the partial widths are given in GeV	140
5.3	Partial width of $H \rightarrow gg$ as the measure of the production cross section, partial widths and branching ratios for various channels in SM (for $m_{H_{SM}} = 125.6$ GeV and total width 4.15E-03 GeV), and the EW ν_R model for row 3 in Table 5.4, also in Eq. (5.52) where $\tilde{H} \sim H_1^{0'}$ (with $m_{\tilde{H}} = 125.6$ GeV and total width 1.34E-03 GeV). All the partial widths are given in GeV	147

5.4	All the masses and the total width of \tilde{H} are given in GeV . Fixed parameters as given in Eq. (5.46).	149
B.1	SV_1V_2 type couplings(V_1 and V_2' are vector gauge bosons and S is a Higgs boson), which contribute to Oblique Corrections. Common factor: $igM_W g^{\mu\nu}$	165
B.2	S_1S_2V type couplings(V is a vector gauge boson and S_1, S_2 are Higgs/Goldstone bosons), which contribute to Oblique Corrections. Common factor: $ig(p-p')^\mu$, where $p(p')$ is the <i>incoming</i> momentum of the $S_1(S_2)$.166	
B.3	$H_1H_2V_1V_2$ type couplings, which contribute to Oblique Corrections. Common factor: $ig^2g^{\mu\nu}$	167
B.4	$H_1H_2V_1V_2$ type couplings, which <i>do not</i> contribute to Oblique Corrections. Common factor: $ig^2g^{\mu\nu}$	168
B.5	$f_1^M f_2^M V$ type couplings, which contribute to the Oblique Corrections. For each Feynman rule the charge conservation is implicit. f_{1R}^M and f_{2R}^M are members of the same mirror fermion doublet with isospins $\frac{1}{2}$ and $-\frac{1}{2}$ respectively (ref. [26], [10] & [11]). Common factor for all couplings: $ig\gamma_\mu$	168
C.1	One-loop diagrams with two internal scalar (S) (Higgs or Goldstone boson) lines, which contribute to W^+ and Z self-energies. Common factor: $g^2/16\pi^2$	170
C.2	Tadpole diagrams with one internal scalar (S) (Higgs or Goldstone boson) line, which contribute to W^+ and Z self-energies. Common factor: $g^2/16\pi^2$	172

C.3	One-loop diagrams with one internal scalar (S) (Higgs or Goldstone boson) line and one internal vector boson line, which contribute to W^+ and Z self-energies. Common factor: $g^2/16\pi^2$	174
C.4	One-loop diagrams with two internal scalar (S) (Higgs or Goldstone boson) lines, which contribute to photon (γ) self-energy and Z - γ transition amplitude. Common factor: $g^2/16\pi^2$	175
C.5	Tadpole diagrams with one internal scalar (S) (Higgs or Goldstone boson) line, which contribute to photon (γ) self-energy and Z - γ transition amplitude. Common factor: $g^2/16\pi^2$	176
C.6	One-loop diagrams with one internal scalar (S) (Higgs or Goldstone boson) line and one internal vector boson line, which contribute to photon (γ) self-energy and Z - γ transition amplitude. Common factor: $g^2/16\pi^2$	177
C.7	One-loop diagrams with two internal scalar (S) (Higgs or Goldstone boson) lines, which contribute to $\Pi_{33}(q^2)$ in T . Common factor: $g^2/16\pi^2$	178
C.8	Tadpole diagrams with one internal scalar (S) (Higgs or Goldstone boson) line, which contribute to $\Pi_{33}(q^2)$ in T . Common factor: $g^2/16\pi^2$	179
C.9	One-loop diagrams with one internal scalar (S) (Higgs or Goldstone boson) line and one internal vector boson line, which contribute to $\Pi_{33}(q^2)$ in T . Common factor: $g^2/16\pi^2$	180
C.10	Fermion loop diagrams with two internal mirror fermion lines, which contribute to $\Pi_{WW}(q^2)$. Here f_{1R}^M 's and f_{2R}^M 's are members of a mirror fermion doublet with isospins (T_3^f) equal to $\frac{1}{2}$ and $-\frac{1}{2}$ respectively. Common factor: $g^2 N_c/16\pi^2$	182
C.11	Fermion loop diagrams with two internal mirror fermion lines, which contribute to $\Pi_{ZZ}(q^2)$. Common factor: $g^2 N_c/16\pi^2$	183

C.12 Fermion loop diagrams with two internal mirror fermion lines, which contribute to $\Pi_{Z\gamma}(q^2)$. Common factor: $g^2 N_c/16\pi^2$	184
C.13 Fermion loop diagrams with two internal mirror fermion lines, which contribute to $\Pi_{\gamma\gamma}(q^2)$. Common factor: $g^2 N_c/16\pi^2$	185
C.14 Fermion loop diagrams with two internal mirror fermion lines, which contribute to $\Pi_{33}(q^2)$. Common factor: $g^2 N_c/16\pi^2$	186
D.1 Yukawa couplings with SM quarks and mirror-quarks in the extended $EW\nu_R$ model. The Yukawa couplings involving <i>charged</i> SM (and mirror) leptons can be obtained by replacing up-type SM (and mirror) quarks by left-handed (and right-handed) neutrinos and down-type SM (and mirror) quarks by the charged SM (and mirror) leptons in this table.	187
D.2 Yukawa couplings with SM quarks and mirror-quarks in the $EW\nu_R$ model. The Yukawa couplings involving <i>charged</i> SM (and mirror) leptons can be obtained by replacing up-type SM (and mirror) quarks by left-handed (and right-handed) neutrinos and down-type SM (and mirror) quarks by the charged SM (and mirror) leptons in this table.	188
D.3 $S_1 S_2 V$ type couplings (V is a vector gauge boson and S_1, S_2 are Higgs/Goldstone bosons), which contribute to Oblique Corrections. Common factor: $i g(p-p')^\mu$, where $p(p')$ is the <i>incoming</i> momentum of the $S_1(S_2)$	189
D.4 $S V_1 V_2$ type couplings (V_1 and V_2' are vector gauge bosons and S is a Higgs boson), which contribute to Oblique Corrections. Common factor: $i g M_W g^{\mu\nu}$	191
D.5 $H_1 H_2 V_1 V_2$ type couplings, which contribute to Oblique Corrections. Common factor: $i g^2 g^{\mu\nu}$	191

D.6	$H_1 H_2 V_1 V_2$ type couplings, which <i>do not</i> contribute to Oblique Corrections. Common factor: $i g^2 g^{\mu\nu}$	193
-----	--	-----

Chapter 1

The Standard Model

Different particles in the Nature influence with each other through one or more of the *Fundamental Forces in the Nature*. There are four known fundamental forces: Gravitational force, Electromagnetic force, Strong nuclear force, and Weak nuclear force.

The latter 3 forces can be theoretically realized through a framework known as *the Standard Model (SM)* of particle physics, while the nature of gravitational force is studied with the help of *the General Theory of Relativity*. The Standard Model (SM) of particle physics is one of the most successful theoretical models in physics. The success of SM is a result of rigorous experimental scrutiny that it has been subjected to over the years.

There exist experimental evidences, such as neutrino oscillations, existence of the dark matter and dark energy, which cannot be accounted for strictly within the SM. However, so far there is no doubt that SM also lays a strong foundation for the physics Beyond the Standard Model (BSM). Hence, it is essential to discuss the SM, before delving into the depths of any facets of particle physics.

In this chapter we will take a historical-cum-physical approach to review the devel-

opment of SM [2]. We will see how the $SU(2)$ symmetry structure of the weak nuclear force in SM emerges as a result of *Unitarity* (requirement that the total probability has to be $\lesssim 1$). We will then discuss how physical requirements dictate “gauging” of SM, and how the electromagnetic and the weak nuclear forces are “unified” into the *electromagnetic force*, governed by a gauge theory abiding $SU(2) \times U(1)$ symmetry.

The final section of the chapter discusses the Higgs mechanism and the Higgs boson in SM.

1.1 How does the $SU(2)$ symmetry emerge?

To develop the SM, we start in a premise that the quantum electrodynamics, which explains the electromagnetic interaction between charged particles, was well understood. Thus, it was known that quantum electrodynamics obeys a local $U(1)$ gauge symmetry (we will shortly discuss what “local symmetry” and “gauging” mean).

1.1.1 Fermi’s model of β -decay

In 1896 Henry Becquerel discovered radioactive emissions, which were classified into α , β and γ emissions by Ernest Rutherford in 1899 [3]. In 1930, Wolfgang Pauli wrote his famous letter [4], postulating the existence of the neutral particle in the β decay, which Enrico Fermi named as *neutrino* in 1934 [5].

The β decay is a process in which a neutron (n^0) decays into a proton (p^+), an electron (e^-) and a neutral particle called the anti-neutrino ($\bar{\nu}$): $n \rightarrow e^- p^+ \bar{\nu}$.

Fermi put forward a model of 4-fermion interaction that explained the β decay remarkably well. At that time, the β decay was thought to be a result of the interaction between a neutron, a proton, an electron and a neutrino. The Lagrangian of the

Fermi interaction was *empirically* written as

$$\mathcal{L}_{Fermi} = -\frac{G_F}{\sqrt{2}} [\bar{p}(x) \gamma_\mu n(x)] [\bar{e}(x) \gamma_\mu \nu(x)] + h.c. \text{ (Hermitian Conjugate)}. \quad (1.1)$$

G_F is known as the Fermi's constant, at that time thought to be given by [6]

$$G_F \approx \frac{10^{-5}}{m_p^2} = 1.1663787(6) \times 10^{-5} \text{ GeV}^{-2}, \quad (1.2)$$

with m_p as the mass of proton and $\hbar = c = 1$, and (..) denotes the uncertainty in the last significant figure. This Fermi's four-fermion interaction can be visualized as

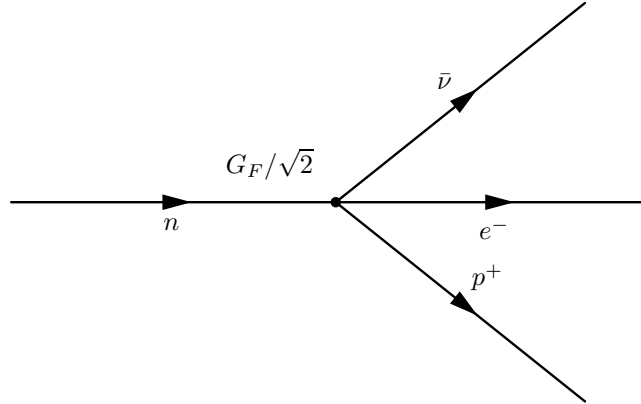


Figure 1.1: Fermi's 4 fermion interaction.

As the β decay has a relatively long lifetime of ≈ 881 s, the Fermi's interaction was referred to as a *weak interaction*. Fermi's constant can also account for the muon decay $\mu^- \rightarrow e^- \bar{\nu}_e \bar{\nu}_\mu$ and the pion decay $\pi^- \rightarrow \mu^- \bar{\nu}_\mu$ (lifetime of about 2.2 μ s and 28 ns, respectively). Remember that the Lagrangian in Eq. (1.1) is purely phenomenological. The *weak currents* like $[\bar{p}(x) \gamma_\mu n(x)]$ and $[\bar{e}(x) \gamma_\mu \nu(x)]$ conserve parity, just like the electromagnetic current $[\bar{e}(x) \gamma_\mu e(x)]$ does.

Note that neutrinos were still considered massless.

Lee and Yang in 1956 [7] proposed a series of experiments to verify the exact parity

structure of weak currents. Chien-Shuing Wu in 1957 demonstrated [8] that parity is, indeed, not conserved in the weak interaction. After a number of experiments by different groups, the exact parity structure of weak currents was proved to be:

$$\mathcal{J}_\mu^{weak} = [\bar{e}(x) \gamma_\mu(1 - \gamma_5) \nu(x)], [\bar{p}(x) \gamma_\mu(1 - \gamma_5) n(x)], \dots \quad (1.3)$$

Under parity operation $\bar{\psi}(x) \gamma_\mu \gamma_5 \psi(x) \rightarrow P \bar{\psi}(x) \gamma_\mu \gamma_5 \psi(x) P^{-1} = -\bar{\psi}(x') \gamma_\mu \gamma_5 \psi(x')$. Thus, \mathcal{J}_μ^{weak} has the ‘ $V - A$ ’ structure, meaning that it is written as a vector (V) current ‘minus’ an axial vector (A) current. With this correct parity structure, \mathcal{L}_{Fermi} was written as

$$\mathcal{L}_{Fermi} = -\frac{G_F}{\sqrt{2}} (\mathcal{J}_\mu^{weak} \mathcal{J}^{\mu,weak}) . \quad (1.4)$$

Note: $(1 - \gamma_5)/2 \psi(x) = \psi_L(x)$ - the component of $\psi(x)$ having left-handed helicity.

1.1.2 Unitarity requires W^\pm , W^0

1.1.2.1 Infinities, unitarity violation and bad high energy behavior

Lagrangian in Eq. (1.4) correctly describes the parity violating and charge changing nature of the weak current $[\bar{e}(x) \gamma_\mu \gamma_5 \bar{\nu}(x)]$. It agrees very well with experimentally measured cross sections of tree level processes such as the β decay and muon decay $\mu^- \rightarrow e^- \bar{\nu}_e \bar{\nu}_\mu$. However, this theory breaks down for one-loop processes such as $\nu_\mu e^- \rightarrow \nu_\mu e^-$.

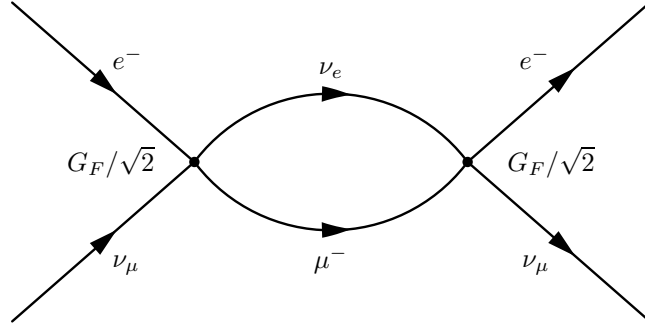


Figure 1.2: One loop process Fermi's 4 fermion interactions.

The Fermi's interaction predicts an infinite cross section for such a process! This problem with the theory can be traced back to the violation of “unitarity” in this theory.

Unitarity is the basic principle that probability cannot exceed 1. In scattering theory, the S -matrix is given by $S = \mathbb{I} + iT$, where \mathbb{I} represents “no scattering”, while iT gives the amplitude of the scattering. Thus, $|S|^2 = S S^\dagger = S^\dagger S = 1$ is the measure of the total probability of the process (with or without scattering) [9].

The cross section of $\nu_\mu e^- \rightarrow \nu_\mu e^-$ can be given, using the Fermi's interaction, as

$$\sigma \sim G_F s, \quad (1.5)$$

where $s = 2 m_e E_\nu$ with E_ν is the energy of ν_μ in the lab frame. Thus, s is a measure of the energy, at which the theory is probed. According to the scattering theory, this cross section can also be written as

$$\sigma \sim \frac{|S_{J=1}|^2}{s} \Rightarrow \sigma \leq \frac{1}{s}, \quad (1.6)$$

because, for unitarity, $|S_{J=1}|^2 \leq 1$.

$$G_F^2 s \leq \frac{1}{s} \Rightarrow \sqrt{s} \leq (G_F)^{-1/2} \Rightarrow \sqrt{s} \lesssim 300 \text{ GeV}. \quad (1.7)$$

This means that the unitarity is violated and the Fermi's theory of weak interaction breaks down beyond about 300 GeV . To be accurate, the weak interaction unitarity is violated at about 1000 GeV . What remedy could avoid such a bad high energy behavior?

1.1.2.2 W^\pm cures infinities

The Quantum Electrodynamics (QED), which has a similar current structure, does not exhibit such a bad high energy behavior. All the infinities in QED can be cancelled through “renormalization”. The renormalizability of QED is possible because of the dimensionless coupling constant ‘ e ’. On the other hand, the coupling constant $G_F \sim 10^{-5}/m_p^2$ of the Fermi interaction has dimensions of $(Energy)^{-2}$. We can thus expect that a theory of weak interaction that has a dimensionless coupling constant could remedy the problem of infinities and unitarity violation.

The QED Lagrangian is written as

$$\mathcal{L}^{QED} = e \mathcal{J}_\mu^{EM} A^\mu, \quad (1.8)$$

where $\mathcal{J}_\mu^{EM} = \bar{e}(x) \gamma_\mu e(x)$ is the electromagnetic current, A_μ is the photon field and ‘ e ’ - the charge of electron - is the *dimensionless* coupling constant of the electromagnetic interaction. Notice that because the electromagnetic force is carried by the vector (spin-1) photon field, the EM coupling constant ‘ e ’ can be dimensionless.

Therefore, physicists tried to write a Lagrangian weak interaction by introducing

a charged spin-1 field W^\pm and a dimensionless coupling constant ‘ g ’:

$$\mathcal{L}^{weak} = g \mathcal{J}_\mu^{weak} W^\mu, \quad (1.9)$$

where \mathcal{J}_μ^{weak} is the charge-changing weak current that was introduced in Eq. (1.3). Thus, all the weak interactions, $[\bar{e}(x) \gamma_\mu \gamma_5 \nu(x)]$, $[\bar{\mu}(x) \gamma_\mu \gamma_5 n(x)]$, have the same coupling constant ‘ g ’. Note that W^\pm is a massive spin-1 field, as opposed to the massless photon field A_μ .

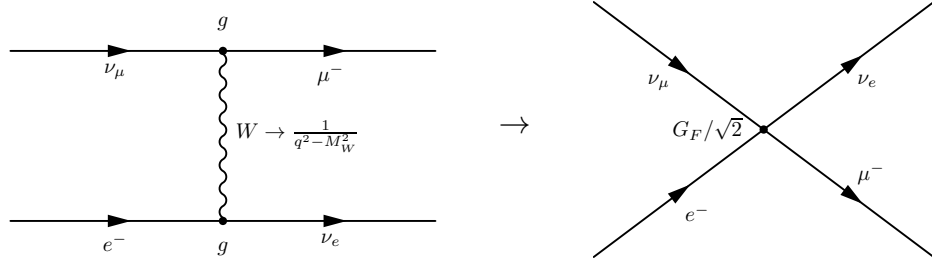


Figure 1.3: $e^- \nu_\mu \rightarrow \mu^- \nu_e$ process with W^\pm reduces to Fermi’s 4 fermion interaction at $q^2 \ll M_W^2$.

Since the weak force is carried by the W^\pm bosons, the process $e^- \nu_\mu \rightarrow \mu^- \nu_e$ can be represented by the Feynman diagram in Fig. 1.3. When the momentum-squared q^2 transferred in the process is much lower than the mass of W^\pm , the $e^- \nu_\mu \rightarrow \mu^- \nu_e$ effectively occurs through the Fermi’s four-fermion interaction. Thus, the coupling constants in the Fermi’s four-fermion interaction and the Lagrangian \mathcal{L}^{weak} are related by:

$$G_F = \frac{\sqrt{2}}{8} \frac{g^2}{M_W^2}, \quad (1.10)$$

where M_W is the mass of W^\pm . \mathcal{L}^{weak} does solve the problem of a coupling constant with dimension. However, the problem of unitarity violation at the high energy still remains.

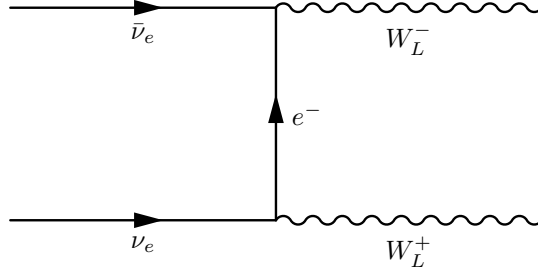


Figure 1.4: $\nu_e \bar{\nu}_e \rightarrow W_L W_L$ by exchanging an electron.

Since, W^\pm are massive, they possess 3 degrees of freedom of polarization: 2 transverse and 1 longitudinal. Let us denote their longitudinally polarized component by W_L^\pm , which has a polarization given by

$$\epsilon_\mu^{(L)} = \frac{k_\mu}{M_W} + \mathcal{O}\left(\frac{M_W}{k_\mu}\right). \quad (1.11)$$

Consider the diagram in Fig. 1.4, whose cross section increases with energy, because the cross section contains

$$\sum_{\text{polarization}} \epsilon_\mu \epsilon_\nu^* = -g_{\mu\nu} + \frac{k_\mu k_\nu}{M_W}, \quad (1.12)$$

where the second term leads to the bad high energy behavior.

The cross section of this process can be given by

$$\sigma = \frac{G_F^2 E_{CM}^2}{3 \pi}, \quad (1.13)$$

where E_{CM} is the energy of the process in the center-of-mass frame. In the S -matrix formulation of scattering theory, this cross section can be given by

$$\sigma = \frac{\pi}{E_{CM}^2} \sum_J (2J + 1) |S_{0,0;1/2,-1/2}|^2, \quad (1.14)$$

where the first two suffixes of $S_{0,0;1/2,-1/2}$ denote the helicities of the longitudinal components W_L^\pm , while the latter two suffixes denote those of the neutrino and the anti-neutrino in Fig. 1.4.

Since only the $J = 1$ term contributes, from Eqs. (1.13) and (1.14) and unitarity, we get

$$|S_{0,0;1/2,-1/2}|^2 = \frac{G_F^2 E_{CM}^4}{9 \pi^2} \leq 1. \quad (1.15)$$

This implies violation of unitarity at $E_{CM} \sim 900$ GeV. Thus, if the charge-changing weak interaction is transmitted through W^\pm bosons, then it does yield a dimensionless coupling constant ‘ g ’ for the interaction. But, to eliminate the bad high energy behavior, we still need something that *cancels* the problematic diagram in Fig. 1.4.

1.1.2.3 W^0 cures bad high energy behavior

What if another diagram contributes to $\nu\bar{\nu} \rightarrow W_L^+W_L^-$, such that it cancels the bad high energy behavior of Fig. 1.4? Considering the zero-charge on both sides of this process, what if we introduce W^0 - a neutral spin-1 particle? Then, in addition to Fig. 1.4, the diagram in Fig. 1.5 also contributes to $\nu\bar{\nu} \rightarrow W_L^+W_L^-$.

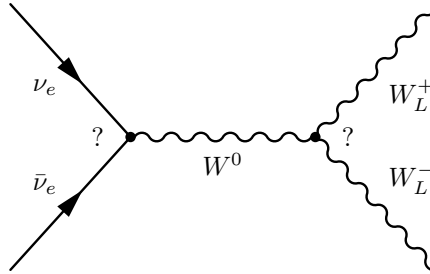
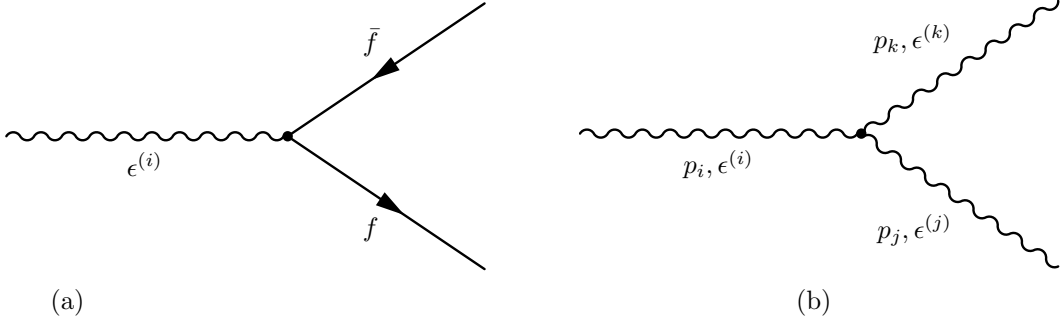


Figure 1.5: $\nu_e\bar{\nu}_e \rightarrow W_L^+W_L^-$ by exchanging the W^0 boson.

The bad high energy behavior of Fig. 1.4 is cancelled, if the couplings at the two vertices in Fig. 1.5 obey the symmetry of a Lie group [10]. Vertex in Fig. 1.6(a) is

Figure 1.6: EW ν_R model mirror fermion loop examples

given by

$$V_{(1)} = \imath g \bar{f}_\alpha \not{\epsilon}^{(i)} \frac{(1 - \gamma_5)}{2} T_{\alpha\beta}^{(i)} f_\beta, \quad (1.16)$$

where ‘ g ’ is the weak coupling in Eq.(1.9). $\not{\epsilon} = \gamma_\mu \epsilon^\mu$, where γ_μ are matrices given by [11]

$$\begin{aligned} \gamma^0 &= \begin{pmatrix} \mathbb{I} & 0 \\ 0 & \mathbb{I} \end{pmatrix}, & \gamma^1 &= \begin{pmatrix} 0 & \sigma_1 \\ -\sigma_1 & 0 \end{pmatrix}, \\ \gamma^2 &= \begin{pmatrix} 0 & \sigma_2 \\ -\sigma_2 & 0 \end{pmatrix}, & \gamma^3 &= \begin{pmatrix} 0 & \sigma_3 \\ -\sigma_3 & 0 \end{pmatrix}, \end{aligned} \quad (1.17)$$

where σ ’s are the Pauli matrices. $T_{\alpha\beta}^{(i)}$ are matrices and f ’s are fermion fields. Since there are three polarizations (thus, the superscript (i) takes three values), *there are three $T^{(i)}$ matrices*. Vertex $V_{(2)}$ in Fig. 1.6(b) is given by

$$\begin{aligned} V_{(2)} = & \imath g \left\{ f^{ij,k} [\epsilon^{(i)} \cdot \epsilon^{(j)}] [\epsilon^{(k)} \cdot (p_i - p_j)] + f^{jk,i} [\epsilon^{(j)} \cdot \epsilon^{(k)}] [\epsilon^{(i)} \cdot (p_j - p_k)] \right. \\ & \left. + f^{ki,j} [\epsilon^{(k)} \cdot \epsilon^{(i)}] [\epsilon^{(j)} \cdot (p_k - p_i)] \right\}. \end{aligned} \quad (1.18)$$

This assumes that $V_{(2)}$ contains the same coupling constant ‘ g ’ as $V_{(1)}$ so as to get the desired cancellation. The structure of $V_{(2)}$ is a result of the fact that W^\pm , W^0 are spin-1 *bosons*, and thus, $V_{(2)}$ must be symmetric under exchange of any two of the i , j , k indices. So far, $f^{ij,k}$, $f^{jk,i}$ and $f^{ki,j}$ are some constants which only satisfy $f^{ij,k} = -f^{ji,k}$, that is $f^{ij,k}$ are completely antisymmetric under exchange of two of its indices.

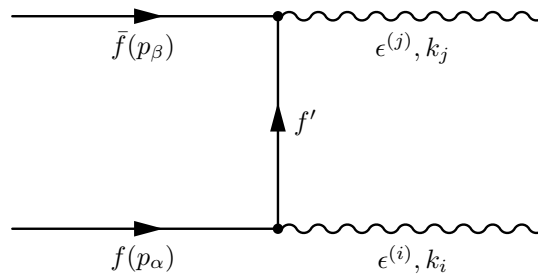


Figure 1.7: $\nu_e \bar{\nu}_e \rightarrow W_L W_L$ by exchanging an electron.

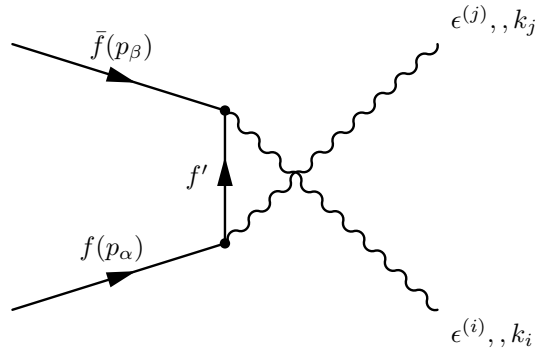


Figure 1.8: $\nu_e \bar{\nu}_e \rightarrow W_L W_L$ by exchanging an electron.

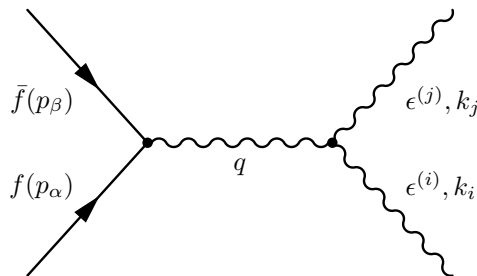


Figure 1.9: $\nu_e \bar{\nu}_e \rightarrow W_L W_L$ by exchanging the W^0 boson.

Using these vertices, we can write the amplitudes for the three diagrams that contribute to $f\bar{f} \rightarrow W_L^+ W_L^-$. These diagrams and their amplitudes are tabulated in Table 1.1. While writing these amplitudes we have ignored all the fermion masses, for simplicity.

Table 1.1: Vertices in the theory of weak interactions.

(a)	$\mathcal{M}_{(a)} = -ig^2 \bar{v}_\alpha \not{\epsilon}^{(i)} \frac{(\not{p}_\beta + \not{k}^{(j)})}{(\not{p}_\beta + \not{k}^{(j)})^2} \not{\epsilon}^{(j)} \times \frac{(1 - \gamma_5)}{2} [T_{\alpha\rho}^{(i)} T_{\rho\beta}^{(j)}] u_\beta$
(b)	$\mathcal{M}_{(b)} = -ig^2 \bar{v}_\alpha \not{\epsilon}^{(j)} \frac{(\not{p}_\alpha - \not{k}^{(j)})}{(\not{p}_\alpha - \not{k}^{(j)})^2} \not{\epsilon}^{(i)} \times \frac{(1 - \gamma_5)}{2} [T_{\alpha\beta}^{(j)} T_{\rho\beta}^{(i)}] u_\beta$
(c)	$\begin{aligned} \mathcal{M}_{(c)} = & -g^2 \bar{v}_\alpha \gamma^\lambda \frac{(1 - \gamma_5)}{2} T_{\alpha\beta}^{(k)} u_\beta \times \frac{1}{(q^2 - M_{W0}^2)} \left\{ f^{ij,k} \epsilon^{(i)} \cdot \epsilon^{(j)} (k^{(i)} - k^{(j)})_\lambda \right. \\ & \left. + f^{jk,i} \epsilon^{(i)} \cdot (-k^{(j)} + q) \epsilon_\lambda^{(j)} + f^{ki,j} \epsilon^{(j)} \cdot (-q - k^{(i)}) \epsilon_\lambda^{(i)} \right\} \end{aligned}$

Adding up all three diagrams, the total amplitude of the process $f\bar{f} \rightarrow W_L^+ W_L^-$ is given by

$$\mathcal{M}_{tot} = \mathcal{M}_a + \mathcal{M}_b + \mathcal{M}_c. \quad (1.19)$$

Remember that $k^{(\rho)} \cdot \epsilon^{(\rho)} = 0$ and as $k^{(j)} \rightarrow \infty$, $\epsilon_\lambda^{(i,j)} = k_\lambda^{(i,j)}/M_W + \mathcal{O}(M_W/k)$.

Therefore,

$$\begin{aligned} \mathcal{M}_{tot} = & - \frac{i}{M_W} g^2 \bar{v}_\alpha \not{\epsilon}^{(i)} \frac{(1 - \gamma_5)}{2} \left[T_{\alpha\rho}^{(i)} T_{\rho\beta}^{(j)} - T_{\alpha\rho}^{(j)} T_{\rho\beta}^{(i)} - i f^{ki,j} T_{\alpha\beta}^{(k)} \right] u_\beta \\ & + g^2 \frac{\epsilon^{(i)} \cdot k^{(j)}}{M_W (k^{(i)} \cdot k^{(j)})} \bar{v}_\alpha \not{k}^{(j)} \frac{(1 - \gamma_5)}{2} T_{\alpha\beta}^{(k)} u_\beta \left(-f^{jk,i} + f^{ij,k} \right) \end{aligned} \quad (1.20)$$

Since also $\epsilon_\lambda^{(i)} \rightarrow k_\lambda^{(i)}/M_W$ as $k_\lambda^{(i)} \rightarrow \infty$, the amplitude \mathcal{M}_{tot} increases with $k^{(j)}$.

The first term increases as $k^{(i)}$, whereas the second one increases as $k^{(j)}$. To cancel

this diagram i.e. for $\mathcal{M}_{tot} = 0$, both the terms in the equation above should cancel separately. A vanishing second term implies $f^{jk,i} = f^{ij,k}$. We already know that $f^{ij,k} = -f^{ji,k}$, by interchange symmetry of bosons in Eq. (1.18). Therefore, (dropping the comma in the superscript)

$$f^{ijk} = f^{jki} = f^{kij}, \quad (1.21)$$

and f^{ijk} is *completely antisymmetric* under exchange of any two indices. For the first term to vanish,

$$[T^i, T^j] = i f^{ijk} T^k, \quad (1.22)$$

i.e. the T^i matrices satisfy the commutator of a Lie algebra, of which they are the generators. f^{ijk} are the *structure constants* of the Lie algebra. Since there are 3 $T^{(i)}$ matrices, the Lie algebra obeyed here must be that of the $SU(2)$ group. Thus, $T^{(i)} = \tau^i/2$, where τ^i 's are the Pauli matrices given by

$$\tau_1 = \begin{pmatrix} 0 & 1 \\ 1 & 0 \end{pmatrix}, \quad \tau_2 = \begin{pmatrix} 0 & -i \\ i & 0 \end{pmatrix}, \quad \tau_3 = \begin{pmatrix} 1 & 0 \\ 0 & -1 \end{pmatrix} \quad (1.23)$$

and $f^{ijk} = \epsilon^{ijk}$ - the Levi-Civita symbol in three dimensions.

1.1.3 Conclusion of the section

We saw that the good high energy behavior of the weak interactions necessitates existence of W^\pm as well as W^0 . Their couplings obey the symmetry of the $SU(2)$ group. Also note that the three point interactions in Figs. 1.6(a) and 1.6(b) have a common coupling constant 'g'.

In other words, **the $SU(2)$ symmetry of the weak interactions emerges out**

of a *physical* requirement of the good high energy behavior of the theory.

It is denoted by $SU(2)_L$ symmetry, since the current \mathcal{J}_μ^{weak} has a ‘ $V - A$ ’ structure.

Thus, only the left-handed components of fermions couple to the spin-1 bosons W^\pm , W^0 . It is important to note that coupling only to the left-handed fermions is not an inherent property of W^\pm , W^0 bosons, but it emerges from the *observed* ‘ $V - A$ ’ structure of the weak currents. Theoretically, they can couple to the right-handed components of some other fermions, but more on this in Chapter 3 onwards.

In the next section we will discuss the concept of gauging a theory in the context of the weak interactions obeying $SU(2)$ symmetry.

1.2 ‘Gauging’ the $SU(2)$ symmetry

This section illustrates the necessity for and implications of gauging the theory of weak interactions that obeys the symmetry of $SU(2)$ group. Note that in Quantum Electrodynamics (QED), the $U(1)$ symmetry is also gauged. It is simpler to discuss the concept of gauging a $U(1)$ theory, but we will skip this step and directly explore the concept of gauging the theory of weak interactions.

Recall from the previous section that unitarity necessitates existence of spin-1 bosons W^\pm , W^0 , which can be thought of as the force carriers of the weak interaction. Under the $SU(2)$ symmetry they can be grouped into a vector $\vec{W}_\mu = (W^1, W^2, W^0)$, where the charged W^\pm are given by

$$W^\pm = \frac{W^1 \mp iW^2}{\sqrt{2}} \tag{1.24}$$

Fermion pairs - neutrino-electron or up-down quarks - also form doublets under the

$SU(2)_L$ symmetry:

$$\psi_L = \begin{pmatrix} \psi_{1L} \\ \psi_{2L} \end{pmatrix}. \quad (1.25)$$

1.2.1 Global vs. local $SU(2)$ symmetry

Ignoring the masses of the fermions for simplicity, let us check if the kinetic Lagrangian of the fermions $\bar{\psi}_L \gamma^\mu \partial_\mu \psi_L$ is invariant under a global $SU(2)_L$ phase transformation:

$$\psi_L \rightarrow e^{-i \vec{T} \cdot \vec{\alpha}} \psi_L, \quad (1.26)$$

where $\vec{T} = (T_1, T_2, T_3)$ is a vector formed by three 2×2 generators of the $SU(2)$ group. $\vec{\alpha} = (\alpha_1, \alpha_2, \alpha_3)$ is a vector that parametrizes the phase transformation. Therefore, under this *global* transformation,

$$\begin{aligned} \bar{\psi}_L \gamma^\mu \partial_\mu \psi_L &\rightarrow (\bar{\psi}_L e^{+i \vec{T} \cdot \vec{\alpha}}) \gamma^\mu \partial_\mu (e^{-i \vec{T} \cdot \vec{\alpha}} \psi_L) \\ &= \bar{\psi}_L e^{+i \vec{T} \cdot \vec{\alpha}} e^{-i \vec{T} \cdot \vec{\alpha}} \gamma^\mu \partial_\mu \psi_L. \end{aligned} \quad (1.27)$$

By global transformation we mean that the same phase transformation is applied to all the points in space-time. In other words, if an electron at a point in the space-time undergoes a phase transformation $\vec{\alpha}$, then all the electrons at all the other space-time points also undergo the same transformation!

In contrast, if the transformation is *local*, then the phase transformation $\vec{\alpha}(x)$ at a point (in space-time) x is independent of all other points:

$$\begin{aligned} \psi_L(x) &\rightarrow e^{-i \vec{T} \cdot \vec{\alpha}(x)} \psi_L(x) \\ &= U(\alpha(x)) \psi_L(x). \end{aligned} \quad (1.28)$$

Then, the kinetic term transforms as follows:

$$\begin{aligned} \bar{\psi}_L(x) \gamma^\mu \partial_\mu \psi_L(x) &\rightarrow \bar{\psi}_L(x) U^{-1}(\alpha(x)) \gamma^\mu \partial_\mu U(\alpha(x)) \psi_L(x) \\ &= \bar{\psi}_L(x) \gamma^\mu \partial_\mu \psi_L(x) + \bar{\psi}_L(x) \gamma^\mu [U^{-1}(\alpha(x)) \partial_\mu U(\alpha(x))] \psi_L(x), \end{aligned} \quad (1.29)$$

where, in general, $[U^{-1}(\alpha(x)) \partial_\mu U(\alpha(x))] \neq 1$. Therefore, the kinetic term of fermions is not invariant under a *local* $SU(2)$ symmetry, like it is under a *global* $SU(2)$ symmetry.

If we demand that we should be able to freely perform an independent $SU(2)$ phase transformation at each space-time point, then we need another term in the Lagrangian to cancel the non-invariant part $\bar{\psi}_L(x) \gamma^\mu [U^{-1}(\alpha(x)) \partial_\mu U(\alpha(x))] \psi_L(x)$.

1.2.2 The covariant derivative and non-invariant mass terms

Looking at the form of the $\vec{T} \cdot \vec{W}_\mu$ -term, if it transforms as

$$\begin{aligned} \vec{T} \cdot \vec{W}_\mu &\rightarrow \vec{T} \cdot \vec{W}'_\mu \\ &= U^{-1}(\alpha(x)) \vec{T} \cdot \vec{W}_\mu U(\alpha(x)) - \frac{i}{g} (\partial_\mu U(\alpha(x))) U^{-1}(\alpha(x)), \end{aligned} \quad (1.30)$$

then the term $-ig \bar{\psi}_L(x) \gamma^\mu \vec{T} \cdot \vec{W}_\mu \psi_L(x)$ in the Lagrangian transforms as follows:

$$\begin{aligned} &-ig \bar{\psi}_L(x) \gamma^\mu \vec{T} \cdot \vec{W}_\mu \psi_L(x) \\ &\rightarrow -ig \bar{\psi}_L(x) \gamma^\mu \vec{T} \cdot \vec{W}_\mu \psi_L(x) - \bar{\psi}_L(x) \gamma^\mu [U^{-1}(\alpha(x)) \partial_\mu U(\alpha(x))] \psi_L(x). \end{aligned} \quad (1.31)$$

Since the two terms above are invariant, when considered together, we can define the kinetic term of the fermions as

$$\bar{\psi}_L(x) \gamma^\mu (\partial_\mu - ig \vec{T} \cdot \vec{W}_\mu) \psi_L(x) \quad (1.32)$$

with the ‘‘covariant derivative’’ $D_\mu = \partial_\mu - ig \vec{T} \cdot \vec{W}_\mu$.

We need to check if the entire Lagrangian in the theory is also invariant with this prescription of how \vec{W}_μ transforms under a local $SU(2)$ transformation. The full Lagrangian is written as

$$\begin{aligned} \mathcal{L} &= \bar{\psi}_L(x) \gamma^\mu D_\mu \psi_L(x) - \frac{1}{4} G_{\mu\nu}^i G^{i\mu\nu} - \frac{1}{2} M_W^2 \vec{W}_\mu \cdot \vec{W}^\mu \\ &= \mathcal{L}_1 + \mathcal{L}_2 + \mathcal{L}_3. \end{aligned} \quad (1.33)$$

Here \mathcal{L}_1 is the covariant kinetic term of the fermions, \mathcal{L}_2 is the kinetic term of \vec{W}_μ and \mathcal{L}_3 is the mass term of \vec{W}_μ . In \mathcal{L}_2 , $G_{\mu\nu}^i \equiv \partial_\mu W_\nu^i - \partial_\nu W_\mu^i + g \epsilon^{ijk} W_\mu^j W_\nu^k$.

Consider

$$\begin{aligned} Tr[\vec{T} \cdot \vec{G}_{\mu\nu} \vec{T} \cdot \vec{G}^{\mu\nu}] &= Tr\left(T^i T^j\right) G_{\mu\nu}^i G^{i\mu\nu} \\ &= \frac{1}{2} G_{\mu\nu}^i G^{i\mu\nu}, \end{aligned} \quad (1.34)$$

where $Tr[\dots]$ denotes trace of a matrix. Hence, it can be easily checked that the prescription of transformation of \vec{W}_μ in Eq.(1.30) implies that under the local transformation

$$\vec{T} \cdot \vec{G}_{\mu\nu} \rightarrow \vec{T} \cdot \vec{G}'_{\mu\nu} = U(x) \vec{T} \cdot \vec{G}_{\mu\nu} U^{-1}(x). \quad (1.35)$$

This gives

$$\begin{aligned} Tr[\vec{T} \cdot \vec{G}_{\mu\nu} \vec{T} \cdot \vec{G}^{\mu\nu}] &\rightarrow Tr[U(x) \vec{T} \cdot \vec{G}_{\mu\nu} U^{-1}(x) U(x) \vec{T} \cdot \vec{G}^{\mu\nu} U^{-1}(x)] \\ &= Tr[\vec{T} \cdot \vec{G}_{\mu\nu} \vec{T} \cdot \vec{G}^{\mu\nu}], \end{aligned} \quad (1.36)$$

as $Tr[ABC] = Tr[CAB]$. Thus, \mathcal{L}_2 is invariant under a local $SU(2)$ transformation.

Now consider how the \mathcal{L}_3 term transforms:

$$- \frac{1}{2} M_W^2 \vec{W}_\mu \cdot \vec{W}^\mu. \quad (1.37)$$

Let us first see how \vec{W}_μ transforms under an *infinitesimal* local transformation i.e. $\vec{\alpha}(x)$ is small, implying $U(\alpha(x)) = \mathbb{I} - \imath \vec{T} \cdot \vec{\alpha}(x)$ and $U^{-1}(x) = \mathbb{I} + \imath \vec{T} \cdot \vec{\alpha}(x)$. Then, from Eq. (1.30),

$$\begin{aligned} \vec{T} \cdot \vec{W}'_\mu &= \vec{T} \cdot \vec{W}_\mu - \imath (\vec{T} \cdot \vec{\alpha}(x)) (\vec{T} \cdot \vec{W}_\mu) + \imath (\vec{T} \cdot \vec{W}_\mu) (\vec{T} \cdot \vec{\alpha}(x)) - \frac{1}{g} (\vec{T} \cdot \partial_\mu \vec{\alpha}(x)) \\ &= \vec{T} \cdot \vec{W}_\mu - \imath \alpha^j W_\mu^k [T^j, T^k] - \frac{\imath}{g} (\vec{T} \cdot \partial_\mu \vec{\alpha}(x)). \end{aligned} \quad (1.38)$$

Since $[T^j, T^k] = \imath \epsilon^{jkl} T^l$,

$$W_\mu^i \rightarrow W_\mu^{i'} = W_\mu^i + \epsilon^{ijk} \alpha^j W_\mu^k - \frac{1}{g} \partial_\mu \alpha^i(x). \quad (1.39)$$

This procedure of fixing how the spin-1 force carriers transform under a local symmetry transformation, so as to make the Lagrangian (with massless bosons and fermions) invariant under the transformation, is called “gauging”. The force carriers are called the “gauge bosons”. The global symmetry of the Lagrangian becomes a local symmetry through the process of gauging. Note that a global symmetry is a special case of a local symmetry, in which $\alpha(x) = \alpha$ is a constant.

From Eq. (1.39), we see that $W_\mu^{i'} \cdot W^{i'\mu} \neq W_\mu^i \cdot W^{i\mu}$ and therefore *the mass term of \vec{W}_μ is not invariant under a local $SU(2)$ transformation.* We cannot eliminate this term by making W^\pm , W^0 massless, since we need them to be massive so that at low energies the weak interaction reduces to Fermi's four-fermion interaction.

W^\pm , W^0 therefore acquire their masses through some other mechanism that we will discuss shortly.

But before that, let us consider the consequences of massive fermions in the context of a local $SU(2)$ symmetry. Because we have so far considered massless fermions, the Lagrangian in Eq. (1.33) does not include a mass term of fermions. A generic mass term of a fermion ψ is given as

$$m\bar{\psi}(x)\psi(x) = m\bar{\psi}_R\psi_L + m\bar{\psi}_L\psi_R, \quad (1.40)$$

where ψ_L and ψ_R are the left- and right-handed (helicity) components of the fermion ψ . Since the ' $(V + A)$ ' current is not observed in the weak interactions i.e. since ψ_R does not interact with W^\pm , W^0 , under a $SU(2)$ transformation (global or local), $\psi_R \rightarrow \psi_R$. Thus, Eq. (1.40) transforms as follows:

$$m(\bar{\psi}_R\psi_L + \bar{\psi}_L\psi_R) \rightarrow m(\bar{\psi}_R U(\alpha(x))\psi_L + \bar{\psi}_L U^{-1}(\alpha(x))\psi_R). \quad (1.41)$$

Thus, the fermion mass term is not invariant under a local $SU(2)$ transformation.

1.2.2.1 Conclusions of the section

We can draw the following conclusions from the discussion in this section:

- If we insist that we should have a freedom of performing a phase transformation independently at all space-time points, then we need to 'gauge' the theory.

While gauging we add a spin-1 boson(s) to the theory and fix how they transform under the phase transformation so as to make the Lagrangian (except the mass terms of the bosons and fermions) invariant under a local phase transformation.

- We can conclude that **so long as the local gauge symmetry is preserved, the gauge bosons and the fermions in the theory are massless.**
- In this process one also defines the “covariant derivative” in the kinetic terms of various fields (not only the fermions - we will see this shortly in the next section).
- For the theory of weak interactions, we gauge the $SU(2)$ symmetry. W^\pm , W^0 are the gauge bosons of this theory.
- After gauging, all the terms in the Lagrangian are invariant under local $SU(2)$ transformations, except the mass terms of the gauge bosons and the fermions. As long as the $SU(2)$ gauge symmetry is preserved, the gauge bosons W^\pm , W^0 and the fermions - leptons and quarks - are massless.
- We need a different mechanism to generate masses for all the particles.

We will discuss this mechanism - the Higgs mechanism - in the next section.

1.3 The Higgs mechanism and generating the masses of gauge bosons and fermions

Based on the previous section, the Lagrangian of the $SU(2)$ gauge theory of weak interactions is given by

$$\mathcal{L} = \bar{\psi}_L(x) \gamma^\mu D_\mu \psi_L(x) - \frac{1}{4} G_{\mu\nu}^i G^{i\mu\nu}. \quad (1.42)$$

Thus, in this theory the gauge bosons W^\pm , W^0 , as well as the fermions ψ are massless. We know for sure that in reality all these particles have masses. However, these are not two contradictory statements, the present state of the Universe is not described directly by the Lagrangian, but by “a ground state” of the Lagrangian (one of the ground states, if there are many).

So all we need is to make the gauge bosons as well as the fermions massive in the ground state of the Lagrangian, which describes the Universe we live in. This is achieved through the Higgs mechanism, which breaks the gauge symmetry spontaneously. Remember that *the local symmetry of the Lagrangian is still preserved, but the ground state solution of the ‘Lagrange’s equation of motion’ is not symmetric under the local symmetry.*

The Higgs mechanism was proposed in 1964 independently by Peter Higgs [12, 13]; by Robert Brout and Francois Englert [14] and by Gerald Guralnik, C. R. Hagen, and Tom Kibble [15]. The non-relativistic version of this mechanism for superconducting material was put forward by Philip Anderson in 1963 [16].

Peter Higgs proposed the mechanism for an $O(2)$ gauge theory. It is simpler to understand the mechanism using an $O(2)$ gauge theory, but we will directly discuss the mechanism for the $SU(2)$ gauge theory of weak interactions. For the electroweak theory in SM, the Higgs mechanism follows the same steps for a $SU(2) \times U(1)$ gauge theory.

In the first subsection we will list the steps to be followed in the Higgs mechanism for a generic gauge theory. The discussion of the mechanism for the $SU(2)$ gauge theory of weak interactions is given in the second subsection.

1.3.1 Steps in the Higgs mechanism

The steps followed in the Higgs mechanism are as follows:

- Introduce a scalar field that possesses the appropriate transformation properties under the gauge symmetry.
- Write the potential for the scalar field and find its ground state by minimizing the potential. If this ground state inherently does not obey the symmetry of the Lagrangian, then the evolution of the system to the ground state is said to “spontaneously” break the symmetry.
- Choose the proper vacuum alignment in the ground state so that one of the degrees of freedom of the scalar field acquires a mass, while the other d.o.f.’s are massless.
- The massive d.o.f. appears as a physical particle, called the “Higgs boson”. The massless d.o.f.’s are called the “Nambu-Goldstone bosons” (N-G bosons).
- The N-G bosons appear as massless physical particles if the spontaneously broken symmetry is a global symmetry. If a local symmetry is spontaneously broken then the N-G bosons are *absorbed* by the longitudinally polarized components of the gauge bosons. This process of the spontaneous breaking of a local symmetry is called the Higgs mechanism.

1.3.2 The Higgs mechanism for the $SU(2)$ gauge theory

To break the $SU(2)_L$ gauge symmetry of weak interactions, we add 4 scalar degrees of freedom, which form a doublet under $SU(2)_L$:

$$\Phi = \begin{pmatrix} \phi_1 \\ \phi_2 \end{pmatrix}. \quad (1.43)$$

Here ϕ_1 and ϕ_2 are complex numbers, thus, both having 2 degrees of freedom each.

The scalar Lagrangian is given by

$$\mathcal{L}_S = (D_\mu \Phi)^\dagger (D^\mu \Phi) - V(\Phi), \quad (1.44)$$

where $V(\Phi)$ is the scalar potential, given by

$$V(\Phi) = -\mu^2 (\Phi^\dagger \Phi) + \lambda (\Phi^\dagger \Phi)^2. \quad (1.45)$$

After minimizing this potential we see that the ground state, which is asymmetrical under a local $SU(2)_L$ transformation can be obtained only if $\mu^2 > 0$ and λ is real. In this case the the ground state is given by

$$\langle \Phi^\dagger \Phi \rangle = \frac{v^2}{2} \quad \text{where} \quad v^2 = \frac{\mu^2}{\lambda} \quad (1.46)$$

This defines a 3D circle formed by all the ground states in the 4D space formed by the scalar d.o.f.'s $Re[\phi_1]$, $Re[\phi_2]$, $Im[\phi_1]$, $Im[\phi_2]$. One of these ground states represents the state, in which we obtain 1 massive and 3 massless particles (not all physical particles).

We choose such a vacuum alignment:

$$\langle \Phi \rangle = \frac{1}{\sqrt{2}} \begin{pmatrix} 0 \\ v \end{pmatrix} \quad (1.47)$$

Here v is called the vacuum expectation value (VEV) of the $Re[\phi_2]$.

Since only those fields can appear as physical particles which have 0 VEV, to clearly see the appearance of the physical particles, we choose a particular vacuum and a particular gauge - ‘‘unitary gauge’’:

$$\Phi(x) = Exp\left(\imath \vec{\tau} \cdot \frac{\vec{\xi}(x)}{v}\right) \begin{pmatrix} 0 \\ \frac{v + \eta(x)}{\sqrt{2}} \end{pmatrix}, \quad (1.48)$$

with $\langle \eta(x) \rangle = 0$.

Particular vacuum:

$$\langle \xi(x) \rangle = 0. \quad (1.49)$$

$Exp\left(\imath \vec{\tau} \cdot \frac{\vec{\xi}(x)}{v}\right)$ parametrizes rotations along the 3D circle formed by all the ground states, defined by Eq. (1.47). $Exp\left(\imath \vec{\tau} \cdot \frac{\vec{\xi}(x)}{v}\right)$ is like the $U(\vec{\alpha}(x))$ in the previous section. We are free to choose x -dependent $\vec{\xi}(x)$ because of the local nature of the symmetry of the Lagrangian. Consequently, we can do such rotations while still being in a ground state.

Eventually $\vec{\xi}(x)$ gives rise to 3 N-G bosons and $\eta(x)$ appears as the Higgs boson.

Denoting $Exp\left(\imath \vec{\tau} \cdot \frac{\vec{\xi}(x)}{v}\right)$ by $U(\vec{\xi}(x))$, Eq. (1.30) gives

$$\frac{\vec{\tau}}{2} \cdot \vec{W}'_\mu = U^{-1}(\vec{\xi}(x)) \frac{\vec{\tau}}{2} \cdot \vec{W}_\mu U(\vec{\xi}(x)) - \frac{\imath}{g} (\partial_\mu U(\vec{\xi}(x))) U^{-1}(\vec{\xi}(x)). \quad (1.50)$$

The second term here absorbs the N-G bosons into the gauge bosons. Note that if

the symmetry is global then this term vanishes and hence, the N-G bosons cannot be absorbed in the gauge bosons. With a local symmetry, the covariant derivative becomes $D'_\mu = \left(\partial_\mu - ig \frac{\vec{\tau}}{2} \cdot \vec{W}'_\mu \right)$, and in the kinetic term of the gauge bosons,

$$G_{\mu\nu}^i \rightarrow G_{\mu\nu}^{i'} = \partial_\mu W_\nu^{i'} - \partial_\nu W_\mu^{i'} + g \epsilon^{ijk} W_\mu^{j'} W_\nu^{k'}. \quad (1.51)$$

Hence, in the chosen ground state, the Lagrangian of the scalars and the gauge bosons becomes (we will talk about fermions shortly).

$$\mathcal{L}_{ground} = (D'_\mu \Phi')^\dagger (D^{\mu'} \Phi') + \left(\frac{\mu^2}{2} (v + \eta(x))^2 - \frac{\lambda}{4} (v + \eta(x))^4 \right) - \frac{1}{4} G_{\mu\nu}^{i'} G^{i',\mu\nu} \quad (1.52)$$

When we expand the first term, we see a mass term for the gauge bosons \vec{W}'_μ :

$$\frac{g^2}{8} \begin{pmatrix} 0 & v \end{pmatrix} \begin{pmatrix} \frac{\vec{\tau}}{2} \cdot \vec{W}'_\mu & \frac{\vec{\tau}}{2} \cdot \vec{W}'^{\mu'} \end{pmatrix} \begin{pmatrix} 0 \\ v \end{pmatrix} = \frac{1}{2} \left(\frac{gv}{2} \right)^2 \vec{W}'_\mu \cdot \vec{W}'^{\mu'}. \quad (1.53)$$

Thus, the gauge bosons W^\pm , W^0 acquire a mass of $M_W = gv / 2$. Notice that this term is invariant under a *global* $SU(2)$ transformation.

In the second term of Eq. (1.52), using $v^2 = (\mu^2/\lambda)$, we find a term

$$\frac{1}{2} (2 \mu^2) \eta^2(x), \quad (1.54)$$

which is the mass term of a physical massive scalar η having mass $m_\eta = \sqrt{2} \mu$ ¹.

This process, through which the gauge symmetry is spontaneously broken, the gauge bosons acquire mass and a massive physical scalar appears, is called the Higgs

¹The second term in Eq. (1.52) also contains a constant term $\sim 1/4 \mu^2/\lambda$. This term is said to contribute to the ‘‘Cosmological constant’’. Unless one is trying to explore the gravitational force or cosmological evolution of the Universe, this term can be ignored as can be any constant shift in the Lagrangian

mechanism. Note that the process of generating fermion masses is not counted in this mechanism. This process involves the Yukawa couplings of the fermions with the scalar, as we will see shortly.

1.3.3 Generating masses of the fermions

The $SU(2)_L$ gauge theory of weak interactions also contains fermions. Their left-handed helicity components form doublets $\psi^T = (\psi_{1L}, \psi_{2L})$ under $SU(2)_L$, while the right-handed parts of the charged fermions are singlets ψ_{1R}, ψ_{2R} . The right-handed parts of neutral fermions - neutrinos - are absent in this theory (more on this later). Even after the Higgs mechanism these fermions are massless. They can acquire masses if they have $SU(2)_L$ gauge invariant interactions with the scalar fields.

Yukawa interaction, which is a tree-level interaction, is $SU(2)_L$ gauge invariant. To give masses to both ψ_1 and ψ_2 , it can be written as:

$$\mathcal{L}_Y = g_{Y1} \bar{\psi}_L \Phi \psi_{2R} + g_{Y2} \bar{\psi}_L \tilde{\Phi} \psi_{1R} + h.c.. \quad (1.55)$$

where $\tilde{\Phi} = i\tau_2 \Phi^*$. When the $SU(2)_L$ gauge symmetry is spontaneously broken through the Higgs mechanism, the \mathcal{L}_Y is written in the chosen ground state as:

$$\begin{aligned} \mathcal{L}_{Y,ground} &= g_{Y1} \begin{pmatrix} \bar{\psi}_{1L} & \bar{\psi}_{2L} \end{pmatrix} \begin{pmatrix} 0 \\ v \\ \sqrt{2} \end{pmatrix} \psi_{2R} \\ &\quad + g_{Y2} \begin{pmatrix} \bar{\psi}_{1L} & \bar{\psi}_{2L} \end{pmatrix} \begin{pmatrix} v \\ \sqrt{2} \\ 0 \end{pmatrix} \psi_{1R} + h.c. \\ &= g_{Y1} \frac{v}{\sqrt{2}} \bar{\psi}_{2L} \psi_{2R} + g_{Y2} \frac{v}{\sqrt{2}} \bar{\psi}_{1L} \psi_{1R} + h.c. \end{aligned} \quad (1.56)$$

Thus, ψ_1 acquires a mass of $(g_{Y1} v/\sqrt{2})$ and ψ_2 acquires a mass of $(g_{Y2} v/\sqrt{2})$.

1.3.4 Summary of this section

- In this section we have discussed the Higgs mechanism and its salient features by considering the $SU(2)_L$ gauge theory of weak interactions as an example.
- By adding a scalar to a gauge theory the masses of gauge bosons can be generated by breaking the gauge symmetry spontaneously through the Higgs mechanism.
- A massive physical scalar particle, popularly known as the Higgs boson, is a byproduct of the Higgs mechanism.
- After such spontaneous symmetry breaking a residual global symmetry remains.
- The masses of fermions in the theory are generated through their Yukawa interactions with the scalar field, when the gauge symmetry is spontaneously broken.

After all this discussion we are ready to talk about the Standard Model, which is the focus of the next section.

1.4 The Standard Model of particle physics

As discussed earlier, the Standard Model is a $SU(3)_C \times SU(2)_L \times U(1)_Y$ gauge theory. The $SU(3)_C$ part of the theory explains the strong-nuclear interactions through the Quantum Chromodynamics (QCD), while the $SU(2)_L \times U(1)_Y$ gauge theory accounts for the weak-nuclear and the electromagnetic interactions with the help of the Electroweak (EW) theory.

Since the strong interactions are not within the scope of this dissertation, we will only discuss the EW part of the SM, which is a $SU(2)_L \times U(1)_Y$ gauge theory.

In the first part of this section we will argue in favor of a $U(1)_Y$ gauge symmetry, under which the leptons transform in a particular way. In the second part, we will gauge the theory with only the leptons and the gauge bosons under consideration. In the third part we will break the EW gauge symmetry spontaneously and derive the mass eigenstates of the gauge bosons as well as the Higgs bosons and we will also briefly depict the necessity for the existence of quarks, and how the leptons and quarks acquire their masses. The final part of this section will list the features and limitations of the SM.

1.4.1 Existence of a $U(1)_Y$ gauge theory

Consider the electron e and the neutrino ν_L , left-handed components of which form a lepton doublet under the $SU(2)_L$ gauge symmetry:

$$l_L = \begin{pmatrix} \nu_L \\ e_L \end{pmatrix}. \quad (1.57)$$

e_R is a singlet under $SU(2)_L$. The ν_L and e_L are eigenstates of the $T_{3L} = \tau_3/2$ generator of $SU(2)_L$, with eigenvalues $+1/2$ and $-1/2$ respectively, and $T_{3L}(e_R) = 0$.

In reality there are 3 “generations” of leptons, each having a doublet of the left-handed components and a charged singlet:

$$l_{eL} = \begin{pmatrix} \nu_{eL} \\ e_L \end{pmatrix}, \quad e_R; \quad l_{\mu L} = \begin{pmatrix} \nu_{\mu L} \\ \mu_L \end{pmatrix}, \quad \mu_R; \quad l_{\tau L} = \begin{pmatrix} \nu_{\tau L} \\ \tau_L \end{pmatrix}, \quad \tau_R. \quad (1.58)$$

Here e , μ , τ are electron, muon, and tau-lepton (or tau-on), respectively. ν_e , ν_μ , ν_τ are the neutrinos associated with them, respectively. While writing the Lagrangian and equations we will consider only one representative generation, formed by electron

and neutrino ν_{eL} . Remember that a sum over the 3 lepton generations is implicit.

If the electric charges $Q(\nu_L)$ and $Q(e_L)$ are considered to be the eigenvalues of a generator of the gauge symmetry of the theory, then $SU(2)_L$ will be a part of the gauge symmetry group. T_{3L} will also then be a part of the generator Q of the symmetry. Thus, we can define

$$Q = T_{3L} + \frac{Y}{2}. \quad (1.59)$$

Here $Y/2$ is the generator of remaining part of the gauge group, such that $Y/2 = -1/2$ for both ν_L and e_L . Also, $Y/2(e_R) = -1$ so that $Q(e_R) = -1$. $Y/2$ is called the ‘‘Hypercharge’’².

Such a generator can be associated with a $U(1)_Y$ symmetry group, under which the lepton components transform as

$$l_L \rightarrow \text{Exp}\left(-i\frac{Y}{2}\alpha_Y(x)\right) l_L = \text{Exp}\left(+i\frac{1}{2}\alpha_Y(x)\right) l_L, \quad (1.60)$$

and

$$e_R \rightarrow \text{Exp}\left(-i\frac{Y}{2}\alpha_Y(x)\right) e_R = \text{Exp}(+i\alpha_Y(x)) e_R. \quad (1.61)$$

Thus, e_R is a singlet under the $SU(2)_L$ gauge symmetry but not under the $U(1)_Y$ symmetry. If the right-handed component of the neutrino ν_R exists, then in the minimal extension to SM

$$T_{3L}(\nu_R) = 0 \quad \text{and} \quad \frac{Y}{2}(\nu_R) = 0. \quad (1.62)$$

Thus, ν_R is a singlet under the entire $SU(2)_L \times U(1)_Y$ symmetry. *In a minimal model*

²Sometimes the Y instead of $Y/2$ is referred to as the hypercharge. This is just a matter of convention. In this dissertation we will stick to the convention of calling $Y/2$ as the hypercharge.

the existence of ν_R is not necessary!

1.4.2 Gauging the $SU(2)_L \times U(1)_Y$ symmetry

If we are to gauge the entire $SU(2)_L \times U(1)_Y$ symmetry, then we have to add a gauge boson B_μ that is associated the $U(1)_Y$ part of the gauge symmetry. Then the covariant derivative is defined as

$$D_\mu = \partial_\mu - ig \vec{T} \cdot \vec{W}_\mu - ig' \frac{Y}{2} B_\mu, \quad (1.63)$$

implying

$$D_\mu l_L = \left(\partial_\mu - ig \frac{\vec{\tau}}{2} \cdot \vec{W}_\mu + ig' \frac{1}{2} B_\mu \right) l_L \quad (1.64)$$

and

$$D_\mu e_R = (\partial_\mu + ig' B_\mu) e_R. \quad (1.65)$$

Here g' is the gauge coupling associated with B_μ .

The Lagrangian for massless leptons can therefore be written as:

$$\mathcal{L}_{lepton} = \bar{l}_L \gamma^\mu D_\mu l_L + \bar{e}_R \gamma^\mu D_\mu e_R. \quad (1.66)$$

The kinetic terms of the gauge bosons are given by

$$\mathcal{L}_{gauge} = -\frac{1}{4} G_{\mu\nu}^i G^{i\mu\nu} - \frac{1}{4} B_{\mu\nu} B^{\mu\nu}, \quad (1.67)$$

where

$$G_{\mu\nu}^i \equiv \partial_\mu W_\nu^i - \partial_\nu W_\mu^i + g \epsilon^{ijk} W_\mu^j W_\nu^k, \quad (1.68)$$

and

$$B_{\mu\nu}^i = \partial_\mu B_\nu^i - \partial_\nu B_\mu^i. \quad (1.69)$$

1.4.3 Breaking the $SU(2)_L \times U(1)_Y$ gauge symmetry spontaneously

In this subsection we will discuss the spontaneous breaking of the $SU(2)_L \times U(1)_Y$ gauge symmetry. First, we will generate the masses of the gauge bosons through the Higgs mechanism. In the second part we will talk about how the masses of leptons and quarks are generated.

1.4.3.1 The Higgs mechanism in the $SU(2)_L \times U(1)_Y$ gauge theory

Remember that the formulation of the $SU(2)_L \times U(1)_Y$ gauge theory is an attempt to unify the weak force and the electromagnetic force. Thus, in the ground state of this theory we must have a massless gauge boson - photon A_μ . In addition we must also have 2 massive charged gauge bosons W_μ^\pm and a neutral massive gauge boson, which we will call Z_μ for now.

We know from our discussion in the previous section that the $SU(2)_L$ gauge theory alone needs 4 scalar degrees of freedom, to generate masses for its 3 gauge bosons. Since also for the $SU(2)_L \times U(1)_Y$ gauge theory we require only 3 massive gauge bosons, it appears that 4 scalar d.o.f.'s could be just sufficient. Let us check this.

We define a scalar doublet:

$$\Phi = \begin{pmatrix} \phi^+ \\ \phi^0 \end{pmatrix}, \quad (1.70)$$

having the hypercharge $Y/2 = 1/2$. ϕ^+ is a positively charged scalar field, having 2

real d.o.f.'s.

Hence,

$$(D_\mu \Phi) = \left(\partial_\mu - ig \vec{T} \cdot \vec{W}_\mu - ig' \frac{Y}{2} B_\mu \right) \Phi. \quad (1.71)$$

The scalar potential is given by

$$V(\Phi) = -\mu^2 (\Phi^\dagger \Phi) + \lambda (\Phi^\dagger \Phi)^2. \quad (1.72)$$

The VEV of Φ is given by

$$\langle \Phi \rangle = \begin{pmatrix} 0 \\ v \\ \frac{v}{2} \end{pmatrix}, \quad \text{where} \quad v = \frac{\mu^2}{\lambda}. \quad (1.73)$$

To see the mass spectrum of the gauge bosons, we choose the “unitary gauge” as before:

$$\Phi(x) = \text{Exp} \left(i \vec{\tau} \cdot \frac{\vec{\xi}(x)}{v} \right) \begin{pmatrix} 0 \\ v + \eta(x) \\ \frac{v}{\sqrt{2}} \end{pmatrix}, \quad (1.74)$$

with $\langle \eta(x) \rangle = 0$ with the vacuum alignment $\langle \xi(x) \rangle = 0$.

In this gauge i.e. under this $SU(2)_L$ transformation (as in the last section):

$$\frac{\vec{\tau}}{2} \cdot \vec{W}'_\mu = U^{-1}(\vec{\xi}(x)) \frac{\vec{\tau}}{2} \cdot \vec{W}_\mu U(\vec{\xi}(x)) - \frac{i}{g} (\partial_\mu U(\vec{\xi}(x))) U^{-1}(\vec{\xi}(x)). \quad (1.75)$$

This time we also have

$$B'_\mu = B_\mu \quad (1.76)$$

Then $(D'_\mu \Phi')^\dagger (D^{\mu'} \Phi')$ contains

$$\frac{g'^2}{8} \begin{pmatrix} 0 & v \end{pmatrix} (B'_\mu B^{\mu'}) \begin{pmatrix} 0 \\ v \end{pmatrix} = \frac{1}{2} \left(\frac{g'v}{2} \right)^2 B'_\mu B^{\mu'}, \quad (1.77)$$

in addition to $\left(\frac{1}{2} \left(\frac{gv}{2} \right)^2 \vec{W}'_\mu \cdot \vec{W}'^{\mu'} \right)$ in Eq. (1.53).

Additionally, $(D'_\mu \Phi')^\dagger (D^{\mu'} \Phi')$ also contains cross terms between W_μ^3 and B_μ :

$$\begin{aligned} \frac{g g'}{2} \begin{pmatrix} 0 & v \end{pmatrix} \left(\frac{\vec{\tau}}{2} \cdot \vec{W}'_\mu \right) B'_\mu \begin{pmatrix} 0 \\ v \end{pmatrix} &= \frac{g g'}{2} \left(-\frac{1}{2} v^2 \right) W_\mu^{3'} B'^\mu \\ &= \frac{1}{2} \left(-\frac{g g' v^2}{2} \right) W_\mu^{3'} B'^\mu \end{aligned} \quad (1.78)$$

Thus, mass terms involving $W_\mu^{3'}$ and B'^μ can be put together into

$$\frac{v^2}{4} \begin{pmatrix} W_\mu^3 & B_\mu \end{pmatrix} \begin{pmatrix} g^2 & -g g' \\ -g g' & g'^2 \end{pmatrix} \begin{pmatrix} W_\mu^3 \\ B_\mu \end{pmatrix}. \quad (1.79)$$

Notice that determinant of the 2×2 matrix above is 0, which implies that one of its eigenvalue is 0, as required for the massless photon.

Diagonalizing this matrix we get the mass eigenstates Z_μ and A_μ of the neutral gauge bosons W_μ^3 and B_μ , such that

$$\begin{pmatrix} Z_\mu \\ A_\mu \end{pmatrix} = \begin{pmatrix} \cos \theta_W & -\sin \theta_W \\ \sin \theta_W & \cos \theta_W \end{pmatrix} \begin{pmatrix} W_\mu^3 \\ B_\mu \end{pmatrix}, \quad (1.80)$$

where

$$\cos \theta_W = \frac{g}{\sqrt{g^2 + g'^2}}, \quad \text{and} \quad \sin \theta_W = \frac{g'}{\sqrt{g^2 + g'^2}}, \quad (1.81)$$

and θ_W is called the “weak mixing angle”.

Thus, now we have 4 gauge bosons of the $SU(2)_L \times U(1)_Y$ gauge theory: 2 charged gauge bosons

$$W^\pm = \frac{W^1 \mp iW^2}{\sqrt{2}} \quad (1.82)$$

having a mass $M_W = g v / 2$ and 2 neutral gauge bosons given by Eq. (1.80) with Z_μ having a mass $M_Z = \sqrt{g^2 + g'^2} v / 2$ and massless photon A_μ . As a result,

$$\frac{M_W}{M_Z} = \frac{g}{\sqrt{g^2 + g'^2}} = \cos \theta_W, \quad (1.83)$$

which is a **prediction of the Standard Model**.

The covariant derivative can be written as

$$D_\mu = \left(\partial_\mu - i g \vec{T} \cdot \vec{W}_\mu - i g' \frac{Y}{2} B_\mu \right) \quad (1.84)$$

Consider the part of the covariant derivative that involves neutral gauge bosons. By inverting Eq. (1.80), we get

$$\begin{aligned} - i g \vec{T} \cdot \vec{W}_\mu - i g' \frac{Y}{2} B_\mu &= - i \left[g \cos \theta_W T_{3L} - g' \sin \theta_W \frac{Y}{2} \right] Z_\mu \\ &\quad - i \left[g \sin \theta_W T_{3L} + g' \cos \theta_W \frac{Y}{2} \right] A_\mu, \end{aligned} \quad (1.85)$$

Therefore, the fermion coupling to photon are given by

$$- i g \sin \theta_W Q \bar{\psi}_L^i \gamma^\mu A_\mu \psi_L, \quad (1.86)$$

which is known from QED to be $-i g e Q \bar{\psi}_L^i \gamma^\mu A_\mu \psi_L$. This gives the second

prediction of the SM:

$$e = g \sin \theta_W . \quad (1.87)$$

Similarly the interaction with W^\pm is given by

$$\frac{g}{\sqrt{2}} (J_\mu^+ W^{+\mu} + J_\mu^- W^{-\mu}) , \quad (1.88)$$

where $J_\mu^+ = 1/2 \bar{\nu} \gamma_\mu (1 - \gamma_5) e$ and $J_\mu^- = 1/2 \bar{e} \gamma_\mu (1 - \gamma_5) \nu$. As a result, the amplitude of the process $e^- \nu_\mu \rightarrow \mu^- \nu_e$ is

$$\sim g^2/2 J_\mu^+ \frac{1}{q^2 - M_W^2} J^{-\mu} \quad (1.89)$$

which reduces to Fermi's four-fermion interaction in the limit $q^2 \ll M_W^2$ (refer to section 1.1.1). We thus recover Eq. (1.10):

$$G_F = \frac{\sqrt{2}}{8} \frac{g^2}{M_W^2} , \quad (1.90)$$

which is also a **prediction of the SM**.

From Eqs. (1.87) and (1.90) the mass of W^\pm was also predicted to be

$$M_W = 2^{-1/4} \frac{(\pi \alpha_{EM})^{1/2}}{\sin \theta_W} G_F^{-1/2} . \quad (1.91)$$

The charge of electron e , the electromagnetic coupling constant $\alpha_{EM} = e^2/4\pi$ and the Fermi's constant G_F were measured to high accuracy by the time SM was put forward. The value of $\sin \theta_W$ was extracted using various low-energy experiments (refer to section 10.3 of [6]). Hence, the masses M_W and M_Z are also **predicted by SM**.

1.4.3.2 Generating masses of leptons and quarks

As seen in the previous section the masses of fermions are generated through Yukawa interactions of fermions and the scalar, when the gauge symmetry is spontaneously broken. In SM, the scalar Φ , l_L and e_R can form $SU(2)_L \times U(1)_Y$ gauge invariant term, similar to section 1.3.3:

$$\mathcal{L}_{Lepton-Yuk} = g_e \bar{l}_L \Phi e_R + h.c., \quad (1.92)$$

which after the spontaneous breaking of the symmetry becomes $g_e \frac{v}{\sqrt{2}} \bar{e}_L e_R + h.c..$ Thus, the mass of electron is given by $m_e = g_e v / \sqrt{2}$, where v can be measured, but g_e cannot be. Hence, the mass of electron cannot be predicted by SM. Similarly, the mass of muon m_μ and of tau m_τ are also not predicted by SM.

Gauge invariance also allows terms of the form $\bar{l}_{eL} \Phi \mu_R$, etc. We will discuss their implications in the next chapter.

In addition to 3 generations of leptons, it is also necessary for 3 generations of quarks to exist, to cancel the gauge anomalies [10] in the SM. Each quark must also occur in three colors. We thus have six quarks: up (u), down (d), charm (c), strange (s), top (t), bottom (b). Their components form doublets and singlets as follows:

$$q_{1L} = \begin{pmatrix} u_L \\ d_L \end{pmatrix}, \quad u_R, \quad d_R; \quad q_{2L} = \begin{pmatrix} c_L \\ s_L \end{pmatrix}, \quad c_R, \quad s_R; \quad q_{3L} = \begin{pmatrix} t_L \\ b_L \end{pmatrix}, \quad t_R, \quad b_R; \quad (1.93)$$

with $Y/2(q_L) = 1/6$, $Y/2(u_R) = 2/3$, $Y/2(d_R) = -1/3$. The electric charge of u , c , t is $\frac{2}{3}e$ and that of d , s , b is $-\frac{1}{3}e$.

Their mass terms arise from the Lagrangian

$$\mathcal{L}_{quark-Yuk} = g_d \bar{q}_{1L} \Phi d_R + g_u \bar{q}_{1L} \tilde{\Phi} u_R + h.c.. \quad (1.94)$$

Thus, after the spontaneous symmetry breaking the up-quark and down-quark attain masses of $(g_u v / \sqrt{2})$ and $(g_d v / \sqrt{2})$, respectively. Masses of the other 2 quark generations arise similarly through the Yukawa interactions with Φ . Note that the numerical values of none of these masses can be predicted by SM, since the Yukawa couplings g_u, g_d, \dots are free parameters.

The $SU(2)_L \times U(1)_Y$ gauge invariance also allows terms such as $g_{ds} q_{1L} \Phi s_R$, $g_{uc} q_{1L} \tilde{\Phi} c_R$, etc. Thus, the mass terms of quarks can be grouped as:

$$\bar{\psi}^u \mathcal{M}_U \psi^u = \frac{v}{\sqrt{2}} \times \bar{\psi}^u \begin{pmatrix} g_{uu} & g_{uc} & g_{ut} \\ g_{cu} & g_{cc} & g_{ct} \\ g_{tu} & g_{tc} & g_{tt} \end{pmatrix} \psi^u, \quad (1.95)$$

and

$$\bar{\psi}^d \mathcal{M}_D \psi^d = \frac{v}{\sqrt{2}} \times \bar{\psi}^d \begin{pmatrix} g_{dd} & g_{ds} & g_{db} \\ g_{sd} & g_{ss} & g_{sb} \\ g_{bd} & g_{bs} & g_{bb} \end{pmatrix} \psi^d, \quad (1.96)$$

where $\psi^u = \begin{pmatrix} u & c & t \end{pmatrix}^T$ and $\psi^d = \begin{pmatrix} d & s & b \end{pmatrix}^T$. The mass matrices \mathcal{M}_U and \mathcal{M}_D are, in general, complex and non-hermitian. These matrices can be diagonalized by two unitary matrices each, as follows:

$$U_{L,u}^\dagger \mathcal{M}_U U_{R,u} = \mathcal{M}_{U,diag} \quad (1.97)$$

$$U_{L,d}^\dagger \mathcal{M}_D U_{R,d} = \mathcal{M}_{D,diag}. \quad (1.98)$$

Using this notation, we can write the charged current of quarks that couples to the W^+ boson as

$$\bar{\psi}_L^u U_{L,u}^\dagger \gamma^\mu U_{L,d} \psi_L^{d'} = \bar{\psi}_L^u V_{CKM} \gamma^\mu \psi_L^{d'}, \quad (1.99)$$

where $\psi_L^u = \begin{pmatrix} u_L \\ c_L \\ t_L \end{pmatrix}^T$, $\psi_L^d = \begin{pmatrix} d_L \\ s_L \\ b_L \end{pmatrix}^T$, $\psi_L^u = U_{L,u}$, $\psi_L^d = U_{L,d}$. $V_{CKM} = U_{L,u}^\dagger \cdot U_{L,d}$ is called the Cabibbo-Kobayashi-Masakawa (CKM) matrix [6], which is a unitary matrix. Its components are measure of different flavor-changing interactions in the quark sector.

We will not go into details of the CKM-matrix. In the next chapter we will discuss the details of an analogous matrix defined for the lepton sector.

1.5 Features and Limitations of the Standard Model

Before discussing any physics beyond the Standard Model, we will briefly review the features and the limitations of the SM in this section. First let us summarize the particle content of SM.

Three generations
of matter (fermions)

	I	II	III		
mass →	2.4 MeV/c ²	1.27 GeV/c ²	171.2 GeV/c ²	0	? GeV/c ²
charge →	2/3	2/3	2/3	0	0
spin →	1/2	1/2	1/2	1	0
name →	u up	c charm	t top	γ photon	H Higgs boson
	4.8 MeV/c ²	104 MeV/c ²	4.2 GeV/c ²	0	
	-1/3	-1/3	-1/3	0	
	1/2	1/2	1/2	1	
Quarks	d down	s strange	b bottom	g gluon	
	<2.2 eV/c ²	<0.17 MeV/c ²	<15.5 MeV/c ²	91.2 GeV/c ²	
	0	0	0	0	
	1/2	1/2	1/2	1	
	ν_e electron neutrino	ν_μ muon neutrino	ν_τ tau neutrino	Z⁰ Z boson	
	0.511 MeV/c ²	105.7 MeV/c ²	1.777 GeV/c ²	80.4 GeV/c ²	
	-1	-1	-1	±1	
	1/2	1/2	1/2	1	
Leptons	e electron	μ muon	τ tau	W[±] W boson	Gauge bosons

Figure 1.10: The Standard Model particle content. Image source: Wikipedia

Notice that we show an image in which there is still a question mark for the mass of the SM Higgs boson. It is because, as we will discuss in detail in Chapter 5, only a scalar having a mass of 125 GeV has been discovered at the Large Hadron Collider, but it is too early to conclude that it is the SM Higgs boson!

Features of the Standard Model:

- SM can theoretically account for 3 of the 4 fundamental forces in the Nature - electromagnetic, weak nuclear and strong nuclear forces.
- SM describes the 3 forces with the help of a gauge theory obeying $SU(3)_C \times SU(2)_L \times U(1)_Y$ local symmetry. Accounting for the 3 forces with these small

groups is a remarkable theoretical success.

- SM is a “renormalizable” theory, meaning that all the infinities in this model can be cancelled to all orders in the perturbation theory [10].
- The model has been extremely successful in explaining various precision phenomena, predicting existence of the W^\pm and Z^0 bosons along with their masses, predicting existence of a CP-even Higgs boson. SM has been rigorously tested at various experiments for more than 3 decades and it has been extremely successful. It is not an exaggeration to say that SM is one of the most successful theories in not just particle physics or in physics, but in all sciences!

Limitations of the Standard Model:

Although SM is an extremely successful model, it cannot account for all the phenomena associated with the electroweak and strong forces. However, we believe that it certainly is a strong foundation on which our understanding of physics beyond SM can be built. Main limitations of SM are as follows:

- Originally, neutrinos are massless within the SM. However, it has been experimentally verified that at least two of the three species of neutrinos have tiny, but non-zero masses. This is a strong piece of evidence for the physics beyond the SM. Various theoretical models have been proposed to explain the origin of the neutrino masses, but none has been experimentally validated.
- SM cannot account for the dark matter, which makes about 86% of all the matter in the Universe and 23% of all the energy content. It also does not account for the dark energy, which makes up about 73% of the total energy content in the Universe.

- SM does predict existence of one Higgs boson, it does not predict its mass. Similarly, masses of all the fermions, their Yukawa couplings, masses of the gauge bosons, etc. cannot be extracted theoretically. Their prediction requires experimental results as inputs.
- If there is no new physics at energies higher than the electroweak scale ($\Lambda_{EW} \sim 246$ GeV) until the Planck scale, then the SM vacuum is considered to be metastable [17].
- There are other questions such as the so-called hierarchy problem, naturalness problem, absence of Grand Unification in SM. However, there is no *experimental* evidence to indicate that any of these questions are serious problems. They might very well be real problems, but as of now there is no evidence that suggests so.

At this juncture we are ready to venture into physics Beyond the Standard Model! In the next chapter we will discuss in detail the evidences for neutrino “oscillations”, masses and mixings. We will also review a few popular theoretical mechanisms that have been proposed to account for the origin of the neutrino masses.

Chapter 2

Neutrino Oscillations and Models of Neutrino Masses

In the previous chapter we discussed in detail the development of $SU(2)_L$ gauge theory of weak interactions. That story started from Pauli's postulate of existence of neutrinos, which were considered 'ghost particles' as they were very illusive for detectors. In fact, Wolfgang Pauli bet a case of champaign that neutrinos would never be detected - a bet that he lost not until 26 years later, in 1956, when Cowen and Reines detected antineutrinos from a nuclear reactor [18].

As discussed in the previous chapter, in Standard Model, neutrinos were thought to be massless. However, experiments since 1998 have confirmed that at least two of the 3 light neutrinos have tiny, but non-zero masses. To the date the mechanism that is responsible for neutrino masses has not been experimentally validated, although numerous theoretical mechanisms have been proposed to theoretically realize this phenomenon. It remains an open question and the strongest pieces of evidence (within the regime of SM, since neutrino is a part of SM) for physics beyond the SM.

In this chapter, we will first review the experimental evidences that point to non-

zero neutrino masses and mixings. In the following section we will review a few mechanisms that explain the origin of neutrino masses. We will also discuss the limitations of these models and motivate the necessity for a new model, which will be discussed in detail in the next chapter onwards.

2.1 The PMNS matrix and various mixing angles

Recall our discussion of Eq. (1.92) in the previous chapter. In SM the charged leptons acquire masses through the following terms in the Lagrangian:

$$\mathcal{L}_{Lepton-Yuk} = g_e \bar{l}_L \Phi e_R + h.c., \quad (2.1)$$

which, after the spontaneous breaking of $SU(2)_L \times U(1)_Y$ gauge symmetry, becomes $g_e \frac{v}{\sqrt{2}} \bar{e}_L e_R + h.c..$ Gauge invariance also allows “flavor-changing” terms of the form $\bar{l}_{eL} \Phi \mu_R, \bar{l}_{eL} \Phi \tau_R, \bar{l}_{\mu L} \Phi \tau_R$, etc.

Therefore, just like mixings in the quark sector, the mass matrix for charged leptons can in general be written as

$$\bar{\psi}_l \mathcal{M}_l \psi_l = \frac{v}{\sqrt{2}} \times \bar{\psi}_l \begin{pmatrix} g_{ee} & g_{e\mu} & g_{e\tau} \\ g_{\mu e} & g_{\mu\mu} & g_{\mu\tau} \\ g_{\tau e} & g_{\tau\mu} & g_{\tau\tau} \end{pmatrix} \psi_l, \quad (2.2)$$

where $\psi_l = \begin{pmatrix} e & \mu & \tau \end{pmatrix}^T$. In general, this matrix is not symmetric. It can be diagonalized by two unitary matrices as follows:

$$U_{L,e}^+ \mathcal{M}_l U_{R,e} = \mathcal{M}_{l,diag}. \quad (2.3)$$

For the moment let us assume that somehow neutrinos also acquire masses through terms of the form $m_{\nu_e} \bar{\nu}_{eL} \nu_{eR}$, etc. Then the neutrino mass matrix can also be written as

$$\begin{aligned} \bar{\psi}_{\nu_L} \mathcal{M}_\nu \psi_{\nu_R} + h.c. &= \bar{\psi}_{\nu_L} U_{\nu_L} U_{\nu_L}^\dagger \mathcal{M}_l U_{\nu_R} U_{\nu_R}^\dagger \psi_{\nu_R} + h.c. \\ &= \bar{\psi}'_{\nu_L} \mathcal{M}_{\nu,diag} \psi'_{\nu_R}. \end{aligned} \quad (2.4)$$

where $\psi_\nu = \begin{pmatrix} \nu_e & \nu_\mu & \nu_\tau \end{pmatrix}^T$ and $\psi'_{\nu_{L,R}} = U_{\nu_{L,R}}^\dagger \psi_{\nu_{L,R}}$. In the same way as we did for the CKM matrix for the quark sector in Eq. (1.99), the charged current of leptons that couples to the W^+ boson can be written as

$$\bar{\psi}'_{e_L} U_{e_L}^{-1} \gamma^\mu U_{\nu_L} \psi'_{\nu_L} = \bar{\psi}'_{e_L} V_{CKM}^l \gamma^\mu \psi'_{\nu_L}, \quad (2.5)$$

where

$$V_{CKM}^l = U_{e_L}^{-1} U_{\nu_L}. \quad (2.6)$$

This is like V_{CKM} , but for leptons. Hence the superscript ‘ l ’. Note that V_{CKM}^l is a unitary matrix.

Note that if the neutrinos are massless, then U_{ν_L} can be arbitrarily chosen so that $U_{e_L} = U_{\nu_L}$ and $V_{CKM}^l = 1$.

Such conversion of one flavor of lepton into another is analogous to coupled oscillators. The coupling strength is defined in terms of the ‘lepton mixing matrix’ V_{CKM}^l [19]. However, Charged Lepton Flavor Violation (CLFV) has not been observed, even if it is not forbidden in SM. Thus, usually it is assumed that $U_{e_L} = \mathbb{I}$, in which case $V_{CKM}^l = U_{\nu_L}$.

2.1.1 PMNS matrix

Pontecorvo first proposed the idea that the electron neutrino is really a linear combination of mass eigenstate neutrinos and that this could lead to $\nu_e \rightarrow \nu_\mu$ oscillations ([19] and references therein). This idea was also independently put forward by Maki, Nakagawa and Sakata. Later Mikheyev, Smirnov and Wolfenstein proposed that these oscillations would be resonantly enhanced in the Sun.

Hence, V_{CKM}^l is named as PMNS (Pontecorvo, Maki, Nakagawa, Sakata) matrix and is denoted by U_{PMNS} . Hereafter we will use this notation. Since U_{PMNS} is a unitary matrix, it can be fully specified in terms of 3 angles and 6 complex phases. If $U_{eL} = \mathbb{I}$, then 3 of these phases can be removed and

$$\begin{pmatrix} \nu_e \\ \nu_\mu \\ \nu_\tau \end{pmatrix} = U_{PMNS} \begin{pmatrix} \nu_1 \\ \nu_2 \\ \nu_3 \end{pmatrix} = \begin{pmatrix} U_{e1} & U_{e2} & U_{e3} \\ U_{\mu1} & U_{\mu2} & U_{\mu3} \\ U_{\tau1} & U_{\tau2} & U_{\tau3} \end{pmatrix} \begin{pmatrix} \nu_1 \\ \nu_2 \\ \nu_3 \end{pmatrix},$$

where ν_1, ν_2, ν_3 are mass eigenstate neutrinos, having masses m_1, m_2, m_3 respectively.

If one assumes that the remaining 3 phases are zero, then U_{PMNS} can be parametrized in terms of three $O(3)$ rotation matrices (three Euler rotations) as

$$U_{PMNS} = R_{23} R_{13} R_{12}, \quad (2.7)$$

where

$$R_{23} = \begin{pmatrix} 1 & 0 & 0 \\ 0 & c_{23} & s_{23} \\ 0 & -s_{23} & c_{23} \end{pmatrix}, \quad R_{13} = \begin{pmatrix} c_{13} & 0 & s_{13} \\ 0 & 1 & 0 \\ -s_{13} & 0 & c_{13} \end{pmatrix}, \quad R_{12} = \begin{pmatrix} c_{12} & s_{12} & 0 \\ -s_{12} & c_{12} & 0 \\ 0 & 0 & 1 \end{pmatrix}, \quad (2.8)$$

with $c_{ij} = \cos \theta_{ij}$, $s_{ij} = \sin \theta_{ij}$ and $0 \leq \theta_{ij} \leq \pi/2$. Thus,

$$U_{PMNS} = \begin{pmatrix} c_{12} c_{13} & s_{12} c_{13} & s_{13} \\ -s_{12} c_{23} - c_{12} s_{13} s_{23} & c_{12} c_{23} - s_{12} s_{13} s_{23} & c_{13} s_{23} \\ s_{12} s_{23} - c_{12} s_{13} c_{23} & -c_{12} s_{23} - s_{12} s_{13} c_{23} & c_{13} c_{23} \end{pmatrix} \quad (2.9)$$

If we consider the 3 phases - 1 ‘‘Dirac phase’’ δ and 2 ‘‘Majorana phases’’ β_1, β_2 , then the PMNS matrix is expressed as:

$$U_{PMNS} = R_{23} U_{13} R_{12} P_{12}, \quad (2.10)$$

where

$$U_{13} = \begin{pmatrix} c_{13} & 0 & s_{13} e^{-i\delta} \\ 0 & 1 & 0 \\ -s_{13} e^{i\delta} & 0 & c_{13} \end{pmatrix}, \quad P_{12} = \begin{pmatrix} e^{i\beta_1} & 0 & 0 \\ 0 & e^{i\beta_2} & 0 \\ 0 & 0 & 1 \end{pmatrix}. \quad (2.11)$$

The most general PMNS matrix is then written as

$$U_{PMNS} = \begin{pmatrix} c_{12} c_{13} & s_{12} c_{13} & s_{13} e^{-i\delta} \\ -s_{12} c_{23} - c_{12} s_{13} s_{23} e^{i\delta} & c_{12} c_{23} - s_{12} s_{13} s_{23} e^{i\delta} & c_{13} s_{23} \\ s_{12} s_{23} - c_{12} s_{13} c_{23} e^{i\delta} & -c_{12} s_{23} - s_{12} s_{13} c_{23} e^{i\delta} & c_{13} c_{23} \end{pmatrix} \cdot P_{12}. \quad (2.12)$$

The three θ_{ij} are measured/probed mainly with three types of experiments.

The probability that a α -flavor neutrino ν_α converts to a β -flavor neutrino is given by [20]

$$P_{\nu_\alpha \rightarrow \nu_\beta} = \delta_{\alpha\beta} - 4 \sum_{i>j} \text{Re} (U_{\alpha i}^* U_{\beta i} U_{\alpha j} U_{\beta j}^*) \sin^2 (X_{ij}) + 2 \sum_{i>j} \text{Im} (U_{\alpha i}^* U_{\beta i} U_{\alpha j} U_{\beta j}^*) \sin (2 X_{ij}), \quad (2.13)$$

where

$$X_{ij} = \frac{\Delta m_{ij}^2}{4} \frac{L}{E} = 1.27 \frac{\Delta m_{ij}^2}{\text{eV}^2} \frac{L}{\text{kms}} \frac{\text{GeV}}{E}. \quad (2.14)$$

Here, U_{ab} are elements of U_{PMNS} in Eq. (2.12), E is the energy of the neutrino beam, L is the baseline from the neutrino source to the detector and $\Delta m_{ij}^2 = m_i^2 - m_j^2$.

2.1.2 Global fit values

In a particular experiment that probes the oscillations $\nu_\alpha \rightarrow \nu_\beta$, a fit of the relevant Δm_{ij}^2 vs. $\sin^2 \theta_{ij}$ is obtained. Different types of experiments probe different Δm_{ij}^2 and $\sin^2 \theta_{ij}$.

E.g. from the oscillations $\nu_\mu \rightarrow \nu_\tau$ in the atmospheric neutrino flux (flux of neutrinos originated in the cascade of cosmic ray air-showers), $|\Delta m_{32}^2|$ and $\sin^2 \theta_{23}$ can be measured. Note that it has not yet been possible to probe the sign of Δm_{32}^2 or Δm_{31}^2 . This results in two different scenarios for the ‘‘hierarchy’’ of the neutrino masses:

1. ‘‘Normal Hierarchy’’: $m_1 < m_2 < m_3$
2. ‘‘Inverted Hierarchy’’: $m_3 < m_1 < m_2$

Since experiments have only been able to probe the difference between mass-squares of neutrinos, the absolute values of neutrino masses are not known. However, there is an upper limit on the sum of neutrino masses $m_\nu \lesssim 1$ eV, set by the cosmological experiments, which measure the limits on the total energy density of the Universe contributed by the light neutrino species ([19] and references therein).

The recent global fit values of neutrino oscillation parameters are given in Table 2.1

Table 2.1: Global fit values of neutrino oscillation measurements, given in [21] for “free fluxes”. “NH” \rightarrow Normal Hierarchy; “IH” \rightarrow Inverted Hierarchy.

Parameter	Global fit value ($\pm 1\sigma$)
$\sin^2 \theta_{12}$	$0.302^{+0.013}_{-0.012}$
θ_{12} (deg.)	$33.36^{+0.81}_{-0.78}$
$\sin^2 \theta_{23}$ (NH)	$0.413^{+0.037}_{-0.025}$
$\sin^2 \theta_{23}$ (IH)	$0.594^{+0.021}_{-0.022}$
θ_{23} (deg.) (NH)	$40.0^{+2.1}_{-1.5}$
θ_{23} (deg.) (IH)	$50.4^{+1.3}_{-1.3}$
$\sin^2 \theta_{13}$	$0.0227^{+0.0023}_{-0.0024}$
θ_{13} (deg.)	$8.66^{+0.44}_{-0.46}$
δ_{CP} (deg.)	300^{+66}_{-138}
Δm_{21}^2 (10^{-5} eV 2)	$7.50^{+0.18}_{-0.19}$
Δm_{31}^2 (10^{-3} eV 2) (NH)	$+2.473^{+0.070}_{-0.067}$
Δm_{32}^2 (10^{-3} eV 2) (IH)	$-2.427^{+0.042}_{-0.065}$

We will not go into the details of these measurements, as the neutrino oscillations are not the focus of this dissertation. However, neutrino oscillation data demonstrates that neutrinos do have tiny, albeit non-zero masses, indicating existence of physics beyond the SM.

The phenomenology of a particular model that explains the origin of neutrino masses is the focus of this dissertation. We therefore move on to review a few popular theoretical models, which attempt to do the similar.

2.2 Seesaw mechanism of neutrino masses

In this section we will review some of the popular theoretical mechanisms, with which the origin of neutrino masses can be theoretically realized. As we saw at the beginning

of the previous section, if the right-handed neutrinos exist, then m_ν can be explained. All the neutrinos which have been detected so far have tiny masses and left-handed neutrinos helicity. This has put an upper limit on the right-handed component in the light neutrinos.

This means that, if the right-handed neutrinos exist, then the mass eigenstates which have ν_R 's as the dominant component must be much heavier than the light neutrinos. That would explain why we have not seen them so far and why they are not among the relativistic species (light neutrinos and photons) in the Universe. Thus, a theoretical mechanism that would give tiny masses to light neutrinos needs to also make the ν_R 's heavy. An attractive way of achieving this is through the ‘‘Seesaw mechanism’’ (light-heavy balance \rightarrow seesaw).

In this section, we will review the so-called type-I, type-II, type-III seesaw mechanisms. We will also briefly discuss the type-I seesaw mechanism in the Left-Right symmetric models, since in this mechanism ν_R transforms non-trivially under the $SU(2)_L \times U(1)_Y$ gauge symmetry. Note that the seesaw mechanism in the EW ν_R model is different from all of these types. The discussion here mainly follows [19, 22].

2.2.1 Different types of ν -mass terms

We can write an ad-hoc mass term for the light neutrino as $\sim H l^T \kappa H l$, where H is a Higgs field, l is the lepton doublet containing ν_L and κ is a (effective) coupling having dimensions (mass) $^{-1}$. When H acquires a VEV, we get a mass term for ν_L . In the seesaw mechanisms this term is generated effectively by the exchange of a right-handed neutrino having appropriate transformation property under $SU(2)_L \times U(1)_Y$, for an appropriate Higgs field.

In general, different types of mass terms for ν can be written as follows:

- **ν_L Majorana mass term:**

If ν_L is a Majorana fermion i.e. if it is an antiparticle of itself, then in the vacuum state of the Lagrangian its Majorana mass term can be written as $m_{LL}^\nu \bar{\nu}_L \nu_L^c$, where ν_L^c is the CP conjugate of ν_L , which is the right-handed antineutrino field. These terms violate the lepton number. They are strictly forbidden for charged particles, due to the electric charge conservation.

If we want this term to be generated through spontaneous breaking of the electroweak symmetry, due to the VEV of scalar doublets (and no higher multiplets such as a scalar triplet), then the Majorana mass terms are forbidden at the renormalizable level by gauge invariance. In seesaw mechanisms such terms are generated effectively in the presence of right-handed neutrinos.

- **ν_R Majorana mass term:**

If one introduces a right-handed neutrino then a Majorana mass term for ν_R can be written as $M_R \bar{\nu}_R^c \nu_R$, where ν_R^c is the left-handed antineutrino field.

- **Dirac mass term:**

In presence of ν_R , one can also write a Dirac mass term of the form $m_{LR} \bar{\nu}_L \nu_R$.

Hence, the neutrino mass matrix can be written as

$$\begin{pmatrix} \bar{\nu}_L & \bar{\nu}_R^c \end{pmatrix} \begin{pmatrix} 0 & m_{LR} \\ m_{LR}^T & M_R \end{pmatrix} \begin{pmatrix} \nu_L^c \\ \nu_R \end{pmatrix}. \quad (2.15)$$

If we are writing the matrix for multiple light neutrino mass eigenstates, then each of the elements is a matrix. If $M_R \gg m_{LR}$, then eigenvalues of this matrix are $\approx M_R$ and a small Majorana mass $m_{LL}^\nu = -m_{LR} M_R^{-1} m_{LR}^T$. Thus, m_{LL}^ν is naturally suppressed by the heavy M_R . If $m_{LR} \sim M_W$ and $M_R \sim \Lambda_{GUT} \sim \mathcal{O}(10^{16} \text{ GeV})$, then

$m_{LL}^\nu \sim 10^{-3}$ eV, which seems to have the appropriate order of magnitude, looking at Table 2.1.

Notice the *huge* mass of ν_R that is necessary to obtain the light-neutrino masses that agree with the data.

2.2.2 Type-I Seesaw mechanism

In the type-I mechanism, the right-handed neutrinos ν_R 's are added to the SM. These ν_R 's are singlets under the $SU(2)_L \times U(1)_Y$ gauge symmetry. Thus, they do not interact with W^\pm and Z , and are called “sterile” ν_R 's. The mass matrix of neutrinos arises from the Lagrangian [22]

$$\mathcal{L} = y_D \bar{l}_L \tilde{\Phi} \nu_R - \frac{1}{2} \nu_R^T M_R \nu_R + h.c., \quad (2.16)$$

where Φ is a $SU(2)_L$ Higgs doublet having VEV $\langle \Phi \rangle = (0, v/\sqrt{2})^T$. After the breaking of the electroweak symmetry, when Φ acquires its VEV, one obtains the neutrino mass matrix of the form in Eq. (2.15). Here, $m_{LR}^T = -y_D v/\sqrt{2}$.

In this mechanism, for each ν_R , only one ν_L gets a mass. Thus, the number of ν_R 's required is the same as the number of massive ν_L 's, i.e. at least two ν_R 's are necessary. Generally, one ν_R per lepton generation is added.

This is a minimal type-I seesaw mechanism with only one Higgs doublet. In 2-Higgs doublet models, the type-I seesaw mechanism is implemented with two scalar doublets - one giving masses to ($T_3 = 1/2$) fermions and the other to ($T_3 = -1/2$) fermions.

Once again notice that a huge mass of $M_R \sim \mathcal{O}(10^{16}$ GeV) is necessary with $y_D \sim \mathcal{O}(1)$ so that $m_\nu \lesssim 1$ eV is satisfied. Such ν_R 's are too heavy to be produced at the Large Hadron Collider or near-future experiments. If the ν_R 's, instead, would

couple to W^\pm , Z , then their masses would also be around the electroweak scale $\Lambda_{EW} \approx 246$ GeV. Thus, they would be non-sterile, but type-I seesaw mechanism cannot generate light enough masses for ν_L 's with non-sterile ν_R 's. In the subsequent chapters of this dissertation, we will discuss in detail a model which achieves this.

2.2.3 Type-II Seesaw mechanism

In the type-II seesaw mechanism, we have a scalar triplet in addition to the SM scalar doublet. The role of ν_R of generating an effective dimension-5 operator is played by a $Y/2 = 1$ complex scalar triplet given by

$$\Delta_L \equiv \frac{1}{\sqrt{2}} \vec{\tau} \cdot \vec{\Delta}_L = \begin{pmatrix} \Delta^+/\sqrt{2} & \Delta^{++} \\ \Delta^{0*} & -\Delta^+/\sqrt{2} \end{pmatrix}. \quad (2.17)$$

Thus, there is no ν_R in the minimal type-II seesaw mechanism. The mass of the light neutrino is directly generated from the Yukawa interaction

$$\mathcal{L} = y_\Delta l_L^T C \sigma_2 \Delta_L l_L + h.c.. \quad (2.18)$$

When Δ_L acquires a VEV of $\langle \Delta_L \rangle$, the ν_L gets a mass of $m_\nu = y_\Delta \langle \Delta \rangle$. This VEV is generated through the cubic scalar terms in the scalar potential:

$$\mu \Phi^T \sigma_2 \Delta_L^* \Phi + M_\Delta^2 Tr(\Delta_L^\dagger \Delta_L). \quad (2.19)$$

In the vacuum state of this potential, $\langle \Delta_L \rangle \approx \mu v^2 / (2 M_\Delta^2)$, where $v/\sqrt{2}$ is the VEV of the real part of Φ .

Thus, for not-so-fine-tuned y_Δ , we get appropriate light neutrino masses when $\mu v^2 \ll M_\Delta^2$. So the VEV of the triplet must be really small, while its mass needs to

be really large, just like M_R in the type-I seesaw. Hence, still the name “seesaw” for this mechanism. Notice that, in this mechanism too, the effective mass term for the light neutrinos comes from a dimension-5 operator with $\kappa \sim \mu/M_\Delta^2$.

There have been attempts to make the VEV $\langle \Delta_L \rangle$ large, but it requires fine tuning of the Yukawa couplings y_Δ and the μ .

2.2.4 Type-III Seesaw mechanism

So far we have seen that for a seesaw mechanism we basically need two mass scales - one heavier than the other. In the type-I seesaw mechanism the heavier one arises from the mass of ν_R ; in the type-II seesaw mechanism, it is the scale of large M_Δ .

Notice that in Eq. (2.16) for the type-I seesaw mechanism, a gauge invariant term can be formed by coupling $\sim (l_L \Phi)$ with a $SU(2)_L$ triplet, such that the neutral component of the triplet couples to ν_L . In the type-III seesaw mechanism this is achieved by adding to the SM one real ($Y/2 = 0$) *fermion* triplet $\vec{T}_F = \begin{pmatrix} T_{F1} & T_{F2} & T_{F3} \end{pmatrix}^T$, for each of the lepton generations. Just like the type-I seesaw, at least 2 fermion triplets are required to give masses to two ν_L .

The mass of ν_L is generated through the Lagrangian

$$\mathcal{L} = y_T l^T C \sigma_2 \vec{\tau} \cdot \vec{T}_F \Phi + M_T \vec{T}_F^T \cdot C \vec{T}_F. \quad (2.20)$$

As usual, we are showing the equation for only one of the 3 lepton generations only for illustration. In this case the mass matrix for neutrino can be written as

$$\begin{pmatrix} 0 & y_T v / \sqrt{2} \\ y_T^T v / \sqrt{2} & M_T \end{pmatrix} \quad (2.21)$$

Hence, just like in the type-I seesaw mechanism, after the breaking of the $SU(2)_L \times$

$U(1)_Y$ gauge symmetry, the light neutrino masses for ν_L are obtained as

$$m_{LL}^\nu = -y_T^T M_T^{-1} y_T v^2. \quad (2.22)$$

Thus, once again the mass of ν_L is generated through an effective dimension-5 operator after integrating out T_F . Here as well, if the Yukawa couplings y_T are not extremely small, M_T must be huge to obtain appropriate masses for ν_L 's.

In the three types of seesaw mechanisms we can notice that:

- To give small enough masses to ν_L 's some physics beyond SM (ν_R , Δ_L or T_F) is added at a very large scale $\gg \Lambda_{EW}$.
- In the type-I seesaw mechanism, which adds ν_R 's to SM particle content, the masses M_R of the right-handed neutrinos need to be huge - of the order of the so-called GUT scale.
- In the type-II seesaw mechanism, which adds a complex scalar triplet Δ_L to the SM, the VEV of Δ_L needs to be very small and its mass very large to generate appropriate masses of ν_L .

If we want ν_R 's in the seesaw mechanism to be lighter so that they can be produced and detected at the LHC or experiments in the future, then it probably is a good idea not to make ν_R a singlet under all the gauge symmetries! If ν_R transforms *non-trivially* under a gauge symmetry, then if the corresponding gauge bosons are produced experimentally, ν_R would also be around the same energy scale and can be produced.

In the next section we will briefly review a class of models, in which ν_R is a singlet under $SU(2)_L$, but a doublet under a BSM gauge group $SU(2)_R$.

2.3 Left-Right symmetric models

Left-Right symmetric (L-R) models are extensions of the SM, which obey a $SU(2)_L \times SU(2)_R \times U(1)_{B-L}$ gauge symmetry ([23, 24] and references therein). Here right-handed fermions in SM are doublets under $SU(2)_R$, while still being singlets under $SU(2)_L$. Parity is an exact symmetry in L-R models. At some energy scale v_R above the electroweak scale, the $SU(2)_L \times SU(2)_R \times U(1)_{B-L}$ gauge symmetry is spontaneously broken to $SU(2)_L \times U(1)_Y$ gauge symmetry.

This is worth mentioning in this dissertation as ν_R 's are part of a $SU(2)_R$ *doublet* in these models, unlike the minimal type-I seesaw mechanisms. In the EW ν_R model too, ν_R 's are members of $SU(2)_L$ *doublet*. Hence, it is of interest to note some implications of the L-R models before building the EW ν_R model.

In the L-R model with parity as the L-R symmetry, the charge assignments for the quark and lepton multiplets, under $SU(2)_L \times SU(2)_R \times U(1)_{B-L}$ are given by $q_L(2, 0, 1/3)$, $q_R(0, 2, 1/3)$, $l_L(2, 0, -1)$, $l_R(0, 2, -1)$. Here l_L and q_L are the SM lepton and quark doublets, and

$$l_R = \begin{pmatrix} \nu_R \\ e_R \end{pmatrix}, \quad q_R = \begin{pmatrix} u_R \\ d_R \end{pmatrix}. \quad (2.23)$$

are doublets under $SU(2)_R$.

In this model the neutrino masses can be generated through either type-I or type-II seesaw mechanism. In a most general scalar structure a hybrid type-I+type-II seesaw mechanism is implemented, with the help of two scalar doublets Φ_1, Φ_2 (both can be combined in a $(2, 2)$ representation of $SU(2)_L \times SU(2)_R$), and two scalar triplets Δ_L

and Δ_R [22, 23]:

$$\Phi = \begin{pmatrix} \phi_1^0 & \phi_1^+ \\ \phi_2^- & \phi_2^0 \end{pmatrix}, \quad \Delta_{L,R} = \begin{pmatrix} \Delta_{L,R}^+/\sqrt{2} & \Delta_{L,R}^{++} \\ \Delta_{L,R}^0 & -\Delta_{L,R}^+/\sqrt{2} \end{pmatrix} \quad (2.24)$$

This model also contains gauge bosons W_R^\pm and Z_R of the $SU(2)_R$ gauge symmetry. The scale of breaking of this symmetry is not bounded from above. Theoretically its bounded from below only by the electroweak scale ≈ 246 GeV.

Signals for the production of the ν_R in this model, primarily $\bar{u} + d \rightarrow W_R^- \rightarrow \nu_R + l$ [24], have been searched for at the LHC. The scale of W_R mass has been bounded from below at ~ 3 TeV by these searches [25].

2.4 Summary of the chapter

- There is a confirmed evidence that at least two of the three flavors of light neutrinos have tiny, but non-zero masses. This is the strongest piece of evidence (within the regime of SM), for physics beyond the SM.
- Many theoretical mechanisms have been proposed to theoretically realize neutrino masses, but none has been experimentally validated.
- The popular seesaw mechanisms extend SM by new physics at very large scales. Unless fine-tuned, the new particles are too heavy to be produced at the LHC or the near-future experiments.
- The Left-Right symmetric models add the right-handed neutrinos, which is a member of the $SU(2)_R$ lepton doublet, to the SM fermion content. These models extend the gauge group of the Standard Model, thus, adding more gauge bosons and a higher symmetry breaking scale.

- Although signals for the L-R models are searched for at the LHC, the scale of new physics in these models is only bounded from below by experiments, currently at about 3 TeV .

This chapter provides only a brief review of the spectrum of theoretical models for the origin of neutrino masses. It can be seen from this discussion that the validation of the origin of neutrino masses remains an open question.

A model of neutrino masses that can be *conclusively* tested at the LHC and/or near-future experiments could go a long way in resolving the mystery of neutrino masses!

Chapter 3

Hung's Minimal EW ν_R Model

From the previous two chapters we realize that, without a doubt, the nature of the electroweak symmetry breaking and the neutrino masses and mixings are two of the most pressing problems in particle physics. Neutrino mixings are the strongest piece of evidence (within the regime of SM) for physics beyond the Standard Model. The discovery of a Higgs boson having a mass of 125 GeV is definitely a significant step in resolving the first of these mysteries. However, absence of a signal for any BSM phenomenon at the Large Hadron Collider has severely constrained many popular BSM models. In this situation, exploring the BSM physics through the portal of neutrinos seems to be a promising direction to pursue.

In the last chapter we reviewed many theoretical mechanisms which are proposed to explain the origin of neutrino masses and mixings. Popularly, neutrino masses are theoretically realized through the so-called seesaw-type mechanisms. But in a general seesaw mechanism, since ν_R is a singlet under the $SU(2)_L \times U(1)_Y$ gauge symmetry (“sterile ν_R ”), its Majorana mass is naturally near the so-called Grand Unification scale ($\mathcal{O}(10^{15-16}$ GeV)). Such ν_R cannot be produced at the LHC or a near future collider, and hence such seesaw mechanisms cannot be directly tested.

On the other hand, there are the Left-Right symmetric models (L-R models), in which ν_R is a member of a doublet under $SU(2)_R$ (still a singlet under $SU(2)_L$) gauge symmetry. However, the scale of breaking of the $SU(2)_R$ and its gauge boson W_R is only bounded from below by experimental constraints, which are currently set at about 3 TeV [25].

With a motivation of exploring the possibility of testing the seesaw mechanism at the LHC (and near-future experiments) [26] attempts to answer:

1. Is it possible to have $M_R \sim \Lambda_{EW}$?
2. And, is it possible within the gauge group of the Standard Model: $SU(3)_C \times SU(2)_L \times U(1)_Y$?

[26] answers both these question affirmatively, through the $EW\nu_R$ model, which is the focus of this dissertation. In the $EW\nu_R$ model, the right-handed neutrinos naturally acquire a mass of $\mathcal{O}(\Lambda_{EW})$ and they are also non-sterile under $SU(2)_L \times U(1)_Y$.

In this chapter we will first review the step-by-step process of building this model. Secondly we will write a general scalar potential in this model that breaks the $SU(2)_L \times U(1)_Y$ spontaneously to $U(1)_{EM}$ and obtain the spectrum of physical particles (gauge bosons, scalars, fermions) in this model. In the third section we will summarize main features of the model, before moving on to analyzing its phenomenology in the subsequent chapters.

3.1 Building the model

In this chapter we will follow the steps in [26] to build the minimal $EW\nu_R$ model. As a starter, we quote Lee and Yang [7]:

“If such asymmetry is indeed found, the question could still be raised whether there could not exist corresponding elementary particles exhibiting opposite asymmetry such that in the broader sense there will still be over-all right-left symmetry.”

3.1.1 The fermion sector

Let us consider the lepton sector and the scalar doublet Φ in SM. For the purpose of illustration we will consider only one generation in the lepton sector. A lepton generation in SM is given by

$$l_L = \begin{pmatrix} \nu_L \\ e_L \end{pmatrix}, e_R, \quad (3.1)$$

where the left-handed components are part of a $SU(2)_L$ doublet, and the right-handed e_R is a singlet under $SU(2)_L$. In a general seesaw mechanism, that we reviewed in the previous chapter, the right-handed neutrino ν_R is also a singlet under $SU(2)_L$. It therefore acquires a Dirac mass by coupling to $\bar{l}_L\Phi$ or $\bar{l}_L\tilde{\Phi}$, which are also $SU(2)_L$ singlet terms. Since this leads to a huge Majorana mass of ν_R , we should avoid that, if we want the ν_R to acquire an EW-scale mass. We therefore make ν_R a member of a $SU(2)_L$ right-handed lepton doublet:

$$l_R^M = \begin{pmatrix} \nu_R \\ e_R^M \end{pmatrix}, e_L^M, \quad (3.2)$$

where the superscript ‘ M ’ stands for “*Mirror Fermions*”. e_R^M and e_L^M are right-handed and left-handed components of the “mirror electron” e^M . Note that e^M is an entirely new particle, different from the SM electron. The word ‘electron’ in its name only suggests that it has the same $SU(2) \times U(1)_Y$ quantum numbers. The word

‘mirror’ signifies that its *chirality* components are swapped as compared to the SM electron components, meaning that the right-handed component e_R^M is a part of a $SU(2)$ doublet and left-handed e_L^M is a $SU(2)$ singlet. Similarly, there are two more generations of mirror leptons and two more ν_R 's.

Note that in the last paragraph, we dropped the subscript ‘ L ’ from $SU(2)_L$. This is because the ‘ L ’ signifies that the left-handed components of the fermions couple to the gauge bosons W^\pm and Z . Now that we have added mirror leptons whose right-handed components are in the doublets, these components would couple to the same gauge bosons. Hence, it is better to drop the subscript ‘ L ’.

To give the Dirac mass to the neutrinos, let us assume existence of a $SU(2)$ scalar singlet ϕ_S . Hence, we can have

$$\begin{aligned}\mathcal{L}_{Sl} &= g_{Sl} \bar{l}_L \phi_S l_R^M + h.c. \\ &= g_{Sl} (\bar{\nu}_L \nu_R + \bar{e}_L e_R^M) \phi_S + h.c.\end{aligned}\tag{3.3}$$

In addition, analogous to Eq. (1.92) for SM, we also have

$$\mathcal{L}_{LY1} = g_l \bar{l}_L \Phi e_R + h.c.,\tag{3.4}$$

$$\mathcal{L}_{LY2} = g_l^M \bar{l}_R^M \Phi e_L^M + h.c.,\tag{3.5}$$

with the VEV $\langle \phi_S \rangle = v_S$ and just like in SM, $\langle \Phi \rangle = \left(0, v_2/\sqrt{2} \right)^T$. Note that VEV of Φ is denoted in terms of v_2 , and not the total $v \approx 246$ GeV. Then from Eqs. (3.3), (3.4), (3.11) we obtain

$$m_\nu^D = g_{Sl} v_S, \quad M_l = \begin{pmatrix} m_l & m_\nu^D \\ m_\nu^D & m_{l^M} \end{pmatrix},\tag{3.6}$$

for Dirac neutrino and charged SM lepton, charged mirror lepton, respectively. Here $m_l = g_l v_2/\sqrt{2}$ for the SM lepton, and $m_{lM} = g_l^M v_2/\sqrt{2}$ for the mirror lepton. Their Dirac masses are obtained by diagonalizing M_l in Eq. (3.6):

$$\tilde{m}_l = m_l - \frac{(m_\nu^D)^2}{m_{lM} - m_l}, \quad \tilde{m}_{lM} = m_{lM} + \frac{(m_\nu^D)^2}{m_{lM} - m_l}. \quad (3.7)$$

We will assume that $m_{lM} \gg m_l$ and, as we will see shortly, to satisfy the constraints on neutrino mass m_ν , we need $m_\nu^D \ll m_{lM}, m_l$. This implies that $\tilde{m}_l \approx m_l$ and $\tilde{m}_{lM} \approx m_{lM}$.

Now that we have added new mirror leptons to the SM fermion spectrum, we must also add ‘‘mirror quarks’’ to ensure anomaly cancellation [10]. Thus, there will be 3 mirror quark generations analogous to:

$$q_R^M = \begin{pmatrix} u_R^M \\ d_R^M \end{pmatrix}, \quad u_L^M, \quad d_L^M. \quad (3.8)$$

Here too, u^M (mirror up-quark) and d^M (mirror down-quark) are new particles different from the up-quark and down-quark in SM. Just like mirror leptons, the right-handed components of the mirror quarks are members of $SU(2)$ doublets, while the left-handed components are singlets.

They acquire masses through Lagrangian terms similar to Eqs. (3.3), (3.4), (3.11):

$$\begin{aligned} \mathcal{L}_{Sq} &= g_{Sq} \bar{q}_L \phi_S q_R^M + h.c. \\ &= g_{Sq} (\bar{u}_L u_R^M + \bar{d}_L d_R^M) \phi_S + h.c. \end{aligned} \quad (3.9)$$

$$\mathcal{L}_{QY1} = g_d \bar{q}_L \Phi d_R + g_u \bar{q}_L \tilde{\Phi} u_R + h.c., \quad (3.10)$$

$$\mathcal{L}_{QY2} = g_{d^M} \bar{q}_R^M \Phi d_L^M + g_{u^M} \bar{q}_R^M \tilde{\Phi} u_L^M + h.c., \quad (3.11)$$

Their masses can be obtained from these equations as:

$$\tilde{m}_q = m_q - \frac{(m_\nu^D)^2 (g_{Sq}/g_{Sl})^2}{m_{q^M} - m_q}, \quad \tilde{m}_{q^M} = m_{q^M} + \frac{(m_\nu^D)^2 (g_{Sq}/g_{Sl})^2}{m_{q^M} - m_q}, \quad (3.12)$$

where $q = u, d$, $m_q = g_q v_2/\sqrt{2}$ and $m_{q^M} = g_{q^M} v_2/\sqrt{2}$. We assume that $m_{q^M} > m_q$, and similar to leptons, we have $\tilde{m}_q \approx m_q$, $\tilde{m}_{q^M} \approx m_{q^M}$.

This completes the fermion sector in the EW ν_R model.

3.1.2 The scalar sector

In the scalar sector, so far we have only added the Φ_S in addition to the SM-like scalar doublet Φ . If we only have these fields in the EW ν_R model, then neutrinos have ‘‘Dirac nature’’ i.e. they have Dirac masses. Since ν_R are part of a $SU(2)$ doublet, they would couple to the Z boson and contribute to its width, unless $m_\nu^D > M_Z/2$. But this contradicts with the experimental constraints (from particle physics as well as cosmology) on the masses of neutrino, namely $m_\nu \lesssim 1\text{eV}$. Hence, neutrinos in the EW ν_R model cannot only have the Dirac mass.

ν_R in this model must also have Majorana masses. We need to obtain neutrino masses through a seesaw mechanism. A Majorana mass of ν_R can be obtained by coupling a fermion bilinear $l_R^{M,T} \sigma_2 l_R^M$, which transforms as $(1 + 3, Y/2 = -1)$ under $SU(2) \times U(1)_Y$, with an appropriate scalar field to construct gauge invariant term in the Lagrangian. A charged scalar with a VEV would be the simplest, but its VEV would break the charge conservation. The next simplest field is a scalar triplet $\tilde{\chi}$ ($3, Y/2 = +1$):

$$\tilde{\chi} = \frac{1}{\sqrt{2}} \vec{\tau} \cdot \vec{\chi} = \begin{pmatrix} \frac{1}{\sqrt{2}}\chi^+ & \chi^{++} \\ \chi^0 & -\frac{1}{\sqrt{2}}\chi^+ \end{pmatrix}. \quad (3.13)$$

Then the Majorana mass of ν_R is generated through:

$$\mathcal{L}_M = g_M l_R^{M,T} \sigma_2 \tau_2 \tilde{\chi} l_R^M, \quad (3.14)$$

where, although σ_2 and τ_2 have same matrix form, their matrix indices are different. σ_2 's matrix indices run over Lorentz indices, whereas τ_2 's indices are those of a $SU(2)$ doublet (more on this can be found in any quantum field theory textbook; review in [11] is also a useful reference). Basically, $(l_R^{M,T} \sigma_2) = \overline{l_R^{M,c}}$, where $l_R^{M,c}$ is the charge conjugate of l_R^M .

When χ^0 acquires a VEV: $\langle \chi \rangle = v_M$, a Majorana mass term is obtained:

$$M_R = g_M v_M, \quad (3.15)$$

where M_R is the Majorana mass of ν_R . Note that Eq. (3.14) also contains a term of the form $e_R^M \chi^{++} e_R^M$, which would result in a like-sign dilepton event - a particle physics counterpart of “neutrino-less doublet β -decay” [27]. This is also a lepton-number violating term.

If M_R is lighter than $M_Z/2$, then ν_R would contribute to the width of the Z boson, which has been measured to a high precision [6]. Since it would contradict the data, this scenario is already ruled out. Thus, ν_R must have a mass $M_R \geq M_Z/2$.

Since we do not want the ν_L to acquire a Majorana mass similarly, a global $U(1)_M$ symmetry is imposed. Different fields transform as follows under this symmetry:

$$\begin{aligned} (q_R^M, l_R^M) &\rightarrow e^{i\alpha_M} (q_R^M, l_R^M), \\ \tilde{\chi} &\rightarrow e^{-2i\alpha_M} \tilde{\chi}, \quad \phi_S \rightarrow e^{-i\alpha_M} \phi_S, \end{aligned} \quad (3.16)$$

and all the other fields are singlets under $U(1)_M$. This symmetry also prevents quarks from acquiring a Majorana mass. Despite the symmetry ν_L does acquire a Majorana mass M_L at the one-loop level:

$$M_L = \lambda_S \frac{1}{16 \pi^2} \frac{m_\nu^{D^2}}{M_R} \log \left(\frac{M_R}{M_{\phi_S}} \right), \quad (3.17)$$

where λ_S and M_{ϕ_S} are the quartic coupling and the mass of ϕ_S respectively. Thus, when $\lambda_S < 1$, M_L is smaller than $m_\nu^{D^2}/M_R$ by at least two orders of magnitude.

The Majorana mass matrix can be written as

$$\mathcal{M} = \begin{pmatrix} M_L & m_\nu^D \\ m_\nu^D & M_R \end{pmatrix}, \quad (3.18)$$

where m_ν^D , M_R and M_L are given by Eqs. (3.6), (3.15) and (3.15), respectively. If $v_M \gg v_S$ and $g_{SI} \sim \mathcal{O}(g_M)$, then the eigenvalues of \mathcal{M} can be given by

$$m_\nu = M_L - \frac{(m_\nu^D)^2}{M_R} = - \left(\frac{g_{SI}^2}{g_M} \right) \frac{v_S}{v_M} v_S (1 - \epsilon) \quad \text{and} \quad M_R, \quad (3.19)$$

where $\epsilon < 10^{-2}$ and m_ν is the mass of a light neutrino.

For $M_R \sim \Lambda_{EW}$, if we consider $v_M \sim \Lambda_{EW}$, then to satisfy $m_\nu \lesssim 1$ eV,

$$v_S \approx \sqrt{v_M \times 1 \text{ eV}} \approx \mathcal{O}(10^5) \text{ eV}. \quad (3.20)$$

Thus, v_S is about 5-6 orders of magnitude smaller than the electroweak scale $\Lambda_{EW} \approx 246$ GeV. If $g_{SI} \sim \mathcal{O}(10^{-6})$, then $v_S \sim \Lambda_{EW}$. The hierarchy between Λ_{EW} and v_S is not as severe as that between the so-called ‘‘Grand Unification’’ scale ($\mathcal{O}(10^{16})$ GeV) and Λ_{EW} in typical Grand Unified Theories. This aspect is discussed in detail in [26].

The story does not end here, since we have to ensure that the ρ parameter equals 1 at the tree level. At the tree level it is defined as

$$\rho \equiv \frac{M_W^2}{M_Z^2 \cos^2 \theta_W} = 1. \quad (3.21)$$

A global $SU(2)$ symmetry, called the ‘‘custodial symmetry’’ and denoted by $SU(2)_D$, ensures that $\rho = 1$ at the tree level. At the loop-level it deviates from 1 due to radiative corrections and the custodial symmetry is broken. At the tree level, a scalar multiplet that transforms as (T, Y) under $SU(2)_L \times U(1)_Y$ and has VEV v_i , contributes to ρ as follows [28]:

$$\rho = \frac{\sum_i [4 T(T+1) - Y^2]_i v_i^2 c_{T,Y}}{2 \sum_i Y^2 v_i^2}, \quad (3.22)$$

where $c_{T,Y} = 1$ if (T, Y) is a complex representation and $c_{T,Y} = 1/2$ if (T, Y) is a real representation. The summations run over all the scalar multiplet in the model.

If one just has the triplet $\tilde{\chi}$ and nothing else, one would obtain $\rho = 1/2$ in contradiction with the fact that experimentally $\rho \approx 1$. Higgs doublets alone would give naturally $\rho = 1$. A mixture with one triplet and one doublet would give $\rho \approx 1$ if the VEV of the triplet, v_M , is much less than that of the doublet, v_2 , i.e. $v_M \ll v_2$. But this is not what we want since we would like to have v_M and v_2 of $\mathcal{O}(\Lambda_{EW})$. To preserve the custodial symmetry with a Higgs triplet, another scalar triplet $\xi = (3, Y/2 = 0)$ is needed in addition to the aforementioned $\tilde{\chi}(3, Y/2 = 1)$ and the usual doublet $\phi = (2, Y/2 = -1/2)$. Under a global $SU(2)_L \times SU(2)_R$ symmetry, the two triplets

can be grouped into a (3, 3) representation as [27, 29, 30, 31, 32]:

$$\chi = \begin{pmatrix} \chi^0 & \xi^+ & \chi^{++} \\ \chi^- & \xi^0 & \chi^+ \\ \chi^{--} & \xi^- & \xi^{0*} \end{pmatrix}. \quad (3.23)$$

Under this symmetry the SM-like scalar doublet Φ ($2, Y/2 = -1/2$) and $\tilde{\Phi} = i\tau_2\Phi^*$ can also be grouped in a (2, 2) representation as

$$\Phi_2 = \begin{pmatrix} \phi^{0*} & \phi^+ \\ \phi^- & \phi^0 \end{pmatrix} \quad (3.24)$$

This completes the field content of the $EW\nu_R$ model. The scalar sector in this minimal $EW\nu_R$ model is identical to that in the model by Georgi and Machacek [30].

3.2 Breaking of the electroweak symmetry

With this representation the kinetic part of the scalar Lagrangian can be written as [30, 32, 27]:

$$(\mathcal{L}_{S^{EW\nu_R}})_{kin} = \frac{1}{2} Tr [(D_\mu\Phi_2)^\dagger(D_\mu\Phi_2)] + \frac{1}{2} Tr [(D_\mu\chi)^\dagger(D_\mu\chi)] + |\partial_\mu\phi_S|^2 \quad (3.25)$$

The notation $(\mathcal{L}_{S^{EW\nu_R}})_{kin}$ is used to denote the kinetic part (denoted by subscript ‘kin’) of the Higgs Lagrangian (denoted by subscript ‘S’ for Scalar) in $EW\nu_R$ model (denoted by ‘ $EW\nu_R$ ’ in the subscript).

$$D_\mu\Phi \equiv \partial_\mu\Phi + \frac{1}{2} ig(\mathbf{W}_\mu \cdot \boldsymbol{\tau})\Phi - \frac{1}{2} ig' \Phi B_\mu \tau_3; \quad (3.26)$$

$$D_\mu \chi \equiv \partial_\mu \chi + ig(\mathbf{W}_\mu \cdot \mathbf{t})\chi - ig'\chi B_\mu t_3 \quad (3.27)$$

The τ_i and t_i are the 2×2 and 3×3 representation matrices of the $SU(2)$ generators respectively, following reference [32]. τ_i 's are explicitly given in Eq. (1.23) and t_i 's are given by

$$t_1 = \frac{1}{\sqrt{2}} \begin{pmatrix} 0 & 1 & 0 \\ 1 & 0 & 1 \\ 0 & 1 & 0 \end{pmatrix}, \quad t_2 = \frac{1}{\sqrt{2}} \begin{pmatrix} 0 & -i & 0 \\ i & 0 & -i \\ 0 & i & 0 \end{pmatrix}, \quad t_3 = \begin{pmatrix} 1 & 0 & 0 \\ 0 & 0 & 0 \\ 0 & 0 & 1 \end{pmatrix}. \quad (3.28)$$

We work under the premise that the hierarchy in neutrino masses in EW ν_R model comes from the VEV of ϕ_S [27]. Thus, $v_S \sim 10^5$ eV and as a result the mixing between ϕ_S and other scalars is negligible. Hence, hereafter in the related calculations we neglect this mixing.

After the spontaneous breaking of $SU(2)_L \times U(1)_Y$ to $U(1)_{EM}$, expanding the Lagrangian in equation (3.25), one can find the Feynman rules for the three point and four point interactions between physical scalars, Nambu-Goldstone bosons and electroweak gauge bosons W , Z and γ . For the corresponding SM Feynman rules it is useful to recall the kinetic part of the SM-Higgs Lagrangian:

$$(\mathcal{L}_{SSM})_{kin} = \frac{1}{2} Tr [(D_\mu \Phi)^\dagger (D_\mu \Phi)] \quad (3.29)$$

The interactions of the SM leptons with the $SU(2)_L \times U(1)_Y$ gauge bosons arise similar to the SM, from the terms:

$$\bar{l}_L \not{D} l_L; \quad \bar{e}_R \not{D} e_R, \quad (3.30)$$

where

$$\begin{aligned}\not{D}l_L &\equiv \gamma^\mu(\partial_\mu - \frac{1}{2}ig(\mathbf{W}_\mu \cdot \boldsymbol{\tau}) + \frac{1}{2}ig'B_\mu)l_L, \\ \not{D}e_R &\equiv \gamma^\mu(\partial_\mu + ig'B_\mu)e_R.\end{aligned}\tag{3.31}$$

The interactions of mirror leptons with the gauge bosons arise from the terms

$$\bar{l}_R^M \not{D}l_R^M; \bar{e}_L^M \not{D}e_L^M,\tag{3.32}$$

where

$$\begin{aligned}\not{D}l_R^M &\equiv \gamma^\mu(\partial_\mu - \frac{1}{2}ig(\mathbf{W}_\mu \cdot \boldsymbol{\tau}) + \frac{1}{2}ig'B_\mu)l_R^M, \\ \not{D}e_L^M &\equiv \gamma^\mu(\partial_\mu + ig'B_\mu)e_L^M.\end{aligned}\tag{3.33}$$

The gauge interactions of the SM quarks and the mirror quarks can similarly be found from

$$\bar{q}_L \not{D}q_L; \bar{d}_R \not{D}d_R; \bar{u}_R \not{D}u_R; \bar{q}_R^M \not{D}q_R^M; \bar{d}_L^M \not{D}d_L^M; \bar{u}_L^M \not{D}u_L^M.\tag{3.34}$$

To generate masses of the gauge bosons and the fermions the $SU(2)_L \times U(1)_Y$ gauge symmetry must be spontaneously broken to $U(1)_{EM}$. To get the physical scalar spectrum, we need to write a general scalar potential that obeys a global

$SU(2)_L \times SU(2)_R$. It can be written as

$$\begin{aligned}
V(\Phi_2, \chi) = & \lambda_1 \left(\text{Tr} \Phi_2^\dagger \Phi_2 - v_2^2 \right)^2 + \lambda_2 \left(\text{Tr} \chi^\dagger \chi - 3v_M^2 \right)^2 \\
& + \lambda_3 \left(\text{Tr} \Phi_2^\dagger \Phi_2 - v_2^2 + \text{Tr} \chi^\dagger \chi - 3v_M^2 \right)^2 \\
& + \lambda_4 \left((\text{Tr} \Phi_2^\dagger \Phi_2) (\text{Tr} \chi^\dagger \chi) - 2 \left(\text{Tr} \Phi_2^\dagger \frac{\tau^a}{2} \Phi_2 \frac{\tau^b}{2} \right) (\text{Tr} \chi^\dagger T^a \chi T^b) \right) \\
& + \lambda_5 \left(3 \text{Tr} \chi^\dagger \chi \chi^\dagger \chi - (\text{Tr} \chi^\dagger \chi)^2 \right), \tag{3.35}
\end{aligned}$$

where repeated indices a, b are summed over. Note that this potential is invariant under $\chi \rightarrow -\chi$ so that the cubic terms in the potential are eliminated. In order for this potential to be positive semidefinite the following conditions must be imposed: $\lambda_1 + \lambda_2 + 2\lambda_3 > 0$, $\lambda_1\lambda_2 + \lambda_1\lambda_3 + \lambda_2\lambda_3 > 0$, $\lambda_4 > 0$, $\lambda_5 > 0$ [27].

When the $SU(2)_L \times U(1)_Y \rightarrow U(1)_{EM}$ in the vacuum state of the scalar potential, the global $SU(2)_L \times SU(2)_R$ symmetry of the potential breaks down to $SU(2)_D$ custodial symmetry if the vacuum alignment of Φ_2 and χ is as follows:

$$\langle \chi \rangle = \begin{pmatrix} v_M & 0 & 0 \\ 0 & v_M & 0 \\ 0 & 0 & v_M \end{pmatrix}, \tag{3.36}$$

and

$$\langle \Phi \rangle = \begin{pmatrix} v_2/\sqrt{2} & 0 \\ 0 & v_2/\sqrt{2} \end{pmatrix}. \tag{3.37}$$

After the spontaneous symmetry breaking one obtains the W^\pm , Z bosons and the photon A , in the same way as in SM (explained in Chapter 1). Also, $M_W = gv/2$ and $M_Z = M_W/\cos\theta_W$, with $v = \sqrt{v_2^2 + 8v_M^2} \approx 246 \text{ GeV}$ and, at tree level, $\rho = M_W^2/(M_Z^2 \cos^2\theta_W) = 1$ as desired.

3.2.1 The physical scalars

To express the physical states we define a few subsidiary fields [27]:

$$\begin{aligned}\phi^0 &\equiv \frac{1}{\sqrt{2}}\left(v_2 + \phi^{0r} + i\phi^{0i}\right), & \chi^0 &\equiv v_M + \frac{1}{\sqrt{2}}\left(\chi^{0r} + i\chi^{0i}\right); \\ \psi^\pm &\equiv \frac{1}{\sqrt{2}}\left(\chi^\pm + \xi^\pm\right), & \zeta^\pm &\equiv \frac{1}{\sqrt{2}}\left(\chi^\pm - \xi^\pm\right)\end{aligned}\quad (3.38)$$

for the complex neutral and charged fields respectively. Here the quantities with superscripts ‘r’ and ‘i’ denote the ‘real’ and the ‘imaginary’ components, respectively. Note that the real components, ϕ^{0r} and χ^{0r} , have *zero* vacuum expectation values. We will also define

$$s_H = \sin\theta_H = \frac{2\sqrt{2}v_M}{v}, \quad c_H = \cos\theta_H = \frac{v_2}{v} \quad (3.39)$$

With this notation, the Nambu-Goldstone bosons are given by

$$G_3^\pm = c_H\phi^\pm + s_H\psi^\pm, \quad G_3^0 = i\left(-c_H\phi^{0i} + s_H\chi^{0i}\right). \quad (3.40)$$

Just like in SM, these N-G bosons are absorbed by the longitudinal polarization of the massive W^\pm and Z bosons.

After the symmetry breaking, the scalar potential in Eq. (5.16) preserves the custodial $SU(2)_D$. Therefore, the *ten* massive physical scalars can be grouped into **5**

+ $\mathbf{3} + \mathbf{1}$ (2 singlets) of the custodial $SU(2)_D$, as follows:

$$\begin{aligned}
\text{five-plet (quintet)} &\rightarrow H_5^{\pm\pm}, H_5^\pm, H_5^0; \\
\text{triplet} &\rightarrow H_3^\pm, H_3^0; \\
\text{two singlets} &\rightarrow H_1^0, H_1^{0'}, \tag{3.41}
\end{aligned}$$

where

$$\begin{aligned}
H_5^{++} &= \chi^{++}, H_5^+ = \zeta^+, H_3^+ = c_H \psi^+ - s_H \phi^+, \\
H_5^0 &= \frac{1}{\sqrt{6}} (2\xi^0 - \sqrt{2}\chi^{0r}), H_3^0 = i(c_H \chi^{0i} + s_H \phi^{0i}), \\
H_1^0 &= \phi^{0r}, H_1^{0'} = \frac{1}{\sqrt{3}} (\sqrt{2}\chi^{0r} + \xi^0), \tag{3.42}
\end{aligned}$$

with $H_5^{--} = (H_5^{++})^*$, $H_5^- = -(H_5^+)^*$, $H_3^- = -(H_3^+)^*$, and $H_3^0 = -(H_3^0)^*$. The Feynman rules, the loop diagrams and the oblique parameters (in Chapter 4), will be expressed in terms of these physical scalar five-plet, triplet, two singlets and their masses, $m_{H_5^{\pm\pm, \pm, 0}}$, $m_{H_3^\pm, 0}$, m_{H_1} , $m_{H_1'}$ respectively.

While the custodial symmetry is preserved, the scalar multiplets are degenerate. Their masses are given as:

$$m_{H_5^{\pm\pm, \pm, 0}}^2 = m_5^2 = 3(\lambda_4 c_H^2 + \lambda_5 s_H^2), \quad m_{H_3^\pm, 0}^2 = m_3^2 = \lambda_4 v^2. \tag{3.43}$$

The two singlets H_1^0 and $H_1^{0'}$ can mix according to the mass-squared matrix given as:

$$\mathcal{M}_{H_1^0, H_1^{0'}}^2 = v^2 \begin{pmatrix} 8c_H^2 (\lambda_1 + \lambda_3) & 2\sqrt{6}s_H c_H \lambda_3 \\ 2\sqrt{6}s_H c_H \lambda_3 & 3s_H^2 (\lambda_2 + \lambda_3) \end{pmatrix} \tag{3.44}$$

The oblique parameters, the Feynman rules and the loop diagrams are expressed in terms of the VEVs of the doublet and triplets, and the masses of the physical scalars- $m_{H_5^{\pm\pm,\pm,0}}, m_{H_3^{\pm,0}}, m_1, m_{H'_1}$.

The custodial symmetry is broken at the loop level, splitting the masses of the scalar multiplet members. However, the symmetry could also be broken explicitly by some terms, which split the masses within the multiplets. We do not list any such terms in this dissertation, but we do keep this at the back of our mind and denote the masses of the multiplet members separately in all the formulas.

The Feynman rules for the gauge interactions of fermions (SM fermions and mirror fermions) in the $EW\nu_R$ model can be evaluated from

$$(\mathcal{L}_{F^{EW\nu_R}})_{int} = (\mathcal{L}_{F^{SM}})_{int} + (\mathcal{L}_{F^M})_{int} , \quad (3.45)$$

where $(\mathcal{L}_{F^{SM}})_{int}$ comes from the fermion sector in the SM and is given by

$$\begin{aligned} (\mathcal{L}_{F^{SM}})_{int} &= \frac{g}{\sqrt{2}} \left[(\bar{u}_L^j \gamma^\mu d_{Lj} + \bar{\nu}_L^j \gamma^\mu e_{Lj}) W_\mu^+ + (\bar{d}_L^j \gamma^\mu u_{Lj} + \bar{e}_L^j \gamma^\mu \nu_{Lj}) W_\mu^- \right] \\ &+ \frac{g}{c_W} \left[\sum_{f=u_j, d_j, \nu_j, e_j} (T_3^f - s_W^2 Q_f) \bar{f}_L^j \gamma^\mu f_{Lj} - \sum_{f=u_j, d_j, e_j} s_W^2 Q_f \bar{f}_R^j \gamma^\mu f_{Rj} \right] Z_\mu \\ &+ e \sum_{f=u_j, d_j, e_j} Q_f (\bar{f}_L^j \gamma^\mu f_{Lj} + \bar{f}_R^j \gamma^\mu f_{Rj}) A_\mu \end{aligned} \quad (3.46)$$

and $(\mathcal{L}_{F^M})_{int}$ includes interaction terms arising due to the mirror fermion-sector in the $EW\nu_R$ model.

To write the mirror fermions part $(\mathcal{L}_{F^M})_{int}$ remember that the W bosons couple only to $SU(2)$ doublets of fermions. Thus, only the right-handed mirror fermions couple to the W^\pm , as opposed to $(\mathcal{L}_{F^{SM}})_{int}$, where only left-handed SM fermions

interact with the W^\pm bosons. Similarly the three-point couplings of the right-handed mirror fermions with Z and γ bosons at the tree-level are same as those for the left-handed SM fermions. Hence, $(\mathcal{L}_{FM})_{int}$, is given by

$$\begin{aligned}
(\mathcal{L}_{FM})_{int} = & \frac{g}{\sqrt{2}} \left[(\bar{u}_R^{Mi} \gamma^\mu d_{Ri}^M + \bar{\nu}_R^i \gamma^\mu e_{Ri}^M) W_\mu^+ + (\bar{d}_R^{Mi} \gamma^\mu u_{Ri}^M + \bar{e}_R^{Mi} \gamma^\mu \nu_{Ri}^M) W_\mu^- \right] \\
& + \frac{g}{c_W} \left[\sum_{f^M = u^M, d^M, \nu^M, e^M} (T_3^{f^M} - s_W^2 Q_{f^M}) \bar{f}_R^{Mi} \gamma^\mu f_{Ri}^M \right. \\
& \quad \left. - \sum_{f^M = u^M, d^M, e^M} s_W^2 Q_{f^M} \bar{f}_L^{Mi} \gamma^\mu f_{Li}^M \right] Z_\mu \\
& + e \sum_{f^M = u^M, d^M, e^M} Q_{f^M} (\bar{f}_R^{Mi} \gamma^\mu f_{Ri}^M + \bar{f}_L^{Mi} \gamma^\mu f_{Li}^M) A_\mu. \tag{3.47}
\end{aligned}$$

In equation (3.47) $i, j = 1, 2, 3$, where i denotes fermions in the i^{th} mirror-quark or mirror-lepton generation. u_i^M and d_i^M denote the up- and the down- members of a mirror-quark generation respectively. Following a similar notation (ν_{Ri} and e_i^M) denote (the neutrino and the ‘electron’) members of a mirror-lepton generation respectively.

In Appendix B we have listed various Feynman rules in the minimal $EW\nu_R$ model, which will be used in the calculation of the ‘‘oblique parameters’’, discussed in the next chapter.

3.3 Summary of the minimal $EW\nu_R$ model

In this section we summarize main features of the minimal $EW\nu_R$ model. First, in Fig. 3.1 we show the physical particle spectrum in the model.

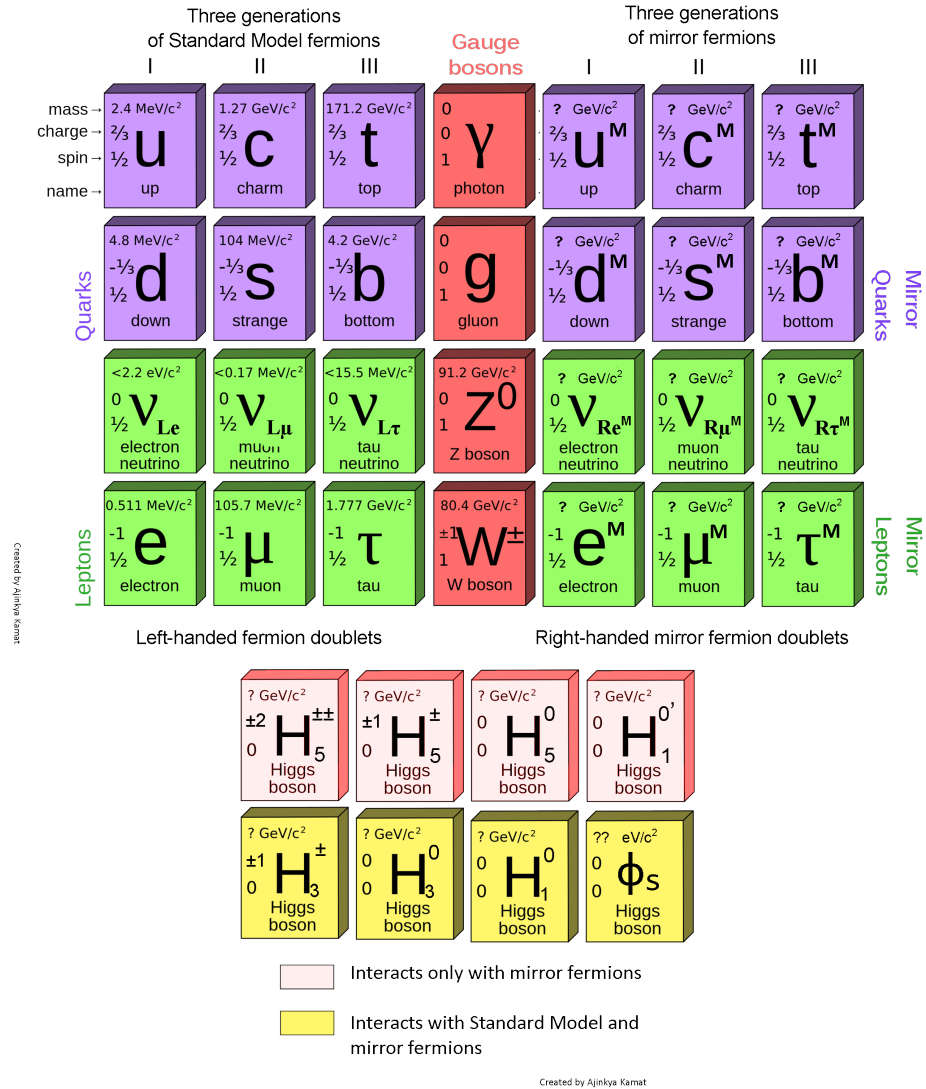


Figure 3.1: Physical particle spectrum in the minimal EWν_R model

3.3.1 What’s the advantage of the mirror fermions?

The EWν_R model predicts the existence of the mirror fermions which have opposite chirality to their SM counterparts having the same $SU(2)_L$ quantum numbers. Since their masses are also expected to be near the electroweak scale, it is possible to probe their phenomenology at the Large Hadron Collider.

3.3.2 Why don't we see mirror fermions today?

As seen in Eqs. (3.3) and (3.9), the mirror fermions couple to the SM fermions through interactions of the form $g_{Sd} \bar{d}_L d_R^M$, $g_{Sl} \bar{e}_L e_R^M$. In particular, since ϕ_S is expected to have a mass of $\mathcal{O}(10^5 \text{ eV})$, the decay modes the following decay modes are possible for the mirror fermions: $e_R^M \rightarrow e_L + \phi_S$, $q_R^M \rightarrow q_L + \phi_S$.

Thus, all the mirror fermions and ν_R 's, created after the big bang, have already decayed to the SM fermions. The mirror quarks could not form mirror-hadrons through their $SU(3)_C$ couplings, since they had already decayed before the baryons were formed.

The same decay modes could be the signals of the mirror fermions at the LHC. If a mirror lepton or mirror quark is created in a process at the LHC, it would decay to the corresponding SM fermion by emitting a ϕ_S . If the couplings g_{Sl} and g_{Sq} are large, then these decays would occur within the beam pipe of the detector, in which case the mirror fermions would not be detected. If these couplings are small enough, then the vertex of the decay would be "displaced". Such decay would have a final state of lepton + missing energy or jet + missing energy. This is an interesting aspect of the phenomenology of the mirror fermions, and could be a subject for future analysis.

3.3.3 Doesn't ν_R contribute to the total energy density?

From Eq. (3.3) we can see that the decay modes such as $\nu_R \rightarrow \nu_L + \phi_S$ and $e_R^M \rightarrow e_L + \bar{\nu}_L + \nu_R \rightarrow e_L + \bar{\nu}_L + \nu_L + \phi_S$ are also possible. Thus, all the ν_R 's also decayed to ν_L 's and ϕ_S . Those ν_R 's created today in astrophysical processes also decay *soon*, and therefore do not contribute to the total energy density of the Universe.

3.3.4 Does this model have a ‘dark matter’ candidate?

The only particle in the $\text{EW}\nu_R$ model that seems to be as sterile as the dark matter is ϕ_S . Since it is as light as $\mathcal{O}(10^5 \text{ eV})$, it would not be a “cold dark matter” candidate.

On the other hand, the mirror fermions in the $\text{EW}\nu_R$ model also occur in a model of dark matter asymmetry - the “Luminogenesis” model [33]. The dark matter candidates in this model are not part of the particle spectrum in the minimal $\text{EW}\nu_R$ model.

3.3.5 Main features of the model

- In the $\text{EW}\nu_R$ model the non-sterile right-handed neutrinos ν_R naturally acquire a Majorana mass near the electroweak scale. A lower limit of $M_Z/2$ is set on this mass M_R , based on data for the Z width. The ν_R in this model can be produced at the LHC and hence, the seesaw mechanism can be directly tested.
- In many other models, when ν_R obtains a Majorana mass from VEV of a singlet or a triplet scalar field, a massless N-G boson, called “Majoron”, arises due to the violation of the lepton number or the $B - L$ number (refer to [26] and references therein). No such N-G bosons arise here.
- The $\text{EW}\nu_R$ model achieves this without adding any more gauge bosons to the SM.
- Although the $\text{EW}\nu_R$ model stands on its own, it is also possible to embed this model in the $E(6)$ Grand Unification group [26, 34].
- The $\text{EW}\nu_R$ model predicts the existence of the mirror fermions which have opposite chirality to their SM counterparts having the same $SU(2)_L$ quantum

numbers. Since their masses are also expected to be near the electroweak scale, it is possible to probe their phenomenology at the Large Hadron Collider.

- This model contains a very interesting scalar sector that includes a doubly charged Higgs and multiple singly charged Higgs'. These can have interesting phenomenology at the Large Hadron Collider [27]. Although there have been searches for charged Higgs at the LHC, the searches did not include the kind of processes that would probe the charged scalar sector in this model.
- In SM the gauge anomalies [10] in the lepton sector can be cancelled only due to the quark sector. In the $EW\nu_R$ model, the anomaly cancellation happens in an interesting way, meaning that the anomalies within the SM lepton sector cancel those in the mirror lepton sector. Similarly the anomalies in the quark sector also cancel among themselves.
- This model also proposes the existence of a $SU(2)$ singlet scalar ϕ_S . An interesting scenario is possible in which the VEV of ϕ_S evolves with time. Thus, ϕ_S can play a role of a slow-rolling field considered in [35, 26].

In the following chapters in this dissertation, we will analyze the phenomenology in the minimal $EW\nu_R$ model, first in the context of the electroweak precision parameters and later in the light of the 125-GeV Higgs at the LHC.

Chapter 4

Contributions to Oblique Parameters in the $EW\nu_R$ Model

As mentioned in the Foreword of this dissertation, for any theoretical model to be viable, it must not contradict with experimental constraints from experiments in the past. In this chapter we discuss relevant constraints on the minimal $EW\nu_R$ model [26] - those coming from the so-called “Oblique Parameters” S and T .

In the first section we explain what oblique parameters are and why are they relevant for the $EW\nu_R$ model. In the two following sections we derive the contributions to the relevant oblique parameters from this model and discuss their agreement with the experimental constraints, respectively.

4.1 Defining Oblique Parameters

4.1.1 What are Oblique Parameters?

Effects of the vacuum polarization diagrams (oblique corrections) on the electroweak-interaction observables can be parametrized by three finite parameters denoted by

S , T and U , known as the *Oblique Parameters* [36, 6, 37]. Their formalism was first put forward by Peskin and T. Takeuchi [36]. These are finite, measurable and renormalization-scheme independent quantities. Since polarization diagrams are higher order processes (one-loop or higher), oblique parameters can be helpful in probing higher-order effects BSM (Beyond the Standard Model) physics.

We will discuss their formulas and derivations shortly, but let us first consider how measurements of the oblique parameters can be used as constraints on new physics.

Based on the Lagrangian of any model vacuum polarization diagrams and oblique parameters can be calculated. Hence, for a set of numerical values of relevant parameters in the model, numerical values of the oblique parameters can be predicted. The Standard Model also predicts certain values for the oblique parameters. On the other hand, the oblique parameters have also been measured experimentally [6]. The SM values lie within the error bars of the experimental values.

Although this is another of many success stories of SM, the error bars also leave a room for new physics. At the same time these error bars also constrain new physics! Let us consider the S parameter, for instance. We can naively write

$$S = S_{SM} + \tilde{S}, \quad (4.1)$$

where S on the left-hand side is the measured/real value of the parameter, S_{SM} is the SM-prediction for it and \tilde{S} is the “new physics” contribution to S (following the notation from [38]). Thus, SM-predicted value of \tilde{S} is 0. Similarly, \tilde{T} , and \tilde{U} are also new-physics contributions to T and U parameters respectively, both of them having SM-predicted value 0. We will refer to all S , T , U , as well as \tilde{S} , \tilde{T} , \tilde{U} as “Oblique Parameters”. There is a small caveat in implementing this procedure to calculate theoretical predictions. We would discuss it after digging a little deeper into the

definitions and derivations of the oblique parameters.

Using these parameters one could probe the effects of new physics on the electroweak interactions at the one-loop level, if the new physics scale is much larger as compared to M_Z .

In a regime where the scale of new physics that is being probed is much larger than M_Z , these parameters were defined using a perturbative expansion as [36]:

$$\begin{aligned}
 \alpha S &\equiv 4e^2[\Pi'_{33}(0) - \Pi'_{3Q}(0)], \\
 \alpha T &\equiv \frac{e^2}{s_W^2 c_W^2 M_Z^2}[\Pi_{11}(0) - \Pi_{33}(0)], \\
 \alpha U &\equiv 4e^2[\Pi'_{11}(0) - \Pi'_{33}(0)],
 \end{aligned} \tag{4.2}$$

where $s_W = \sin \theta_W$, $c_W = \cos \theta_W$ are the functions of the weak-mixing angle θ_W . Π_{11} and Π_{33} are vacuum polarizations of the isospin currents and Π_{3Q} the vacuum polarization of one isospin and one electromagnetic current. The Π' functions are defined as $\Pi'(0) = (\Pi(q^2) - \Pi(0)) / q^2$ in general. We will be using $q^2 = M_Z^2$.

After the electroweak symmetry breaking the weak gauge boson triplet (W_1, W_2, W_3^0) and the hypercharge gauge boson B mix to yield W^\pm, Z^0 and γ . Therefore, Π_{11}, Π_{33} and Π_{3Q} and hence, the oblique parameters can also be expressed in terms of the self energies of W, Z, γ and the $Z - \gamma$ mixing [36].

S , T and U can be expressed as:

$$\frac{\hat{\alpha}}{4\hat{s}_W^2\hat{c}_W^2}S = \frac{1}{M_Z^2} \left[\bar{\Pi}_{ZZ}(M_Z^2) - \left(\frac{\hat{c}_W^2 - \hat{s}_W^2}{\hat{c}_W^2\hat{s}_W^2} \right) \bar{\Pi}_{Z\gamma}(M_Z^2) - \bar{\Pi}_{\gamma\gamma}(M_Z^2) \right]^{\text{EW}\nu_R} \quad (4.3)$$

$$\hat{\alpha}T = \frac{1}{M_W^2} \left[\Pi_{11}(0) - \Pi_{33}(0) \right]^{\text{EW}\nu_R} \quad (4.4)$$

$$\frac{\hat{\alpha}}{4\hat{s}_W^2}U = \left[\frac{\bar{\Pi}_{WW}(M_W^2)}{M_W^2} - \hat{c}_W^2 \frac{\bar{\Pi}_{ZZ}(M_Z^2)}{M_Z^2} - 2\hat{s}_W\hat{c}_W \frac{\bar{\Pi}_{Z\gamma}(M_Z^2)}{M_Z^2} - \hat{s}_W^2 \frac{\bar{\Pi}_{\gamma\gamma}(M_Z^2)}{M_Z^2} \right]^{\text{EW}\nu_R} \quad (4.5)$$

The superscript ‘EW ν_R ’ denotes the contribution in the EW ν_R model. They can be defined for any other model in a similar way. Hence, the new physics contributions to the oblique parameters in the EW ν_R model should be calculated using

$$\begin{aligned} \frac{\hat{\alpha}}{4\hat{s}_W^2\hat{c}_W^2}\tilde{S} &= \frac{1}{M_Z^2} \left[\bar{\Pi}_{ZZ}(M_Z^2) - \left(\frac{\hat{c}_W^2 - \hat{s}_W^2}{\hat{c}_W^2\hat{s}_W^2} \right) \bar{\Pi}_{Z\gamma}(M_Z^2) - \bar{\Pi}_{\gamma\gamma}(M_Z^2) \right]^{\text{EW}\nu_R} \\ &\quad - \frac{1}{M_Z^2} \left[\bar{\Pi}_{ZZ}(M_Z^2) - \left(\frac{\hat{c}_W^2 - \hat{s}_W^2}{\hat{c}_W^2\hat{s}_W^2} \right) \bar{\Pi}_{Z\gamma}(M_Z^2) - \bar{\Pi}_{\gamma\gamma}(M_Z^2) \right]^{\text{SM}} \end{aligned} \quad (4.6)$$

$$\hat{\alpha}\tilde{T} = \frac{1}{M_W^2} \left[\Pi_{11}(0) - \Pi_{33}(0) \right]^{\text{EW}\nu_R} - \frac{1}{M_W^2} \left[\Pi_{11}(0) - \Pi_{33}(0) \right]^{\text{SM}} \quad (4.7)$$

$$\begin{aligned} \frac{\hat{\alpha}}{4\hat{s}_W^2}\tilde{U} &= \left[\frac{\bar{\Pi}_{WW}(M_W^2)}{M_W^2} - \hat{c}_W^2 \frac{\bar{\Pi}_{ZZ}(M_Z^2)}{M_Z^2} - 2\hat{s}_W\hat{c}_W \frac{\bar{\Pi}_{Z\gamma}(M_Z^2)}{M_Z^2} - \hat{s}_W^2 \frac{\bar{\Pi}_{\gamma\gamma}(M_Z^2)}{M_Z^2} \right]^{\text{EW}\nu_R} \\ &\quad - \left[\frac{\bar{\Pi}_{WW}(M_W^2)}{M_W^2} - \hat{c}_W^2 \frac{\bar{\Pi}_{ZZ}(M_Z^2)}{M_Z^2} - 2\hat{s}_W\hat{c}_W \frac{\bar{\Pi}_{Z\gamma}(M_Z^2)}{M_Z^2} - \hat{s}_W^2 \frac{\bar{\Pi}_{\gamma\gamma}(M_Z^2)}{M_Z^2} \right]^{\text{SM}} \end{aligned} \quad (4.8)$$

where all quantities with a hat on top ($\hat{}$) i.e. \hat{s}_W , \hat{c}_W , $\hat{\alpha} \equiv \hat{g}^2\hat{s}_W^2/(4\pi)$ are defined in the \overline{MS} renormalization scheme evaluated at M_Z [6]. $\bar{\Pi}(q^2) = \Pi(q^2) - \Pi(0)$ [36].

Hereafter, in this chapter and in the context of oblique parameters elsewhere in this dissertation the hats on top of these and other quantities are omitted, but implied, unless otherwise is stated.

We can see that

- S is associated with the difference between the Z self-energy at $q^2 = M_Z^2$ and $q^2 = 0$
- T is proportional to the difference between the isospin currents Π_{11} and Π_{33} at $q^2 = 0$.
- U is proportional to the difference between the charged and the neutral currents

The new physics contribution to U in the $\text{EW}\nu_R$ model is small as compared to that to S and T . Also, this contribution is constrained only by M_W , and the width, Γ_W , of the W boson. Thus, we can project the STU parameter space on the 2-D $S - T$ parameter space in the $U = 0$ plane [39]. Hence, we focus on the constraints on S and T parameters only.

Another way to define T is in terms of the ‘ ρ parameter’:

$$T = \rho = \frac{M_W^2}{M_Z^2 \cos^2 \theta_W} \quad \text{or} \quad \tilde{T} = 1 - \rho = 1 - \frac{M_W^2}{M_Z^2 \cos^2 \theta_W} \quad (4.9)$$

The SM prediction for T at the *tree-level* is 1. T or ρ are measures of the breaking of custodial symmetry i.e. of the splitting between the masses of different members within a multiplet in fermion and scalar sectors.

Experimentally measured values of the oblique parameters \tilde{S} and \tilde{T} should be used to constrain the new physics contribution in any model. When we performed

this analysis, we used the latest values then, with 2σ constraints [40]:

$$\tilde{S} = -0.02 \pm 0.14 \quad \text{and} \quad \tilde{T} = 0.06 \pm 0.14 \quad (4.10)$$

with a statistical correlation 0.88 between the two [6].

4.1.2 Why are Oblique Parameters relevant?

Any model that adds extra chiral fermion doublets (doublets of fermions which have definite ‘handedness’ or ‘chirality’ or definite eigenvalues corresponding to the γ_5 operator) to SM raises a question of potential large contributions from these extra doublets to the oblique parameters. It is known that such extra chiral doublets yield a large positive contribution to the S parameter. Even if the \tilde{T} parameter is set to 0 by making members of the chiral fermion doublets degenerate, the \tilde{S} contribution still remains large in magnitude *with a positive sign*. This is, in fact, a major problem that ‘Technicolor’ models run into [41].

The $\text{EW}\nu_R$ model also introduces one right-handed mirror fermion doublet for every SM left-handed doublet, and similarly one left-handed singlet for every right-handed SM singlet. Thus, this model contains *twice* as many chiral fermion doublets as SM. Therefore, constraints from the oblique parameters are the most relevant ones to test the agreement of the $\text{EW}\nu_R$ model with the experimental results (Step 1 in the analysis of a theoretical model).

The $\text{EW}\nu_R$ model can agree with these constraints if the large negative contribution from the fermion sector in the model are somehow canceled by the contribution from the scalar sector in the model. We will present numerical results in section 4.4 to show that this, indeed, happens and the $\text{EW}\nu_R$ model does not contradict with the electroweak precision constraints coming from the oblique parameters.

4.2 Calculating new physics contributions to Oblique Parameters

The self energies relevant for calculating the oblique parameters can be obtained from the loop-level contributions to corresponding gauge boson propagators. We are interested in oblique corrections calculated up to one-loop level i.e. considering only one-loop radiative contributions to the oblique parameters.

In the $EW\nu_R$ model (refer to Chapter 3), quantum numbers of fermions and scalars under $SU(2) \times U(1)_Y$ gauge symmetry are such that a fermion and a scalar do not simultaneously enter in a one-loop interaction that contributes to an electroweak gauge boson propagator. The scalar and fermion sectors in the $EW\nu_R$ model, thus contribute to the radiative corrections through separate one-loop interactions. Same is also true for the Standard Model (recall that to calculate \tilde{S} and \tilde{T} we need to consider contributions from the $EW\nu_R$ model and SM). We can therefore calculate contributions to \tilde{S} and \tilde{T} from the scalar sector and the fermion sector separately and add them up to obtain the total contributions.

Similarly, due to opposite chirality of mirror fermion and SM fermion doublets (and singlets), mirror fermions and SM fermions contribute to \tilde{S} and \tilde{T} independently. Thus, from Eqs. (4.6,4.7), only mirror fermions contribute to \tilde{S} and \tilde{T} . Also note that the scalar sector contributions and mirror fermion sector contributions in $EW\nu_R$ model are separately finite. We denote the scalar contributions to \tilde{S} and \tilde{T} by \tilde{S}_{scalar} , \tilde{T}_{scalar} respectively. Contributions from the mirror fermion sector in $EW\nu_R$ model are denoted by $\tilde{S}_{fermion}$, $\tilde{T}_{fermion}$ respectively. Thus,

$$\tilde{S} = \tilde{S}_{scalar} + \tilde{S}_{fermion} \quad (4.11)$$

$$\tilde{T} = \tilde{T}_{scalar} + \tilde{T}_{fermion} . \quad (4.12)$$

New physics contributions to S and T due to the scalar sector of the $\text{EW}\nu_R$ model are given in Eq. (4.15) and Eq. (4.17) respectively. The corresponding new physics contributions to S and T due to the lepton sector in the $\text{EW}\nu_R$ model are given in Eq. (4.18) and Eq.(4.20) respectively. Similarly, the new physics contributions to S and T due to the quarks in the $\text{EW}\nu_R$ model are given in Eq. (4.21) and Eq. (4.22) respectively. It should be noted that in this dissertation we assume that the mixings between different mirror-quark and mirror-lepton generations are negligible. Thus, the mass matrices for these fermion sectors are already diagonal. To compare the new physics contributions from the $\text{EW}\nu_R$ model with the experimental constraints (refer to the plots in section 4.4) we have considered wide ranges of the mirror fermions masses. Hence, even if small non-zero mixings between different mirror fermion generations are included, it will only move individual points in the available parameter space, but will not significantly affect the total available parameter space and will not influence the conclusions of this chapter. We will discuss step-by-step derivations of new physics contributions to S and T in Section 4.3.

4.3 Calculation of One Loop Contributions to the Oblique Parameters in the $\text{EW}\nu_R$ model

One loop contributions to the oblique parameters in the $\text{EW}\nu_R$ model can be calculated from the cubic and quartic couplings listed in Appendix B and using the loop integral functions illustrated in Appendix A and C. The SM loop diagrams contributing to S , T can be similarly obtained from the SM cubic and quartic couplings in equations (3.29), $(\mathcal{L}_{FSM})_{int}$ and using loop integrals from Appendix A and C. The new physics contributions to S from the scalar sector and mirror fermion sector in

EW ν_R model will be calculated separately and then added to find the total contribution \tilde{S} (Eq. (4.6)). Similar procedure will be followed to calculate \tilde{T} (Eq. (4.7)). Thus, as in eqns. (4.11), (4.12),

$$\tilde{S} = \tilde{S}_{scalar} + \tilde{S}_{fermion}, \quad \tilde{T} = \tilde{T}_{scalar} + \tilde{T}_{fermion}. \quad (4.13)$$

Recall (Eq. (4.6)) that the contributions to \tilde{S} come from Z and γ self-energies, $Z\gamma$ mixing, each calculated up to one-loop level. To evaluate \tilde{T} using equation (4.7) the isospin current Π_{11} and electromagnetic current Π_{33} are used. The W and Z self-energies are related to these isospin currents by [36],

$$\begin{aligned} \Pi_{WW} &= \frac{e^2}{s_W^2} \Pi_{11}; \\ \Pi_{ZZ} &= \frac{e^2}{s_W^2 c_W^2} (\Pi_{33} - 2s_W^2 \Pi_{3Q} + s_W^4 \Pi_{QQ}) \end{aligned} \quad (4.14)$$

Using these relations Π_{11} can be obtained from the loop contributions to Π_{WW} listed in tables C.1, C.3, C.4. From equation (4.14) the one-loop contributions to Π_{33} can be obtained using $\lim_{g' \rightarrow 0} (\Pi_{ZZ})$. These contributions are listed below, separately from Π_{ZZ} for scalar as well as fermion sectors in the EW ν_R model.

4.3.1 Contributions to Oblique Parameters from the scalar sector in the EW ν_R model

Using tables C.1, C.2, C.3, C.4, C.5, C.6 and Eq. (4.6) the new physics contribution, \tilde{S}_{scalar} is given by (as in Eq. (4.15))

$$\begin{aligned}
\tilde{S}_{scalar} &= S_{scalar}^{EW\nu_R} - S_{scalar}^{SM} \\
&= \frac{1}{M_Z^2 \pi} \left\{ \frac{4}{3} s_H^2 \left[\bar{B}_{22}(M_Z^2; M_Z^2, m_{H_5^0}^2) - M_Z^2 \bar{B}_0(M_Z^2; M_Z^2, m_{H_5^0}^2) \right] \right. \\
&\quad + 2 s_H^2 \left[\bar{B}_{22}(M_Z^2; M_Z^2, m_{H_5^+}^2) - M_W^2 \bar{B}_0(M_Z^2; M_Z^2, m_{H_5^+}^2) \right] \\
&\quad + c_H^2 \left[\bar{B}_{22}(M_Z^2; M_Z^2, m_{H_1}^2) - M_Z^2 \bar{B}_0(M_Z^2; M_Z^2, m_{H_1}^2) \right] \\
&\quad + \frac{8}{3} s_H^2 \left[\bar{B}_{22}(M_Z^2; M_Z^2, m_{H_1'}^2) - M_Z^2 \bar{B}_0(M_Z^2; M_Z^2, m_{H_1'}^2) \right] \\
&\quad + \frac{4}{3} c_H^2 \bar{B}_{22}(M_Z^2; m_{H_5^0}^2, m_{H_3}^2) + 2 c_H^2 \bar{B}_{22}(M_Z^2; m_{H_5^+}^2, m_{H_3}^2) \\
&\quad + s_H^2 \bar{B}_{22}(M_Z^2; m_{H_3}^2, m_{H_1}^2) + \frac{8}{3} c_H^2 \bar{B}_{22}(M_Z^2; m_{H_3}^2, m_{H_1'}^2) \\
&\quad - 4 \bar{B}_{22}(M_Z^2; m_{H_5^{++}}^2, m_{H_5^{++}}^2) - \bar{B}_{22}(M_Z^2; m_{H_5^+}^2, m_{H_5^+}^2) - \bar{B}_{22}(M_Z^2; m_{H_3^+}^2, m_{H_3^+}^2) \\
&\quad \left. - \left[\bar{B}_{22}(M_Z^2; M_Z^2, m_H^2) - M_Z^2 \bar{B}_0(M_Z^2; M_Z^2, m_H^2) \right] \right\}, \tag{4.15}
\end{aligned}$$

Although it is not apparent from Eq. (4.15), \tilde{S}_{scalar} decreases with increasing mass-splitting within a $SU(2)_D$ scalar multiplet and between two $SU(2)_D$ scalar singlets of the $EW\nu_R$ model. For large enough splitting(s) it becomes negative, which is desired to compensate for the large positive contribution from mirror fermions (refer to section 4.4). To obtain \tilde{T}_{scalar} the contributions to Π_{11} in Eq. (4.7) are obtained from the Π_{WW} contributions in tables C.1, C.2, C.3, C.4, C.5, C.6 and using Eq. (4.14). The corresponding Π_{ZZ} contributions are obtained using Eq. (4.14) and tables C.7, C.8, C.9. Thus, we get

$$\begin{aligned}
\tilde{T}_{scalar} &= T_{scalar}^{EW\nu R} - T_{scalar}^{SM} \\
&= \frac{1}{4\pi s_W^2 M_W^2} \left\{ 2 B_{22}(0; m_{H_5^{++}}^2; m_{H_5^+}^2) + 3 B_{22}(0; m_{H_5^+}^2; m_{H_5^0}^2) + B_{22}(0; m_{H_3^+}^2; m_{H_3^0}^2) \right. \\
&\quad + c_H^2 \left[2 B_{22}(0; m_{H_5^{++}}^2; m_{H_3^+}^2) + B_{22}(0; m_{H_5^+}^2; m_{H_3^0}^2) + \frac{1}{3} B_{22}(0; m_{H_3^+}^2; m_{H_5^0}^2) \right. \\
&\quad \left. \left. + \frac{8}{3} B_{22}(0; m_{H_3^+}^2; m_{H_1^+}^2) - \frac{8}{3} B_{22}(0; m_{H_3^0}^2; m_{H_1^+}^2) \right] \right. \\
&\quad + s_H^2 \left[2 B_{22}(0; M_W^2; m_{H_5^{++}}^2) - B_{22}(0; M_W^2; m_{H_5^+}^2) - B_{22}(0; M_W^2; m_{H_5^0}^2) \right. \\
&\quad + B_{22}(0; m_{H_3^+}^2; m_{H_1^+}^2) - B_{22}(0; m_{H_3^0}^2; m_{H_1^+}^2) + M_W^2 \left(B_0(0; M_W^2, m_{H_5^0}^2) \right. \\
&\quad \left. \left. + B_0(0; M_W^2, m_{H_5^+}^2) - 2 B_0(0; M_W^2, m_{H_5^{++}}^2) \right) \right] + A_0(m_{H_5^{++}}^2) - \frac{1}{2} A_0(m_{H_5^+}^2) \\
&\quad \left. - \frac{1}{2} A_0(m_{H_5^0}^2) - \left(\frac{1}{2} - s_H^2 \right) A_0(m_{H_3^+}^2) + \frac{1}{2} A_0(m_{H_3^0}^2) - \left(\frac{1}{2} + s_H^2 \right) A_0(M_W^2) \right\} \\
&\hspace{15em} (4.16)
\end{aligned}$$

Hence, using Eq. (A.11),

$$\begin{aligned}
\tilde{T}_{scalar} = & \frac{1}{4\pi s_W^2 M_W^2} \left\{ \frac{1}{2} \mathcal{F}(m_{H_5^{++}}^2, m_{H_5^0}^2) + \frac{3}{4} \mathcal{F}(m_{H_5^+}^2, m_{H_5^0}^2) + \frac{1}{4} \mathcal{F}(m_{H_3^+}^2, m_{H_3^0}^2) \right. \\
& + \frac{c_H^2}{2} \mathcal{F}(m_{H_5^{++}}^2, m_{H_3^+}^2) + \frac{c_H^2}{4} \mathcal{F}(m_{H_5^+}^2, m_{H_3^0}^2) + \frac{c_H^2}{12} \mathcal{F}(m_{H_5^0}^2, m_{H_3^+}^2) \\
& - \frac{c_H^2}{2} \mathcal{F}(m_{H_5^+}^2, m_{H_3^+}^2) - \frac{c_H^2}{3} \mathcal{F}(m_{H_5^0}^2, m_{H_3^0}^2) \\
& + \frac{s_H^2}{4} \left[\mathcal{F}(m_{H_3^+}^2, m_{H_1}^2) - \mathcal{F}(m_{H_3^0}^2, m_{H_1}^2) \right] \\
& + \frac{2}{3} c_H^2 \left[\mathcal{F}(m_{H_3^+}^2, m_{H_1}^2) - \mathcal{F}(m_{H_3^0}^2, m_{H_1}^2) \right] + \frac{s_H^2}{2} \mathcal{F}(M_W^2, m_{H_5^{++}}^2) \\
& - \frac{s_H^2}{4} \mathcal{F}(M_W^2, m_{H_5^+}^2) - \frac{s_H^2}{4} \mathcal{F}(M_W^2, m_{H_5^0}^2) + M_W^2 s_H^2 B_0(0; M_W^2, m_{H_5^0}^2) \\
& \left. + M_W^2 s_H^2 B_0(0; M_W^2, m_{H_5^+}^2) - M_W^2 s_H^2 B_0(0; M_W^2, m_{H_5^{++}}^2) \right\}. \tag{4.17}
\end{aligned}$$

It should be noted that the individual loop integral functions on the RHS of Eqs. (4.15), (4.17) do contain divergences by definition, but these divergences cancel as expected resulting in finite \tilde{S}_{scalar} and \tilde{T}_{scalar} respectively. Similar cancellations ensure that \tilde{S}_{lepton} , \tilde{T}_{lepton} and \tilde{S}_{quark} , \tilde{T}_{quark} are all separately finite.

4.3.2 Contributions to the Oblique Parameters from the fermion sector in the $EW\nu_R$ model

Using these loop diagrams and the definitions of S , T in eqns. (4.6), (4.7), we obtain the new physics contributions, \tilde{S}_{lepton} , \tilde{T}_{lepton} and \tilde{S}_{quark} , \tilde{T}_{quark} . We also use

$Q_f = T_3^f + \frac{Y_f}{2}$. Thus, for \tilde{S}_{lepton} we get (as given in Eq. (4.18)):

$$\begin{aligned}\tilde{S}_{lepton} &= S_{lepton}^{EW\nu R} - S_{lepton}^{SM} \\ &= \frac{(N_C)_{lepton}}{6\pi} \sum_{i=1}^3 \left\{ -2 Y_{lepton} x_{\nu i} + 2 \left(-4 \frac{Y_{lepton}}{2} + 3 \right) x_{ei} - Y_{lepton} \ln \left(\frac{x_{\nu i}}{x_{ei}} \right) \right. \\ &\quad \left. + (1 - x_{\nu i}) \frac{Y_{lepton}}{2} G(x_{\nu i}) + \left[\left(\frac{3}{2} - \frac{Y_{lepton}}{2} \right) x_{ei} - \frac{Y_{lepton}}{2} \right] G(x_{ei}) \right\} \quad (4.18)\end{aligned}$$

For \tilde{T}_{lepton} we obtain,

$$\begin{aligned}\tilde{T}_{lepton} &= T_{lepton}^{EW\nu R} - T_{lepton}^{SM} \\ &= \frac{(N_C)_{lepton}}{4\pi s_W^2 M_W^2} \times \sum_{i=1}^3 \left[m_{\nu i}^2 \left(B_1(0; m_{\nu i}^2, m_{\nu i}^2) \right. \right. \\ &\quad \left. \left. - B_1(0; m_{\nu i}^2, m_{ei}^2) \right) + m_{ei}^2 \left(B_1(0; m_{ei}^2, m_{ei}^2) - B_1(0; m_{ei}^2, m_{\nu i}^2) \right) \right] \quad (4.19)\end{aligned}$$

Hence,

$$\tilde{T}_{lepton} = \frac{(N_C)_{lepton}}{8\pi s_W^2 M_W^2} \sum_{i=1}^3 \mathcal{F}(m_{\nu i}^2, m_{ei}^2). \quad (4.20)$$

Here, because we have subtracted the contribution from three generations of SM leptons, the summation is over three generations of mirror leptons only. Subscripts νi and ei represent the mass eigenstates, right-handed neutrino (ν_{Ri}) and mirror electron (e_i^M) member, of the i^{th} mirror lepton generation respectively. $(N_C)_{lepton} = 1$ is the lepton color factor and $Y_{lepton} = -1$ is the hypercharge of the mirror leptons. $x_{\nu i, ei} = (m_{\nu i, ei}/M_Z)^2$, where $m_{\nu i, ei}$ are masses of ν_{Ri} and e_i^M respectively. And $G(x)$ is given by Eq. (A.19). The new physics contributions to S and T from the quark

sector in $\overline{EW\nu_R}$ model are given by

$$\begin{aligned}
\tilde{S}_{quark} &= S_{quark}^{EW\nu_R} - S_{quark}^{SM} \\
&= \frac{(N_C)_{quark}}{6\pi} \sum_{i=1}^3 \left\{ 2 \left(4 \frac{Y_{quark}}{2} + 3 \right) x_{ui} + 2 \left(-4 \frac{Y_{quark}}{2} + 3 \right) x_{di} \right. \\
&\quad - Y_{quark} \ln \left(\frac{x_{ui}}{x_{di}} \right) + \left[\left(\frac{3}{2} + Y_{quark} \right) x_{ui} + \frac{Y_{quark}}{2} \right] G(x_{ui}) \\
&\quad \left. + \left[\left(\frac{3}{2} - Y_{quark} \right) x_{di} - \frac{Y_{quark}}{2} \right] G(x_{di}) \right\}
\end{aligned} \tag{4.21}$$

and

$$\begin{aligned}
\tilde{T}_{quark} &= T_{quark}^{EW\nu_R} - T_{quark}^{SM} \\
&= \frac{(N_C)_{quark}}{4\pi s_W^2 M_W^2} \times \sum_{i=1}^3 \left[m_{ui}^2 \left(B_1(0; m_{ui}^2, m_{ui}^2) - B_1(0; m_{ui}^2, m_{di}^2) \right) \right. \\
&\quad \left. + m_{di}^2 \left(B_1(0; m_{di}^2, m_{di}^2) - B_1(0; m_{di}^2, m_{ui}^2) \right) \right] \\
&= \frac{(N_C)_{quark}}{8\pi s_W^2 M_W^2} \sum_{i=1}^3 \mathcal{F}(m_{ui}^2, m_{di}^2),
\end{aligned} \tag{4.22}$$

respectively. Once again, because we have subtracted the contribution from three generations of SM quarks, the summation is over three generations of mirror quarks only. Subscripts ui and di represent the mass eigenstates of the mirror up- (u_i^M) and the mirror down- (d_i^M) member of the i^{th} mirror-quark generation respectively (refer to the arguments about negligible mirror fermion mixings given after Eq. (4.12)). $(N_C)_{quark} = 3$ is the quark color factor and $Y_{quark} = -1/3$ is hypercharge for mirror quarks. $x_{ui, di} = (m_{ui, di}/M_Z)^2$, where $m_{ui, di}$ are masses of u_i^M and d_i^M respectively. Refer to Appendix C.2 for the mirror fermion loop diagrams contributing to S and

T . As in section 4.4.2, both \tilde{S}_{lepton} and \tilde{S}_{quark} favor positive values more than the negative values, although this trend is not apparent in eqns. (4.18), (4.21). It can be seen in eqns. (4.20) and (4.22) that both \tilde{T}_{lepton} and \tilde{T}_{quark} are always positive. Also contributions to these quantities from a mirror lepton and a mirror quark generation increase with the mass splittings within the doublet of the mirror generation. These behaviors are expected in the $EW\nu_R$ model so that the total \tilde{S} and \tilde{T} satisfy the experimental constraints given in section 4.4.2.

4.4 Comparison with the experimental constraints

In this section we present the results of numerical analysis of oblique parameters, discussed in Section 3 ([42], [43]). In the first subsection we present the ranges for all the relevant parameters. In the second subsection, we show the scatter plots of the S and T parameters coming from the mirror sector and the scalar sector, without imposing the experimental constraints. Contributions from these two sectors, separately plotted in $\tilde{T} - \tilde{S}$ plane are also discussed. In the next subsection, we combine the contributions from both the sectors and show the scatter plot of the predictions of $\tilde{T} - \tilde{S}$ in the $EW\nu_R$ model overlapping the 1σ and 2σ experimental constraints, in the $\tilde{T} - \tilde{S}$ plane.

4.4.1 Ranges of relevant parameters

As seen in Section 4.3, the S and T parameters depend on many parameters, including the masses of the scalars, the masses of the mirror fermions and the right-handed neutrino and the ratio of VEV's θ_H (recall the definition from Eq. (3.39) in Chapter 3).

Among these parameters, the upper limits on the masses M_R of the right-handed

neutrinos and those on the masses of mirror fermions are correlated. A few remarks about this correlation are in order here. Last but not the least in this mini review is the question of charged fermion masses, in particular the top quark and mirror fermion masses and the perturbative Yukawa couplings they arise from. This is a topic for a detailed discussion on its own, but such an endeavor is beyond the scope of this dissertation. A few words are in order here for sure. Since $v = \sqrt{v_2^2 + 8v_M^2} \approx 246 \text{ GeV}$, it is evident that $v_2 < 246 \text{ GeV}$ and $v_M < 87 \text{ GeV}$. This has implications regarding fermion masses, since charged fermion masses are proportional to v_2 while the ν_R masses are proportional to v_M . The requirement that the Yukawa couplings giving rise to these masses, namely g_f 's and g_M , are perturbative (i.e. $\alpha_{f,M} \equiv g_{f,M}^2/(4\pi) \leq 1$) imposes constraints on the allowed ranges of v_2 and v_M respectively, and also on the allowed ranges of masses of the mirror fermions. Since $M_R = g_M v_M$ and since the Yukawa mass of a charged fermion is given by (ignoring mixings in the mass matrix for now) $m_f = g_f v_2/\sqrt{2}$, for a given mass of a charged mirror fermion (m_{fM}) the upper limit on masses of ν_R 's can be given by

$$M_R \leq \frac{\sqrt{2} g_{M,\max} v_{M,\max}}{g_{fM,\min} v_{2,\min}} m_{fM} \quad (4.23)$$

Let us estimate each quantity in the fraction on the right hand side of this equation. As mentioned before, $g_{M,\max} = \sqrt{4\pi}$. Because the top quark mass is known, (*naively* expressing it as $m_{\text{top}} = g_{\text{top}} v_2/\sqrt{2} \approx 170 \text{ GeV}$), the perturbative limit on g_{top} gives $v_2 \geq 68 \text{ GeV}$. This constrains v_M further such that $v_M \leq 84 \text{ GeV}$. Since $M_R \geq M_Z/2$, it follows that $v_M \geq 13 \text{ GeV}$ to ensure that $g_M \leq \sqrt{4\pi}$. This limit on v_M implies that $v_2 \leq 243 \text{ GeV}$. Hence, considering the charged mirror fermion masses to be heavier than 150 GeV it is straight forward to see that $g_f \geq 0.87$ for $v_2 \sim 243 \text{ GeV}$. Thus, Eq. (4.23) becomes $M_R \leq 7.1 m_{fM}$. On the other hand $g_M \leq \sqrt{4\pi}$ and

$v_M \leq 84$ GeV also imply that $M_R \leq 300$ GeV. Both these constraints are plotted in FIG. 4.1. In addition to any other constraints, the aforementioned constraints are also to be incorporated while studying the phenomenology of the $EW\nu_R$ model.

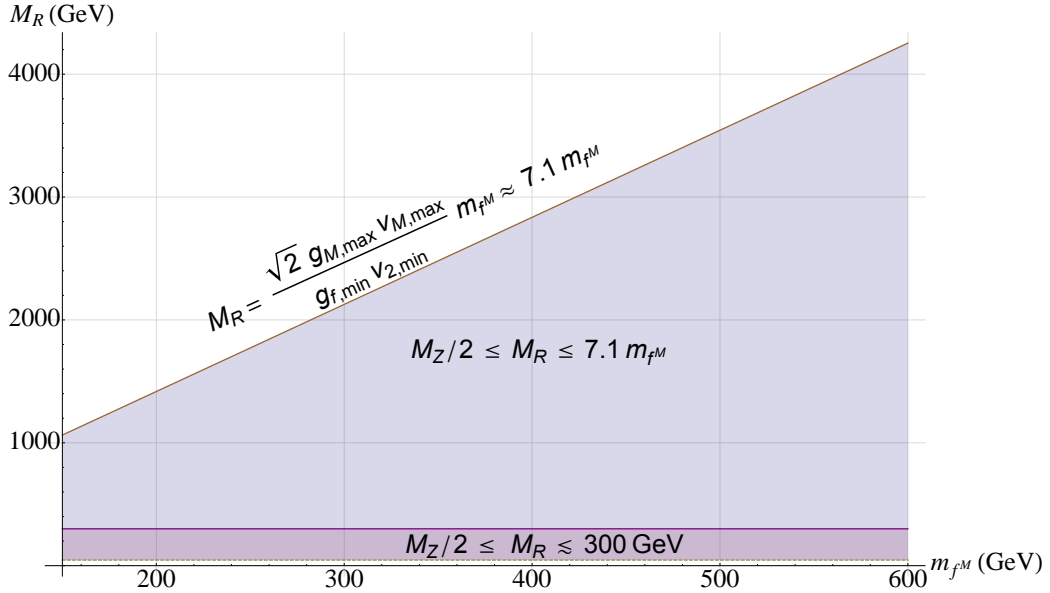


Figure 4.1: Mass of ν_R versus mass of charged mirror fermion f^M with constraints due to perturbativity of the Yukawa couplings. Thus, the final constraints are $M_Z/2 \leq M_R \leq 300$ GeV and $m_{f^M} \leq 610$ GeV (small purple area).

Considering $m_f = g_f v_2 / \sqrt{2} \leq g_f 148$ GeV, one expects a Yukawa coupling $g_{\text{top}} \sim 1.2$ for the top quark. This coupling can actually be even smaller if the SM quark mass matrix is of the “democratic type” i.e. having all matrix elements being equal to 1 [44]. (A more “realistic” version differs slightly from this one.) The largest mass eigenvalue in such a model is $\sim 3 g_f 148$ GeV giving $g_t \sim 0.4$. For very heavy mirror quarks, the Yukawa couplings might be larger, but, because the requirement for a perturbative $\alpha_f \equiv g_f^2 / 4\pi \leq 1$, a value of $g_f \sim 2$ or 3 might not be problematic. There is also an interesting twist in the situation when the Yukawa couplings become large: A possibility that the electroweak symmetry can be broken dynamically by condensates of heavy fermions through the exchange of a fundamental scalar as it has

been done for a heavy fourth generation [45, 46].

In our numerical calculations we fixed the ranges of the relevant parameters as follows:

- Scalar masses: from M_Z to 650 GeV . The upper limit was chosen since the results of Higgs searches at CMS and ATLAS were available up to about 650 GeV .
- M_R : from $M_Z/2$ to 300 GeV .
- Masses of the mirror fermions: from M_Z to 600 GeV .
- $\sin \theta_H = 2\sqrt{2} v_M/v$: from 0.1 to 0.89, as discussed in [27]. We Stretched the lower limit to 0.1 for numerical purposes.

4.4.2 Unconstrained \tilde{S} and \tilde{T} parameters for the scalar and the mirror fermion sectors

We generated 10,000 random combinations of the parameters in the ranges given above and calculated the \tilde{S} and \tilde{T} parameters using their expressions given in the previous section. For these combinations the ranges of the contributions from the scalar and the mirror fermion sectors were as follows:

- \tilde{S}_{scalar} or \tilde{S}_S : $-0.5 \leq \tilde{S}_S \leq 0.5$
- \tilde{T}_{scalar} or \tilde{T}_S : $-5 \leq \tilde{T}_S \leq 22$
- $\tilde{S}_{fermion}$ or \tilde{S}_{MF} : $-0.1 \leq \tilde{S}_{MF} \leq 1$
- $\tilde{T}_{fermion}$ or \tilde{T}_{MF} : $0 \leq \tilde{T}_{MF} \leq 32$

We show 500 of these points in Figs. 4.2 and 4.3. Scatter plot of \tilde{T} versus \tilde{S} for the scalar sector *with* the 1 and 2 σ experimental contours from [40]:

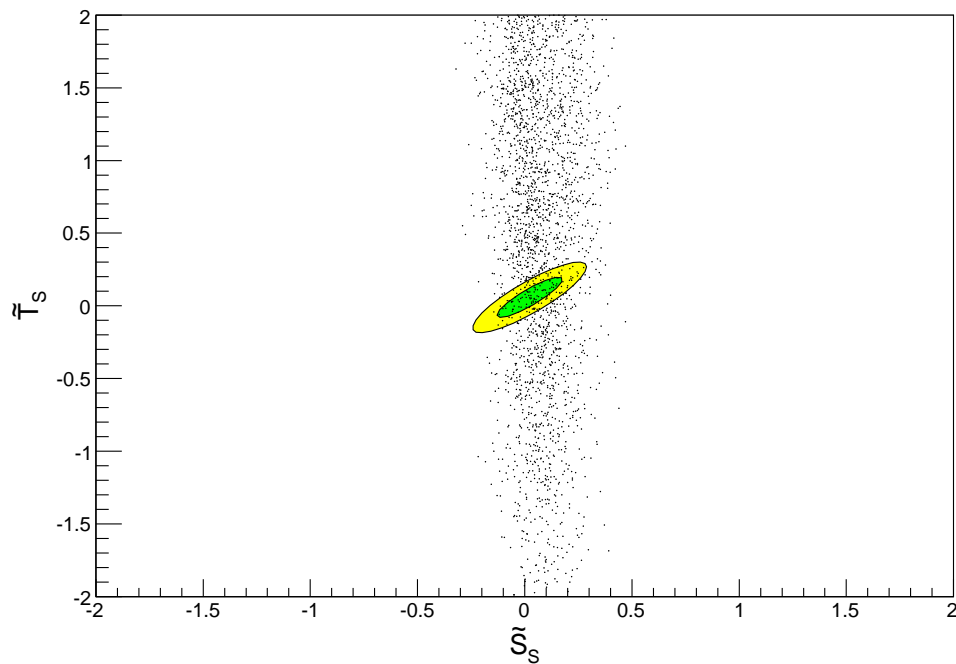


Figure 4.2: \tilde{T} versus \tilde{S} for the scalar sector with the 1 and 2 σ experimental contours (about 500 points). Plotted by Vinh V. Hoang.

Scatter plot of \tilde{T} versus \tilde{S} for the mirror fermion sector *with* the 1 and 2 σ experimental contours from [40]

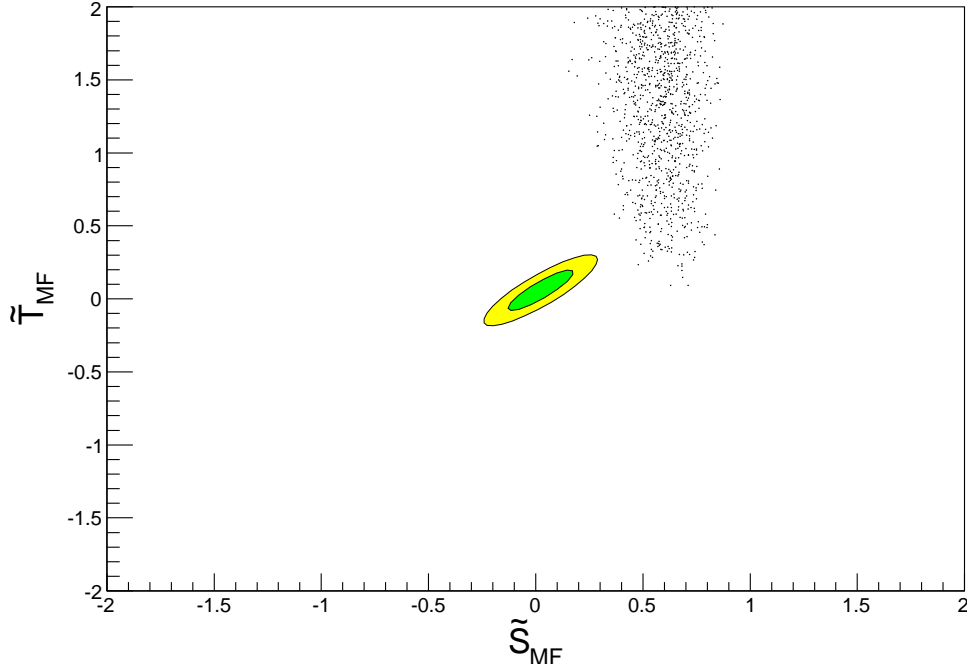


Figure 4.3: \tilde{T} versus \tilde{S} for the mirror fermion sector with the 1 and 2 σ experimental contours (about 500 points). Plotted by Vinh V. Hoang.

Notice in Fig. 4.3 that $\tilde{S}_{fermion}$ is almost always positive, as expected. On the other hand, \tilde{S}_{scalar} in Fig. 4.2 can have positive as well as negative value. Thus, negative \tilde{S}_{scalar} can almost cancel $\tilde{S}_{fermion}$ to yield the total \tilde{S} that agrees with the experimental constraints. We will verify this when we discuss constrained $EW\nu_R$ predictions in the next subsection.

4.4.3 Constrained \tilde{S} and \tilde{T} parameters for the scalar and the mirror fermion sectors

To verify whether the expected cancellation of \tilde{S}_{scalar} and $\tilde{S}_{fermion}$ really occurs, we generated random combinations of the parameters in the ranges given in section 4.4.1 and calculated the \tilde{S} and \tilde{T} parameters using their expressions given in the previous section. In this way we generated about 3,500 combinations of the parameters, for which the calculated values of these parameters are within the 1σ or 2σ experimental results given in Eq. (4.10):

$$\tilde{S} = -0.02 \pm 0.14 \quad \text{and} \quad \tilde{T} = 0.06 \pm 0.14 \quad (4.24)$$

with a statistical correlation 0.88 between the two. About 100 among these 3,500 combinations satisfy the 1σ constraints.

Fig. 4.4 shows the these calculated values, along with the imposed experimental constraints. We can see that a significant part of the parameter space in the $EW\nu_R$ model is consistent with the electroweak precision constraints from \tilde{S} and \tilde{T} .

We also noticed that for these constrained combinations of the parameters, the \tilde{S}_{scalar} and \tilde{T}_{scalar} really *almost* cancel $\tilde{S}_{fermion}$ and $\tilde{T}_{fermion}$, respectively [42].

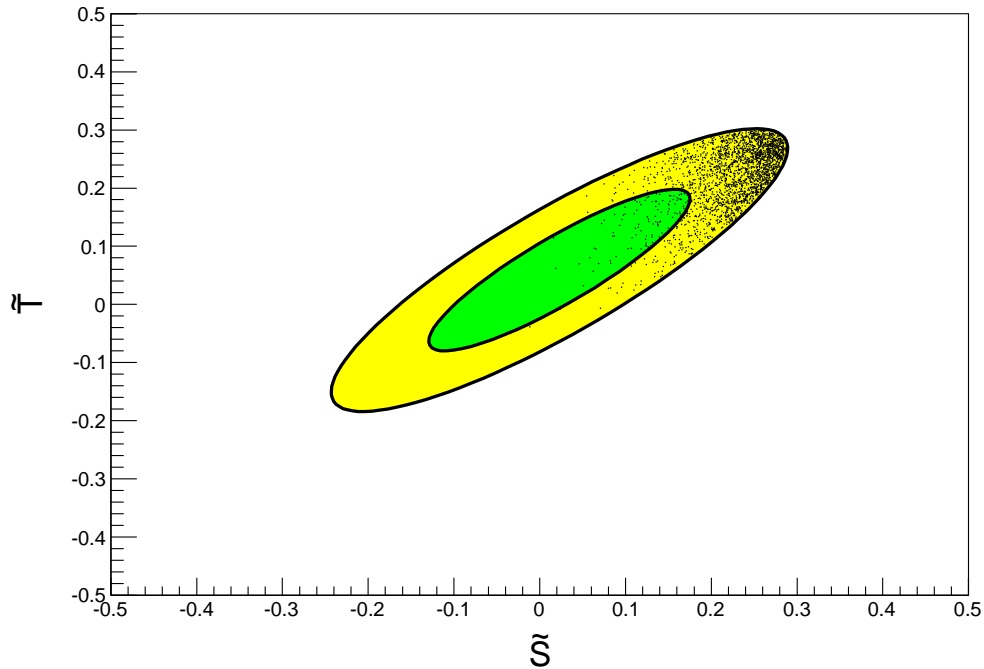


Figure 4.4: Total \tilde{T} versus \tilde{S} with the 1 and 2 σ experimental contours. Plotted by Vinh V. Hoang.

4.4.3.1 A few remarks

A remark about the allowed range of θ_H parameter is in order here. As can be seen in Appendix C, this parameter enters in calculation of various loop diagrams that contribute to the oblique parameters. One might think that the constraints on these parameters restrict the allowed range of θ_H to $\cos\theta_H \sim 1$ (i.e. where VEV v_2 of SM-like scalar doublet Φ_2 is dominant in v). However, we noticed that all the values of $\sin\theta_H$ were equally allowed by oblique constraints [42]. This is interesting, since in many other models which add extra scalar multiplets to the particle content in SM, the VEV's of the extra scalars are restricted by the constraints on the ρ parameter

(and hence, on the \tilde{T}), so as to make v_2 dominant in v .

In the plots above, the value of $m_{H_3^0}$ was fixed at 126 GeV. Recall that this is a pure-CP-odd pseudoscalar. The reason behind this choice and the implications of the spin-parity of the 125-GeV spin-0 state at the LHC for the $\text{EW}\nu_R$ model will be discussed in the next chapter. We will also discuss what extension is needed in the scalar sector of the $\text{EW}\nu_R$ model, as a result.

In these figures, the masses of H_1^0 and $H_1^{0'}$ were arbitrarily chosen to be $m_{H_1^0} = 600$ GeV and $m_{H_1^{0'}} = 100, 500, 650$ GeV. These values, although arbitrary, were chosen for illustrative purposes. A number of features of how different contributions to \tilde{S} and \tilde{T} vary with θ_H , the scalar masses and mass splittings are discussed in detail in [42].

4.5 Conclusions of the chapter

- For any model that adds extra chiral fermions to the SM fermion sector, it is crucial to verify its agreement with the experimental constraints on the electroweak precision parameters - the oblique parameters \tilde{S} and \tilde{T} .
- Since the $\text{EW}\nu_R$ model contains the mirror fermions, it is important to first check whether it satisfies the experimental constraints on \tilde{S} and \tilde{T} , before analyzing its phenomenology further.
- We demonstrated that a significant part of the parameter space of the $\text{EW}\nu_R$ model is consistent with these constraints.
- We observed that these constraints do not restrict the ratio of VEV's of the triplet χ and doublet Φ_2 , through the θ_H parameter. It is only restricted by the

perturbative limit on various Yukawa couplings and the lower limit of $M_Z/2$ on M_R .

- The particular choices of scalar masses in our calculations were only for illustrative purposes. Changing these choices should only move the region of the parameter space that agrees with the experimental constraints. We believe that it will not change the conclusion of our analysis.

As the minimal $\text{EW}\nu_R$ model does not violate the electroweak precision constraints, we can now discuss the phenomenology of the model further. When this analysis was coming to its conclusion, the 125-GeV Higgs was discovered at the Large Hadron Collider. In the next chapter we will discuss the implications of this discovery from the perspective of the $\text{EW}\nu_R$ model.

Chapter 5

An Extended $EW\nu_R$ Model and the Dual Nature of the 125-GeV Scalar

The agreement between the minimal $EW\nu_R$ model in Chapter 3 with the experimental constraints from the oblique parameters demonstrates the validity of the model from the perspective of *Step 1* illustrated in the Foreword of the dissertation. In the present chapter we will investigate the implications and a generalization of the $EW\nu_R$ model in the context of Steps 2 and 3 - relevance of a theoretical model to contemporary experiments and its predictions which can be tested at the experiments.

When the analysis in the previous chapter of this dissertation was in progress, only one of all the particles in the Standard Model remained to be experimentally discovered - the Higgs boson. The ATLAS and CMS experiments at the Large Hadron Collider (LHC) were excluding different mass ranges between ~ 115 GeV (LEP bound [6]) and ~ 600 GeV. After excluding a broad low-mass region, the search for the SM-like Higgs boson was narrowed down to the mass regions around certain values where the data was not conclusive enough [47, 48]. These regions for both CMS and ATLAS included the masses around 125 GeV .

On July 4, 2012 the CMS and ATLAS experiments announced the “discovery” of a spin-0 state with a mass of 125 GeV , which was then hoped to be a Higgs-boson-like particle [49, 50]. Further data revealed that the signal strengths of this particle, indeed, looked similar to those of the SM Higgs boson [51, 52, 53, 54]. Hence, for every model of physics beyond the Standard Model (BSM) it became imperative to

1. have at least one Higgs particle with a mass of about 125 GeV , having SM-like signal strengths, and
2. study the implications of these properties in the ‘allowed’ parameter space of the model (e.g. allowed masses of any BSM particles in the model, etc.).

To test the viability of a model or to search for the model experimentally at the LHC, the signal strengths of the 125-GeV Higgs boson candidate in the model must be studied.

In phenomenology of the $EW\nu_R$ model can be studied also by focusing on the signals for the mirror fermions. However, in the light of the Higgs discovery, agreement with the signal strengths of the 125-GeV particle is the *veto* criteria for any region in the parameter space. We therefore decided to analyze the implications of this discovery for the $EW\nu_R$ model, which truly revealed many interesting features of the scalar sector in the model.

The organization of this chapter is as follows: In Section 5.1, we will explore the viability of the neutral scalars in the minimal $EW\nu_R$ model as 125-GeV candidates. Section 5.2 shows step-by-step development of an extended $EW\nu_R$ model. Sections 5.4, 5.4.1, 5.3 discuss “the dual nature” of the 125-GeV Higgs, and the implications of the heavier CP-even neutral scalars in this model.

5.1 Can the minimal EW ν_R model accommodate a 125-GeV Higgs?

By “the minimal model” we refer to the Hung’s model explained in Chapter 3. The scalar sector in this model contains one doublet Φ_2 and two triplets χ, ξ . The SM fermions as well as the mirror fermions in the model couple to the same $SU(2)$ scalar doublet Φ_2 .

After the electroweak symmetry is spontaneously broken, 4 neutral physical spin-0 states are obtained - $H_1^0, H_1^{0'}, H_3^0$, and H_5^0 . For now we focus our attention only on H_1^0 and H_3^0 , as the other 2 states do not couple to SM or mirror fermions (remember that the right-handed neutrinos are not counted among the mirror fermions). Thus, we can say that either H_1^0 or H_3^0 could be the 125-GeV candidates in this model. Recall that H_1^0 is a CP-even (scalar) eigenstate, while H_3^0 is a CP-odd (pseudoscalar) eigenstate. The Feynman rules of the Yukawa couplings of SM fermions to H_1^0, H_3^0 and H_3^\pm can be obtained from the Lagrangian

$$\mathcal{L}_Y^{SM} = -h_{ij} \bar{\Psi}_{Li} \Phi_2 \Psi_{Rj} + h.c.$$

The corresponding Feynman Rules for SM quarks [27] are given by

$$\begin{aligned} g_{H_1^0 q\bar{q}} &= -i \frac{m_q g}{2 M_W c_H} \dots (q = t, b) \\ g_{H_3^0 t\bar{t}} &= i \frac{m_t g s_H}{2 M_W c_H} \gamma_5, & g_{H_3^0 b\bar{b}} &= -i \frac{m_b g s_H}{2 M_W c_H} \gamma_5, \\ g_{H_3^\pm t\bar{b}} &= i \frac{g s_H}{2\sqrt{2} M_W c_H} [m_t(1 + \gamma_5) - m_b(1 - \gamma_5)]. \end{aligned} \quad (5.1)$$

For the mirror quarks the Yukawa interactions are obtained from

$$\mathcal{L}_Y^{MF} = -h_{ij} \bar{\Psi}_{Ri} \Phi_{2M} \Psi_{Lj} + h.c. . \quad (5.2)$$

Thus, the Feynman Rules for mirror quarks are

$$\begin{aligned} g_{H_1^0 q^M \bar{q}^M} &= -i \frac{m_{q^M} g}{2 M_W c_H}, \\ g_{H_3^0 u_i^M \bar{u}_i^M} &= -i \frac{m_{u_i^M} g s_H}{2 M_W c_H} \gamma_5, & g_{H_3^0 d_i^M \bar{d}_i^M} &= i \frac{m_{d_i^M} g s_H}{2 M_W c_H} \gamma_5 \\ g_{H_3^- u_i^M \bar{d}_i^M} &= i \frac{g s_H}{2\sqrt{2} M_W c_H} [m_{u_i^M} (1 - \gamma_5) - m_{d_i^M} (1 + \gamma_5)] \end{aligned} \quad (5.3)$$

A spin-0 state can be a viable candidate for the 125-GeV scalar at the LHC, if and only if the decay properties of the latter agree with those predicted for the candidate particle. At a hadron collider such as the LHC, only the relative signal strengths μ , and not the partial decay widths Γ can be experimentally measured for any decay channel. Since the production cross section appears in calculations of μ for all the decay channels, it is reasonable to believe that, in the minimal EW ν_R model, if the production cross section of a candidate particle deviates a lot from that of the SM Higgs boson, then it is difficult to compensate for this deviation for all the decay channels. For example, consider the production cross section of H_1^0 in the gluon-gluon (gg) fusion channel, $\sigma(gg \rightarrow H_1^0)$. In this model, the top-quark as well as the mirror quark loops must be considered while calculating $\sigma(gg \rightarrow H_1^0)$. For a back-of-the-envelope calculation, assuming that mirror quarks are as massive as the

top quark,

$$\begin{aligned}\sigma(gg \rightarrow H_1^0) &= |\mathcal{A}(gg \rightarrow \text{top loop} \rightarrow H_1^0) + \mathcal{A}(gg \rightarrow 6 \text{ mirror quark loops} \rightarrow H_1^0)|^2 \\ &\sim \frac{49}{c_H^2} \times \sigma(gg \rightarrow H_{SM}^0),\end{aligned}$$

where ‘ \mathcal{A} ’ denotes amplitude of the production process. Therefore,

$$\sigma(gg \rightarrow H_1^0) \gtrsim 49 \times \sigma(gg \rightarrow H_{SM}^0). \quad (5.4)$$

At the LHC, gg -fusion is the most dominant production channel for a SM-like Higgs. From the structure of the $\text{EW}\nu_R$ model, it is also the most dominant production channel for $H_{1,3}^0$. Consequently, μ 's of all the decay channels of H_1^0 agree with the data at LHC, if all the corresponding partial decay widths are suppressed at least by a factor of about 49 as compared to the SM-Higgs-decay widths. However, it can be seen from Eq. (5.1) and Table D.4 that $\mathcal{A}(H_1^0 f \bar{f}) \gtrsim \mathcal{A}(H_{SM}^0 f \bar{f})$, while $\mathcal{A}(H_1^0 V V^\dagger) \lesssim \mathcal{A}(H_{SM}^0 V V^\dagger)$. Therefore, it is not possible to suppress all the partial decay widths by a factor of 49, to compensate for the factor of ~ 49 in the production cross section. This implies that H_1^0 cannot be a viable candidate for the 125-GeV scalar at the LHC¹.

The other possible 125-GeV candidate could be H_3^0 . The Yukawa couplings of H_3^0 with fermions are proportional to $\tan\theta_H$, and it couples to the up and down members of $SU(2)$ fermion doublets with opposite signs (refer to Eq. (5.1)). For a back-of-the-envelope calculation assuming that the up- and down-type mirror quarks

¹Maybe it is possible that H_1^0 still satisfies all the constraints from decay properties of the 125-GeV Higgs boson, but only in a highly constrained parameter space

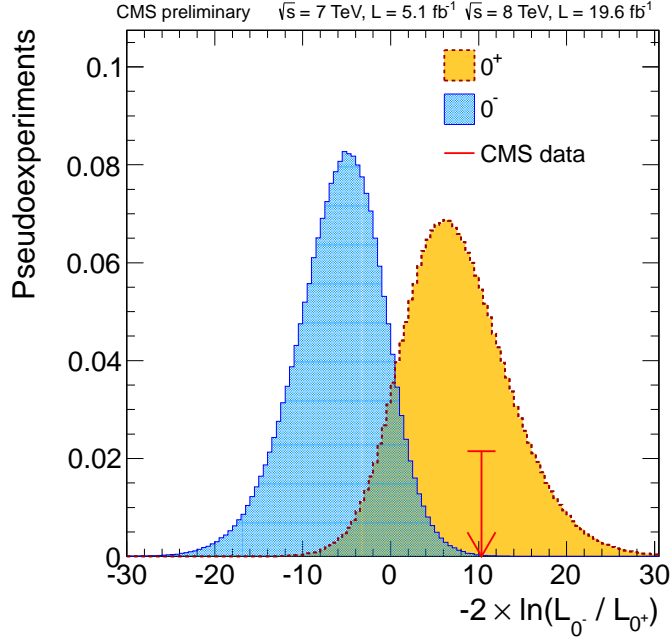


Figure 5.1: Courtesy: CMS collaboration, CMS-PAS-HIG-13-002, March 2013

have degenerate masses,

$$\sigma(gg \rightarrow H_1^0) \sim \tan^2 \theta_H \times \sigma(gg \rightarrow H_{SM}^0). \quad (5.5)$$

In general, $\tan^2 \theta_H$ can be ~ 1 and therefore, $\sigma(gg \rightarrow H_1^0) \sim \sigma(gg \rightarrow H_{SM}^0)$. Thus, in the light of recent results from the LHC, only H_3^0 (CP-odd) can potentially have relative signal strengths μ 's close to that of the SM-Higgs boson.

On the other hand, the preliminary likelihood analysis with different spin-parity hypotheses for the 125-GeV particle disfavors 0^- (CP-odd pseudoscalar) hypothesis by more than 3σ as compared to the 0^+ (CP-even scalar) [55]. Refer to FIG. 5.1. Consequently, H_3^0 is not a viable candidate for the 125-GeV scalar at the LHC.

The question under investigation now becomes *how the 125-GeV particle can be accommodated in the $EW\nu_R$ model as a scalar (CP-even) mass eigenstate*².

²The possibility that the 125-GeV Higgs boson is a linear combination of CP-even and CP-

The minimal $\text{EW}\nu_R$ model cannot answer this question affirmatively. Hence an extension of the model is required, particularly in the scalar sector of the minimal model. We will discuss a simple extension of the model in the next section.

5.2 An extended $\text{EW}\nu_R$ model

5.2.1 Field content of the model

As the minimal $\text{EW}\nu_R$ model in [26] cannot accommodate the 125-GeV particle as a scalar, an extension to the model is needed. Adding a scalar $SU(2)$ doublet to the field content of the model is the simplest extension, and it is expected to work, because:

- We need at least one additional scalar degree of freedom (d.o.f.), which can appear as a physical state with a mass of ~ 125 GeV. But a $SU(2)$ singlet scalar would not do the job, as it cannot interact with electroweak gauge bosons. Hence, the next simplest option is adding a $SU(2)$ scalar doublet.
- With this addition the $\text{EW}\nu_R$ model will have *two* $SU(2)$ scalar doublets, in which case we can expect to obtain one ‘light’ and one ‘heavy’ physical scalar, under the premise of having SM-like signal strengths - just like what happens in case of 2HDM model [56].

odd state has not been thoroughly tested experimentally yet. Here we will stick to CP-eigenstate hypothesis based on the likelihood analysis

When a $Y = 1$ complex scalar doublet is added to the minimal $\text{EW}\nu_R$ model, under the global $SU(2)_L \times SU(2)_R$ we have

$$\Phi_2 = \begin{pmatrix} \phi_2^{0,*} & \phi_2^+ \\ \phi_2^- & \phi_2^0 \end{pmatrix}, \quad \Phi_{2M} = \begin{pmatrix} \phi_{2M}^{0,*} & \phi_{2M}^+ \\ \phi_{2M}^- & \phi_{2M}^0 \end{pmatrix}, \quad \chi = \begin{pmatrix} \chi^0 & \xi^+ & \chi^{++} \\ \chi^- & \xi^0 & \chi^+ \\ \chi^{--} & \xi^- & \chi^{0*} \end{pmatrix}. \quad (5.6)$$

However, if both $\text{Re}[\phi_2^0]$ and $\text{Re}[\phi_{2M}^0]$ interact with SM as well as mirror fermions, then it might severely restrict their vacuum expectation values (VEV). If both of them contribute to the masses of charged SM-fermions (most of which are significantly light) and much heavier ($\gtrsim 100$ GeV; more on this later) charged mirror fermions, that could create difficulties in agreement between the allowed parameter space in the model and experimental constraints. To prevent such cross couplings, a global symmetry will be imposed such that only one doublet couples to the charged SM-fermions and the other one only to the mirror fermions. We introduce the following global symmetries and scalar doublets:

$$U(1)_{SM} : \quad \Phi_2 \rightarrow e^{i\alpha_{SM}} \Phi_2 \\ (q_L^{SM}, l_L^{SM}) \rightarrow e^{i\alpha_{SM}} (q_L^{SM}, l_L^{SM}), \quad (5.7)$$

$$U(1)_{MF} : \quad \Phi_{2M} \rightarrow e^{i\alpha_{MF}} \Phi_{2M} \\ (q_R^M, l_R^M) \rightarrow e^{i\alpha_{MF}} (q_R^M, l_R^M), \quad (5.8)$$

$$\phi_S \rightarrow e^{-i(\alpha_{MF} - \alpha_{SM})} \phi_S, \quad (5.9)$$

$$\tilde{\chi}, \xi \rightarrow e^{-2i\alpha_{MF}} \tilde{\chi}, \xi. \quad (5.10)$$

All the other fields ($SU(2)$ -singlet right-handed SM fermions, left-handed mirror fermions) are singlets under the global $U(1)_{\text{SM}} \times U(1)_{\text{MF}}$.

These symmetries will forbid Yukawa couplings of the form $g_Y \bar{f}_L \Phi_2 M f_R$ and $g_Y \bar{f}_R^M \Phi_2 f_L^M$, at tree level. Only Yukawa interactions of the type $g_Y \bar{f}_L \Phi_2 f_R$ and $g_Y \bar{f}_R^M \Phi_{2M} f_L^M$ are allowed. The Yukawa couplings of the physical spin-0 states to SM and mirror fermions will involve mixing angles between different $SU(2)$ scalar multiplets.

5.2.2 Symmetry breaking

Proper vacuum alignment that results in $SU(2)_L \times U(1)_Y \rightarrow U(1)_{em}$ follows the pattern below:

$$\langle \Phi_2 \rangle = \begin{pmatrix} v_2/\sqrt{2} & 0 \\ 0 & v_2/\sqrt{2} \end{pmatrix}, \quad \langle \Phi_{2M} \rangle = \begin{pmatrix} v_{2M}/\sqrt{2} & 0 \\ 0 & v_{2M}/\sqrt{2} \end{pmatrix}, \quad (5.11)$$

and

$$\langle \chi \rangle = \begin{pmatrix} v_M & 0 & 0 \\ 0 & v_M & 0 \\ 0 & 0 & v_M \end{pmatrix}, \quad (5.12)$$

Thus, the VEVs of real parts of Φ_2 , Φ_{2M} and χ are $(v_2/\sqrt{2})$, $(v_{2M}/\sqrt{2})$ and v_M respectively such that

$$v_2^2 + v_{2M}^2 + 8v_M^2 = v^2, \quad (5.13)$$

where $v \approx 246$ GeV. We define

$$s_2 = \frac{v_2}{v}; \quad s_{2M} = \frac{v_{2M}}{v}; \quad s_M = \frac{2\sqrt{2}v_M}{v}. \quad (5.14)$$

A generic $SU(2)_L \times SU(2)_R$ preserving potential for these scalars can now be written as

$$\begin{aligned}
V(\Phi_2, \Phi_{2M}, \chi) = & \lambda_1 \left[\text{Tr} \Phi_2^\dagger \Phi_2 - v_2^2 \right]^2 + \lambda_2 \left[\text{Tr} \Phi_{2M}^\dagger \Phi_{2M} - v_{2M}^2 \right]^2 + \lambda_3 \left[\text{Tr} \chi^\dagger \chi - 3v_M^2 \right]^2 \\
& + \lambda_4 \left[\text{Tr} \Phi_2^\dagger \Phi_2 - v_2^2 + \text{Tr} \Phi_{2M}^\dagger \Phi_{2M} - v_{2M}^2 + \text{Tr} \chi^\dagger \chi - 3v_M^2 \right]^2 \\
& + \lambda_5 \left[(\text{Tr} \Phi_2^\dagger \Phi_2) (\text{Tr} \chi^\dagger \chi) - 2 \left(\text{Tr} \Phi_2^\dagger \frac{\tau^a}{2} \Phi_2 \frac{\tau^b}{2} \right) (\text{Tr} \chi^\dagger T^a \chi T^b) \right] \\
& + \lambda_6 \left[(\text{Tr} \Phi_{2M}^\dagger \Phi_{2M}) (\text{Tr} \chi^\dagger \chi) - 2 \left(\text{Tr} \Phi_{2M}^\dagger \frac{\tau^a}{2} \Phi_{2M} \frac{\tau^b}{2} \right) (\text{Tr} \chi^\dagger T^a \chi T^b) \right] \\
& + \lambda_7 \left[(\text{Tr} \Phi_2^\dagger \Phi_2) (\text{Tr} \Phi_{2M}^\dagger \Phi_{2M}) - (\text{Tr} \Phi_2^\dagger \Phi_{2M}) (\text{Tr} \Phi_{2M}^\dagger \Phi_2) \right] \\
& + \lambda_8 \left[3 \text{Tr} \chi^\dagger \chi \chi^\dagger \chi - (\text{Tr} \chi^\dagger \chi)^2 \right], \tag{5.15}
\end{aligned}$$

where $M_W = gv/2$. Note that this potential, like the one in the minimal $\text{EW}\nu_R$ model is also invariant under $\chi \rightarrow -\chi$. The vacuum alignment given above breaks the global $SU(2)_L \times SU(2)_R$ down to the custodial $SU(2)_D$.

It is found that three ‘massless’ Nambu-Goldstone bosons can be obtained after spontaneous breaking of $SU(2)_L \times U(1)_Y$ to $U(1)_{em}$, when a condition $\lambda_5 = \lambda_6 = \lambda_7$ is imposed on the potential above. Thus, the final form of the scalar potential, which

is to be used to find the physical Higgs states, is

$$\begin{aligned}
V(\Phi_2, \Phi_{2M}, \chi) = & \lambda_1 \left[\text{Tr} \Phi_2^\dagger \Phi_2 - v_2^2 \right]^2 + \lambda_2 \left[\text{Tr} \Phi_{2M}^\dagger \Phi_{2M} - v_{2M}^2 \right]^2 + \lambda_3 \left[\text{Tr} \chi^\dagger \chi - 3v_M^2 \right]^2 \\
& + \lambda_4 \left[\text{Tr} \Phi_2^\dagger \Phi_2 - v_2^2 + \text{Tr} \Phi_{2M}^\dagger \Phi_{2M} - v_{2M}^2 + \text{Tr} \chi^\dagger \chi - 3v_M^2 \right]^2 \\
& + \lambda_5 \left[(\text{Tr} \Phi_2^\dagger \Phi_2) (\text{Tr} \chi^\dagger \chi) - 2 \left(\text{Tr} \Phi_2^\dagger \frac{\tau^a}{2} \Phi_2 \frac{\tau^b}{2} \right) (\text{Tr} \chi^\dagger T^a \chi T^b) + (\text{Tr} \Phi_{2M}^\dagger \Phi_{2M}) (\text{Tr} \chi^\dagger \chi) \right. \\
& - 2 \left(\text{Tr} \Phi_{2M}^\dagger \frac{\tau^a}{2} \Phi_{2M} \frac{\tau^b}{2} \right) (\text{Tr} \chi^\dagger T^a \chi T^b) + (\text{Tr} \Phi_2^\dagger \Phi_2) (\text{Tr} \Phi_{2M}^\dagger \Phi_{2M}) \\
& \left. - (\text{Tr} \Phi_2^\dagger \Phi_{2M}) (\text{Tr} \Phi_{2M}^\dagger \Phi_2) \right] + \lambda_8 \left[3 \text{Tr} \chi^\dagger \chi \chi^\dagger \chi - (\text{Tr} \chi^\dagger \chi)^2 \right] \tag{5.16}
\end{aligned}$$

After $SU(2)_L \times U(1)_Y \rightarrow U(1)_{em}$, besides the three Nambu-Goldstone bosons, there are *twelve* physical scalars grouped into $5 + 3 + 3 + 1$ of the custodial $SU(2)_D$. This includes 3 custodial scalar singlets.

To express the Nambu-Goldstone bosons and the physical scalars in terms of $SU(2)$ scalar d.o.f.'s, let us adopt the following convenient notation:

$$\begin{aligned}
s_2 = \frac{v_2}{v}, \quad s_{2M} = \frac{v_{2M}}{v}, \quad s_M = \frac{2\sqrt{2} v_M}{v}, \\
c_2 = \frac{\sqrt{v_{2M}^2 + 8v_M^2}}{v}, \quad c_{2M} = \frac{\sqrt{v_2^2 + 8v_M^2}}{v}, \quad c_M = \frac{\sqrt{v_2^2 + v_{2M}^2}}{v}. \tag{5.17}
\end{aligned}$$

Thus, $s_2^2 + c_2^2 = s_{2M}^2 + c_{2M}^2 = s_M^2 + c_M^2 = 1$. Notice that in the limit $s_{2M} \rightarrow 0$, $s_M \rightarrow s_H$ and $c_M \rightarrow c_H$. Like we did for the minimal EW ν_R model, let us also define:

$$\begin{aligned}
\phi_2^0 & \equiv \frac{1}{\sqrt{2}} \left(v_2 + \phi_2^{0r} + i\phi_2^{0i} \right), \quad \phi_{2M}^0 \equiv \frac{1}{\sqrt{2}} \left(v_{2M} + \phi_{2M}^{0r} + i\phi_{2M}^{0i} \right), \\
\chi^0 & \equiv v_M + \frac{1}{\sqrt{2}} \left(\chi^{0r} + i\chi^{0i} \right), \quad \psi^\pm \equiv \frac{1}{\sqrt{2}} \left(\chi^\pm + \xi^\pm \right), \quad \zeta^\pm \equiv \frac{1}{\sqrt{2}} \left(\chi^\pm - \xi^\pm \right) \tag{5.18}
\end{aligned}$$

With these fields the Nambu-Goldstone bosons are given by

$$G_3^\pm = s_2\phi_2^\pm + s_{2M}\phi_{2M}^\pm + s_M\psi^\pm \quad \text{and} \quad G_3^0 = i\left(-s_2\phi_2^{0i} - s_{2M}\phi_{2M}^{0i} + s_M\chi^{0i}\right). \quad (5.19)$$

The physical scalars can be grouped, based on their transformation properties under $SU(2)_D$ as follows:

$$\begin{aligned} \text{five-plet (quintet)} &\rightarrow H_5^{\pm\pm}, H_5^\pm, H_5^0; \\ \text{triplet} &\rightarrow H_3^\pm, H_3^0; \\ \text{triplet} &\rightarrow H_{3M}^\pm, H_{3M}^0; \\ \text{three singlets} &\rightarrow H_1^0, H_{1M}^0, H_1^{0'} \end{aligned} \quad (5.20)$$

where

$$\begin{aligned} H_5^{++} &= \chi^{++}, \quad H_5^+ = \zeta^+, \quad H_5^0 = \frac{1}{\sqrt{6}}\left(2\xi^0 - \sqrt{2}\chi^{0r}\right), \\ H_3^+ &= -\frac{s_2s_M}{c_M}\phi_2^+ - \frac{s_{2M}s_M}{c_M}\phi_{2M}^+ + c_M\psi^+, \\ H_3^0 &= i\left(\frac{s_2s_M}{c_M}\phi_2^{0i} + \frac{s_{2M}s_M}{c_M}\phi_{2M}^{0i} + c_M\chi^{0i}\right), \\ H_{3M}^+ &= -\frac{s_{2M}}{c_M}\phi_2^+ + \frac{s_2}{c_M}\phi_{2M}^+, \quad H_{3M}^0 = i\left(-\frac{s_{2M}}{c_M}\phi_2^{0i} + \frac{s_2}{c_M}\phi_{2M}^{0i}\right), \\ H_1^0 &= \phi_2^{0r}, \quad H_{1M}^0 = \phi_{2M}^{0r}, \quad H_1^{0'} = \frac{1}{\sqrt{3}}\left(\sqrt{2}\chi^{0r} + \xi^0\right). \end{aligned} \quad (5.21)$$

with phase conventions $H_5^{--} = (H_5^{++})^*$, $H_5^- = -(H_5^+)^*$, $H_3^- = -(H_3^+)^*$, $H_{3M}^- = -(H_{3M}^+)^*$, $H_3^0 = -(H_3^0)^*$ and $H_{3M}^0 = -(H_{3M}^0)^*$. The masses of these physical scalars can easily be obtained from eq. (5.16).

As long as the $SU(2)_D$ custodial symmetry is preserved, members of the physical scalar multiplets have degenerate masses. These masses are

$$\begin{aligned} m_5^2 &= 3(\lambda_5 c_M^2 + \lambda_8 s_M^2)v^2, \\ m_3^2 &= \lambda_5 v^2, \quad m_{3M}^2 = \lambda_5(1 + c_M^2)v^2. \end{aligned} \quad (5.22)$$

In general, H_1^0 , H_{1M}^0 and $H_1^{0'}$ can mix according to the mass-squared matrix

$$\mathcal{M}_{\text{singlets}}^2 = v^2 \times \begin{pmatrix} 8s_2^2(\lambda_1 + \lambda_4) & 8s_2s_{2M}\lambda_4 & 2\sqrt{6}s_2s_M\lambda_4 \\ 8s_2s_{2M}\lambda_4 & 8s_{2M}^2(\lambda_2 + \lambda_4) & 2\sqrt{6}s_{2M}s_M\lambda_4 \\ 2\sqrt{6}s_2s_M\lambda_4 & 2\sqrt{6}s_{2M}s_M\lambda_4 & 3s_M^2(\lambda_3 + \lambda_4) \end{pmatrix}. \quad (5.23)$$

It should be noted that in the limit $\lambda_4 \rightarrow 0$ the off-diagonal elements in the matrix above vanish. Also note that, in general, we have six parameters in the physical scalar potential and we *can* have six independent physical scalar masses. Thus, given the masses of the physical scalar states the parameters (these include quadratic coupling parameters, λ_4 , λ_5 , λ_8) in the potential can be uniquely determined and vice versa. Hence, the generic mass eigenstates are given by

$$\begin{pmatrix} \tilde{H} \\ \tilde{H}' \\ \tilde{H}'' \end{pmatrix} = \begin{pmatrix} a_{1,1} & a_{1,1M} & a_{1,1'} \\ a_{1M,1} & a_{1M,1M} & a_{1M,1'} \\ a_{1',1} & a_{1',1M} & a_{1',1'} \end{pmatrix} \begin{pmatrix} H_1^0 \\ H_{1M}^0 \\ H_1^{0'} \end{pmatrix}, \quad (5.24)$$

the lightest of which is \tilde{H} , while \tilde{H}'' is the heaviest.

Tables D.2 - D.6 list couplings of the physical Higgs states with fermions and gauge bosons.

5.2.3 Physical particle spectrum in the extended EW ν_R model

The total particle content in this model is shown in Fig. 5.2 below.

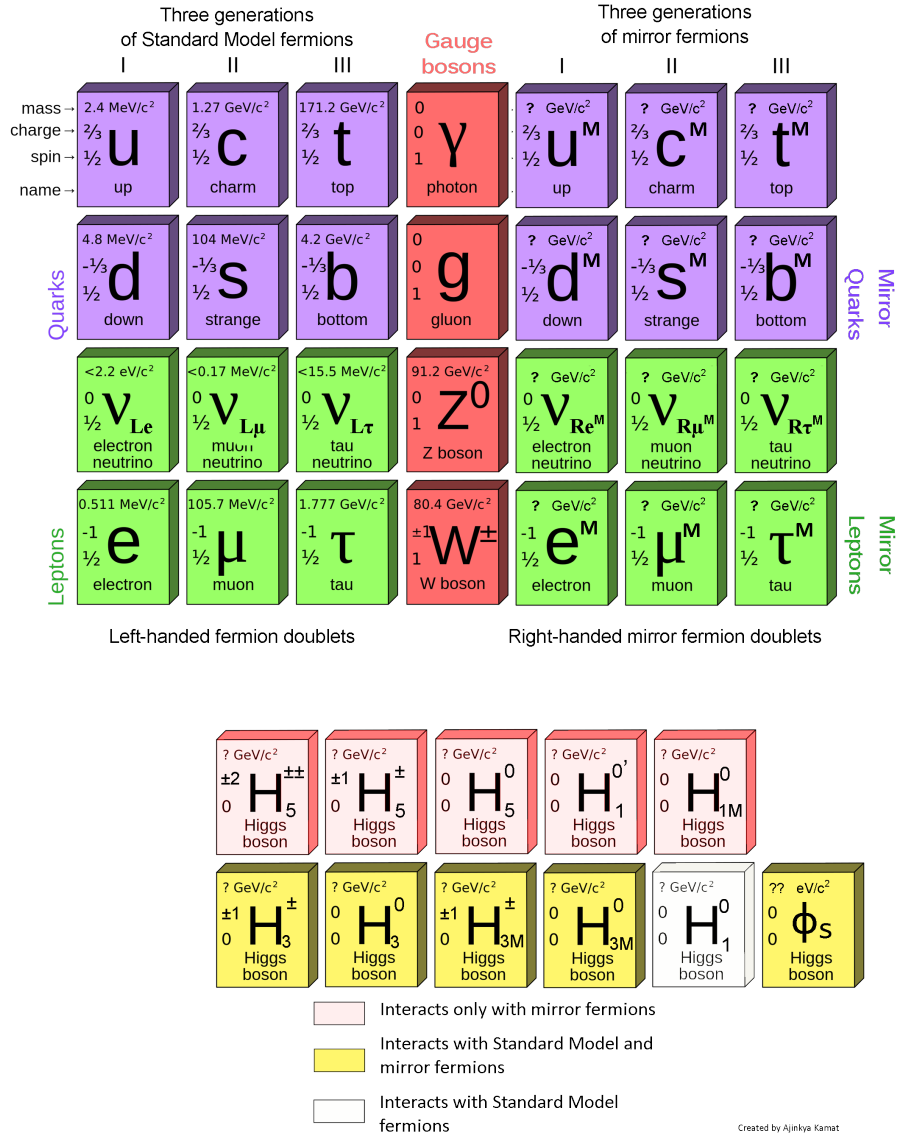


Figure 5.2: Physical particle spectrum in the extended EW ν_R model.

Note the difference between the figure above and Fig. 3.1 in Chapter 3. Since we have added 4 scalar degrees of freedom to the original model, we obtain 4 additional physical scalars.

5.2.4 A comment on oblique contributions in the extended EW ν_R model

We know from the analysis in Chapter 4 that those combinations of parameters of the EW ν_R model would agree with the experimental constraints on \tilde{S} and \tilde{T} , for which the positive fermion contributions to \tilde{S} are compensated by the negative contributions from the scalar sector of the model. We saw that the scalar contributions \tilde{S}_S can take negative as well as positive values. Therefore, even after adding an additional scalar doublet to the minimal model, it is reasonable to expect existence of a significant region in the parameter space to result in negative \tilde{S}_{scalar} that can compensate for the positive $\tilde{S}_{fermion}$. We therefore believe that the contribution due to these extra d.o.f.'s will not change the conclusion about the agreement between the contributions to \tilde{S} and \tilde{T} in the extended EW ν_R model and the electroweak precision constraints from experiments.

Hence, we argue that \tilde{S} and \tilde{T} in the extended EW ν_R model would also satisfy the experimental constraints, just like the minimal EW ν_R model.

5.2.5 A comment on the pseudo Nambu-Goldstone bosons in the EW ν_R model

Before proceeding to analyze the decay properties of the scalars in the EW ν_R model, an important clarification is in order here, regarding whether or not the Nambu-Goldstone (N-G) bosons arise due to breaking of the $U(1)_{SM} \times U(1)_{MF}$ symmetry.

When any symmetry is broken *spontaneously* there arise massless N-G bosons. If a local symmetry is spontaneously broken in the vacuum state of the Lagrangian, then the N-G bosons are absorbed by the longitudinal-polarization components of the corresponding gauge bosons [57] (refer to Chapter 1). On the other hand, if a global

symmetry is broken, then the N-G bosons appear as physical massless particles. In a different scenario the global symmetry is not exact i.e. it is broken “explicitly” by symmetry breaking term(s) in the Lagrangian. In such a case, the would-be N-G bosons acquire masses proportional to the symmetry-breaking term(s). Such massive would-be N-G bosons are referred to as “pseudo Nambu-Goldstone bosons” [10].

Keeping this in mind let us look at what happens to the N-G bosons associated with breaking of the $U(1)_{\text{SM}} \times U(1)_{\text{MF}}$ symmetry.

In the context of the minimal $\text{EW}\nu_R$ model this question arises for the $U(1)_{\text{MF}}$ symmetry (referred to as $U(1)_M$ in [26]). How different fields transform under this symmetry is given in Eq. (3.16). This question of N-G bosons has been addressed in detail in [29] and, specifically in the $\text{EW}\nu_R$ model, in [26]. Recall the scalar potential in the minimal $\text{EW}\nu_R$ model, in Eq. (3.35). The term proportional to λ_4 is necessary for the proper vacuum alignment of Φ_2 and χ , so that $SU(2) \times U(1)_Y \rightarrow U(1)_{\text{EM}}$. This term includes interactions such as $(\xi^0 \chi^0 \xi^+ \chi^-)$. It can be seen from Eq. (3.16) that these terms *explicitly* break the $U(1)_{\text{MF}}$ symmetry. As a result, after the *spontaneous* breaking of $SU(2) \times U(1)_Y$ to $U(1)_{\text{EM}}$, the pseudo N-G bosons of the global $U(1)_{\text{MF}}$, which are the triplet $H_3^{0,\pm}$, acquire mass proportional to λ_4 , as given in Eq. (3.43).

Similarly, in the extended $\text{EW}\nu_R$ model we have the global $U(1)_{\text{SM}} \times U(1)_{\text{MF}}$ symmetry. Notice the terms proportional to λ_5 in the potential in Eq. (5.15). These terms are necessary to ensure the proper vacuum alignment of Φ_2 , Φ_{2M} and χ . However, as can be seen from Eqs. (5.7), (5.8) and (5.10), these terms *explicitly* break the $U(1)_{\text{SM}} \times U(1)_{\text{MF}}$ symmetry. Hence, when $SU(2) \times U(1)_Y \rightarrow U(1)_{\text{EM}}$, the pseudo-N-G-bosons pick up masses proportional to λ_5 and become $H_3^{0,\pm}$ and $H_{3M}^{0,\pm}$ (refer to Eq. (5.22)).

Thus, in both, the minimal and the extended, $\text{EW}\nu_R$ models the $U(1)_{\text{MF}}$ and $U(1)_{\text{SM}} \times U(1)_{\text{MF}}$ symmetries (respectively) are broken explicitly to ensure proper

vacuum alignment for the *spontaneous* breaking of the electroweak symmetry. Hence, there arise no massless N-G bosons associated with these symmetries!

In the next section we will discuss how the different partial widths of a CP-even scalar can be calculated in the $\text{EW}\nu_R$ model. The signal strengths of a scalar in this model depend on these partial widths. It is therefore important to review their calculation before proceeding to numerical analysis of the 125-GeV candidate in this model.

5.3 Partial decay widths of neutral Higgs

In this section we will discuss various production and decay channels that are relevant for studying properties of the 125-GeV Higgs from the perspective of the $\text{EW}\nu_R$ model. We will focus on tree- and one-loop decays of CP-even physical states in this model. These include tree-level decays: $H^0 \rightarrow WW, ZZ, f\bar{f}$, and one-loop processes: $H^0 \rightarrow \gamma\gamma, gg$ - type decays (and also the Higgs boson production through $gg \rightarrow H$). We show calculation of the decay width $\Gamma(H \rightarrow \gamma\gamma)$ up to LO in QCD.

We also show how partial widths of all other than the $\gamma\gamma$ decay channel can be calculated easily from the corresponding SM values modified by a multiplicative factor. We calculate these widths in $\text{EW}\nu_R$ model from the SM values given in [58].

5.3.1 $H \rightarrow gg$

The decay of a custodial singlet Higgs boson to two gluons proceeds through one-loops at LO. Unlike $H^0 \rightarrow \gamma\gamma$ channel, this channel does not give a ‘clean’ signal at a hadron collider like the LHC due to large QCD background. However, the gluon-gluon fusion channel ($gg \rightarrow H$) is the most dominant production channel for a neutral Higgs and hence, Hgg coupling becomes important while studying $\mu(H^0\text{-decay})$ for

various decay channels.

The production cross section of $gg \rightarrow H^0$ is related to the width of $H^0 \rightarrow gg$ by

$$\sigma(gg \rightarrow H^0) \propto \Gamma(H^0 \rightarrow gg), \quad (5.25)$$

where the constant of proportionality includes phase space integrals and the mass of H^0 (refer Eq. (2.30) in [28]). Therefore, for a given mass of Higgs

$$\frac{\sigma_{\text{EW}\nu_R}(gg \rightarrow H^0)}{\sigma_{SM}(gg \rightarrow H^0)} = \frac{\Gamma_{\text{EW}\nu_R}(H^0 \rightarrow gg)}{\Gamma_{SM}(H^0 \rightarrow gg)}. \quad (5.26)$$

Hence, to calculate signal strengths $\mu(H\text{-decay})$, we use $\Gamma(H^0 \rightarrow gg)$ instead of $\Gamma(H^0 \rightarrow gg)$, since we are only interested in the ratios of production cross-sections.

Consider a general scalar mass-eigenstate H that is also a CP-even state in some model of BSM Physics. The relevant part of the interaction Lagrangian is [28]

$$\mathcal{L}_{int} = \frac{-m_f}{v_{H^0}} \bar{\psi}\psi H^0 + g M_W \lambda_W W_\mu^+ W^{\mu-} H^0 + \frac{g \lambda_S}{M_W} S^+ S^- H^0, \quad (5.27)$$

where v_{H^0} is the vacuum expectation value of H^0 , $v = 2M_W/g \sim \sqrt{\sum_{\text{all } H^{0,s}} v_{H^0}^2}$, ψ is a fermion of mass m_f , S^\pm is a charged BSM scalar. For SM $\lambda_W = 1/\sqrt{2}$, $\lambda_S = 0$. For a general (CP-even) Higgs boson H^0 that couples to the SM quarks with Yukawa coupling in the equation above, the decay width of $H^0 \rightarrow gg$ is given by

$$\Gamma(H^0 \rightarrow gg) = \frac{\alpha_S^2 g^2 m_{H^0}^3}{128\pi^3 M_W^2} \left| \sum_i \frac{1}{2 v_{H^0}/v} F_{1/2}(\tau_i) \right|^2, \quad (5.28)$$

where, for a loop of quark having mass m_i , $\tau_i = 4m_i^2/m_{H^0}^2$ [28], and $F_{1/2}(\tau)$ is given by

$$F_{1/2}(\tau) = -2\tau[1 + (1-\tau)f(\tau)]. \quad (5.29)$$

and

$$\begin{aligned}
 f(\tau) &= [\sin^{-1}(1/\sqrt{\tau})]^2, & \text{if } \tau \geq 1, \\
 &= \frac{1}{4} [\text{Log}(\eta_+/\eta_-) - i\pi]^2, & \text{if } \tau < 1;
 \end{aligned} \tag{5.30}$$

where

$$\eta_{\pm} \equiv (1 \pm \sqrt{1 - \tau}). \tag{5.31}$$

In [58] the width for $H^0 \rightarrow gg$ in SM is calculated up to the NLO QCD calculations. We calculate $\Gamma(\tilde{H} \rightarrow gg)$ in the $EW\nu_R$ model using these SM values. Using Eq. (5.24), Tables D.2 and D.1 this decay width can be given by

$$\Gamma^{EW\nu_R}(\tilde{H} \rightarrow gg) = \Gamma^{SM}(H_{SM}^0 \rightarrow gg) \times \frac{\left| \frac{a_{1,1}}{s_2} F_{1/2}(\tau_{top}) + \frac{a_{1,1M}}{s_{2M}} \sum_i F_{1/2}(\tau_{MF_i}) \right|^2}{|F_{1/2}(\tau_{top})|^2} \tag{5.32}$$

where \tilde{H} denotes \tilde{H} , \tilde{H}' and \tilde{H}'' ; \sum_i is over all the mirror quarks; $\tau_{MF_i} = 4 m_{MF_i}^2/m_{H^0}^2$. $a_{1,1}$ and $a_{1,1M}$ are elements of the square matrix in Eq (5.24) - they are coefficients of H_1^0 and H_{1M}^0 in \tilde{H} respectively.

5.3.2 $H^0 \rightarrow \gamma\gamma$

For a custodial singlet Higgs boson decay to two photons also proceeds through one-loops at LO. It is a ‘clean’ channel due to the absence of large QCD background. Therefore, in the study of 125-GeV Higgs boson, decay to diphoton is an important channel at CMS and ATLAS [59, 60].

For a general Higgs mass eigenstate H^0 having couplings as given in Eq (5.27) the

decay width of $H^0 \rightarrow \gamma\gamma$ is given by [28]:

$$\Gamma(H^0 \rightarrow \gamma\gamma) = \frac{\alpha^2 g^2}{1024 \pi^3} \frac{m_{H^0}^3}{M_W^2} \left| \sum_i N_{ci} Q_i^2 F_s(\tau_i) \right|^2. \quad (5.33)$$

Here \sum_i is performed over all the particles of spin- s which contribute to $H^0 \rightarrow \gamma\gamma$, $s = \text{spin-0, spin-1/2, and spin-1}$ is the spin of i^{th} particle, Q_i is the electric charge in units of e , and

$$\begin{aligned} F_1(\tau) &= \lambda_W \tau [3 + (4 - 3\tau)f(\tau)], \\ F_{1/2}(\tau) &= -2 \tau [1 + (1 - \tau)f(\tau)], \\ F_0(\tau) &= 2 \lambda_S [1 - \tau f(\tau)], \end{aligned} \quad (5.34)$$

with $\tau = 4 m_i^2/m_{H^0}^2$ and $f(\tau)$ is given by Eq (5.30).

Considering the contribution from W^\pm loop, the charged fermion loops in SM (all except the top quark loop are negligible) and setting $v_{H^0} = v$ gives the $H_{SM}^0 \rightarrow \gamma\gamma$ decay width. Note that $F_1(\tau)$ includes contributions from only the transverse polarization of W-boson; the contribution from Goldstone boson must be added separately using $F_0(\tau_W)$.³

Based on Eq (5.33) we define partial amplitude of $H^0 \rightarrow \gamma\gamma$ as

$$\mathcal{A}(H^0 \rightarrow \gamma\gamma) = \sqrt{\frac{\alpha^2 g^2}{1024 \pi^3} \frac{m_{H^0}^3}{M_W^2}} \left(\sum_i N_{ci} Q_i^2 F_s(\tau_i) \right). \quad (5.35)$$

³The formulas given above in Eq (5.27), Eq (5.34) are a bit different from Eqs.(2.15), (2.17) in [28]. We try to give formulas for a general BSM model (e.g. using a general v_{H^0} , λ_W and λ_S)

Then, in the $EW\nu_R$ model, we see from Eq (5.24) that

$$\begin{aligned} \Gamma^{EW\nu_R}(\tilde{H} \rightarrow \gamma\gamma) &= \left| a_{1,1} \mathcal{A}^{EW\nu_R}(H_1^0 \rightarrow \gamma\gamma) + a_{1,1M} \mathcal{A}^{EW\nu_R}(H_{1M}^0 \rightarrow \gamma\gamma) \right. \\ &\quad \left. + a_{1,1'} \mathcal{A}^{EW\nu_R}(H_1^{0'} \rightarrow \gamma\gamma) \right|^2, \end{aligned} \quad (5.36)$$

where $a_{1,i}$ with $(i = 1, 1M, 1')$ are the coefficients of H_1^0 , H_{1M}^0 and $H_1^{0'}$ in \tilde{H} mass eigenstate, respectively; these are the elements in the \tilde{H} -row of the mixing matrix in Eq (5.24). To calculate $\mathcal{A}^{EW\nu_R}(H_1^0 \rightarrow \gamma\gamma)$, in addition to the W^\pm , G_3^\pm and top-loop contributions we have to also consider one loop contributions involving H_3^\pm , H_{3M}^\pm , H_5^\pm and $H_5^{\pm\pm}$, whereas for $\mathcal{A}^{EW\nu_R}(H_{1M}^0 \rightarrow \gamma\gamma)$ we need to consider the W^\pm , G_3^\pm loops, the loops with the charged mirror fermion and the loops with H_3^\pm , H_{3M}^\pm , H_5^\pm and $H_5^{\pm\pm}$. Various Feynman rules necessary for these calculations can be read from Tables D.2-D.6 and the three point scalar Feynman rules can be obtained from Eq. (5.16).

In Eq. (5.22) all the members of a scalar custodial multiplet are degenerate, e.g. H_3^0 and H_3^+ have same masses and so on. But once custodial symmetry is broken at the loop level, different custodial multiplet members can have different masses. This mass splitting can also be due to some custodial symmetry-breaking terms in the Lagrangian (not given explicitly in this dissertation). In that case, the partial width of $\tilde{H} \rightarrow \gamma\gamma$ depends on the following variable parameters in $EW\nu_R$ models are:

- Masses of H_3^\pm , H_{3M}^\pm , H_5^\pm and $H_5^{\pm\pm}$;
- s_2 , s_{2M} , s_M ;
- Masses of charged mirror leptons and mirror quarks;
- Scalar self-couplings: λ_1 , λ_2 , λ_3 , λ_4 , λ_5 , λ_8 ;

- Elements of 3×3 mixing matrix in Eq (5.24).

Note that all of these parameters are not completely independent, e.g. once we fix s_2 , s_{2M} , then s_M is automatically fixed; scalar self-couplings and mixing matrix elements must vary so as to give at least one scalar mass eigenstate at the mass of about 125 GeV .

5.3.3 Tree level decays of \tilde{H}

Tree level decay channels of a neutral (CP-even) Higgs include decays to two fermions and to WW , ZZ . In this subsection first we show how the decay widths of these decays in the $EW\nu_R$ model are related to the widths in SM. Although at the LO these decays have only the tree level contributions, NLO QCD+EW corrections become significant at about 5% accuracy for [58]. Because the decay widths of these channels at tree level in the $EW\nu_R$ model and in SM are related by a multiplicative factor as described below, by using SM decay widths to calculate the decay widths in $EW\nu_R$ model these NLO contributions will be automatically included in our results. For vertices involving mirror fermions the QCD+EW corrections are different from the corrections for SM quarks (in SM non-negligible QCD corrections only come from top quark). Because mirror quark masses are of the same order as the top quark, for $\sim 5\%$ accuracy the NLO corrections due to mirror quarks can be assumed to have the same magnitude as those due to the top quark. The different tree level couplings in $EW\nu_R$ model can be found in Tables D.2, D.1, D.4, and Eq.[eqn. with relevant Lagrangian terms]). Note that the predictions for μ of various decay channels in the $EW\nu_R$ model are stated up to 5% accuracy, because Yukawa couplings of H_{1M}^0 with the mirror fermions can be large and at these large values extra QCD corrections can be dominant and reduce the accuracy to $\sim 5\%$.

5.3.3.1 $\tilde{\mathbf{H}} \rightarrow \mathbf{W}\mathbf{W}, \mathbf{Z}\mathbf{Z}$

The $H_1^0 VV$, $H_{1M}^0 VV$ and $H_1^{0'} VV$ couplings ($V = W^\pm, Z$) in $EW\nu_R$ model are suppressed by $s_2 = v_2/v$, $s_{2M} = v_{2M}/v$ and $s_M = 2\sqrt{2}v_M/v$ respectively, as compared to $H_{SM}^0 VV$ couplings in SM. Hence, using Eq (5.24) the decay widths for custodial singlet Higgs mass eigenstates \tilde{H} are given by

$$\Gamma^{EW\nu_R}(\tilde{H} \rightarrow WW, ZZ) = \Gamma^{SM}(H_{SM}^0 \rightarrow WW, ZZ) \times \left| a_{1,1} s_2 + a_{1,1M} s_{2M} + a_{1,1'} \frac{2\sqrt{2}}{\sqrt{3}} s_M \right|^2. \quad (5.37)$$

5.3.3.2 $\tilde{\mathbf{H}} \rightarrow \mathbf{f}\bar{\mathbf{f}}$

The decays of $\tilde{H}, \tilde{H}', \tilde{H}''$ to two fermions take place through the tree level Yukawa couplings at LO, when mass of the decaying scalar is at least twice as much as mass of the fermions. It can be seen from Tables D.2 and D.1 that the Yukawa couplings of charged SM fermions with H_1^0 and H_{1M}^0 are enhanced by factors $1/s_2$ and $1/s_{2M}$ respectively as compared to the corresponding couplings with H_{SM}^0 in SM. Also, $H_1^{0'}$ does not couple to particle-antiparticle pairs of charged fermions. Hence, the decay widths to SM fermions can be calculated from corresponding SM decay widths given in [58] and using Eq (5.24). Decay widths calculated in this way also include NLO QCD corrections that are taken into account in [58]. The partial widths of decays to SM fermions are given in terms of corresponding widths in SM by

$$\Gamma^{EW\nu_R}(\tilde{H} \rightarrow f \bar{f}) = \Gamma^{SM}(H^0 \rightarrow f \bar{f}) \times \left| \frac{a_{1,1}}{s_2} \right|^2, \quad (5.38)$$

On the other hand, the partial widths of decays to two charged mirror fermions need to be calculated explicitly. We calculate these up to LO, i.e. up to $\sim 5\%$ accuracy, since for further accuracy NLO QCD corrections become important. These partial widths are given by

$$\Gamma^{EW\nu_R}(\tilde{H} \rightarrow f^M \bar{f}^M) = \frac{g^2}{32\pi} \frac{m_{f^M}^2}{M_W^2} \frac{a_{1,1M}^2}{s_{2M}^2} m_{\tilde{H}} \times \left(1 - \frac{4 m_{f^M}^2}{m_{\tilde{H}}^2}\right)^{3/2}. \quad (5.39)$$

We are now equipped well enough to explore the signal strengths of the 125-GeV \tilde{H} , which will be the focus of the next section. We will now see what features and implications of the 125-GeV Higgs at the LHC are revealed through the analysis of the parameter space in the $EW\nu_R$ model.

5.4 The Dual Nature of the 125-GeV Scalar

Measured properties of the 125-GeV scalar particle that was discovered at the LHC so far tend to be close to the properties of SM Higgs boson. Hence, in every model of BSM Physics it is imperative to (i) have at least one Higgs particle with a mass of about 125 GeV having SM-like decay signal strengths, and (ii) study the implications of these properties in the ‘allowed’ parameter space of the model (e.g. allowed masses of any BSM particles in the model, etc.). To check the viability of a model or to search for the model experimentally, decay properties of the 125-GeV Higgs boson candidate in the model must be studied.

We denote the 125-GeV candidate in the $EW\nu_R$ model by \tilde{H} . From Eq. (5.24) we see that it is a mixture of H_1^0 , H_{1M}^0 and $H_1^{0'}$. Recall that H_1^0 comes from the SM-like scalar doublet Φ_2 , H_{1M}^0 comes from doublet Φ_{2M} and $H_1^{0'}$ from triplet χ .

Because the measured decay signal strengths of the 125-GeV Higgs boson are

close to SM predictions, intuitively one might expect that H_1^0 has to be the dominant component of \tilde{H} . But our investigation shows that the 125-GeV \tilde{H} can have SM-like decay signal strengths, even if H_1^0 is a sub-dominant component in it. Hence the dual-like nature of 125-GeV Higgs boson from perspective of the $\text{EW}\nu_R$ model. In this section we will discuss this dual-like nature and its implications.

In the first subsection we will explain the methodology used in the analysis; the next subsection presents the analysis and results for $\tilde{H} \sim H_1^0$ case. In the third subsection, we present a more interesting case, where, although H_1^0 is a subdominant component of 125-GeV \tilde{H} , it still satisfies the experimental constraints on the signal strengths.

A note on CP of the 125-GeV Higgs in the $\text{EW}\nu_R$ model:

As seen in Sec. 5.2, the $\text{EW}\nu_R$ model has 6 neutral physical scalars, of which 3 are CP-even states (H_1^0, H_{1M}^0, H_1') and 3 are CP-odd states (H_3^0, H_{3M}^0, H_5^0). Their couplings to fermions and gauge bosons are listed in Tables D.2 - D.6 in Appendix D. Among these H_5^0 does not couple to charged fermions.

It can be seen from Tables D.2 and D.1 that decay widths of $H_3^0/H_{3M}^0 \rightarrow f \bar{f}$ can be close to the SM predictions for some combinations of the BSM parameters in the couplings. But as mentioned in Section 5.1, H_3^0, H_{3M}^0 are disfavored as 125-GeV candidates as compared to the CP-even hypothesis [55].

Hence, in this chapter while considering 125-GeV candidate in the $\text{EW}\nu_R$ model, we proceed with the hypothesis that this candidate is a CP-even eigenstate ⁴.

Out of the 3 CP-even Higgs bosons, only H_1^0 can have decay widths to SM fermions similar to the SM predictions. Therefore, one might expect that in the $\text{EW}\nu_R$ model

⁴The possibility that the 125-GeV Higgs boson is a linear combination of CP-even and CP-odd state has not been thoroughly checked experimentally yet. The spin and parity of the 125-GeV scalar are yet to be measured at CMS and ATLAS. Thus, we will stick to the CP-eigenstate hypothesis based on the likelihood analysis

H_1^0 is the candidate for 125-GeV Higgs boson. However, in the absence of explicit decay widths and based on current available signal strengths for various decay channels, we will show that the 125-GeV Higgs boson can be very different from the standard expectation. It is in the spirit of our analysis that we may coin the term “Dr. Jekyll” to the Standard Model expectation (a mild impostor) and the term “Mr. Hyde” to the definite “impostor” (which mainly comes from the scalar triplet) scenario presented in this chapter.

5.4.1 Methodology for comparing the $\text{EW}\nu_R$ model predictions with data

For any given decay channel of a Higgs, CMS and ATLAS experiments at the LHC measure the total cross section of the decay process. The cross section of any decay channel of the Higgs boson that is measured at the LHC is given by

$$\sigma(H\text{-decay}) = \sigma(H\text{-production}) \times BR(H\text{-decay}), \quad (5.40)$$

where $\sigma(H\text{-production})$ is the production cross section of H and $BR(H\text{-decay})$ is the Branching Ratio of the decay channel of H that is under consideration.

$$BR(H\text{-decay}) = \frac{\Gamma(H\text{-decay})}{\Gamma_H}, \quad (5.41)$$

where $\Gamma(H\text{-decay})$ is the partial width of the H -decay channel, and Γ_H is the total width of H . To compare the data with the Standard Model predictions, the ratio of the measured signal strength to its SM-predicted value is presented, denoted by μ .

$$\mu(H\text{-decay}) = \frac{\sigma(H\text{-decay})}{\sigma_{SM}(H\text{-decay})}, \quad (5.42)$$

$\sigma(H\text{-decay})$ being measured experimentally or predicted by a model.

Therefore, to compare the $\text{EW}\nu_R$ -predicted decay signal strengths with the data, we investigate the agreement between the ratio of $\text{EW}\nu_R$ prediction with the SM prediction $\mu_{\text{EW}\nu_R} = \sigma_{\text{EW}\nu_R}(H\text{-decay})/\sigma_{\text{SM}}(H\text{-decay})$, to the ratio of measured decay cross section with the SM-prediction $\mu_{\text{data}} = \sigma_{\text{data}}(H\text{-decay})/\sigma_{\text{SM}}(H\text{-decay})$. $\sigma_{H\text{-decay}}$ in the $\text{EW}\nu_R$ model with the predictions SM for that decay channel.

Hence, we need to calculate

- partial decay widths for these channels,
- the total width of \tilde{H} and
- the production cross-section of $gg \rightarrow \tilde{H}$.

The analysis is done in the following steps:

1. Identify all the decay channels that contribute significantly to the total width of the 125-GeV \tilde{H} . Identify the variables on which the aforementioned three quantities depend.
2. Identify the limits on the variables.
3. Select a set of values for the variables within their respective limits.
4. Calculate the signal strengths μ in various channels for the 125-GeV \tilde{H} , and compare them with the measured values from CMS.

5.4.1.1 Decay channels under consideration

For this analysis we calculate signal strengths μ for decay channels $\tilde{H} \rightarrow ZZ, W^+W^-, \gamma\gamma, b\bar{b}, \tau\bar{\tau}$. We calculate the production cross-section and partial widths of various

decay channels as explained in Section 5.3. The total width of the 125-GeV \tilde{H} is calculated by adding individual partial decay widths:

$$\Gamma_{\tilde{H}} = \Gamma_{\tilde{H} \rightarrow b\bar{b}} + \Gamma_{\tilde{H} \rightarrow \tau\bar{\tau}} + \Gamma_{\tilde{H} \rightarrow c\bar{c}} + \Gamma_{\tilde{H} \rightarrow W^+W^-} + \Gamma_{\tilde{H} \rightarrow ZZ} + \Gamma_{\tilde{H} \rightarrow gg} + \Gamma_{\tilde{H} \rightarrow \gamma\gamma}. \quad (5.43)$$

Among all the partial widths considered above, $\Gamma_{\tilde{H} \rightarrow b\bar{b}}$ and $\Gamma_{\tilde{H} \rightarrow W^+W^-}$ are the most dominant for the SM-Higgs. Because of the constraint $m_{f^M} > 100$ GeV, the decay channel $\tilde{H} \rightarrow f^M \bar{f}^M$ does not occur at the leading order, when f^M is on-shell.

In what follows we identify the relevant variables in the analysis and estimate their allowed ranges.

5.4.1.2 Lower limit on the masses of charged mirror fermions

The lower limit of 102 GeV on the masses of charged mirror leptons and mirror quarks is imposed based on the results of search for sequential heavy charged leptons and quarks at LEP3 (refer ‘Heavy Charged Leptons’ and ‘Heavy Quarks’ sections in [6] and references therein). Strictly speaking these constraints apply only to sequential heavy fermions, such as $L' \rightarrow \tau Z \rightarrow \tau l \bar{l}$, $\tau q \bar{q}$ or $Q' \rightarrow b Z \rightarrow b l \bar{l}$, $b q \bar{q}$ or $Q' \rightarrow b W^+ \rightarrow b l \bar{\nu}$, $b q \bar{q}'$ etc.

However, charged mirror fermions in the $EW\nu_R$ model couple to the SM fermions in an altogether different way, through the scalar singlet ϕ_S [26, 61]: $q^M \rightarrow q\phi_S$, $l^M \rightarrow l\phi_S$. This ϕ_S would appear as missing energy in the detector. Thus, the signature of final states in charged mirror fermion decay would involve a lepton + missing E_T or a jet + missing E_T . Moreover, at CMS or ATLAS these decays could occur outside the beam-pipe and inside the silicon vertex detector [26, 61]. Therefore, the constraints from the aforementioned searches do not directly apply to charged mirror fermions. We still impose these constraints on charged mirror fermions, arguing

that if these mirror fermions were lighter than ~ 100 GeV, they would have been discovered at 200 GeV LEP3 [6].

5.4.1.3 Limits on VEVs, scalar and Yukawa couplings

We consider only the cases where the scalar couplings and Yukawa couplings of mirror fermions are perturbative. The perturbative constraint on scalar and Yukawa couplings are $\lambda_i/4\pi \lesssim \mathcal{O}(1)$ and $\alpha_{fM} = g_{MF}^2/4\pi \lesssim \mathcal{O}(1)$ respectively. For numerical analysis we limit ourselves to cases, where $\lambda_i/4\pi \leq 1.3$ and $\alpha_{fM} \leq 1.5$.

As discussed towards the end of Sec. 5.2, the $SU(2)_D$ singlet mass eigenstates depend on s_2 , s_{2M} and s_M . Therefore, they also depend on the vacuum expectation values (VEVs) of the real parts of Φ_2 , Φ_{2M} and χ . While investigating different numerical forms of $\{a_{ij}\}$, one needs to vary the VEV's. Hence, it is necessary to estimate the limits on these VEVs before analyzing the 125-GeV candidate in detail.

Recall that the charged SM fermions, the charged mirror fermions and the right handed neutrinos get their masses due to v_2 , v_{2M} , and v_M respectively. Various constraints on these masses constrain the ranges of the VEVs.

If the pole mass of top quark (173.5 GeV), the heaviest SM fermion, is *perturbative* and comes from v_2 , then $v_2 \gtrsim 69$ GeV (because $g_{top}^2 \leq 4\pi$). We set the lower bound on the masses of all the charged mirror fermions at 102 GeV, which is the LEP3 [6] bound on the heavy BSM quarks and BSM charged leptons. Hence, considering a constraint of $g_{MF}^2/4\pi \leq 1.5$ on the Yukawa couplings of all the charged mirror fermions, $v_{2M} \gtrsim 27$ GeV, implying $v_M \lesssim 80$ GeV. Thus, for perturbative determination of M_R requires $M_R \lesssim 283$ GeV. We also know that $M_R \geq M_Z/2 \approx 45.5$ GeV [26], and, hence, $v_M \gtrsim 13$ GeV. This implies that $v_2 \lesssim 241$ GeV and $v_{2M} \lesssim 233$ GeV. This limit on v_{2M} along with the perturbative limit on g_{MF} sets an upper limit on the masses of the mirror fermions: $m_{MF} \lesssim 715$ GeV. The allowed ranges for VEVs and for parameters

defined in Eq (5.14) are summarized in the table below.

Table 5.1: Allowed ranges of VEVs and parameters defined in Eq. (5.14). All values are given in GeV .

$69 \lesssim v_2 \lesssim 241$	$0.28 \lesssim s_2 \lesssim 0.98$
$33 \lesssim v_{2M} \lesssim 233$	$0.13 \lesssim s_{2M} \lesssim 0.95$
$13 \lesssim v_M \lesssim 83$	$0.15 \lesssim s_M \lesssim 0.95$

5.4.1.4 Common predictions for multiple decay channels

In the $EW\nu_R$ model, predictions for the signal strengths of $\tilde{H} \rightarrow W^+W^-$ and $\tilde{H} \rightarrow ZZ$ are equal. Similarly, predictions for the signal strengths of $\tilde{H} \rightarrow b\bar{b}$ are equal to those for $\tilde{H} \rightarrow \tau\bar{\tau}$. This is expected, since as seen in Section 5.3,

$$\begin{aligned} \frac{\Gamma^{EW\nu_R}(\tilde{H} \rightarrow W^+W^-)}{\Gamma^{SM}(H_{SM}^0 \rightarrow W^+W^-)} &= \frac{\Gamma^{EW\nu_R}(\tilde{H} \rightarrow ZZ)}{\Gamma^{SM}(H_{SM}^0 \rightarrow ZZ)}, \\ \frac{\Gamma^{EW\nu_R}(\tilde{H} \rightarrow b\bar{b})}{\Gamma^{SM}(H_{SM}^0 \rightarrow b\bar{b})} &= \frac{\Gamma^{EW\nu_R}(\tilde{H} \rightarrow \tau\bar{\tau})}{\Gamma^{SM}(H_{SM}^0 \rightarrow \tau\bar{\tau})}. \end{aligned} \quad (5.44)$$

Keeping all this in mind, in the next two subsections we analyze in detail the decay properties of the 125-GeV candidate in the $EW\nu_R$ model.

5.4.1.5 Numerical Analysis

For this analysis a C++ code was written, also using some functionality of ROOT [62]. We investigated this case in following steps:

- We generated random combinations of s_2 , s_{2M} , s_M , λ_1 , λ_2 , λ_3 and λ_4 , using TRandom3 random number generator in ROOT. These parameters were varied

over the following ranges:

$$\begin{aligned}
 -4\pi &\leq \lambda_1, \quad \lambda_2, \lambda_3, \quad \lambda_4 \leq 4\pi, \\
 0.28 &\leq s_2 \leq 0.98, \\
 0.13 &\leq s_{2M} \leq 0.95, \\
 0.15 &\leq s_M \leq 0.95.
 \end{aligned} \tag{5.45}$$

The limits $|\lambda|/4\pi \lesssim 1$ are set so that λ 's are perturbative. Limits on s_2 , s_{2M} , s_M are based on Table 5.1.

- We numerically diagonalized the singlet mass matrix in Eq. (5.23) formed by every combination of the parameters to find the mass eigenvalues and corresponding eigenvector matrix (mixing matrix) in Eq. (5.24). Only those combinations of parameters, which yielded the lightest mass eigenvalue in the range 125.7 ± 1.0 GeV, were saved. 4 million such parameter combinations were found.
- For all the saved combinations we calculated various signal strengths for each of these combinations. The gluon-gluon fusion channel was considered to calculate the predicted production cross section of the \tilde{H} . The partial decay widths were calculated according to Section 5.3, and the total width was calculated using Eq. (5.43).
- In addition to the parameters in Eq (5.45), following parameters are required to calculate the partial widths of $\tilde{H} \rightarrow \gamma\gamma$ and $\tilde{H} \rightarrow gg$, and the cross section

of $gg \rightarrow \tilde{H}$:

$$\begin{aligned}
0 &\leq \lambda_5 \leq 15, \text{ varied with } \Delta\lambda_5 \sim 1.07, \\
\lambda_8 &= -1, m_{H_3^+} = m_{H_{3M}^+} = 500 \text{ GeV}, \\
m_{H_5^+} &= 200 \text{ GeV}, m_{H_5^{++}} = 320 \text{ GeV}, m_{q_3^M} = 120 \text{ GeV}, \\
m_{q_1^M} &= m_{q_2^M} = m_{l^M} = 102 \text{ GeV}.
\end{aligned} \tag{5.46}$$

- We checked if the signal strengths μ 's of the 125-GeV \tilde{H} in various decay channels are within the 1σ constraints on the signal strengths, as measured by CMS experiment. We did not impose constraints from both the CMS and ATLAS, because for some of the decay channels considered here, the signal strength measurements from CMS and ATLAS do not agree with each other within the 1σ constraints. Also, CMS and ATLAS have not published their combined measurements from the recent analyses. We therefore chose to check agreement with the CMS measurements.

Depending on their 1σ constraints, certain combinations out of the 4 million would agree with either only with CMS or with ATLAS results. Thus, imposing the constraints from ATLAS would discard some of the combinations that the CMS constraints would allow and vice versa. However, this would not change any of the conclusions of this chapter.

- We found 1501 out of 4 million combinations of the parameters that satisfy 1σ constraints from CMS on the 125-GeV Higgs signal strengths in WW , ZZ , $b\bar{b}$, $\tau\bar{\tau}$ and $\gamma\gamma$ decay channels. Table 5.4 lists 16 examples out of 1501 cases, with the masses of \tilde{H} , \tilde{H}' , \tilde{H}'' , their mixing-matrix elements, and the signal strengths

of the 125-GeV \tilde{H} for various decay channels.

- In the code, there was no constraint imposed as to what is to be the dominant component in \tilde{H} . Interestingly, hardly any combinations among the 4 million had H_1^0 as a dominant component in the 125-GeV \tilde{H} . This means that either
 1. at the mass of about 125-GeV, 4 million combinations do not yield enough resolution in the parameter space so as to find the $\tilde{H} \sim H_1^0$ case, OR
 2. the $\tilde{H} \sim H_1^0$ case cannot be found with the imposed limits on the parameters, and it requires at least some of these parameters to have values outside of these limits.
- Thus, this scan of the parameter space only yielded *Mr. Hyde* cases, where the SM-like H_1^0 is a subdominant component in the 125-GeV \tilde{H} . Implications of these cases will be further discussed in section 5.4.3.
- On the other hand, to find the combinations of the parameters for which the 125-GeV \tilde{H} has a dominant SM-like H_1^0 component, and which also satisfy the CMS constraints on the signal strengths, we had to choose some of the scalar couplings to have values outside $[-4\pi, 4\pi]$. These *Dr. Jekyll* cases thus require some interactions within the scalar sector to be in the strong-coupling regime. In the next subsection we discuss this scenario in detail.

5.4.2 \tilde{H} as 125-GeV Higgs candidate with a dominant SM-like component

We illustrate the step-by-step process which we followed to analyze this case.

- A Mathematica code was written to numerically diagonalize the custodial-singlet mass matrix in Eq. (5.23) and obtain its mass eigenvalues and eigenvector matrix i.e. the mixing matrix in Eq. (5.24).
- In this code, the values of $s_2 = 0.92$, $s_{2M} = 0.16$ (and thus, $s_M \approx 0.36$) were fixed. The analysis was performed for different s_2 values, but, for $\tilde{H} \sim H_1^0$, only the cases with $s_2 \gtrsim 0.9$ were found to satisfy the experimental constraints on the signal strengths of the 125-GeV Higgs at LHC.
- After fixing s_2 and s_{2M} , the scalar couplings λ_1 , λ_2 , λ_3 and λ_4 were manually varied so that $|\lambda|/4\pi \leq 1.3$, in order to find the combinations of λ 's that yield the lowest eigenvalue of the mass matrix to be 125.7 ± 1.0 GeV and the corresponding eigenstate to have dominant H_1^0 component.
- Recall (refer to Eq.(5.16)) that λ_1 , λ_2 and λ_3 are the self-couplings of Φ_2 , Φ_{2M} and χ respectively. λ_5 is the measure of cross couplings of Φ_2 , Φ_{2M} and χ .
- As stated in section 5.4.1.5, we found combinations of the parameters which satisfy the CMS constraints on the signal strengths, when λ_2 , $\lambda_5 > 4\pi$. $|\lambda_1|$, $|\lambda_4|$, $|\lambda_8|$ are still $\leq 4\pi$, while $\lambda_3 \approx 15$. For illustrative purpose, we show below two of many cases which satisfy the CMS constraints.
- The calculation of the partial width of the $\tilde{H} \rightarrow \gamma\gamma$ channel necessitates fixing the values or ranges for the remaining parameters. In the example cases shown below we fix other parameters as follows:

- $m_{H_3^+} = 600$ GeV, $m_{H_{3M}^+} = 700$ GeV,

- masses of all three charged mirror leptons $m_{lM} = 102$ GeV,

- mass of lightest two generations of mirror quarks $m_{q_1^M} = m_{q_2^M} = 102$ GeV,

- for the purpose of partial widths of \tilde{H} -decays in scenarios above, we also fix mass of the third mirror quark generation at $m_{q^M} = 120$ GeV. This mass will be varied to analyze constraints on $\tilde{H} \sim H_{1M}^0$.
- The values of $m_{H_3^+}$ and $m_{H_{3M}^+}$ are chosen so as to have largest allowed ranges for $m_{H_5^+}$ and $m_{H_5^{++}}$. We vary the latter two over the range $\sim 400 - 730$ GeV for Example 1 and 2. This variation does not affect much the predictions for the signal strengths of the \tilde{H} decays to W^+W^- , ZZ and $f\bar{f}$, but only changes that for $\tilde{H} \rightarrow \gamma\gamma$. $m_{H_5^+}$ and $m_{H_5^{++}}$ vary in correlation when the CMS constraints on the signal strength of the diphoton decay channel are imposed. For the numerical calculation of other signal strengths in the following two examples we chose on of these correlated pairs of the two masses.
- Example 1: $\lambda_1 = -0.077$, $\lambda_2 = 14.06$, $\lambda_3 = 15.4$, $\lambda_4 = 0.1175$, $\lambda_5 = 15$, $\lambda_8 = -1$ and $m_{H_5^+} = 500$ GeV, $m_{H_5^{++}} = 540$ GeV. Fixing these along with $s_2 = 0.92$, $s_{2M} = 0.16$, $s_M \approx 0.36$, fully determines the singlet mass matrix, and hence the mixing matrix, given by:

$$\begin{pmatrix} \tilde{H} \\ \tilde{H}' \\ \tilde{H}'' \end{pmatrix} = \begin{pmatrix} 0.998 & -0.0518 & -0.0329 \\ 0.0514 & 0.999 & -0.0140 \\ 0.0336 & 0.0123 & 0.999 \end{pmatrix} \begin{pmatrix} H_1^0 \\ H_{1M}^0 \\ H_1^{0'} \end{pmatrix}, \quad (5.47)$$

with $\tilde{H} \sim H_1^0$, $\tilde{H}' \sim H_{1M}^0$, $\tilde{H}'' \sim H_1^{0'}$ and $m_{\tilde{H}} = 125.7$ GeV, $m_{\tilde{H}'} = 420$ GeV, $m_{\tilde{H}''} = 601$ GeV. $a_{1,1M}$ - the (1,2) element of the 3×3 matrix can actually vary between (-0.0515, -0.05295) and still satisfy CMS constraints.

Another example is Example 2: $\lambda_1 = 0.0329$, $\lambda_2 = 14.2$, $\lambda_3 = 15.4$, $\lambda_4 =$

0.0056, $\lambda_5 = 15$, $\lambda_8 = -1$, and $m_{H_5^+} = 590$ GeV, $m_{H_5^{++}} = 600$ GeV,

$$\begin{pmatrix} \tilde{H} \\ \tilde{H}' \\ \tilde{H}'' \end{pmatrix} = \begin{pmatrix} 0.99999\dots & -2.49 \times 10^{-3} & -1.60 \times 10^{-3} \\ 2.49 \times 10^{-3} & 0.99999\dots & -5.30 \times 10^{-4} \\ 1.60 \times 10^{-3} & 5.26 \times 10^{-4} & 0.99999\dots \end{pmatrix} \begin{pmatrix} H_1^0 \\ H_{1M}^0 \\ H_1^{0'} \end{pmatrix}, \quad (5.48)$$

with $\tilde{H} \sim H_1^0$, $\tilde{H}' \sim H_{1M}^0$, $\tilde{H}'' \sim H_1^{0'}$ and $m_{\tilde{H}} = 125.7$ GeV, $m_{\tilde{H}'} = 420$ GeV, $m_{\tilde{H}''} = 599$ GeV. The allowed range for $a_{1,1M}$ - the (1,2) element of the 3×3 matrix is $(-1.20, -3.40) \times 10^{-3}$.

Table 5.2: Partial width of $H \rightarrow gg$ as the measure of the production cross section, partial widths and branching ratios for various channels in SM (for $m_{H_{SM}} = 125.7$ GeV with total width = 4.17E-3 GeV, and the EW ν_R model for *Dr. Jekyll* example 2 scenario: $a_{1,1M} = -0.0025$, where $m_{\tilde{H}} = 125.7$ GeV, total width = 4.45E-3 GeV and $\tilde{H} \sim H_1^0$). All the partial widths are given in GeV.

	SM			EW ν_R			μ
	$\Gamma_{H \rightarrow gg}$ $\propto \sigma_{gg \rightarrow H}$	Partial width	BR	$\Gamma_{\tilde{H} \rightarrow gg}$ $\propto \sigma_{gg \rightarrow H}$	Partial width	BR	
$\tilde{H} \rightarrow W^+W^-$	3.55E-04	9.42E-04	2.26E-01	3.46E-04	7.63E-04	1.72E-01	0.74
$\tilde{H} \rightarrow ZZ$	3.55E-04	1.17E-04	2.81E-02	3.46E-04	9.49E-05	2.13E-02	0.74
$\tilde{H} \rightarrow b\bar{b}$	3.55E-04	2.36E-03	5.66E-01	3.46E-04	2.79E-03	6.26E-01	1.07
$\tilde{H} \rightarrow \tau\bar{\tau}$	3.55E-04	2.59E-04	6.21E-02	3.46E-04	3.06E-04	6.87E-02	1.07
$\tilde{H} \rightarrow \gamma\gamma$	3.55E-04	9.51E-06	2.28E-03	3.46E-04	1.26E-05	2.82E-03	1.21

- Notice that, although Examples 1 and 2 have very different values for the off-diagonal elements in $\{a_{ij}\}$, they yield comparable numerical signal strength predictions, the reason being principally that in both the cases $\tilde{H} \sim H_1^0$. We can also find other cases having intermediate values for the off-diagonal elements yielding comparable signal strengths.

- Table 5.2 shows cross section of 125-GeV $H \rightarrow gg$ (as a measure of production cross section), partial widths and branching ratios in the SM and the $EW\nu_R$ model, for example 2. We see that these partial widths are not very different from those in SM. This is expected as, in this case, the couplings of H_1^0 with the SM gauge bosons and fermions are also close to those of the SM Higgs.
- The partial widths and the signal strengths for W^+W^- and ZZ decay channels are smaller, whereas those for $b\bar{b}$, $\tau\bar{\tau}$ and $\gamma\gamma$ decay channels are larger, than the corresponding values in SM.

It is because, for the example in Table 5.2, $s_2 < |a_{1,1}| < 1$, and as per Eq. (5.37) the partial width $\Gamma^{EW\nu_R}(\tilde{H} \rightarrow W^+W^-, ZZ) \sim |s_2 a_{1,1}|^2 \times \Gamma^{SM}(H_{SM}^0 \rightarrow W^+W^-, ZZ)$. On the other hand, as seen in Eq. (5.38), $\Gamma^{EW\nu_R}(\tilde{H} \rightarrow f\bar{f}) \sim |a_{1,1}/s_2|^2 \Gamma^{SM}(H^0 \rightarrow f\bar{f}) > \Gamma^{SM}(H^0 \rightarrow f\bar{f})$.

$\Gamma^{EW\nu_R}(\tilde{H} \rightarrow \gamma\gamma)$ is larger than the corresponding SM value, because in the $EW\nu_R$ model, charged scalars and mirror fermions also contribute to this decay through triangle loops (refer to Section 5.3.2). Recall that in SM this decay is dominated only by the W loop.

- Fig. 5.3 shows the comparison between the CMS data for signal strengths $\mu(H\text{-decay})$ of the 125-GeV Higgs boson, and the corresponding predictions for the 125-GeV \tilde{H} in the $EW\nu_R$ model, for examples 1 and 2 in *Dr. Jekyll* scenario and examples 1, 2 and 3 in *Mr. Hyde* scenario, discussed in the next subsection.

For calculating the $EW\nu_R$ predictions, we have considered the gluon-gluon fusion production channel ($gg \rightarrow \tilde{H}$), which is the most dominant Higgs-production channel at the LHC. Calculations of the predictions in the $EW\nu_R$

model are explained in Section 5.3.

- Notice that the predicted ranges for $\mu(\tilde{H} \rightarrow W^+W^-, ZZ)$ and $\mu(\tilde{H} \rightarrow b\bar{b}, \tau\bar{\tau})$ are much narrower than the allowed ranges by the CMS constraints.

A wider range of $a_{1,1M}$ than shown in Eqs. (5.47), (5.48) is allowed if we impose the constraints on only, say, $\tilde{H} \rightarrow W^+W^-$ decay. However, for a part of the $a_{1,1M}$ range that satisfies the constraints on $\mu(\tilde{H} \rightarrow W^+W^-)$, the constraints on one or more of the other decay channels are not satisfied, and vice versa. So is true for all the other decay channels. Hence, when we seek the range of $a_{1,1M}$ that satisfies the constraints on *all* 4 of the $\tilde{H} \rightarrow W^+W^-, ZZ, b\bar{b}, \tau\bar{\tau}$ decay channels, the predicted ranges for the signal strengths of these different channels are correlated. This shortens the range of $a_{1,1M}$ and of the signal strength predictions. These correlated predictions are shown in Fig. 5.3.

- The predicted range for $\mu(\tilde{H} \rightarrow \gamma\gamma)$ spans over the range 0 – 2.5, because over the ranges of $m_{H_5^+}$ and $m_{H_5^{++}}$, $\mu(\tilde{H} \rightarrow \gamma\gamma)$ can easily vary without significantly affecting the predictions for the signal strengths of other decay channels.
- **Conclusions from Fig. 5.3:** We see that in the $\tilde{H} \sim H_1^0$ scenario predictions of the $EW\nu_R$ model for various signal strengths agree with those of the 125-GeV Higgs boson, as measured by CMS. A slightly, but not very, different mixing matrices can also agree with the ATLAS measurements. Future measurements of partial widths would therefore be required to disentangle this scenario from that the SM.

We now come to the most interesting part of our analysis, the one in which the 125-GeV Higgs boson is very unlike the SM Higgs.

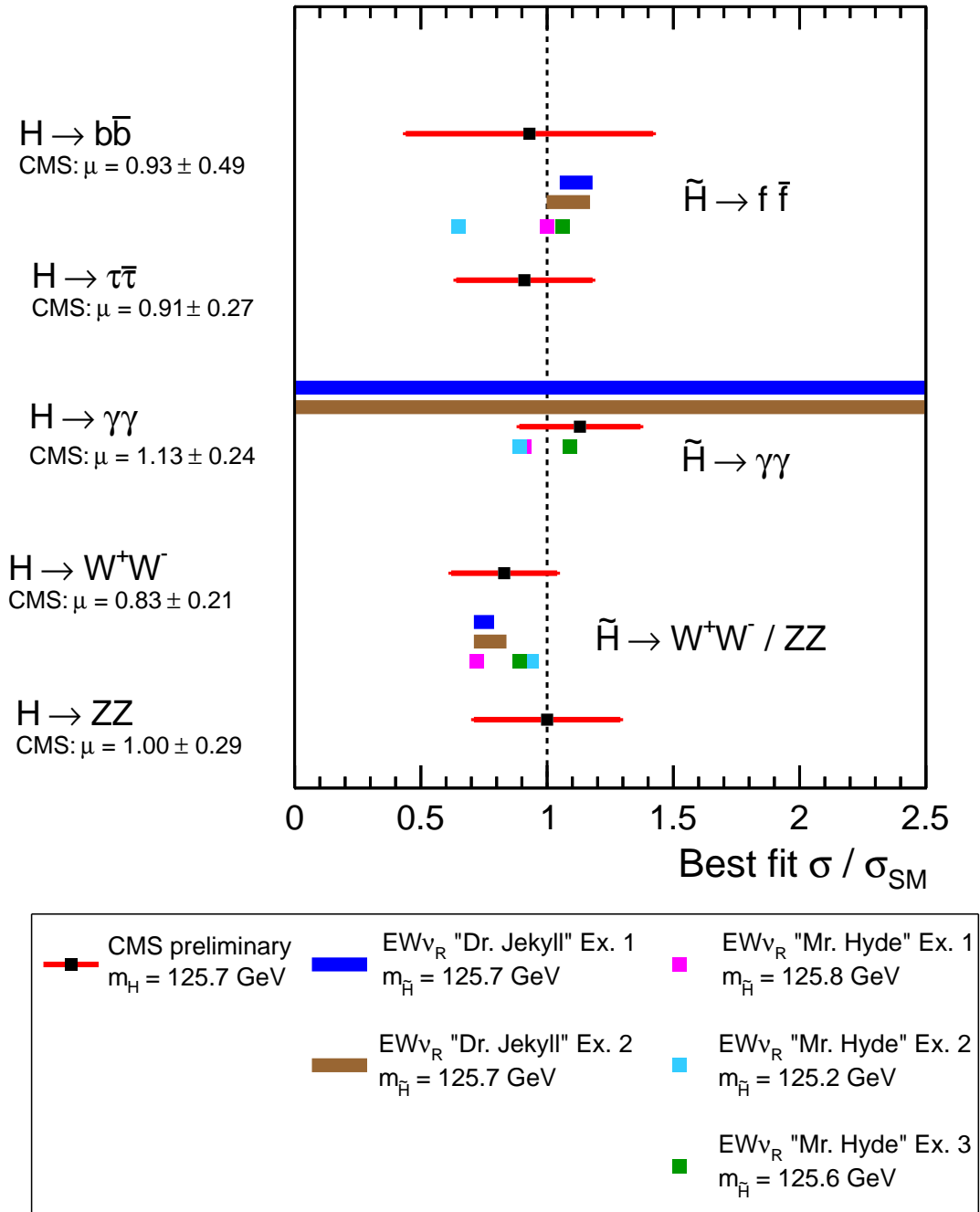


Figure 5.3: Figure shows the predictions of $\mu(\tilde{H} \rightarrow b\bar{b}, \tau\bar{\tau}, \gamma\gamma, W^+W^-, ZZ)$ in the EW ν_R model for examples 1 and 2 in *Dr. Jekyll* and example 1, 2 and 3 in *Mr. Hyde* scenarios, in comparison with corresponding best fit values by CMS [51, 52, 53, 54].

5.4.3 \tilde{H} as the 125-GeV Higgs candidate with a sub-dominant SM-like component

Can the 125-GeV \tilde{H} in the $\text{EW}\nu_R$ model have H_1^0 as a subdominant component and still satisfy the experimental constraints on its signal strengths? There are only two CP-even, neutral scalar states other than H_1^0 , and they are H_{1M}^0 and $H_1^{0'}$. The analysis explained in section 5.4.1.5 revealed 1501 out of 4 million parameter combinations, for which H_1^0 can, indeed, be a subdominant component in 125-GeV \tilde{H} while agreeing with the measured signal strengths of the 125-GeV Higgs at the LHC - the scenario we earlier referred to as *Mr. Hyde* scenario.

5.4.3.1 Results of the analysis

- Table 5.4 shows 16 out of the 1501 combinations of the parameters.
- It can be seen from Table 5.4 that in *Mr. Hyde* scenario, the CMS constraints on the signal strength can be satisfied, even when the scalar couplings satisfy $|\lambda/4\pi| < 1$. This means that the scalar particles heavier than the 125-GeV Higgs, need not be strongly coupled, and could be potentially detected as *narrow resonances* at the LHC.
- Similarly, s_{2M} can be larger than in *Dr. Jekyll* scenario. The mirror fermion masses are given in terms of s_{2M} by

$$m_{fM} = \frac{g_{MF}s_{2M}v}{\sqrt{2}}. \quad (5.49)$$

Consequently, larger (than in *Dr. Jekyll* scenario) masses of the mirror fermions are allowed by the perturbative limit on their Yukawa couplings. In other words,

for a given mass of the mirror fermions, their Yukawa couplings in *Mr. Hyde* scenario can be smaller than those in *Dr. Jekyll* scenario.

- To highlight interesting features of this scenario, we consider three examples listed in Table 5.4.

- Example 1 (row 1 of Table 5.4): $s_2 = 0.900$, $s_{2M} = 0.270$, $s_M = 0.341$, $\lambda_1 = -0.481$, $\lambda_2 = 6.00$, $\lambda_3 = 1.46$, $\lambda_4 = 2.99$, $\lambda_5 = 2$, $\lambda_8 = -1$,

$$\begin{pmatrix} \tilde{H} \\ \tilde{H}' \\ \tilde{H}'' \end{pmatrix} = \begin{pmatrix} 0.300 & -0.094 & -0.949 \\ 0.334 & -0.921 & -0.197 \\ 0.893 & 0.376 & 0.246 \end{pmatrix} \begin{pmatrix} H_1^0 \\ H_{1M}^0 \\ H_1^{0'} \end{pmatrix}, \quad (5.50)$$

with $\tilde{H} \sim H_1^{0'}$, $\tilde{H}' \sim H_{1M}^0$, $\tilde{H}'' \sim H_1^0$; $m_{\tilde{H}} = 125.8$ GeV, $m_{\tilde{H}'} = 416$ GeV, $m_{\tilde{H}''} = 1100$ GeV, $M_R \lesssim 105$ GeV, and $\mu(\tilde{H} \rightarrow W^+W^-/ZZ) = 0.72$, $\mu(\tilde{H} \rightarrow \gamma\gamma) = 0.91$, $\mu(\tilde{H} \rightarrow b\bar{b}/\tau\bar{\tau}) = 1.00$.

- Example 2 (row 2 of Table 5.4): $s_2 = 0.514$, $s_{2M} = 0.841$, $s_M = 0.168$, $\lambda_1 = 6.15$, $\lambda_2 = 7.68$, $\lambda_3 = 8.84$, $\lambda_4 = -2.131502$, $\lambda_5 = 5$, $\lambda_8 = -1$,

$$\begin{pmatrix} \tilde{H} \\ \tilde{H}' \\ \tilde{H}'' \end{pmatrix} = \begin{pmatrix} 0.188 & 0.091 & 0.978 \\ -0.941 & -0.268 & 0.207 \\ -0.281 & 0.959 & -0.035 \end{pmatrix} \begin{pmatrix} H_1^0 \\ H_{1M}^0 \\ H_1^{0'} \end{pmatrix}, \quad (5.51)$$

with $\tilde{H} \sim H_1^{0'}$, $\tilde{H}' \sim H_1^0$, $\tilde{H}'' \sim H_{1M}^0$; $m_{\tilde{H}} = 125.2$ GeV, $m_{\tilde{H}'} = 633$ GeV, $m_{\tilde{H}''} = 1427$ GeV, $M_R \lesssim 52.0$ GeV, and $\mu(\tilde{H} \rightarrow W^+W^-/ZZ) = 0.94$, $\mu(\tilde{H} \rightarrow \gamma\gamma) = 0.89$, $\mu(\tilde{H} \rightarrow b\bar{b}/\tau\bar{\tau}) = 0.65$.

- Example 3 (row 3 of Table 5.4): $s_2 = 0.401$, $s_{2M} = 0.900$, $s_M = 0.151$, $\lambda_1 = 4.76$, $\lambda_2 = 3.41$, $\lambda_3 = 7.71$, $\lambda_4 = -1.29$, $\lambda_5 = 4$, $\lambda_8 = -1$,

$$\begin{pmatrix} \tilde{H} \\ \tilde{H}' \\ \tilde{H}'' \end{pmatrix} = \begin{pmatrix} 0.187 & 0.115 & 0.976 \\ 0.922 & 0.321 & -0.215 \\ 0.338 & -0.940 & 0.046 \end{pmatrix} \begin{pmatrix} H_1^0 \\ H_{1M}^0 \\ H_1^{0'} \end{pmatrix}, \quad (5.52)$$

with $\tilde{H} \sim H_1^{0'}$, $\tilde{H}' \sim H_1^0$, $\tilde{H}'' \sim H_{1M}^0$; $m_{\tilde{H}} = 125.6$ GeV, $m_{\tilde{H}'} = 454$ GeV, $m_{\tilde{H}''} = 959$ GeV, $M_R \lesssim 46.4$ GeV, and $\mu(\tilde{H} \rightarrow W^+W^-/ZZ) = 0.89$, $\mu(\tilde{H} \rightarrow \gamma\gamma) = 1.09$, $\mu(\tilde{H} \rightarrow b\bar{b}/\tau\bar{\tau}) = 1.06$.

- In example 1, H_{1M}^0 is the dominant component in \tilde{H}' , whereas H_1^0 is the dominant in \tilde{H}' in examples 2 and 3. Although the mixing matrices in examples 2 and 3 are not very different, the ratio of VEV's s_2 , s_{2M} are different enough to result in the signal strengths that are not very similar (especially for $\tilde{H} \rightarrow f\bar{f}$). As the partial width of $\tilde{H} \rightarrow f\bar{f}$ is proportional to $|a_{1,1}/s_2|^2$, it changes rapidly with s_2 . Also, because we have 6 mirror quarks which contribute to the cross section of gluon-gluon fusion, the production cross section dominantly changes as $\sim |a_{1,1}/s_2 + 6 a_{1,1M}/s_{2M}|^2$. Thus, any change in $a_{1,1M}/s_{2M}$ is amplified while calculating the signal strengths.
- Comparison of the signal strengths for the three examples with the CMS constraints on them can be seen in Fig. 5.3. Notice the agreement between the predictions for the signal strengths with the CMS constraints in the figure. This agreement demonstrates that the *SM-like signal strengths of 125-GeV Higgs at the LHC are not sufficient to conclude that it is a SM-like Higgs, or even if it*

has a dominant SM-like component.

- Table 5.3 shows the partial widths, branching ratios and the signal strengths for *Mr. Hyde* scenario in the $\text{EW}\nu_R$ model and SM. It can be seen that the partial widths in this scenario are very different from the SM (smaller by a factor of ~ 5 for the example in the table), but it results in similar signal strengths. Measurements of the partial widths are therefore necessary to be able to experimentally distinguish between *Mr. Hyde* scenario and SM.

Table 5.3: Partial width of $H \rightarrow gg$ as the measure of the production cross section, partial widths and branching ratios for various channels in SM (for $m_{H_{SM}} = 125.6$ GeV and total width $4.15\text{E-}03$ GeV), and the $\text{EW}\nu_R$ model for row 3 in Table 5.4, also in Eq. (5.52) where $\tilde{H} \sim H_1^{0'}$ (with $m_{\tilde{H}} = 125.6$ GeV and total width $1.34\text{E-}03$ GeV). All the partial widths are given in GeV .

	SM			$\text{EW}\nu_R$			μ
	$\Gamma_{H \rightarrow gg}$ $\propto \sigma_{gg \rightarrow H}$	Partial width	BR	$\Gamma_{\tilde{H} \rightarrow gg}$ $\propto \sigma_{gg \rightarrow H}$	Partial width	BR	
$\tilde{H} \rightarrow W^+W^-$	3.54E-04	9.30E-04	2.24E-01	5.75E-04	1.64E-04	1.23E-01	0.89
$\tilde{H} \rightarrow ZZ$	3.54E-04	1.16E-04	2.79E-02	5.75E-04	2.04E-05	1.53E-02	0.89
$\tilde{H} \rightarrow b\bar{b}$	3.54E-04	2.35E-03	5.67E-01	5.75E-04	5.07E-04	3.79E-01	1.06
$\tilde{H} \rightarrow \tau\bar{\tau}$	3.54E-04	2.58E-04	6.22E-02	5.75E-04	5.42E-05	4.06E-02	1.06
$\tilde{H} \rightarrow \gamma\gamma$	3.54E-04	9.46E-06	2.28E-03	5.75E-04	2.04E-06	1.53E-03	1.09

5.4.3.2 Remarks on the H_{1M}^0 component in \tilde{H}

A few remarks are in order here:

- Notice that for all the cases listed in Table 5.4 $H_1^{0'}$ is the dominant component in the 125-GeV \tilde{H} . In all 1501 cases we found, the modulus of the coefficient of H_{1M}^0 in the 125-GeV \tilde{H} was ≤ 0.32 .

- In the gluon-gluon fusion channel H_{1M}^0 is produced through triangle loops of 6 mirror quarks. Therefore, if H_{1M}^0 is the dominant component in \tilde{H} , then the production cross section of \tilde{H} could become too high to be compensated by small branching ratios. Thus, it makes sense that H_{1M}^0 is disfavored to be the dominant component in \tilde{H} , by the constraints on the signal strengths.
- Even if H_{1M}^0 is a sub-dominant component in \tilde{H} , one should not think that it has decoupled from the other two singlets. In other words, the scalar doublet Φ_{2M} does not really decouple from Φ_2 and χ . This is because:
 - Even if H_{1M}^0 has a small coefficient in \tilde{H} , its production amplitude through 6 mirror quarks has a significant contribution to the production cross section of \tilde{H} .
 - The real degree of freedom of Φ_{2M} leads to H_{1M}^0 . But its other degrees of freedom also contribute to other physical particles such as $H_3^{0,\pm}$, $H_{3M}^{0,\pm}$. These particles contribute to $\tilde{H} \rightarrow \gamma\gamma$ and the total width. Hence, they play a role in ensuring that the branching ratios are in the appropriate range to achieve an agreement with the signal strength constraints.
- Thus, although H_{1M}^0 is a sub-dominant component in \tilde{H} , the scalar doublet Φ_{2M} , newly added to the minimal EW ν_R model, plays a crucial role in accommodating the 125-GeV Higgs boson in the EW ν_R model, in *Mr. Hyde* as well as *Dr. Jekyll* scenario.

Before concluding this section, we will briefly discuss some indirect constraints on the next heavier scalar \tilde{H}' , in both these scenarios.

Table 5.4: All the masses and the total width of \tilde{H} are given in GeV. Fixed parameters as given in Eq. (5.46).

	s_2	s_{2M}	s_M	λ_1	λ_2	λ_3	λ_4	λ_5	$m_{\tilde{H}}$	$m_{\tilde{H}'}$	$m_{\tilde{H}''}$			
1	0.90	0.27	0.34	-0.48	6.00	1.46	2.99	2	125.8	416	1100			
2	0.51	0.84	0.17	6.15	7.68	8.84	-2.13	5	125.2	633	1427			
3	0.41	0.90	0.15	4.76	3.41	7.71	-1.29	4	125.6	454	959			
4	0.87	0.32	0.36	-0.39	4.40	1.21	4.48	1	126.2	420	1382			
5	0.35	0.91	0.22	8.73	5.26	4.88	-1.59	9	126.1	617	1237			
6	0.31	0.87	0.38	4.99	9.67	2.10	-1.02	1	126.4	435	1786			
7	0.31	0.87	0.38	4.99	9.67	2.10	-1.02	2	126.4	435	1786			
8	0.92	0.21	0.31	-0.73	9.34	1.83	9.25	5	125.6	412	1988			
9	0.36	0.92	0.16	6.78	3.10	7.16	-1.34	4	126.1	501	905			
10	0.92	0.19	0.35	-0.34	11.69	1.17	2.79	1	126.7	428	1067			
11	0.95	0.12	0.29	-0.46	9.71	1.68	3.37	9	126.0	248	1167			
12	0.38	0.89	0.26	3.47	5.24	3.25	-0.99	10	125.2	409	1281			
13	0.30	0.93	0.22	5.01	2.67	3.06	-0.75	12	125.1	415	906			
14	0.36	0.89	0.28	2.34	2.56	2.04	-0.52	12	126.0	333	890			
15	0.48	0.86	0.20	2.26	2.90	4.11	-0.74	6	126.0	376	896			
16	0.32	0.91	0.26	2.76	2.07	2.18	-0.49	11	126.3	323	804			
	$a_{1,1}$	$a_{1,1M}$	$a_{1,1V}$	$a_{1M,1}$	$a_{1M,1M}$	$a_{1M,1V}$	$a_{1V,1}$	$a_{1V,1M}$	$a_{1V,1V}$	$\Gamma_{\tilde{H}}$	$\mu_{WW/ZZ}$	$\mu_{\gamma\gamma}$	$\mu_{bb/\tau\tau}$	$M_R \lesssim$
1	0.301	-0.094	-0.949	0.334	-0.922	0.197	0.893	0.376	0.246	1.66E-03	0.719	0.914	1.002	105.0
2	0.189	0.091	0.978	-0.941	-0.268	0.207	-0.281	0.959	-0.035	9.61E-04	0.941	0.895	0.647	52.0
3	0.187	0.115	0.976	0.922	0.321	-0.215	0.338	-0.940	0.046	1.34E-03	0.891	1.089	1.062	46.4
4	0.303	-0.087	-0.949	0.357	-0.913	0.197	0.884	0.398	0.246	1.12E-03	0.753	1.108	0.849	111.9
5	0.143	0.090	0.986	0.966	0.204	-0.159	0.216	-0.975	0.057	1.12E-03	0.994	0.995	0.682	69.2
6	0.238	0.041	0.970	0.970	0.035	-0.239	0.044	-0.999	0.031	2.62E-03	0.953	1.128	1.092	118.1
7	0.238	0.041	0.970	0.970	0.035	-0.239	0.044	-0.999	0.031	2.62E-03	0.954	0.894	1.093	118.1
8	0.239	-0.096	-0.966	0.210	-0.966	0.148	0.948	0.239	0.211	2.91E-03	0.882	1.341	0.708	95.7
9	0.156	0.129	0.979	-0.901	-0.388	0.195	-0.405	0.912	-0.056	1.37E-03	1.031	1.001	1.043	49.6
10	0.272	-0.047	-0.961	0.237	-0.965	0.114	0.932	0.259	0.251	9.77E-04	0.729	1.107	0.663	108.4
11	0.230	-0.126	-0.965	0.113	-0.981	0.155	0.967	0.145	0.211	1.57E-02	0.742	1.083	0.678	89.2
12	0.241	0.065	0.968	0.964	0.097	-0.247	0.110	-0.993	0.039	1.82E-03	0.849	0.967	1.080	79.6
13	0.131	0.075	0.989	0.979	0.146	-0.141	0.155	-0.986	0.054	1.06E-03	0.770	1.266	0.666	69.0
14	0.211	0.071	0.975	0.971	0.104	-0.217	0.117	-0.992	0.047	1.74E-03	1.006	1.267	0.984	87.0
15	0.217	0.090	0.972	0.950	0.208	-0.231	0.223	-0.974	0.040	1.29E-03	1.012	0.917	0.857	60.9
16	0.182	0.076	0.980	0.975	0.115	-0.190	0.127	-0.991	0.053	1.69E-03	0.919	0.930	1.019	80.6

5.4.4 The next heavier neutral scalar \tilde{H}'

In *Dr. Jekyll* scenario, examples 1 and 2 that we considered have H_{1M}^0 as the dominant component in \tilde{H}' , which is the next heavier physical scalar after the 125-GeV \tilde{H} . Here the total width of \tilde{H}' is also greater than its mass, with the scalar coupling $\lambda_2 > 4\pi$. Thus, it is a strongly coupled scalar, which is difficult to detect as a narrow resonance.

In example 1 of *Mr. Hyde* scenario, H_{1M}^0 is the dominant component in \tilde{H}' , while in examples 2 and 3 H_1^0 is the dominant component in \tilde{H}' . In all 3 examples, \tilde{H}' has a total width $< 10\%$ of its mass.

This subsection compares the signal strength of $\tilde{H}' \rightarrow W^+W^-$ and the $\sigma \times BR(\tilde{H}' \rightarrow \gamma\gamma)$ with the CMS constraints on SM-like heavy Higgs, for examples having $m_{\tilde{H}'} \lesssim 600$ GeV. These CMS constraints [63, 64, 59, 65] assume the Standard model background, whereas, in the $EW\nu_R$ model, extra processes involving mirror fermions and extra scalars also contribute to the background in addition to the SM processes. The background in this model is therefore expected to be larger than that in the SM. A detailed study of this background is out of the scope of this dissertation.

Although the SM background does not strictly apply to \tilde{H}' in the $EW\nu_R$ model, we show how the $EW\nu_R$ predictions compare with the experimental constraints.

For our calculations we computed the total width of \tilde{H}' using

$$\begin{aligned} \Gamma_{\tilde{H}'} = & \sum_{i=1}^3 \Gamma_{\tilde{H}' \rightarrow q_i^M \bar{q}_i^M} + \sum_{j=1}^3 \times \Gamma_{\tilde{H}' \rightarrow l_j^M \bar{l}_j^M} + \Gamma_{\tilde{H}' \rightarrow t\bar{t}} + \Gamma_{\tilde{H}' \rightarrow b\bar{b}} + \Gamma_{\tilde{H}' \rightarrow \tau\bar{\tau}} \\ & + \Gamma_{\tilde{H}' \rightarrow c\bar{c}} + \Gamma_{\tilde{H}' \rightarrow W^+W^-} + \Gamma_{\tilde{H}' \rightarrow ZZ} + \Gamma_{\tilde{H}' \rightarrow gg} + \Gamma_{\tilde{H}' \rightarrow \gamma\gamma}. \end{aligned} \quad (5.53)$$

The partial decay widths were calculated using the method illustrated in Section 5.3.

5.4.4.1 Constraints on the signal strength of $\tilde{H}' \rightarrow W^+W^-$

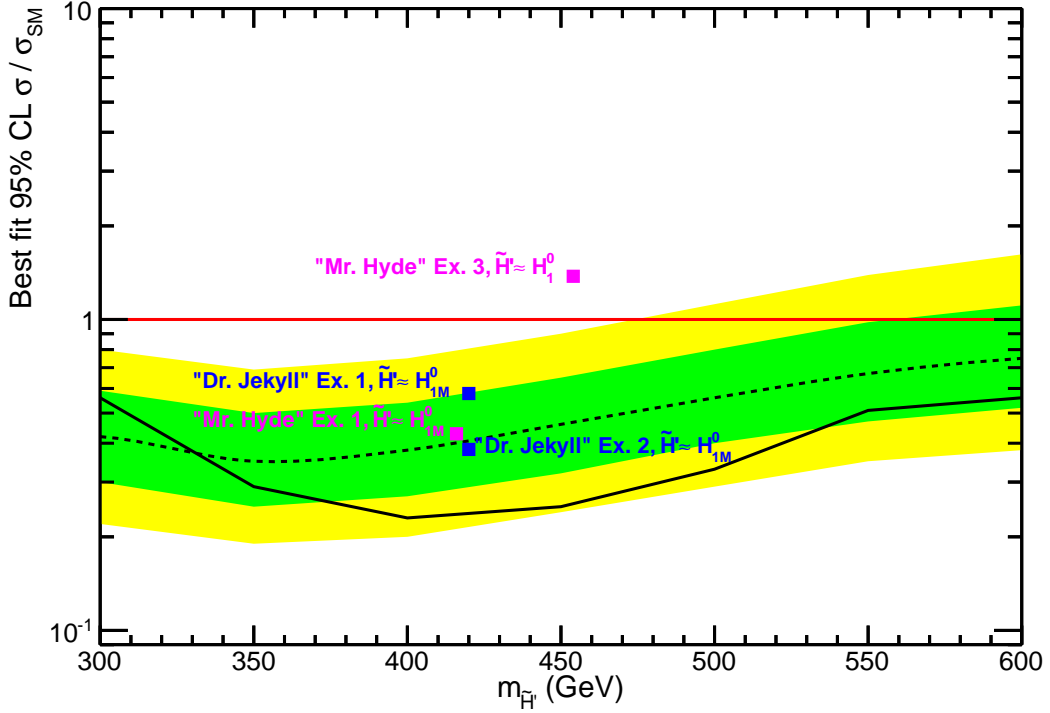


Figure 5.4: Predicted signal strength of $\tilde{H}' \rightarrow W^+W^-$ in 4 example scenarios (blue and purple squares). The results of the search for SM-like Higgs boson up to 600 GeV with the 1σ (green band) and 2σ (yellow band) limits on the SM background (dotted curve) and CMS data (solid black curve) are also displayed.

- Fig. 5.4 shows the signal strength of $\tilde{H}' \rightarrow W^+W^-$ for examples 1 and 2 in *Dr. Jekyll* scenario (blue squares) and examples 1 and 3 in *Mr. Hyde* scenario (purple squares). The 1σ and 2σ SM background bands and the CMS data [63, 64] are also displayed. The signal strength for example 2 in *Mr. Hyde* scenario is not displayed as $m_{\tilde{H}'} = 633$ GeV for this example, but the CMS data for this decay channel are only available up to 600 GeV.
- In the figure, notice that the predicted signal strengths for examples 1 and 2 in *Dr. Jekyll* case and example 1 in *Mr. Hyde* case are within the $\pm 1\sigma$

SM-background bands. Therefore, the CMS data are surely not conclusive for confirming or ruling out these examples.

- Example 1 in *Mr. Hyde* scenario predicts a signal strength $\mu(\tilde{H}' \rightarrow W^+W^-) \approx 1.3$, which is certainly larger the SM-background band and the data. H_1^0 - the SM-like Higgs is the dominant component in \tilde{H}' in this example. However, the SM-background still does not strictly apply here, since additional background processes can contribute to it. For example, production of W^+W^- from two gluons through a box loop of mirror quarks.

5.4.4.2 Constraints on $\tilde{H}' \sim H_{1M}^0$ from $\gamma\gamma$ -decay channel

The constraints on $\sigma(gg \rightarrow \tilde{H}') \times BR(\tilde{H}' \rightarrow \gamma\gamma)$ from CMS [65] and ATLAS [59] are accompanied by assumptions that the total width of the SM-like heavy Higgs is 0.1 GeV or 10% of its mass. The total width of \tilde{H}' in our scenarios does not follow either of these patterns. We observed that $\sigma(gg \rightarrow \tilde{H}') \times BR(\tilde{H}' \rightarrow \gamma\gamma)$ predictions for all the examples in both the scenarios is consistently lower than the CMS and ATLAS constraints.

5.4.4.3 A comment on \tilde{H}''

In the examples of *Dr. Jekyll* scenario considered in this section, $\tilde{H}'' \sim H_1^{0'}$, and in the examples of *Mr. Hyde* scenario that we have considered, $\tilde{H}'' \sim H_1^0$ or H_{1M}^0 . For all these examples, $m_{\tilde{H}''} \gtrsim 600$ GeV. So far, the CMS data in Fig 5.4 are not sensitive to the signal strengths of the order of SM predictions in this mass range. A detailed analysis of its signal strengths will be of interest, when more data for this higher mass range are available and are analyzed with full $EW\nu_R$ background.

5.4.5 Conclusions about the 125-GeV Higgs candidate in the EW ν_R model

- In this section we investigated two very different scenarios of the 125-GeV Higgs boson at the LHC from the perspective of the EW ν_R model:
 1. *Dr. Jekyll*: H_1^0 , which is the real part of the SM-like scalar doublet Φ_2 , is the dominant component in the 125-GeV \tilde{H} , and
 2. *Mr. Hyde*: H_1^0 is a sub-dominant component in the 125-GeV \tilde{H} - a more interesting scenario.
- We demonstrated that in both these scenarios the signal strengths of the 125-GeV \tilde{H} in W^+W^- , ZZ , $\gamma\gamma$, $b\bar{b}$ and $\tau\bar{\tau}$ decay channels agree with the constraints from CMS (and also ATLAS) data. Thus, from the perspective of the EW ν_R model, the present data at the LHC are inconclusive about whether SM-like H_1^0 is *the dominant* or *a sub-dominant component* in the 125-GeV particle. Hence “the dual nature” of the 125-GeV Higgs in the EW ν_R model.

More data, measurements of the individual partial widths and study of the heavier physical scalars in the EW ν_R model are necessary to distinguish between either of these scenarios and the SM-Higgs.

- As expected, the individual partial widths of the 125-GeV \tilde{H} in *Dr. Jekyll* scenarios are not very different from those in SM. Here, the scalar couplings $|\lambda_2|$, $|\lambda_3|$, $|\lambda_5|$ need to be greater than 4π to satisfy the constraints on the signal strengths. This means that the heavier scalars in this scenario tend to be strongly coupled and have large widths.

Dominant SM-like component in the 125-GeV Higgs also leads to v_2 (the VEV of Φ_2) being the dominant part in v , and smaller v_{2M} , which gives masses to

the mirror fermions. Consequently, the masses of the mirror fermions, allowed by the perturbative limit on their Yukawa couplings, cannot be much greater than ~ 120 GeV. We adopt a lower limit of 102 GeV set by the constraints from LEP3 [6].

- Hence, if future measurements of the individual decay widths of the 125-GeV Higgs result in SM-like widths, then it is more likely to be consistent with *Dr. Jekyll* scenario. In this case, the heavier scalars would appear not as narrow resonances, but as broad resonances or enhancement in the background in this model.

Since the SM-like H_1^0 is the dominant component in the 125-GeV \tilde{H} , the effective theory around this energy looks like SM, in which the heavier scalars are *integrated out*.

- In contrast, the individual partial widths of the 125-GeV \tilde{H} are very different from those in SM, in *Mr. Hyde* scenario. In all 1501 combinations of the parameters that we found to agree with the experimental 1σ constraints on the signal strengths contain $H_1^{0'}$ as the dominant component in the 125-GeV \tilde{H} . The predicted signal strengths of this \tilde{H} agree with the experimental 1σ constraints on the signal strengths even when the scalar couplings $|\lambda|$'s are smaller than 4π . The heavier scalars in this case are not strongly coupled, as a result.

The H_{1M}^0 as a dominant component in \tilde{H} is disfavored to agree with the constraints on the signal strengths, due to its large contribution to the cross section of $gg \rightarrow \tilde{H}$.

Because v_{2M} is not constrained to be small in this case, the perturbative upper limit on the masses of the mirror fermions is about 700 GeV .

- Therefore, if the partial widths of the 125-GeV \tilde{H} are measured to be very different from those in SM, it would point towards *Mr. Hyde* scenario. The heavier scalars in this case have narrow widths and can be detected as resonances.

The SM-like H_1^0 is the dominant component in one of the heavier scalars, \tilde{H}' or \tilde{H}'' . Thus, the effective theory around 125 GeV is very different from SM, while the SM-like H_1^0 is *integrated out* with the heavier scalars.

- As can be seen from Eq (5.46) we scanned only a part of the entire parameter space in the $EW\nu_R$ model, by fixing the values or the ranges of a few parameters. A more thorough scan of the parameter space could be of interest, especially if more data from the LHC Run II show any signs of physics Beyond the Standard Model.

Chapter 6

Conclusions

In this dissertation we have presented a detailed analysis of the phenomenology of the non-sterile Electroweak-scale Right-handed Neutrino ($\text{EW}\nu_R$) model. We started by reviewing the development of the Standard Model of particle physics (Chapter 1) and then extensions to SM that accommodate massive neutrinos (Chapter 2). Our discussion provided the motivation for the development of a model, in which the right-handed neutrino ν_R is accessible to the Large Hadron Collider (LHC) and other experiments in the near-future.

In Chapter 3 we then reviewed Hung's minimal $\text{EW}\nu_R$ model [26], in which the ν_R 's naturally acquire a Majorana mass near the electroweak scale $\Lambda_{EW} \approx 246$ GeV. These ν_R 's are non-sterile, meaning that they are members of $SU(2)_L$ right-handed fermion doublets. Their mass M_R is bounded from below at $M_Z/2$ so that ν_R 's do not contribute to the total width of the Z bosons. To achieve the EW-scale M_R , without extending the gauge group of SM, the $\text{EW}\nu_R$ model also adds the mirror leptons, mirror quarks and two scalar triplets $\tilde{\chi}$ and ξ to the SM.

For any model that adds extra chiral fermions to the SM fermion sector, it is crucial to verify its agreement with the experimental constraints on the electroweak

precision parameters - the oblique parameters \tilde{S} and \tilde{T} . These parameters are measure of the radiative corrections to the self-energies of the electroweak gauge bosons W^\pm , Z and γ . They are finite observables, independent of any renormalization scheme. Their experimentally measured values are close to zero, explicitly given in Eq (4.10).

Since the $\text{EW}\nu_R$ model adds the mirror fermions to the SM fermion sector, it is important to first check whether it satisfies the experimental constraints on \tilde{S} and \tilde{T} , before analyzing its phenomenology further. Generally, new chiral fermions lead to a large positive contribution to the \tilde{S} parameter.

We have presented our extensive analysis of the parameter space in the minimal $\text{EW}\nu_R$ model in Chapter 4. We calculated the predicted \tilde{S} and \tilde{T} parameters. We demonstrated that a non-negligible region in the parameter space of the $\text{EW}\nu_R$ model agrees with the experimental constraints from the measurements of the oblique parameters. This result is shown in Fig. 4.4. This agreement is achieved because the large positive contributions to \tilde{S} from the mirror fermion sector are almost cancelled by the negative contributions from the scalar sector in this model.

It is worth noting that these electroweak precision constraints do not restrict the VEV of the triplet χ to be very small. It is only restricted by the perturbative limit on various Yukawa couplings and the lower limit: $M_R > M_Z/2$.

As the minimal $\text{EW}\nu_R$ model does not violate the electroweak precision constraints, we further discussed how the $\text{EW}\nu_R$ model can accommodate the 125-GeV Higgs boson. We argued that in the light of the spin-parity likelihood analysis for the 125-GeV scalar, an extension to the minimal $\text{EW}\nu_R$ model is needed to accommodate the new scalar easily. The simplest possible extension is to add a complex scalar doublet Φ_{2M} to the minimal model. In Chapter 5, we first discussed this extended $\text{EW}\nu_R$ model and derived the physical particle spectrum in it by breaking the $SU(2)_L \times U(1)_Y$ gauge symmetry to the global $SU(2)_D$ custodial symmetry.

Our detailed analysis of the extended $EW\nu_R$ model revealed a very interesting feature of the Higgs sector of this model. This Higgs sector includes a 125-GeV candidate \tilde{H} , which yields the signal strengths for its decays to W^+W^- , ZZ , $\gamma\gamma$, $b\bar{b}$ and $\tau\bar{\tau}$ that are compatible with measurements at CMS and ATLAS. This agreement is achieved, when \tilde{H} is dominantly like the SM Higgs - “Dr. Jekyll” scenario, and also when it is very different from the SM Higgs - “Mr. Hyde” scenario. This result for a few examples of parameter combinations is displayed in Fig. 5.3.

Thus, from the perspective of the $EW\nu_R$ model, the present data at the LHC are inconclusive about whether SM-like H_1^0 is *the dominant or a sub-dominant component* in the 125-GeV particle. Hence “the dual nature” of the 125-GeV Higgs in the $EW\nu_R$ model. More data, measurements of the individual partial widths and study of the heavier physical scalars in the $EW\nu_R$ model are necessary to distinguish between either of these scenarios and the SM-Higgs.

As expected, the individual partial widths of the 125-GeV \tilde{H} in *Dr. Jekyll* scenarios are not very different from those in SM. The heavier scalars in this scenario tend to be strongly coupled and have large widths. Also, the masses of the mirror fermions, allowed by the perturbative limit on their Yukawa couplings, cannot be much greater than ~ 120 GeV. Hence, if future measurements of the individual decay widths of the 125-GeV Higgs result in SM-like widths, then it is more likely to be consistent with *Dr. Jekyll* scenario. In this case, the heavier scalars would appear not as narrow resonances, but as broad resonances or enhancement in the background in this model.

In contrast, the individual partial widths of the 125-GeV \tilde{H} are very different from those in SM, in *Mr. Hyde* scenario. In this scenario, all the combinations of the parameters that we found to agree with the experimental 1σ constraints on the signal strengths contain $H_1^{0'}$ as the dominant component in the 125-GeV \tilde{H} . The perturbative upper limit on the masses of the mirror fermions is about 700 GeV .

Therefore, if the partial widths of the 125-GeV \tilde{H} are measured to be very different from those in SM, it would point towards *Mr. Hyde* scenario. The heavier scalars in this case have narrow widths and can be detected as resonances. The SM-like H_1^0 is the dominant component in one of the heavier scalars, \tilde{H}' or \tilde{H}'' . Thus, the effective theory around 125 GeV is very different from SM, while the SM-like H_1^0 is *integrated out* with the heavier scalars.

We scanned only a part of the entire parameter space in the EW ν_R model, by fixing the values or ranges of a few parameters. A more thorough scan of the parameter space could be of interest, especially if more data from the LHC Run II show any signs of physics Beyond the Standard Model.

Appendix A

Loop Integrals and Functions

Different contributions to the oblique parameters are expressed using loop integrals like A_0 , B_0 , B_{22} , B_1 , B_2 . and functions like \mathcal{F} , G , etc. Therefore, we define all the loop integrals and functions that we have used in the calculations of different loop diagrams before listing contributions from loop diagrams.

For the calculation of oblique parameters we need the loop diagrams with two external vector bosons. These diagrams have a general form

$$\Pi_{\mu\nu} = \Pi_A g_{\mu\nu} + \Pi_B q_\mu q_\nu \tag{A.1}$$

For the purpose of oblique parameters we only need the ‘ $g^{\mu\nu}$ ’ term in this equation. Hence, hereafter in this paper $\Pi_{\mu\nu}$ denotes only the first term on RHS above.

The loop diagrams involving one or two internal scalars or one or two internal fermions appear in the calculation of one-loop vector boson self-energy diagrams and $Z\gamma$ - diagrams. Following loop integrals appear in the calculation of loops with scalar particles [66]:

One-point integral:

$$\int \frac{d^4k}{(2\pi)^4} \frac{1}{(k^2 - m^2)} \equiv \frac{i}{16\pi^2} A_0(m^2) \quad (\text{A.2})$$

Two-point integrals:

$$\begin{aligned} \int \frac{d^4k}{(2\pi)^4} \frac{1}{(k^2 - m_1^2)((k+q)^2 - m_2^2)} \\ \equiv \frac{i}{16\pi^2} B_0(q^2; m_1^2, m_2^2), \end{aligned} \quad (\text{A.3})$$

$$\begin{aligned} \int \frac{d^4k}{(2\pi)^4} \frac{k_\mu k_\nu}{(k^2 - m_1^2)((k+q)^2 - m_2^2)} \\ \equiv \frac{i}{16\pi^2} g_{\mu\nu} B_{22}(q^2; m_1^2, m_2^2) \end{aligned} \quad (\text{A.4})$$

The expansion of LHS in the latter equation also has term with $q_\mu q_\nu$ [66], but this term is omitted as it does not contribute to the oblique parameters [36].

Following [66], in the dimensional regularization these integrals can be simplified to

$$A_0(m^2) = m^2 \left(\Delta + 1 - \ln(m^2) \right) \quad (\text{A.5})$$

$$B_0(q^2; m_1^2, m_2^2) = \Delta - \int_0^1 dx \ln(X - i\epsilon) \quad (\text{A.6})$$

$$\begin{aligned} B_{22}(q^2; m_1^2, m_2^2) = \frac{1}{4}(\Delta + 1) \left(m_1^2 + m_2^2 - \frac{q^2}{3} \right) \\ - \frac{1}{2} \int_0^1 dx X \ln(X - i\epsilon) \end{aligned} \quad (\text{A.7})$$

where

$$X \equiv m_1^2 x + m_2^2(1-x) - q^2 x(1-x), \quad (\text{A.8})$$

$$\Delta \equiv \frac{2}{4-d} + \ln(4\pi) - \gamma. \quad (\text{A.9})$$

in d space-time dimensions with $\gamma = 0.577216\dots$, the Euler's constant [10]. The integrals in eqns. (A.6), (A.7) can be calculated numerically up to desired accuracy. Note that these equations involve the logarithm of a dimensionful quantity, X and the scale of this logarithm is hidden in the $2/(4-d)$ term in Δ (refer to section 7.5 of [10]). It is useful, especially in deriving \tilde{T}_{scalar} in Eq. (4.17), to note that [56]

$$B_0(0; m_1^2, m_2^2) = \frac{A_0(m_1^2) - A_0(m_2^2)}{m_1^2 - m_2^2}, \quad (\text{A.10})$$

$$4B_{22}(0; m_1^2, m_2^2) = \mathcal{F}(m_1^2, m_2^2) + A_0(m_1^2) + A_0(m_2^2), \quad (\text{A.11})$$

where

$$\begin{aligned} \mathcal{F}(m_1^2, m_2^2) &= \frac{m_1^2 + m_2^2}{2} - \frac{m_1^2 m_2^2}{m_1^2 - m_2^2} \ln \left(\frac{m_1^2}{m_2^2} \right), \\ &\quad \text{if } m_1 \neq m_2, \\ &= 0 \quad \text{if } m_1 = m_2. \end{aligned} \quad (\text{A.12})$$

Note that

$$\mathcal{F}(m_1^2, m_2^2) = \mathcal{F}(m_2^2, m_1^2). \quad (\text{A.13})$$

Also notice that

$$\begin{aligned} B_{22}(q^2; m_1^2, m_2^2) &= B_{22}(q^2; m_2^2, m_1^2) \\ B_0(q^2; m_1^2, m_2^2) &= B_0(q^2; m_2^2, m_1^2). \end{aligned} \quad (\text{A.14})$$

While evaluating the fermion loops which contribute to the oblique parameters following two-point loop integrals are useful (refer section 21.3 of [10]):

$$B_1(q^2; m_1^2, m_2^2) = \int_0^1 dx (1-x) \ln\left(\frac{X-i\epsilon}{M^2}\right), \quad (\text{A.15})$$

$$B_2(q^2; m_1^2, m_2^2) = \int_0^1 dx x(1-x) \ln\left(\frac{X-i\epsilon}{M^2}\right), \quad (\text{A.16})$$

where X is as defined in Eq. (A.8). The logarithms in these integrals involve a mass scale M . All the terms, which depend on this scale cancel while evaluating the final expressions for oblique parameters. For $m_1 = m_2 = m$ and $q^2 = M_Z^2$,

$$B_1(M_Z^2; m^2, m^2) = -1 - \frac{G(x)}{4} + \ln\left(\frac{m^2}{M^2}\right), \quad (\text{A.17})$$

$$\begin{aligned} B_2(M_Z^2; m^2, m^2) &= \frac{1}{18} \left[-\frac{3}{2} G(x)(2x+1) \right. \\ &\quad \left. + \left(-12x - 5 + 3 \ln\left(\frac{m^2}{M^2}\right) \right) \right], \end{aligned} \quad (\text{A.18})$$

where

$$G(x) = -4 \sqrt{4x-1} \operatorname{Arctan}\left(\frac{1}{\sqrt{4x-1}}\right). \quad (\text{A.19})$$

While deriving $\tilde{T}_{fermion}$ in Eq.(4.12) we need to evaluate integrals in Eq. (A.15) for

$q = 0$ and $m_1 \neq m_2$. One of the integrals, which appear in this calculation is

$$\begin{aligned} & \int_0^1 dx (m_1^2 x + m_2^2(1-x)) \ln\left(\frac{m_1^2 x + m_2^2(1-x)}{M^2}\right) \\ &= \frac{(m_2^4 - m_1^4) + 2 m_1^4 \ln\left(\frac{m_1^2}{M^2}\right) - 2 m_2^4 \ln\left(\frac{m_1^2}{M^2}\right)}{4(m_1^2 - m_2^2)}. \end{aligned} \quad (\text{A.20})$$

Using the loop integrals and functions defined and enlisted in this appendix we can derive the expressions for the oblique parameters, which are suitable for the numerical analysis.

Appendix B

Feynman rules in the minimal EW ν_R Model

Various Feynman rules in the minimal EW ν_R model and SM are listed in this appendix. We work in the 't Hooft Feynman gauge (gauge parameter, $\xi_{gauge} = 1$) throughout the calculations in this appendix and all the appendices, which follow. To calculate the new Physics contributions due to EW ν_R model to the oblique parameters we also need the corresponding contributions from SM (refer to equations (4.6, 4.7, 4.8)). Therefore, in this section we also list the related SM couplings.

Table B.1: SV_1V_2 type couplings (V_1 and V_2' are vector gauge bosons and S is a Higgs boson), which contribute to Oblique Corrections. Common factor: $igM_W g^{\mu\nu}$

$g_{H_5^0 W^+ W^-}$	$\frac{s_H}{\sqrt{3}}$	$g_{H_5^0 Z Z}$	$-\frac{2}{\sqrt{3}} \frac{s_H}{c_W^2}$
$g_{H_5^{++} W^- W^-}$	$\sqrt{2} s_H$	$g_{H_5^+ W^- Z}$	$-\frac{s_H}{c_W}$
$g_{H_1^0 W^+ W^-}$	c_H	$g_{H_1^0 Z Z}$	$\frac{c_H}{c_W^2}$
$g_{H_1^{0'} W^+ W^-}$	$\frac{2\sqrt{2}}{\sqrt{3}} s_H$	$g_{H_1^{0'} Z Z}$	$\frac{2\sqrt{2}}{\sqrt{3}} \frac{s_H}{c_W^2}$

Table B.2: $S_1 S_2 V$ type couplings (V is a vector gauge boson and S_1, S_2 are Higgs/Goldstone bosons), which contribute to Oblique Corrections. Common factor: $ig(p - p')^\mu$, where $p(p')$ is the *incoming* momentum of the $S_1(S_2)$.

$g_{H_5^0 H_5^- W^+}$	$-\frac{\sqrt{3}}{2}$	$g_{H_5^{++} H_5^{--} Z}$	$-\frac{(1-2s_W^2)}{2c_W}$
$g_{H_5^+ H_5^{--} W^+}$	$-\frac{1}{\sqrt{2}}$	$g_{H_3^+ H_3^- Z}$	$\frac{(1-2s_W^2)}{2c_W}$
$g_{H_3^0 H_3^- W^+}$	$-\frac{1}{2}$	$g_{H_3^+ H_5^- Z}$	$-\frac{1}{2c_W}$
$g_{H_3^+ H_5^{--} W^+}$	$-\frac{1}{\sqrt{2}}CH$	$g_{H_3^0 H_5^0 Z}$	$\frac{1}{\sqrt{3}}\frac{c_H}{c_W}$
$g_{H_3^0 H_5^- W^+}$	$-\frac{1}{2}CH$	$g_{G_3^+ G_3^- Z}$	$\frac{(1-2s_W^2)}{2c_W}$
$g_{H_5^0 H_3^- W^+}$	$-\frac{1}{2\sqrt{3}}CH$	$g_{G_3^0 H_5^0 Z}$	$\frac{1}{\sqrt{3}}\frac{s_H}{c_W}$
$g_{G_3^0 G_3^- W^+}$	$-\frac{1}{2}$	$g_{G_3^+ H_5^- Z}$	$-\frac{1}{2c_W}SH$
$g_{G_3^+ H_5^{--} W^+}$	$-\frac{1}{\sqrt{2}}SH$	$g_{H_1^0 G_3^0 Z}$	$\frac{c_H}{c_W}$
$g_{G_3^0 H_5^- W^+}$	$-\frac{1}{2}SH$	$g_{H_1^{0'} G_3^0 Z}$	$\sqrt{\frac{2}{3}}\frac{s_H}{c_W}$
$g_{H_5^0 G_3^- W^+}$	$\frac{1}{2\sqrt{3}}SH$	$g_{H_1^0 H_3^0 Z}$	$-\frac{s_H}{2c_W}$
$g_{H_1^0 G_3^- W^+}$	$\frac{1}{2}CH$	$g_{H_1^{0'} H_3^0 Z}$	$\sqrt{\frac{2}{3}}\frac{c_H}{c_W}$
$g_{H_1^{0'} G_3^- W^+}$	$\sqrt{\frac{2}{3}}SH$	$g_{H_5^+ H_5^- \gamma}$	$-s_W$
$g_{H_1^0 H_3^- W^+}$	$-\frac{1}{2}SH$	$g_{H_5^{++} H_5^{--} \gamma}$	$-2s_W$
$g_{H_1^{0'} H_3^- W^+}$	$\sqrt{\frac{2}{3}}CH$	$g_{H_3^+ H_3^- \gamma}$	s_W
$g_{H_5^+ H_5^- Z}$	$\frac{(1-2s_W^2)}{2c_W}$	$g_{G_3^+ G_3^- \gamma}$	s_W

Table B.3: $H_1 H_2 V_1 V_2$ type couplings, which contribute to Oblique Corrections. Common factor: $ig^2 g^{\mu\nu}$

$\mathcal{G}_{H_5^0 H_5^0 W^+ W^-}$	$\frac{5}{3}$	$\mathcal{G}_{H_5^0 H_5^0 ZZ}$	$\frac{2}{3} \frac{1}{c_W^2}$
$\mathcal{G}_{H_5^+ H_5^- W^+ W^-}$	$-\frac{3}{2}$	$\mathcal{G}_{H_5^+ H_5^- ZZ}$	$-\frac{(c_W^4 + s_W^4)}{c_W^2}$
$\mathcal{G}_{H_5^{++} H_5^{--} W^+ W^-}$	1	$\mathcal{G}_{H_5^{++} H_5^{--} ZZ}$	$2 \frac{(1 - 2s_W^2)^2}{c_W^2}$
$\mathcal{G}_{H_3^0 H_3^0 W^+ W^-}$	$-(c_H^2 + \frac{s_H^2}{2})$	$\mathcal{G}_{H_3^0 H_3^0 ZZ}$	$-\frac{(1 + c_H^2)}{2c_W^2}$
$\mathcal{G}_{H_3^+ H_3^- W^+ W^-}$	$-(\frac{1}{2} + c_H^2)$	$\mathcal{G}_{H_3^+ H_3^- ZZ}$	$-\left[\frac{s_H^2}{2} \frac{(1 - s_W^2)^2}{c_W^2} + c_H^2 \frac{(c_W^4 + s_W^4)}{c_W^2} \right]$
$\mathcal{G}_{G_3^0 G_3^0 W^+ W^-}$	$-\frac{(1 + s_H^2)}{2}$	$\mathcal{G}_{G_3^0 G_3^0 ZZ}$	$-\frac{1}{2c_W^2} (1 + 3s_H^2)$
$\mathcal{G}_{G_3^+ G_3^- W^+ W^-}$	$-(\frac{1}{2} + s_H^2)$	$\mathcal{G}_{G_3^+ G_3^- ZZ}$	$-\left[\frac{1}{2} c_H^2 (1 - 2s_W^2)^2 + s_H^2 (c_W^4 + s_W^4) \right]$
$\mathcal{G}_{H_1^0 H_1^0 W^+ W^-}$	$\frac{1}{2}$	$\mathcal{G}_{H_1^0 H_1^0 ZZ}$	$\frac{1}{2c_W^2}$
$\mathcal{G}_{H_1^{0'} H_1^{0'} W^+ W^-}$	$\frac{4}{3}$	$\mathcal{G}_{H_1^{0'} H_1^{0'} ZZ}$	$\frac{4}{3c_W^2}$
$\mathcal{G}_{H_5^+ H_5^- \gamma\gamma}$	$-2s_W^2$	$\mathcal{G}_{H_5^+ H_5^- Z\gamma}$	$-\frac{s_W}{c_W} (1 - 2s_W^2)$
$\mathcal{G}_{H_5^{++} H_5^{--} \gamma\gamma}$	$8s_W^2$	$\mathcal{G}_{H_5^{++} H_5^{--} Z\gamma}$	$4 \frac{s_W}{c_W} (1 - 2s_W^2)$
$\mathcal{G}_{H_3^+ H_3^- \gamma\gamma}$	$-2s_W^2$	$\mathcal{G}_{H_3^+ H_3^- Z\gamma}$	$-\frac{s_W}{c_W} (1 - 2s_W^2)$
$\mathcal{G}_{G_3^+ G_3^- \gamma\gamma}$	$-2s_W^2$	$\mathcal{G}_{G_3^+ G_3^- Z\gamma}$	$-\frac{s_W}{c_W} (1 - 2s_W^2)$

Table B.4: $H_1 H_2 V_1 V_2$ type couplings, which *do not* contribute to Oblique Corrections. Common factor: $ig^2 g^{\mu\nu}$

$g_{H_1^{0'} H_5^0 W^+ W^-}$	$\frac{\sqrt{2}}{3}$	$g_{H_1^{0'} H_5^0 Z Z}$	$-\frac{2\sqrt{2}}{3c_W^2}$
$g_{H_3^+ H_5^- W^+ W^-}$	$-\frac{c_H}{2}$	$g_{H_3^+ H_5^- Z Z}$	$c_H \frac{(1-2s_W^2)}{c_W^2}$
$g_{H_3^0 G_3^0 W^+ W^-}$	$-\frac{c_H s_H}{2}$	$g_{H_3^0 G_3^0 Z Z}$	$-\frac{3}{2} \frac{c_H s_H}{c_W^2}$
$g_{H_3^+ G_3^- W^+ W^-}$	$-c_H s_H$	$g_{H_3^+ G_3^- Z Z}$	$-\frac{c_H s_H}{2c_W^2}$
$g_{H_5^+ G_3^- W^+ W^-}$	$-\frac{s_H}{2}$	$g_{H_5^+ G_3^- Z Z}$	$s_H \frac{(1-2s_W^2)}{c_W^2}$
		$g_{H_3^+ H_5^- Z \gamma}$	$c_H \frac{s_W}{c_W}$

Table B.5: $f_1^M f_2^M V$ type couplings, which contribute to the Oblique Corrections. For each Feynman rule the charge conservation is implicit. f_{1R}^M and f_{2R}^M are members of the same mirror fermion doublet with isospins $\frac{1}{2}$ and $-\frac{1}{2}$ respectively (ref. [26], [10] & [11]). Common factor for all couplings: $ig\gamma_\mu$

$g_{\bar{f}_{1R}^M f_{2R}^M W^+}$	$\frac{1}{\sqrt{2}}$
$g_{\bar{f}_R^M f_R^M Z}$	$\frac{1}{c_W} (T_3^f - s_W^2 Q_f)$
$g_{\bar{f}_R^M f_R^M \gamma}$	$s_W Q_f$
$g_{\bar{f}_L^M f_L^M Z}$	$-\frac{s_W^2}{c_W} Q_f$
$g_{\bar{f}_L^M f_L^M \gamma}$	$s_W Q_f$

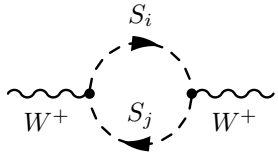
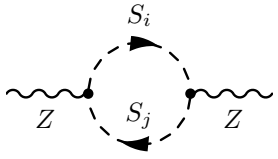
Appendix C

Loop Contributions to Oblique Parameters in the $EW\nu_R$ model

C.1 One Loop Contributions to \tilde{S}_{scalar} and \tilde{T}_{scalar}

In this section the one-loop contributions to \tilde{S}_{scalar} and \tilde{T}_{scalar} are listed. In every table the loop contributions in $EW\nu_R$ model are listed first and then the corresponding contributions in SM are also listed. The one-loop diagrams, which contribute to \tilde{S}_{scalar} can be found in tables C.1, C.3, C.4, C.6, C.2, C.5 below. To calculate \tilde{T}_{scalar} , Π_{11} contributions from scalar sector in $EW\nu_R$ model can be obtained from contributions to Π_{WW} listed in tables C.1, C.3, C.4. The scalar-loop diagrams contributing to Π_{33} are listed in tables C.7, C.9, C.8.

Table C.1: One-loop diagrams with two internal scalar (S) (Higgs or Goldstone boson) lines, which contribute to W^+ and Z self-energies. Common factor: $g^2/16\pi^2$

Contributions to $\Pi_{WW}(q^2)$			Contributions to $\Pi_{ZZ}(q^2)$		
					
S_i	S_j		S_i	S_j	
H_5^+	H_5^0	$3B_{22}(q^2; m_{H_5^+}^2, m_{H_5^0}^2)$	H_5^+	H_5^+	$\frac{c_{2W}^2}{c_W^2} B_{22}(q^2; m_{H_5^+}^2, m_{H_5^+}^2)$
H_5^{++}	H_5^+	$2B_{22}(q^2; m_{H_5^{++}}^2, m_{H_5^+}^2)$	H_5^{++}	H_5^{++}	$4\frac{c_{2W}^2}{c_W^2} B_{22}(q^2; m_{H_5^{++}}^2, m_{H_5^{++}}^2)$
H_3^+	H_3^0	$B_{22}(q^2; m_{H_3^+}^2, m_{H_3^0}^2)$	H_3^+	H_3^+	$\frac{c_{2W}^2}{c_W^2} B_{22}(q^2; m_{H_3^+}^2, m_{H_3^+}^2)$
H_5^{++}	H_3^+	$2c_H^2 B_{22}(q^2; m_{H_5^{++}}^2, m_{H_3^+}^2)$	H_5^+	H_3^+	$\frac{c_H^2}{c_W^2} B_{22}(q^2; m_{H_5^+}^2, m_{H_3^+}^2)$
H_5^+	H_3^0	$c_H^2 B_{22}(q^2; m_{H_5^+}^2, m_{H_3^0}^2)$	H_5^-	H_3^-	$\frac{c_H^2}{c_W^2} B_{22}(q^2; m_{H_5^+}^2, m_{H_3^+}^2)$
H_5^0	H_3^+	$\frac{c_H^2}{3} B_{22}(q^2; m_{H_5^0}^2, m_{H_3^+}^2)$	H_5^0	H_3^0	$\frac{4}{3} \frac{c_H^2}{c_W^2} B_{22}(q^2; m_{H_5^0}^2, m_{H_3^0}^2)$
H_3^+	H_1^0	$s_H^2 B_{22}(q^2; m_{H_3^+}^2, m_{H_1^0}^2)$	H_3^0	H_1^0	$\frac{s_H^2}{c_W^2} B_{22}(q^2; m_{H_3^0}^2, m_{H_1^0}^2)$
H_3^+	$H_1^{0'}$	$\frac{8}{3} c_H^2 B_{22}(q^2; m_{H_3^+}^2, m_{H_1^{0'}}^2)$	H_3^0	$H_1^{0'}$	$\frac{8}{3} \frac{c_H^2}{c_W^2} B_{22}(q^2; m_{H_3^0}^2, m_{H_1^{0'}}^2)$
G_3^+	H_5^{++}	$2s_H^2 B_{22}(q^2; M_W^2, m_{H_5^{++}}^2)$	G_3^+	H_5^+	$\frac{s_H^2}{c_W^2} B_{22}(q^2; M_W^2, m_{H_5^+}^2)$

Continued on next page...

Table C.1 – continued from previous page

S_i	S_j		S_i	S_j	
G_3^0	H_5^+	$s_H^2 B_{22}(q^2; M_Z^2, m_{H_5^+}^2)$	G_3^-	H_5^-	$\frac{s_H^2}{c_W^2} B_{22}(q^2; M_W^2, m_{H_5^+}^2)$
G_3^+	H_5^0	$\frac{s_H^2}{3} B_{22}(q^2; M_W^2, m_{H_5^0}^2)$	G_3^0	H_5^0	$\frac{4}{3} \frac{s_H^2}{c_W^2} B_{22}(q^2; M_Z^2, m_{H_5^0}^2)$
G_3^+	H_1^0	$c_H^2 B_{22}(q^2; M_W^2, m_{H_1^0}^2)$	G_3^0	H_1^0	$\frac{c_H^2}{c_W^2} B_{22}(q^2; M_Z^2, m_{H_1^0}^2)$
G_3^+	$H_1^{0'}$	$\frac{8}{3} s_H^2 B_{22}(q^2; M_W^2, m_{H_1^{0'}}^2)$	G_3^0	$H_1^{0'}$	$\frac{8}{3} \frac{s_H^2}{c_W^2} B_{22}(q^2; M_Z^2, m_{H_1^{0'}}^2)$
G_3^+	G_3^0	$B_{22}(q^2; M_W^2, M_Z^2)$	G_3^+	G_3^+	$\frac{c_{2W}^2}{c_W^2} B_{22}(q^2; M_W^2, M_W^2)$
Standard Model contributions					
H	G_{SM}^+	$B_{22}(q^2; M_W^2, m_H^2)$	H	G_{SM}^0	$\frac{1}{c_W^2} B_{22}(q^2; M_Z^2, m_H^2)$
G_{SM}^+	G_{SM}^0	$B_{22}(q^2; M_W^2, M_Z^2)$	G_{SM}^+	G_{SM}^+	$\frac{c_{2W}^2}{c_W^2} B_{22}(q^2; M_W^2, M_W^2)$

Table C.2: Tadpole diagrams with one internal scalar (S) (Higgs or Goldstone boson) line, which contribute to W^+ and Z self-energies. Common factor: $g^2/16\pi^2$

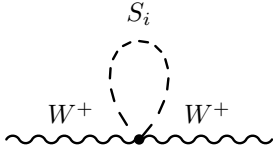
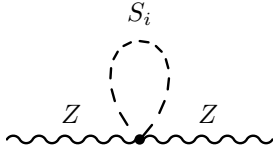
Contributions to $\Pi_{WW}(q^2)$	Contributions to $\Pi_{ZZ}(q^2)$
	
S_i	S_i
H_5^0 $-\frac{5}{6}A_0(m_{H_5^0}^2)$	H_5^0 $-\frac{2}{6c_W^2}A_0(m_{H_5^0}^2)$
H_5^+ $-\frac{3}{2}A_0(m_{H_5^+}^2)$	H_5^+ $-\frac{c_W^4 + s_W^4}{c_W^2}A_0(m_{H_5^+}^2)$
H_5^{++} $-A_0(m_{H_5^{++}}^2)$	H_5^{++} $-2\frac{c_{2W}^2}{c_W^2}A_0(m_{H_5^{++}}^2)$
H_3^0 $-\frac{1}{4}(1 + c_H^2)A_0(m_{H_3^0}^2)$	H_3^0 $-\frac{1}{4c_W^2}(1 + 3c_H^2)A_0(m_{H_3^0}^2)$
H_3^+ $-\frac{1}{2}(1 + 2c_H^2)A_0(m_{H_3^+}^2)$	H_3^+ $-\frac{c_{2W}^2}{2c_W^2}(1 + c_H^2)A_0(m_{H_3^+}^2)$
H_1^0 $-\frac{1}{4}A_0(m_{H_1^0}^2)$	H_1^0 $-\frac{1}{4c_W^2}A_0(m_{H_1^0}^2)$
$H_1^{0'}$ $-\frac{2}{3}A_0(m_{H_1^{0'}}^2)$	$H_1^{0'}$ $-\frac{2}{3c_W^2}A_0(m_{H_1^{0'}}^2)$
G_3^0 $-\frac{1}{4}(1 + s_H^2)A_0(M_Z^2)$	G_3^0 $-\frac{1}{4c_W^2}(1 + 3s_H^2)A_0(M_Z^2)$
G_3^+ $-\frac{1}{2}(1 + 2s_H^2)A_0(M_W^2)$	G_3^+ $-\frac{c_{2W}^2}{2c_W^2}(1 + s_H^2)A_0(M_W^2)$
Continued on next page...	

Table C.2 – continued from previous page

S_i		S_i	
Standard Model contributions			
H	$-\frac{1}{4}A_0(m_H^2)$	H	$-\frac{1}{4c_W^2}A_0(m_H^2)$
G_{SM}^0	$-\frac{1}{4}A_0(M_Z^2)$	G_{SM}^0	$-\frac{1}{4c_W^2}A_0(M_Z^2)$
G_{SM}^+	$-\frac{1}{2}A_0(M_W^2)$	G_{SM}^+	$-\frac{c_W^2}{2c_W^2}A_0(M_W^2)$

Table C.3: One-loop diagrams with one internal scalar (S) (Higgs or Goldstone boson) line and one internal vector boson line, which contribute to W^+ and Z self-energies. Common factor: $g^2/16\pi^2$

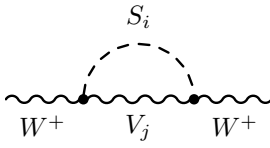
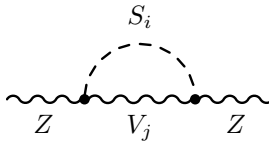
Contributions to $\Pi_{WW}(q^2)$		Contributions to $\Pi_{ZZ}(q^2)$			
					
S_i	V_j	S_i	V_j		
H_5^0	W^+	$-\frac{s_H^2}{3} M_W^2 B_0(q^2; M_W^2, m_{H_5^0}^2)$	H_5^0	Z	$-\frac{4}{3} \frac{s_H^2}{c_W^2} M_Z^2 B_0(q^2; M_Z^2, m_{H_5^0}^2)$
H_1^0	W^+	$-c_H^2 M_W^2 B_0(q^2; M_W^2, m_{H_1^0}^2)$	H_1^0	Z	$-\frac{c_H^2}{c_W^2} M_Z^2 B_0(q^2; M_Z^2, m_{H_1^0}^2)$
$H_1^{0'}$	W^+	$-\frac{8}{3} s_H^2 M_W^2 B_0(q^2; M_W^2, m_{H_1^{0'}}^2)$	$H_1^{0'}$	Z	$-\frac{8}{3} \frac{s_H^2}{c_W^2} M_Z^2 B_0(q^2; M_Z^2, m_{H_1^{0'}}^2)$
H_5^+	Z	$-\frac{s_H^2}{c_W^2} M_W^2 B_0(q^2; M_Z^2, m_{H_5^+}^2)$	H_5^+	W^-	$-\frac{s_H^2}{c_W^2} M_W^2 B_0(q^2; M_W^2, m_{H_5^+}^2)$
H_5^{++}	W^-	$-2s_H^2 M_W^2 B_0(q^2; M_W^2, m_{H_5^{++}}^2)$	H_5^-	W^+	$-\frac{s_H^2}{c_W^2} M_W^2 B_0(q^2; M_W^2, m_{H_5^-}^2)$
Standard Model contributions					
H	W^+	$-M_W^2 B_0(q^2; M_W^2, m_H^2)$	H	Z	$-\frac{M_Z^2}{c_W^2} B_0(q^2; M_Z^2, m_H^2)$
G_{SM}^+	Z	$-\frac{s_W^4}{c_W^2} M_W^2 B_0(q^2; M_Z^2, M_W^2)$	G_{SM}^+	W^-	$-2\frac{s_W^4}{c_W^2} M_W^2 B_0(q^2; M_W^2, M_W^2)$
G_{SM}^+	γ	$-s_W^2 M_W^2 B_0(q^2; 0, M_W^2)$	G_{SM}^-	W^+	$-2\frac{s_W^4}{c_W^2} M_W^2 B_0(q^2; M_W^2, M_W^2)$

Table C.4: One-loop diagrams with two internal scalar (S) (Higgs or Goldstone boson) lines, which contribute to photon (γ) self-energy and Z - γ transition amplitude. Common factor: $g^2/16\pi^2$

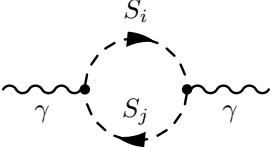
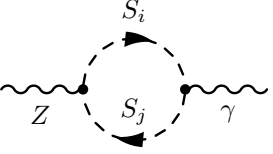
Contributions to $\Pi_{\gamma\gamma}(q^2)$			Contributions to $\Pi_{Z\gamma}(q^2)$		
					
S_i	S_j		S_i	S_j	
H_5^+	H_5^+	$4s_W^2 B_{22}(q^2; m_{H_5^+}^2, m_{H_5^+}^2)$	H_5^+	H_5^+	$2\frac{s_W}{c_W} c_{2W} B_{22}(q^2; m_{H_5^+}^2, m_{H_5^+}^2)$
H_5^{++}	H_5^{++}	$16s_W^2 B_{22}(q^2; m_{H_5^{++}}^2, m_{H_5^{++}}^2)$	H_5^{++}	H_5^{++}	$8\frac{s_W}{c_W} c_{2W} B_{22}(q^2; m_{H_5^{++}}^2, m_{H_5^{++}}^2)$
H_3^+	H_3^+	$4s_W^2 B_{22}(q^2; m_{H_3^+}^2, m_{H_3^+}^2)$	H_3^+	H_3^+	$2\frac{s_W}{c_W} c_{2W} B_{22}(q^2; m_{H_3^+}^2, m_{H_3^+}^2)$
G_3^+	G_3^+	$4s_W^2 B_{22}(q^2; M_W^2, M_W^2)$	G_3^+	G_3^+	$2\frac{s_W}{c_W} c_{2W} B_{22}(q^2; M_W^2, M_W^2)$
Standard Model contributions					
G_{SM}^+	G_{SM}^+	$4s_W^2 B_{22}(q^2; M_W^2, M_W^2)$	G_{SM}^+	G_{SM}^+	$2\frac{s_W}{c_W} c_{2W} B_{22}(q^2; M_W^2, M_W^2)$

Table C.5: Tadpole diagrams with one internal scalar (S) (Higgs or Goldstone boson) line, which contribute to photon (γ) self-energy and Z - γ transition amplitude. Common factor: $g^2/16\pi^2$

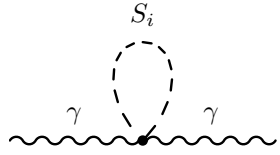
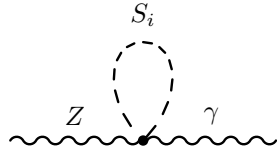
Contributions to $\Pi_{\gamma\gamma}(q^2)$		Contributions to $\Pi_{Z\gamma}(q^2)$	
			
S_i		S_i	
H_5^+	$-2s_W^2 A_0(m_{H_5^+}^2)$	H_5^+	$-\frac{s_W}{c_W} c_{2W} A_0(m_{H_5^+}^2)$
H_5^{++}	$-8s_W^2 A_0(m_{H_5^{++}}^2)$	H_5^{++}	$-4\frac{s_W}{c_W} c_{2W} A_0(m_{H_5^{++}}^2)$
H_3^+	$-2s_W^2 A_0(m_{H_3^+}^2)$	H_3^+	$-\frac{s_W}{c_W} c_{2W} A_0(m_{H_3^+}^2)$
G_3^+	$-2s_W^2 A_0(M_W^2)$	G_3^+	$-\frac{s_W}{c_W} c_{2W} A_0(M_W^2)$
Standard Model contributions			
G_{SM}^+	$-2s_W^2 A_0(M_W^2)$	G_{SM}^+	$-\frac{s_W}{c_W} c_{2W} A_0(M_W^2)$

Table C.6: One-loop diagrams with one internal scalar (S) (Higgs or Goldstone boson) line and one internal vector boson line, which contribute to photon (γ) self-energy and Z - γ transition amplitude. Common factor: $g^2/16\pi^2$

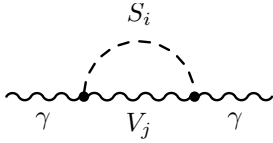
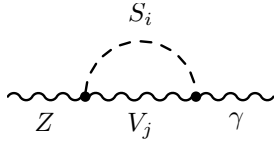
<p style="text-align: center;">Contributions to $\Pi_{\gamma\gamma}(q^2)$</p> 	<p style="text-align: center;">Contributions to $\Pi_{Z\gamma}(q^2)$</p> 
$S_i \quad V_j$	$S_i \quad V_j$
$G_3^+ \quad W^- \quad -s_W^2 M_W^2 B_0(M_Z^2; M_W^2, M_W^2)$ $G_3^- \quad W^+ \quad -s_W^2 M_W^2 B_0(M_Z^2; M_W^2, M_W^2)$	$G_3^+ \quad W^- \quad \frac{s_W^3}{c_W} M_W^2 B_0(M_Z^2; M_W^2, M_W^2)$ $G_3^- \quad W^+ \quad \frac{s_W^3}{c_W} M_W^2 B_0(M_Z^2; M_W^2, M_W^2)$
<p>Standard Model contributions</p>	
$G_{SM}^+ \quad W^- \quad -s_W^2 M_W^2 B_0(M_Z^2; M_W^2, M_W^2)$ $G_{SM}^- \quad W^+ \quad -s_W^2 M_W^2 B_0(M_Z^2; M_W^2, M_W^2)$	$G_{SM}^+ \quad W^- \quad \frac{s_W^3}{c_W} M_W^2 B_0(M_Z^2; M_W^2, M_W^2)$ $G_{SM}^- \quad W^+ \quad \frac{s_W^3}{c_W} M_W^2 B_0(M_Z^2; M_W^2, M_W^2)$

Table C.7: One-loop diagrams with two internal scalar (S) (Higgs or Goldstone boson) lines, which contribute to $\Pi_{33}(q^2)$ in T . Common factor: $g^2/16\pi^2$

Contributions to $\Pi_{33}(q^2)$					
S_i	S_j		S_i	S_j	
H_5^+	H_5^+	$B_{22}(q^2; m_{H_5^+}^2, m_{H_5^+}^2)$	H_5^{++}	H_5^{++}	$4B_{22}(q^2; m_{H_5^{++}}^2, m_{H_5^{++}}^2)$
H_3^+	H_3^+	$B_{22}(q^2; m_{H_3^+}^2, m_{H_3^+}^2)$	H_5^+	H_3^+	$c_H^2 B_{22}(q^2; m_{H_5^+}^2, m_{H_3^+}^2)$
H_5^-	H_3^-	$c_H^2 B_{22}(q^2; m_{H_5^-}^2, m_{H_3^-}^2)$	H_5^0	H_3^0	$\frac{4}{3} c_H^2 B_{22}(q^2; m_{H_5^0}^2, m_{H_3^0}^2)$
H_3^0	H_1^0	$s_H^2 B_{22}(q^2; m_{H_3^0}^2, m_{H_1^0}^2)$	H_3^0	$H_1^{0'}$	$\frac{8}{3} c_H^2 B_{22}(q^2; m_{H_3^0}^2, m_{H_1^{0'}}^2)$
G_3^+	H_5^+	$s_H^2 B_{22}(q^2; M_W^2, m_{H_5^+}^2)$	G_3^-	H_5^-	$s_H^2 B_{22}(q^2; M_W^2, m_{H_5^-}^2)$
G_3^0	H_5^0	$\frac{4}{3} s_H^2 B_{22}(q^2; M_W^2, m_{H_5^0}^2)$	G_3^0	H_1^0	$c_H^2 B_{22}(q^2; M_W^2, m_{H_1^0}^2)$
G_3^0	$H_1^{0'}$	$\frac{8}{3} s_H^2 B_{22}(q^2; M_W^2, m_{H_1^{0'}}^2)$	G_3^+	G_3^+	$B_{22}(q^2; M_W^2, M_W^2)$
Standard Model contributions					
H	G_{SM}^0	$B_{22}(q^2; M_W^2, m_H^2)$	G_{SM}^+	G_{SM}^+	$B_{22}(q^2; M_W^2, M_W^2)$

Table C.8: Tadpole diagrams with one internal scalar (S) (Higgs or Goldstone boson) line, which contribute to $\Pi_{33}(q^2)$ in T . Common factor: $g^2/16\pi^2$

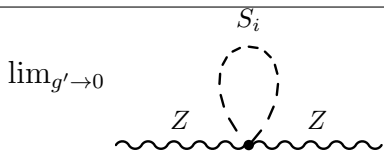
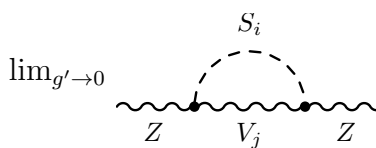
Contributions to $\Pi_{33}(q^2)$			
$\lim_{g' \rightarrow 0}$ 			
S_i		S_i	
H_5^0	$-\frac{2}{6}A_0(m_{H_5^0}^2)$	H_5^+	$-A_0(m_{H_5^+}^2)$
H_5^{++}	$-2A_0(m_{H_5^{++}}^2)$	H_3^0	$-\frac{1}{4}(1+3c_H^2)A_0(m_{H_3^0}^2)$
H_3^+	$-\frac{1}{2}(1+c_H^2)A_0(m_{H_3^+}^2)$	H_1^0	$-\frac{1}{4}A_0(m_{H_1^0}^2)$
$H_1^{0'}$	$-\frac{2}{3}A_0(m_{H_1^{0'}}^2)$	G_3^0	$-\frac{1}{4}(1+3s_H^2)A_0(M_W^2)$
G_3^+	$-\frac{1}{2}(1+s_H^2)A_0(M_W^2)$		
Standard Model contributions			
H	$-\frac{1}{4}A_0(m_H^2)$	G_{SM}^0	$-\frac{1}{4}A_0(M_W^2)$
G_{SM}^+	$-\frac{1}{2}A_0(M_W^2)$		

Table C.9: One-loop diagrams with one internal scalar (S) (Higgs or Goldstone boson) line and one internal vector boson line, which contribute to $\Pi_{33}(q^2)$ in T . Common factor: $g^2/16\pi^2$

Contributions to $\Pi_{33}(q^2)$			
			
S_i	V_j		S_i V_j
H_5^0	Z	$-\frac{4}{3} s_H^2 M_W^2 B_0(q^2; M_W^2, m_{H_5^0}^2)$	H_1^0 Z $-c_H^2 M_W^2 B_0(q^2; M_W^2, m_{H_1^0}^2)$
$H_1^{0'}$	Z	$-\frac{8}{3} s_H^2 M_W^2 B_0(q^2; M_W^2, m_{H_1^{0'}}^2)$	H_5^+ W^- $-s_H^2 M_W^2 B_0(q^2; M_W^2, m_{H_5^+}^2)$
H_5^-	W^+	$-s_H^2 M_W^2 B_0(q^2; M_W^2, m_{H_5^-}^2)$	
Standard Model contributions			
H	Z	$-M_W^2 B_0(q^2; M_W^2, m_H^2)$	

C.2 One Loop Contributions to $\tilde{S}_{fermion}$ and $\tilde{T}_{fermion}$

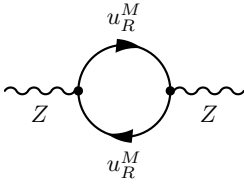
The new Physics contributions, $\tilde{S}_{fermion}$ and $\tilde{T}_{fermion}$, due to fermion sector in EW ν_R model can be calculated by adding the respective contributions due to the lepton-

and quark-sectors in $EW\nu_R$ model that is,

$$\tilde{S}_{fermion} = \tilde{S}_{lepton} + \tilde{S}_{quark} \quad (C.1)$$

$$\tilde{T}_{fermion} = \tilde{T}_{lepton} + \tilde{T}_{quark} \quad (C.2)$$

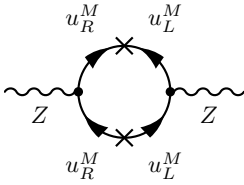
In this section the one-loop contributions to $\tilde{S}_{fermion}$ and $\tilde{T}_{fermion}$ are listed in tables C.10, C.11, C.12, C.14. In each of these tables only the loop contributions due to the mirror fermions in $EW\nu_R$ model are listed. The same expressions for the loop contributions can be used to calculate the lepton loop diagrams and the quark loop diagrams. The fermion loop contributions in SM can be obtained from the mirror fermion loop having fermions with the opposite chirality going in the loop. Consider, for example, the mirror-up-quark-loop diagrams in FIG. C.1 and SM-up-quark-loop diagrams in FIG. C.2.



=

$$-\frac{4}{c_W^2} (T_3^{u^M} - s_W^2 Q_{u^M})^2 \left[\left(\frac{q^2}{6} - \frac{m_{u^M}^2}{2} \right) \Delta - q^2 B_2(q^2; m_{u^M}^2, m_{u^M}^2) + m_{u^M}^2 B_1(q^2; m_{u^M}^2, m_{u^M}^2) \right]$$

(a)



=

$$-\frac{2}{c_W^2} m_{u^M}^2 (T_3^{u^M} - s_W^2 Q_{u^M}) s_W^2 Q_{u^M} [\Delta - 2B_1(q^2; m_{u^M}^2, m_{u^M}^2)]$$

(b)

Figure C.1: $EW\nu_R$ model mirror fermion loop examples

$$\begin{aligned}
\text{(a)} \quad \begin{array}{c} \text{Diagram: A circular fermion loop with two external wavy lines labeled } Z. \text{ The top vertex is labeled } u_L \text{ and the bottom vertex is labeled } u_L. \end{array} &= -\frac{4}{c_W^2} (T_3^u - s_W^2 Q_u)^2 \left[\left(\frac{q^2}{6} - \frac{m_u^2}{2} \right) \Delta \right. \\
&\quad \left. - q^2 B_2(q^2; m_u^2, m_u^2) + m_u^2 B_1(q^2; m_u^2, m_u^2) \right] \\
\text{(b)} \quad \begin{array}{c} \text{Diagram: A circular fermion loop with two external wavy lines labeled } Z. \text{ The top-left vertex is } u_L, \text{ top-right is } u_R, \text{ bottom-left is } u_L, \text{ and bottom-right is } u_R. \end{array} &= -\frac{2}{c_W^2} m_u^2 (T_3^u - s_W^2 Q_u) s_W^2 Q_u [\Delta - 2B_1(q^2; m_u^2, m_u^2)]
\end{aligned}$$

Figure C.2: Standard Model fermion loop examples

Table C.10: Fermion loop diagrams with two internal mirror fermion lines, which contribute to $\Pi_{WW}(q^2)$. Here f_{1R}^M 's and f_{2R}^M 's are members of a mirror fermion doublet with isospins (T_3^f) equal to $\frac{1}{2}$ and $-\frac{1}{2}$ respectively. Common factor: $g^2 N_c / 16\pi^2$

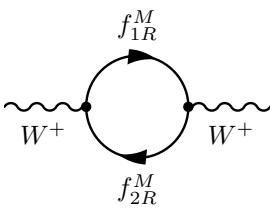
Contributions to $\Pi_{WW}(q^2)$	
	$ -2 \left[\left(\frac{q^2}{6} - \frac{1}{4} (m_{1f}^2 + m_{2f}^2) \right) \Delta - q^2 B_2(q^2; m_{1f}^2, m_{2f}^2) \right. \\ \left. + \frac{1}{2} (m_{1f}^2 B_1(q^2; m_{1f}^2, m_{2f}^2) + m_{2f}^2 B_1(q^2; m_{2f}^2, m_{1f}^2)) \right] $

Table C.11: Fermion loop diagrams with two internal mirror fermion lines, which contribute to $\Pi_{ZZ}(q^2)$. Common factor: $g^2 N_c / 16\pi^2$

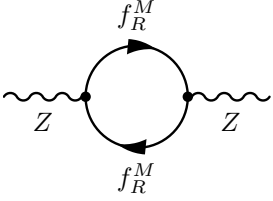
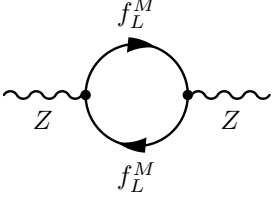
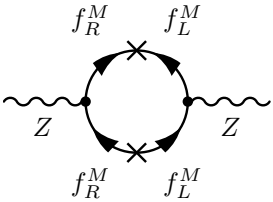
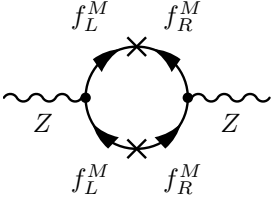
Contributions to $\Pi_{ZZ}(q^2)$	
	$-\frac{4}{c_W^2} (T_3^f - s_W^2 Q_f)^2 \left[\left(\frac{q^2}{6} - \frac{m_f^2}{2} \right) \Delta - q^2 B_2(q^2; m_f^2, m_f^2) + m_f^2 B_1(q^2; m_f^2, m_f^2) \right]$
	$-\frac{4}{c_W^2} s_W^4 Q_f^2 \left[\left(\frac{q^2}{6} - \frac{m_f^2}{2} \right) \Delta - q^2 B_2(q^2; m_f^2, m_f^2) + m_f^2 B_1(q^2; m_f^2, m_f^2) \right]$
	$-\frac{2}{c_W^2} m_f^2 (T_3^f - s_W^2 Q_f) s_W^2 Q_f \left[\Delta - 2B_1(q^2; m_f^2, m_f^2) \right]$
	$-\frac{2}{c_W^2} m_f^2 (T_3^f - s_W^2 Q_f) s_W^2 Q_f \left[\Delta - 2B_1(q^2; m_f^2, m_f^2) \right]$

Table C.12: Fermion loop diagrams with two internal mirror fermion lines, which contribute to $\Pi_{Z\gamma}(q^2)$. Common factor: $g^2 N_c / 16\pi^2$

Contributions to $\Pi_{Z\gamma}(q^2)$	
	$-\frac{4}{c_W}(T_3^f - s_W^2 Q_f) s_W Q_f \left[\left(\frac{q^2}{6} - \frac{m_f^2}{2} \right) \Delta - q^2 B_2(q^2; m_f^2, m_f^2) + m_f^2 B_1(q^2; m_f^2, m_f^2) \right]$
	$\frac{4}{c_W} s_W^3 Q_f^2 \left[\left(\frac{q^2}{6} - \frac{m_f^2}{2} \right) \Delta - q^2 B_2(q^2; m_f^2, m_f^2) + m_f^2 B_1(q^2; m_f^2, m_f^2) \right]$
	$\frac{2}{c_W} m_f^2 (T_3^f - s_W^2 Q_f) s_W Q_f \left[\Delta - 2B_1(q^2; m_f^2, m_f^2) \right]$
	$-\frac{2}{c_W} m_f^2 s_W^3 Q_f^2 \left[\Delta - 2B_1(q^2; m_f^2, m_f^2) \right]$

Table C.13: Fermion loop diagrams with two internal mirror fermion lines, which contribute to $\Pi_{\gamma\gamma}(q^2)$. Common factor: $g^2 N_c / 16\pi^2$

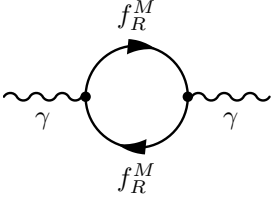
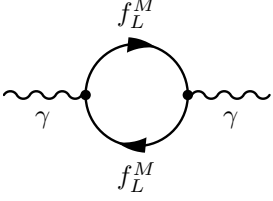
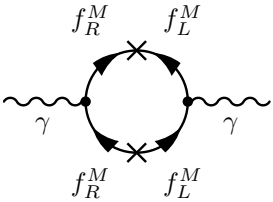
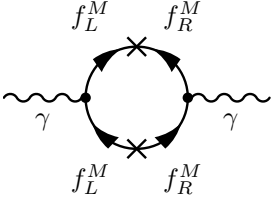
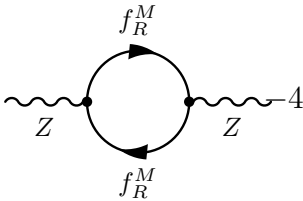
Contributions to $\Pi_{\gamma\gamma}(q^2)$	
	$-4s_W^2 Q_f^2 \left[\left(\frac{q^2}{6} - \frac{m_f^2}{2} \right) \Delta \right. \\ \left. -q^2 B_2(q^2; m_f^2, m_f^2) + m_f^2 B_1(q^2; m_f^2, m_f^2) \right]$
	$-4s_W^2 Q_f^2 \left[\left(\frac{q^2}{6} - \frac{m_f^2}{2} \right) \Delta \right. \\ \left. -q^2 B_2(q^2; m_f^2, m_f^2) + m_f^2 B_1(q^2; m_f^2, m_f^2) \right]$
	$2m_f^2 s_W^2 Q_f^2 \left[\Delta - 2B_1(q^2; m_f^2, m_f^2) \right]$
	$2m_f^2 s_W^2 Q_f^2 \left[\Delta - 2B_1(q^2; m_f^2, m_f^2) \right]$

Table C.14: Fermion loop diagrams with two internal mirror fermion lines, which contribute to $\Pi_{33}(q^2)$. Common factor: $g^2 N_c / 16\pi^2$

Contributions to $\Pi_{33}(q^2)$	
	$4 \left(T_3^f\right)^2 \left[\left(\frac{q^2}{6} - \frac{m_f^2}{2} \right) \Delta \right. \\ \left. - q^2 B_2(q^2; m_f^2, m_f^2) + m_f^2 B_1(q^2; m_f^2, m_f^2) \right]$

The contribution due to the loop diagram in FIG. C.2(a) (with two left-handed SM up quarks in the loop) has similar form of expression as the loop diagram in FIG. C.1(a) with two right-handed mirror-up-quarks in the loop. Also, if the SM up quark loop diagram has mass-insertion propagators as in FIG. C.2(b), then it has similar form of expression as the loop diagram with mass-insertion propagators of mirror up quarks, FIG. C.1(b), when the left-handed-up-quarks-side of the loop is replaced by the right-handed-mirror-up-quark side of the loop and vice versa. The same correspondence exists between other one loop diagrams involving mirror fermions listed in tables C.10, C.11, C.12, C.14 and the diagrams involving SM fermions. Therefore, we have not listed separately the SM fermion loop diagrams in this paper.

Definitions of the loop functions used in these tables are given in Appendix A.

Appendix D

Feynman rules in the extended EW ν_R model

Table D.1: Yukawa couplings with SM quarks and mirror-quarks in the extended EW ν_R model. The Yukawa couplings involving *charged* SM (and mirror) leptons can be obtained by replacing up-type SM (and mirror) quarks by left-handed (and right-handed) neutrinos and down-type SM (and mirror) quarks by the charged SM (and mirror) leptons in this table.

SM Leptons		Mirror Leptons	
$g_{H_1^0 \bar{l} l}$	$-\imath \frac{m_l g}{2 M_W s_2} \dots (l = \tau, \mu, e)$	$g_{H_{1M}^0 l^M \bar{l}^M}$	$-\imath \frac{m_l^M g}{2 M_W s_{2M}}$
$g_{H_3^0 \bar{l} l}$	$-\imath \frac{m_l g s_M}{2 M_W c_M} \gamma_5$	$g_{H_{3M}^0 l_i^M \bar{l}_i^M}$	$\imath \frac{m_{l_i}^M g s_M}{2 M_W c_M} \gamma_5$
$g_{H_3^- \nu_L \bar{l}}$	$-\imath \frac{g m_l s_M}{2\sqrt{2} M_W c_M} (1 - \gamma_5)$	$g_{H_3^- \nu_{Ri} \bar{l}_i^M}$	$-\imath \frac{g m_{l_i}^M s_M}{2\sqrt{2} M_W c_M} (1 + \gamma_5)$
$g_{H_{3M}^0 \bar{l} l}$	$\imath \frac{m_l g s_{2M}}{2 M_W s_2} \gamma_5$	$g_{H_{3M}^0 l_i^M \bar{l}_i^M}$	$\imath \frac{m_{l_i}^M g s_2}{2 M_W s_{2M}} \gamma_5$
$g_{H_{3M}^- \nu_L \bar{l}}$	$-\imath \frac{g m_l s_{2M}}{2\sqrt{2} M_W s_2 c_M} (1 - \gamma_5)$	$g_{H_{3M}^- \nu_{Ri} \bar{l}_i^M}$	$-\imath \frac{g m_{l_i}^M s_2}{2\sqrt{2} M_W s_{2M} c_M} (1 + \gamma_5)$

Table D.2: Yukawa couplings with SM quarks and mirror-quarks in the EW ν_R model. The Yukawa couplings involving *charged* SM (and mirror) leptons can be obtained by replacing up-type SM (and mirror) quarks by left-handed (and right-handed) neutrinos and down-type SM (and mirror) quarks by the charged SM (and mirror) leptons in this table.

SM Quarks		Mirror Quarks	
$g_{H_1^0 q \bar{q}}$	$-\imath \frac{m_q g}{2 M_W s_2} \dots (q = t, b)$	$g_{H_{1M}^0 q^M \bar{q}^M}$	$-\imath \frac{m_q^M g}{2 M_W s_{2M}}$
$g_{H_3^0 t \bar{t}}$	$\imath \frac{m_t g s_M}{2 M_W c_M} \gamma_5$	$g_{H_3^0 u_i^M \bar{u}_i^M}$	$-\imath \frac{m_{u_i^M} g s_M}{2 M_W c_M} \gamma_5$
$g_{H_3^0 b \bar{b}}$	$-\imath \frac{m_b g s_M}{2 M_W c_M} \gamma_5$	$g_{H_3^0 d_i^M \bar{d}_i^M}$	$\imath \frac{m_{d_i^M} g s_M}{2 M_W c_M} \gamma_5$
$g_{H_3^- t \bar{b}}$	$\imath \frac{g s_M}{2\sqrt{2} M_W c_M}$	$g_{H_3^- u_i^M \bar{b}_i^M}$	$\imath \frac{g s_M}{2\sqrt{2} M_W c_M}$
	$\times [m_t(1 + \gamma_5) - m_b(1 - \gamma_5)]$		$\times [m_{u_i^M}(1 - \gamma_5) - m_{d_i^M}(1 + \gamma_5)]$
$g_{H_{3M}^0 t \bar{t}}$	$-\imath \frac{m_t g s_{2M}}{2 M_W s_2} \gamma_5$	$g_{H_{3M}^0 u_i^M \bar{u}_i^M}$	$-\imath \frac{m_{u_i^M} g s_2}{2 M_W s_{2M}} \gamma_5$
$g_{H_{3M}^0 b \bar{b}}$	$\imath \frac{m_b g s_{2M}}{2 M_W s_2} \gamma_5$	$g_{H_{3M}^0 d_i^M \bar{d}_i^M}$	$\imath \frac{m_{d_i^M} g s_2}{2 M_W s_{2M}} \gamma_5$
$g_{H_{3M}^- t \bar{b}}$	$\imath \frac{g s_{2M}}{2\sqrt{2} M_W s_2 c_M} [m_t(1 + \gamma_5) - m_b(1 - \gamma_5)]$	$g_{H_{3M}^- u_i^M \bar{d}_i^M}$	$\imath \frac{g s_2}{2\sqrt{2} M_W s_{2M} c_M} [m_{u_i^M}(1 - \gamma_5) - m_{d_i^M}(1 + \gamma_5)]$

Table D.3: $S_1 S_2 V$ type couplings (V is a vector gauge boson and S_1, S_2 are Higgs/Goldstone bosons), which contribute to Oblique Corrections. Common factor: $ig(p - p')^\mu$, where $p(p')$ is the *incoming* momentum of the $S_1(S_2)$.

$g_{H_3^0 H_5^- W^+}$	$-\frac{\sqrt{3}}{2}$	$g_{H_5^{++} H_5^- Z}$	$-\frac{(1 - 2s_W^2)}{c_W}$
$g_{H_5^+ H_5^- W^+}$	$-\frac{1}{\sqrt{2}}$	$g_{H_5^+ H_5^- Z}$	$\frac{(1 - 2s_W^2)}{2c_W}$
$g_{H_3^0 H_3^- W^+}$	$-\frac{1}{2}s_M^2$	$g_{H_3^+ H_3^- Z}$	$\frac{(1 - 2s_W^2)}{2c_W}$
$g_{H_{3M}^0 H_{3M}^- W^+}$	$\frac{1}{2}$	$g_{H_{3M}^+ H_{3M}^- Z}$	$\frac{(1 - 2s_W^2)}{2c_W}$
$g_{H_3^+ H_5^- W^+}$	$-\frac{1}{\sqrt{2}}c_M$	$g_{H_3^+ H_5^- Z}$	$-\frac{1}{2c_W}c_M$
$g_{H_3^0 H_5^- W^+}$	$-\frac{1}{2}c_M$	$g_{H_3^0 H_5^0 Z}$	$\frac{1}{\sqrt{3}}\frac{c_M}{c_W}$
$g_{H_3^0 H_3^- W^+}$	$-\frac{1}{2\sqrt{3}}c_M$	$g_{G_3^+ G_3^- Z}$	$\frac{(1 - 2s_W^2)}{2c_W}$
$g_{G_3^0 G_3^- W^+}$	$-\frac{1}{2}$	$g_{G_3^0 H_5^0 Z}$	$\frac{1}{\sqrt{3}}\frac{s_M}{c_W}$
$g_{G_3^+ H_5^- W^+}$	$-\frac{1}{\sqrt{2}}s_M$	$g_{G_3^+ H_5^- Z}$	$-\frac{1}{2c_W}s_M$
$g_{G_3^+ H_5^- W^+}$	$-\frac{1}{\sqrt{2}}s_M$	$g_{H_1^0 G_3^0 Z}$	$\frac{s_2}{c_W}$
$g_{G_3^0 H_5^- W^+}$	$-\frac{1}{2}s_M$	$g_{H_{1M}^0 G_3^0 Z}$	$\frac{s_{2M}}{c_W}$
$g_{H_3^0 G_3^- W^+}$	$\frac{1}{2\sqrt{3}}s_M$	$g_{H_1^0 G_3^0 Z}$	$\sqrt{\frac{2}{3}}\frac{s_M}{c_W}$

Continued on the next page.

$g_{H_5^0 G_3^- W^+}$	$\frac{1}{2\sqrt{3}} s_M$	$g_{H_1^0 H_3^0 Z}$	$-\frac{s_2 s_M}{2c_M c_W}$
$g_{H_1^0 G_3^- W^+}$	$\frac{1}{2} s_2$	$g_{H_{1M}^0 H_3^0 Z}$	$-\frac{s_2 s_M}{2c_M c_W}$
$g_{H_{1M}^0 G_3^- W^+}$	$\frac{1}{2} s_{2M}$	$g_{H_1^{0'} H_3^0 Z}$	$\sqrt{\frac{2}{3}} \frac{c_M}{c_W}$
$g_{H_1^{0'} G_3^- W^+}$	$\sqrt{\frac{2}{3}} s_M$	$g_{H_5^+ H_5^- \gamma}$	s_W
$g_{H_1^0 H_3^- W^+}$	$-\frac{s_2 s_M}{2c_M}$	$g_{H_5^{++} H_5^{--} \gamma}$	$-2s_W$
$g_{H_{1M}^0 H_3^- W^+}$	$-\frac{s_2 s_M}{2c_M}$	$g_{H_3^+ H_3^- \gamma}$	s_W
$g_{H_1^{0'} H_3^- W^+}$	$\sqrt{\frac{2}{3}} c_M$	$g_{H_{3M}^+ H_{3M}^- \gamma}$	s_W
$g_{H_1^0 H_{3M}^- W^+}$	$-\frac{s_2 s_M}{2c_M}$	$g_{G_3^+ G_3^- \gamma}$	s_W
$g_{H_{1M}^0 H_{3M}^- W^+}$	$\frac{s_2}{2c_M}$	$g_{H_1^0 H_{3M}^0 Z}$	$\frac{s_2 s_M}{2c_M}$
		$g_{H_{1M}^0 H_{3M}^0 Z}$	$-\frac{s_2}{2c_M}$

Table D.4: SV_1V_2 type couplings(V_1 and V_2' are vector gauge bosons and S is a Higgs boson), which contribute to Oblique Corrections. Common factor: $i g M_W g^{\mu\nu}$

$g_{H_5^0 W^+ W^-}$	$\frac{s_M}{\sqrt{3}}$	$g_{H_5^0 Z Z}$	$-\frac{2}{\sqrt{3}} \frac{s_M}{c_W^2}$
$g_{H_5^{++} W^- W^-}$	$\sqrt{2} s_M$	$g_{H_5^+ W^- Z}$	$-\frac{s_M}{c_W}$
$g_{H_1^0 W^+ W^-}$	s_2	$g_{H_1^0 Z Z}$	$\frac{s_2}{c_W^2}$
$g_{H_{1M}^0 W^+ W^-}$	s_{2M}	$g_{H_{1M}^0 Z Z}$	$\frac{s_{2M}}{c_W^2}$
$g_{H_1^0 W^+ W^-}$	$\frac{2\sqrt{2}}{\sqrt{3}} s_M$	$g_{H_1^0 Z Z}$	$\frac{2\sqrt{2}}{\sqrt{3}} \frac{s_M}{c_W^2}$

Table D.5: $H_1 H_2 V_1 V_2$ type couplings, which contribute to Oblique Corrections. Common factor: $i g^2 g^{\mu\nu}$

$g_{H_5^0 H_5^0 W^+ W^-}$	$\frac{5}{3}$	$g_{H_5^0 H_5^0 Z Z}$	$\frac{2}{3c_W^2}$
$g_{H_5^+ H_5^- W^+ W^-}$	$-\frac{3}{2}$	$g_{H_5^+ H_5^- Z Z}$	$-\frac{(c_W^4 + s_W^4)}{c_W^2}$
$g_{H_5^{++} H_5^{--} W^+ W^-}$	1	$g_{H_5^{++} H_5^{--} Z Z}$	$2 \frac{(1 - 2s_W^2)^2}{c_W^2}$
$g_{H_3^0 H_3^0 W^+ W^-}$	$-\frac{(1 + c_M^2)}{2}$	$g_{H_3^0 H_3^0 Z Z}$	$-\frac{1}{2c_W^2} (1 + 3c_M^2)$
$g_{H_3^+ H_3^- W^+ W^-}$	$-\left(\frac{1}{2} + c_M^2\right)$	$g_{H_3^+ H_3^- Z Z}$	$-\left[\frac{s_M^2}{2} \frac{(1 - s_W^2)^2}{c_W^2} + c_M^2 \frac{(c_W^4 + s_W^4)}{c_W^2} \right]$
Continued on the next page.			

$g_{H_{3M}^0 H_{3M}^0 W^+ W^-}$	$-\frac{1}{2}$	$g_{H_{3M}^0 H_{3M}^0 ZZ}$	$\frac{1}{2c_W^2}$
$g_{H_{3M}^+ H_{3M}^- W^+ W^-}$	$-\frac{1}{2}$	$g_{H_{3M}^+ H_{3M}^- ZZ}$	$-\frac{(1-2s_W^2)^2}{2c_W^2}$
$g_{G_3^0 G_3^0 W^+ W^-}$	$-\frac{(1+s_M^2)}{2}$	$g_{G_3^0 G_3^0 ZZ}$	$-\frac{1}{2c_W^2}(1+3s_M^2)$
$g_{H_1^0 H_1^0 W^+ W^-}$	$\frac{1}{2}$	$g_{H_1^0 H_1^0 ZZ}$	$\frac{1}{2c_W^2}$
$g_{G_3^+ G_3^- W^+ W^-}$	$-\left(\frac{1}{2} + s_M^2\right)$	$g_{G_3^+ G_3^- ZZ}$	$-\left[\frac{c_M^2}{2} \frac{(1-s_W^2)^2}{c_W^2} + s_M^2 \frac{(c_W^4 + s_W^4)}{c_W^2}\right]$
$g_{H_{1M}^0 H_{1M}^0 W^+ W^-}$	$\frac{1}{2}$	$g_{H_{1M}^0 H_{1M}^0 ZZ}$	$\frac{1}{2c_W^2}$
$g_{H_1^{0'} H_1^{0'} W^+ W^-}$	$\frac{4}{3}$	$g_{H_1^{0'} H_1^{0'} ZZ}$	$\frac{4}{3c_W^2}$
$g_{H_5^+ H_5^- \gamma\gamma}$	$-2s_W^2$	$g_{H_5^+ H_5^- Z\gamma}$	$-\frac{s_W}{c_W}(1-2s_W^2)$
$g_{H_5^{++} H_5^{--} \gamma\gamma}$	$8s_W^2$	$g_{H_5^{++} H_5^{--} Z\gamma}$	$4\frac{s_W}{c_W}(1-2s_W^2)$
$g_{H_3^+ H_3^- \gamma\gamma}$	$-2s_W^2$	$g_{H_3^+ H_3^- Z\gamma}$	$-\frac{s_W}{c_W}(1-2s_W^2)$
$g_{H_{3M}^+ H_{3M}^- \gamma\gamma}$	$-2s_W^2$	$g_{H_{3M}^+ H_{3M}^- Z\gamma}$	$-\frac{s_W}{c_W}(1-2s_W^2)$
$g_{G_3^+ G_3^- \gamma\gamma}$	$-2s_W^2$	$g_{G_3^+ G_3^- Z\gamma}$	$-\frac{s_W}{c_W}(1-2s_W^2)$

Table D.6: $H_1 H_2 V_1 V_2$ type couplings, which *do not* contribute to Oblique Corrections.
Common factor: $i g^2 g^{\mu\nu}$

$g_{H_1^0 H_5^0 W^+ W^-}$	$\frac{\sqrt{2}}{3}$	$g_{H_1^0 H_5^0 Z Z}$	$-\frac{2\sqrt{2}}{3c_W^2}$
$g_{H_3^+ H_5^- W^+ W^-}$	$-\frac{c_M}{2}$	$g_{H_3^+ H_5^- Z Z}$	$c_M \frac{(1 - 2s_W^2)}{c_W^2}$
$g_{H_3^0 G_3^0 W^+ W^-}$	$-\frac{c_M s_M}{2}$	$g_{H_3^0 G_3^0 Z Z}$	$-\frac{3}{2} \frac{c_M s_M}{c_W^2}$
$g_{H_3^+ G_3^- W^+ W^-}$	$-c_M s_M$	$g_{H_3^+ G_3^- Z Z}$	$-\frac{c_M s_M}{2c_W^2}$
$g_{H_5^+ G_3^- W^+ W^-}$	$-\frac{s_M}{2}$	$g_{H_5^+ G_3^- Z Z}$	$s_M \frac{(1 - 2s_W^2)}{c_W^2}$
		$g_{H_3^+ H_5^- Z \gamma}$	$c_M \frac{s_W}{c_W}$

Bibliography

- [1] Building for Discovery: Strategic Plan for U.S. Particle Physics In the Global Context. Report of the Particle Physics Project Prioritization Panel (P5), May 2014.
- [2] P. Q. Hung. Notes on Quantum Field Theory, Elementary Particle Physics and Cosmology.
- [3] The Discovery of Radioactivity,
<http://www2.lbl.gov/abc/wallchart/chapters/03/4.html>.
- [4] Translation by Kurt Riesselmann Wolfgang Pauli, 1930.
- [5] F. L. Wilson. Fermi's Theory of Beta Decay. *American Journal of Physics*, 36:1150–1160, December 1968.
- [6] J. Beringer et al. Review of Particle Physics (RPP). *Phys.Rev.*, D86:010001, 2012.
- [7] T.D. Lee and Chen-Ning Yang. Question of Parity Conservation in Weak Interactions. *Phys.Rev.*, 104:254–258, 1956.
- [8] C. S. Wu". Experimental test of parity conservation in beta decay. *Physical Review*, 105(4):1413–1415, 1957.

- [9] Jun John Sakurai and Jim Napolitano. Modern quantum physics. 2011.
- [10] Michael E. Peskin and Daniel V. Schroeder. An Introduction to quantum field theory. 1995.
- [11] Herbi K. Dreiner, Howard E. Haber, and Stephen P. Martin. Two-component spinor techniques and Feynman rules for quantum field theory and supersymmetry. *Phys.Rept.*, 494:1–196, 2010.
- [12] Peter W. Higgs. Broken symmetries, massless particles and gauge fields. *Phys.Lett.*, 12:132–133, 1964.
- [13] Peter W. Higgs. Broken Symmetries and the Masses of Gauge Bosons. *Phys.Rev.Lett.*, 13:508–509, 1964.
- [14] F. Englert and R. Brout. Broken Symmetry and the Mass of Gauge Vector Mesons. *Phys.Rev.Lett.*, 13:321–323, 1964.
- [15] G.S. Guralnik, C.R. Hagen, and T.W.B. Kibble. Global Conservation Laws and Massless Particles. *Phys.Rev.Lett.*, 13:585–587, 1964.
- [16] Philip W. Anderson. Plasmons, Gauge Invariance, and Mass. *Phys.Rev.*, 130:439–442, 1963.
- [17] Paul H. Frampton and Pham Q. Hung. A Possible Reason for $M_H \simeq 126$ GeV. *Mod.Phys.Lett.*, A29(1):1450006, 2014.
- [18] C.L. Cowan, F. Reines, F.B. Harrison, H.W. Kruse, and A.D. McGuire. Detection of the free neutrino: A Confirmation. *Science*, 124:103–104, 1956.
- [19] Stephen F. King and Christoph Luhn. Neutrino Mass and Mixing with Discrete Symmetry. *Rept.Prog.Phys.*, 76:056201, 2013.

- [20] M.C. Gonzalez-Garcia and Michele Maltoni. Phenomenology with Massive Neutrinos. *Phys.Rept.*, 460:1–129, 2008.
- [21] M.C. Gonzalez-Garcia, Michele Maltoni, Jordi Salvado, and Thomas Schwetz. Global fit to three neutrino mixing: critical look at present precision. *JHEP*, 1212:123, 2012.
- [22] Goran Senjanovic. Neutrino Mass: from LHC to Grand Unification - lecture notes, Balkan Summer Institute 2011, Serbia. extracted from <http://bsw2011.seenet-mtp.info/pub/GSenjanovic-bs2011.pdf> in April 2015.
- [23] Gabriela Barenboim, Martin Gorbahn, Ulrich Nierste, and Martti Raidal. Higgs sector of the minimal left-right symmetric model. *Phys.Rev.*, D65:095003, 2002.
- [24] Wai-Yee Keung and Goran Senjanovic. Majorana Neutrinos and the Production of the Right-handed Charged Gauge Boson. *Phys.Rev.Lett.*, 50:1427, 1983.
- [25] Vardan Khachatryan et al. Search for heavy neutrinos and W bosons with right-handed couplings in proton-proton collisions at $\sqrt{s} = 8$ TeV. *Eur.Phys.J.*, C74(11):3149, 2014.
- [26] P.Q. Hung. A Model of electroweak-scale right-handed neutrino mass. *Phys.Lett.*, B649:275–279, 2007.
- [27] Alfredo Aranda, J. Hernandez-Sanchez, and P.Q. Hung. Implications of the discovery of a Higgs triplet on electroweak right-handed neutrinos. *JHEP*, 0811:092, 2008.
- [28] John F. Gunion, Howard E. Haber, Gordon L. Kane, and Sally Dawson. The Higgs Hunter’s Guide. *Front.Phys.*, 80:1–448, 2000.

- [29] Michael S. Chanowitz and Mitchell Golden. Higgs Boson Triplets With $M(W) = M(Z) \cos \theta \omega$. *Phys.Lett.*, B165:105, 1985.
- [30] Howard Georgi and Marie Machacek. DOUBLY CHARGED HIGGS BOSONS. *Nucl.Phys.*, B262:463, 1985.
- [31] Rohini Godbole, Biswarup Mukhopadhyaya, and Marek Nowakowski. Triplet Higgs bosons at $e^+ e^-$ colliders. *Phys.Lett.*, B352:388–393, 1995.
- [32] J.F. Gunion, R. Vega, and J. Wudka. Higgs triplets in the standard model. *Phys.Rev.*, D42:1673–1691, 1990.
- [33] Paul H. Frampton and Pham Q. Hung. Luminogenesis from Inflationary Dark Matter. 2013.
- [34] P.Q. Hung and Paola Mosconi. E(6) unification in a model of dark energy and dark matter. 2006.
- [35] P.Q. Hung. Sterile neutrino and accelerating universe. 2000.
- [36] Michael E. Peskin and Tatsu Takeuchi. Estimation of oblique electroweak corrections. *Phys.Rev.*, D46:381–409, 1992.
- [37] Hong-Jian He, Nir Polonsky, and Shu-fang Su. Extra families, Higgs spectrum and oblique corrections. *Phys.Rev.*, D64:053004, 2001.
- [38] Gautam Bhattacharyya, Sunanda Banerjee, and Probir Roy. Oblique electroweak corrections and new physics. *Phys.Rev.*, D45:729, 1992.
- [39] M. Baak, M. Goebel, J. Haller, A. Hoecker, D. Kennedy, et al. The Electroweak Fit of the Standard Model after the Discovery of a New Boson at the LHC. *Eur.Phys.J.*, C72:2205, 2012.

- [40] We would like to thank Tim Tait for an earlier update on updated constraints on oblique parameters S and T .
- [41] Christopher T. Hill and Elizabeth H. Simmons. Strong dynamics and electroweak symmetry breaking. *Phys.Rept.*, 381:235–402, 2003.
- [42] Vinh Hoang, Pham Q. Hung, and Ajinkya Shrish Kamat. Electroweak precision constraints on the electroweak-scale right-handed neutrino model. *Nucl.Phys.*, B877:190–232, 2013.
- [43] Vinh Hoang, Pham Q. Hung, and Ajinkya Shrish Kamat. Non-sterile electroweak-scale right-handed neutrinos and the dual nature of the 126-GeV scalar. *Submitted to Nucl. Phys. B*, 2015, [hep-ph 1412.0343].
- [44] See e.g. G. C. Branco, J. I. Silva-Marcos and M. N. Rebelo, *Phys. Lett. B* **237**, 446 (1990) for a model of democratic quark mass matrices. For a scenario of quasi-democratic mass matrix models in the context of large extra dimensions, see e.g. P. Q. Hung and M. Seco, *Nucl. Phys. B* **653**, 123 (2003) [hep-ph/0111013].
- [45] P.Q. Hung and Chi Xiong. Renormalization Group Fixed Point with a Fourth Generation: Higgs-induced Bound States and Condensates. *Nucl.Phys.*, B847:160–178, 2011.
- [46] P.Q. Hung and Chi Xiong. Dynamical Electroweak Symmetry Breaking with a Heavy Fourth Generation. *Nucl.Phys.*, B848:288–302, 2011.
- [47] Serguei Chatrchyan et al. Combined results of searches for the standard model Higgs boson in pp collisions at $\sqrt{s} = 7$ TeV. *Phys.Lett.*, B710:26–48, 2012.

- [48] Georges Aad et al. Search for the Standard Model Higgs boson in the decay channel $H \rightarrow ZZ^{(*)} \rightarrow 4\ell$ with 4.8 fb⁻¹ of pp collision data at $\sqrt{s} = 7$ TeV with ATLAS. *Phys.Lett.*, B710:383–402, 2012.
- [49] Serguei Chatrchyan et al. Observation of a new boson at a mass of 125 GeV with the CMS experiment at the LHC. *Phys.Lett.*, B716:30–61, 2012.
- [50] Georges Aad et al. Observation of a new particle in the search for the Standard Model Higgs boson with the ATLAS detector at the LHC. *Phys.Lett.*, B716:1–29, 2012.
- [51] Serguei Chatrchyan et al. Measurement of Higgs boson production and properties in the WW decay channel with leptonic final states. *JHEP*, 1401:096, 2014.
- [52] Serguei Chatrchyan et al. Measurement of the properties of a Higgs boson in the four-lepton final state. *Phys.Rev.*, D89(9):092007, 2014.
- [53] Serguei Chatrchyan et al. Search for the standard model Higgs boson produced in association with a W or a Z boson and decaying to bottom quarks. *Phys.Rev.*, D89(1):012003, 2014.
- [54] Serguei Chatrchyan et al. Evidence for the 125 GeV Higgs boson decaying to a pair of τ leptons. *JHEP*, 1405:104, 2014.
- [55] Serguei Chatrchyan et al. Study of the Mass and Spin-Parity of the Higgs Boson Candidate Via Its Decays to Z Boson Pairs. *Phys.Rev.Lett.*, 110(8):081803, 2013.
- [56] Howard E. Haber and Deva O’Neil. Basis-independent methods for the two-Higgs-doublet model III: The CP-conserving limit, custodial symmetry, and the oblique parameters S, T, U. *Phys.Rev.*, D83:055017, 2011.

- [57] J. Goldstone, A. Salam, and S. Weinberg. Broken Symmetries. *Physical Review*, 127:965–970, August 1962.
- [58] S Heinemeyer et al. Handbook of LHC Higgs Cross Sections: 3. Higgs Properties. 2013.
- [59] Georges Aad et al. Search for Scalar Diphoton Resonances in the Mass Range 65 – 600 GeV with the ATLAS Detector in pp Collision Data at $\sqrt{s} = 8$ TeV. *Phys.Rev.Lett.*, 113(17):171801, 2014.
- [60] Vardan Khachatryan et al. Observation of the diphoton decay of the Higgs boson and measurement of its properties. *Eur.Phys.J.*, C74(10):3076, 2014.
- [61] P.Q. Hung. Electroweak-scale mirror fermions, $\mu \rightarrow e$ gamma and $\tau \rightarrow \mu$ gamma. *Phys.Lett.*, B659:585–592, 2008.
- [62] ROOT: a data analysis package by CERN.
- [63] Serguei Chatrchyan et al. Search for a standard-model-like Higgs boson with a mass in the range 145 to 1000 GeV at the LHC. *Eur.Phys.J.*, C73:2469, 2013.
- [64] Results of sm-like higgs search at cms plotted with the help of numerical data provided by giuseppe cerati.
- [65] CMS Collaboration. Search for an Higgs Like resonance in the diphoton mass spectra above 150 GeV with 8 TeV data. 2014.
- [66] Wolfgang Hollik. Renormalization of the Standard Model. 1993.